TARGETED DELIVERY OF CYTOKINES, GROWTH FACTORS AND PRE-DIFFERENTIATED CELLS FOR MI TREATMENT

by

Kamila Raziyeva

A Thesis

submitted in partial fulfillment

of the requirements for the degree of

Doctor of Philosophy

In Biomedical Science

School of Medicine Nazarbayev University

Supervised by

Arman Saparov, MD, PhD, DSc

December 2023

DECLARATION

I hereby declare that the research contained in this thesis, unless otherwise formally indicated within the text, is the author's original work. The thesis has not been previously submitted to this or any other university for a degree and does not incorporate any material already submitted for a degree.

Signed Dated

04.12.2023

CONTENTS

ABSTRACT

Following myocardial infarction (MI), cardiac tissue undergoes irreversible cellular alterations, with cardiomyocytes being replaced by fibrotic tissue. To combat this our lab synthesized a novel chitosan-based cryogel containing heparin and poly-vinyl alcohol, showcasing distinct porosity and interconnected pore design. A novel cryogel system was previously established as efficacious for tissue regeneration and sustained drug delivery and has been optimized for the repair of cardiac tissue post-MI in a murine model.

The treatment regime involved the systematic loading and sequential injection of the cryogel with specific cytokines, growth factors, and pre-differentiated cells. Initially, the cryogel loaded with interleukin-10 (IL-10) and transforming growth factor-β (TGF-β) was injected intramyocardially immediately post-MI, targeting the acute inflammatory response. On day 4 post-MI, a second injection was administered, this time utilizing cryogel loaded with vascular endothelial growth factor (VEGF) and fibroblast growth factor-2 (FGF-2), aiming at promoting tissue regeneration and neo-angiogenesis. Subsequently, on day 6 post-MI, the group received cells previously differentiated from mouse mesenchymal stem cells: cardiomyocyte-like cells, smooth muscle cells, and endothelial cells. These cells, in synergy with cytokines and growth factors, aim to repopulate the lost cellular populations, thereby enhancing myocardial repair.

Our results highlighted significant myocardial repair in cohorts treated with the combination of cryogel loaded with IL-10,TGF-β and VEGF,FGF-2 and pre-differentiated cells (Cryo/GFs/Cells). Echocardiographic assessments revealed amplified ejection fraction, fractional shortening, and reduced fibrotic regions, as confirmed by Masson Trichrome staining. Further analyses confirmed the immunomodulatory and regenerative capacity of the treatment. Our novel chitosan-based cryogel, enriched with anti-inflammatory and proangiogenic factors, serves as a promising platform for the controlled release of therapeutics, significantly helping tissue repair and regeneration post-MI. In addition, the separate administration of pre-differentiated cells acts in synergy with the Cryo/GFs, further enhancing the regenerative process. The combination of cellular therapy with the Cryo/GFs treatment provides a comprehensive approach for myocardial recovery, using the unique benefits of both techniques to maximize the efficacy of the therapy.

Key words: MI, biomaterials, mesenchymal stem cells, tissue regeneration, cryogel.

1. INTRODUCTION

The Current Study: Hypothesis, Aims, Objects, Novelty and Significance

After experiencing a MI, the heart undergoes significant structural alterations, primarily characterized by the replacement of cardiomyocytes with stiff fibrotic tissue. To address this issue, our research group has developed a novel treatment regimen involving the use of cryogel, growth factors and pre-differentiated cells. The cryogel has been specifically tailored for repairing cardiac tissue in mice following a MI by altering the form of the cryogel from the disk shape used in previous studies to an injectable powder form. This modification makes the treatment less invasive and potentially accelerates the recovery process.

Our treatment strategy involved a sequential administration of a cocktail of cells as well as cryogel, loaded with specific growth factors. Right after the infarction, the cryogel filled with interleukin-10 (IL-10) and transforming growth factor-β (TGF-β) was injected directly into the infarct zone, targeting the acute inflammatory phase. On the day four post-operation, a second injection of cryogel carrying vascular endothelial growth factor (VEGF) and fibroblast growth factor-2 (FGF-2) was introduced. Finally, on day six, pre-differentiated cells from mouse mesenchymal stem cells including cardiomyocytes, smooth muscle cells and endothelial cells were administered. These cells were intended to work in tandem with the growth factors to replenish lost cellular populations, thereby helping in the recovery of myocardial function after the infarction.

Hypothesis:

The sequential delivery of cryogel loaded with a combination of factors (IL-10,TGF-B and VEGF,FGF-2), followed by the injection of mesenchymal stem cells pre-differentiated in vitro into cardiomyocytes, smooth muscle cells and endothelial cells will significantly improve heart regeneration after MI.

Aims:

The primary aim of this study is to identify the most effective treatment strategy for promoting cardiac tissue regeneration post-MI in a murine model. The goal of the study is to compare different regimens, such as the use of pre-differentiated cells, cryogel loaded with growth factors (Cryo/GF), and their combination, to determine which approach offers the most significant benefits in terms of myocardial repair and regeneration. By a comprehensive evaluation of these strategies, the study is aimed to establish a clear understanding of their relative effectiveness and

potentially establish a synergistic impact that could lead to improved outcomes in cardiac regenerative therapy.

Objectives:

Optimization of Cryogel Formulation and Delivery: Optimize the cryogel formulation and its delivery method, focusing on transitioning from disk to injectable powder form to enhance application and efficacy.

In Vitro Differentiation of MSCs: To successfully differentiate mesenchymal stem cells into cardiomyocytes, smooth muscle cells, and endothelial cells under controlled in vitro conditions. This objective aims to prepare and characterize these cells for subsequent use in in vivo treatments.

Comparative Analysis of Treatment Regimens: Systematically evaluate and compare the effectiveness of various treatment strategies for cardiac regeneration post-MI in a murine model. This includes the use of differentiated cells, cryogel with growth factors (Cryo/GFs), and their combinations.

Novelty:

Our research introduces an innovative approach to cardiac regenerative therapy post-MI. The key novel aspects of our study include:

Utilization of Powdered Cryogel: The study introduces a unique adaptation of our lab-developed chitosan-based cryogel, transforming it from its original disc form to a powdered, injectable format for MI treatment.

Sequential Delivery of Therapeutics: Our strategy involves a sequential delivery approach where the cryogel, loaded with specific factors, is first introduced to precondition the injured myocardium. This is a novel approach in creating an optimal environment for cardiac repair.

Integration of Pre-Differentiated MSCs: The study introduces a novel step of injecting pre-differentiated MSCs – into cardiomyocytes, smooth muscle cells, and endothelial cells – in the later phase of treatment. This ensures the integration of cells that have been prepared for heart repair, thus enhancing the effectiveness of the regenerative process.

Synergistic Combination of Treatments: The study is exploring the synergistic effects of combining cryogel with growth factors and pre-differentiated cells. This combination approach is aimed at maximizing the regenerative potential of each component, offering a comprehensive treatment strategy.

Significance:

Cardiovascular diseases remain the predominant cause of death among adults, with their prevalence continuing to rise in developing countries. Among those, MI is particularly significant. Statistics reveal that nearly 50% of patients who have suffered from MI die within five years. Traditional treatments, while commonly employed, have several limitations, highlighting the critical need for novel therapeutic approaches.

Stem cell therapy is a promising strategy in regenerative medicine. However, it still faces challenges, including low engraftment and survival rates when injected into the injured heart environment. To overcome those barriers we have established a strategy to precondition the heart environment with specific factors. This preparatory step optimizes the myocardial environment, creating optimal conditions for cell engraftment and survival, thereby potentially enhancing the efficacy of the therapy.

Furthermore, a significant concern in stem cell therapy is the unpredictable differentiation of transplanted cells in vivo. There is a risk that introduced cells may not evolve into the desired phenotype. Our methodology bypasses this issue by pre-differentiating the MSCs into cardiac-specific cell types under controlled in vitro conditions. This ensures that the transplanted cells are already primed for their intended function and minimizes the risk of undesirable differentiation post-transplantation.

Additionally, the use of cryogel in powder form allows for a minimally invasive injectable approach compared to more invasive open-chest operation, which has considerable risks and requires an extended recovery period for patients. This not only reduces surgical risks but also ensures a faster recovery for patients, highlighting the innovative approach of our study.

Summary:

In conclusion, the primary objective of this research is to evaluate the potential benefits of a sequential delivery of various growth factors loaded into cryogel, followed by the administration

of differentiated cells. The hypothesis behind claims that such a strategy will considerably enhance cardiac functionality post-MI.

2. LITERATURE REVIEW

2.1 Myocardial Infarction

2.1.1 Definition and Prevalence of MI

Cardiovascular Diseases (CVDs) stand as the leading cause of mortality among adults. Their incidence continues to rise in developing countries. Also, despite all the advancements in diagnostic capabilities and therapeutic options, CVDs persist as the predominant factor behind heart-related deaths in developed countries, with 17.8 million deaths in 2017 alone (Pamukçu, 2019; Martin-Rendon et al., 2008; Roth et al., 2018). Worldwide, the number of prevalent cases of total CVDs nearly doubled from 271 million in 1990 to 523 million in 2019. Concurrently, the count of CVD-related deaths steadily increased from 12.1 million in 1990 to 18.6 million in 2019. Global trends in disability-adjusted life years (DALYs) and years of life lost also exhibited significant growth, with years lived with disability doubling from 17.7 million to 34.4 million over the same period. Specifically, the total number of DALYs attributed to ischemic heart disease (IHD) has consistently risen since 1990, reaching 182 million DALYs, along with 9.14 million deaths in the year 2019 and 197 million prevalent cases of IHD in 2019. Additionally, the total number of DALYs associated with stroke has experienced a steady increase since 1990, culminating in 143 million DALYs, 6.55 million deaths in the year 2019, and 101 million prevalent cases of stroke in 2019 (Valgimigli et al., 2021).

Regarding gender, in 2019, CVD resulted in 9.6 million fatalities among men and 8.9 million fatalities among women. Of these, more than 6 million occurred in individuals aged 30-70. The highest number of CVD-related deaths was observed in China, followed by India, Russia, the United States, and Indonesia. France, Peru, and Japan had the lowest age-standardized mortality rates from CVD. The authors of the study highlight that between 1990 and 2019, there was a significant drop in age-adjusted death rates, DALYs, and YLLs. Meanwhile, there were minor decreases in the rates of prevalent cases and YLDs. This indicates that the rise in overall CVD is largely due to population growth and aging (American College of Cardiology, 2020).

According to "European Society of Cardiology: cardiovascular disease statistics 2021" the total number of CVD deaths across all ESC member countries exceeds the number of cancer deaths for both sexes, where ischemic heart disease (IHD) accounts for 45% of deaths from CVD in

females and 39% in males. Large disparities exist between high- and middle-income countries in Europe in the proportion of premature deaths (before 70 years of age) caused by CVD. For females, 36% of all premature deaths are caused by CVD in middle-income countries compared to 16% in high-income countries. For males, the figures are 36% in middle-income countries and 24% in high-income countries. Age-standardized mortality rates (ASMRs) for CVD have declined since 1990 by 47% in males and 42% in females. In high-income European countries, reductions in ASMRs have exceeded 50% for both sexes. However, in middle-income countries, declines have been smaller, not exceeding 15%, with some countries even experiencing increases in ASMRs (Timmis et al., 2022).

Compared to western countries, the majority of Asian countries, with the exception of Japan, South Korea, Singapore, and Thailand, experienced higher age-adjusted death rates from CVD. Also, most Asian countries, excluding Japan, Kuwait, and Singapore, had 2-5 times higher mortality from strokes compared to Western nations. The annual age-adjusted mortality from stroke ranged between 82-215 per 100,000 for Asian countries and 26-46 per 100,000 for Western countries.

South Asian countries, including India and Bangladesh, are witnessing a stark rise in CVDs, with a younger onset age and elevated mortality rates. By 2030, predictions suggest that Asia will see over 20 million annual CVD-related deaths, accounting for over half of the global CVD fatalities. This surge in CVD prevalence is gendered, with certain Asian countries reporting higher rates among men due to increased smoking. Japan has made remarkable progress by having a consistent decline in CVD-related deaths from the 1960s to the 2000s. Similarly, South Korea observed a 57% decrease in CVD for men and 48% for women between 1984 and 1999. In contrast, China's CVD mortality remains alarming, with the disease being the primary cause of death with 41% of all deaths in 2009. Singapore also has made strides, reducing its age-standardized CVD mortality from 99 per 100,000 in 1976 to 59 per 100,000 in 1994. As Japan struggles with risk factors like high blood pressure, smoking, and diabetes, its male smoking prevalence remains relatively higher than Western countries (Ohira et al., 2013)

Overall, nutritional and metabolic factors such as obesity, diabetes mellitus, hypercholesterolemia and overuse of dietary salt significantly contribute to the global surge in cardiovascular complications and fatalities (Roth et al., 2020)

CVD includes a wide group of disorders such as coronary heart disease, stroke, and rheumatic heart disease (Bugiardini et al., 2020)

Among all, MI occupies the leading position. As follows, approximately 50% of patients who have experienced MI die within the next 5 years (Cambria et al., 2018).

While MI is predominantly identified in developed countries, it is also frequently observed in developing countries. A study involving 19,781 coronary artery disease patients reported a 23.3% prevalence of MI. In recent years, there has been a notable decline in the incidence of MI in Europe and the US. Additionally, MI-related heart failure (HF) has significant mortality and morbidity rates. HF poses a substantial burden on the U.S. healthcare system, impacting 6 million people, causing 300,000 deaths annually, and incurring costs around $40 billion. Furthermore, MI has a considerable economic toll. In 2010, the U.S. recorded over 1.1 million hospitalizations due to MI, with associated costs estimated at $450 billion (Salari et al., 2023).

Based on the gender distribution, although the female population seems to have a reduced susceptibility to coronary heart disease and, by extension, CVDs compared to male population, recent results showed significant gender disparities in MI. 1979-2005 National Hospital Discharge Survey showed that the in-hospital fatality rate was higher for females (14.9%) than males (10.2%). Post the acute phase of a MI, females also exhibited a heightened mortality risk at the one-year mark compared to males (Roth et al., 2020).

In one of the recent studies 35,320 articles were reviewed and data of the major risk factors in 12.7 million participants across 58 countries were extracted. Several risk factors for MI were identified. Those factors included a family history of cardiac disease, current smoking, diabetes mellitus, dyslipidemia, and hypertension. Elevated body mass index (≥25 kg/m^2) also increased the risk. Additionally, specific biomarkers such as cholesterol levels over 200 mg/dL, triglyceride levels above 150 mg/dL, and HDL cholesterol levels below 60 mg/dL were associated with a heightened risk of MI (Dugani et al., 2021). Notably, among MI patients younger than 55 years, 80% had smoking as a unique MI risk factor (Salari et al., 2023).

Another study conducted in Norway revealed that the incidence and mortality rates of acute AMI were observed to be lower among younger individuals compared to older ones. Out of 33,439 AMI patients aged ≤80 years, only 1468 (4.4%) were under 45 years old. The occurrence rate of AMI was 2.1 for every 100,000 person-years in individuals aged 20-29 years, 16.9 for those aged 30-39 years, and 97.6 for 40-49 years old. Younger AMI patients were predominantly male, with

a significant proportion of current smokers, obese, or having a family history of premature AMI. However, despite the low AMI rate in this age group, nearly 10% faced a new cardiovascular event or death within a follow-up period of 2.4 years, underscoring the need for enhanced risk factor management in younger patients (Jortveit et al., 2020).

Overall, MI, that is also known as a heart attack, is a pathological condition, which is characterized by the presence of acute myocardial injury that occurs when the blood flow to a part of the heart becomes blocked, preventing the heart muscle from receiving the oxygen-rich blood it needs (Ojha et al., 2023) This blockage leads to damage or destruction of part of the heart muscle. The blockage is most often a result of a formation of fatty deposits, known as atherosclerosis and plaques in coronary arteries, that supply blood to the heart muscle. In case the blood flow is not restored quickly, the section of the heart muscle becomes damaged from lack of oxygen and starts to die (Raziyeva et al., 2022).

The clinical manifestations of MI can differ significantly depending on the age of the patient (Goch et al., 2009). Young adults under 40 years old account for a small percentage of acute MI cases, constituting from 2% to 6% of all AMI cases. AMI in this age group often presents differently than in older individuals, with coronary angiography detecting a higher incidence of normal coronary arteries or non-severe blockages (Shiraishi et al., 2005). However, although young patients often have less extensive coronary artery disease, they are more prone to multi-vessel diseases, suggesting a potential for more severe future cardiac events (Wong, 2012). In addition to risk factors listed earlier , AMI in young people may be caused due to intake of cocaine, amphetamine, ephedrine, or caffeine (Shiraishi et al., 2005). Unlike young patients, whose primary MI symptom is a chest pain, older patients, especially those above 85, often don't feel the pain. However, for up to 20% of patients aged over 85, acute MI might first appear as confusion or a change in mental clarity. Additionally, elderly individuals tend to experience undetected MI or MI without the typical ECG changes unlike young adults. Compared to younger individuals, the elderly are more prone to complications like heart failure, atrial fibrillation, cardiac rupture, and shock: factors highly associated with increased mortality percentage. This poorer outcome in the elderly can be attributed to reduced heart adaptability, other existing health issues, less use of standard treatments, and higher chances of treatment-related complications. Finally, the other characteristics that influence the unfavorable outcomes post-AMI in elderly patients include pronounced reduction in cardiovascular capacity, a higher incidence of coexisting medical

conditions, underutilization of evidence-based therapies, and increased risk of iatrogenic complications (Rich, 2006).

An acute myocardial injury is usually detected by abnormal cardiac biomarkers identifying acute myocardial ischemia. The primary biomarkers used for detection are cardiac troponin I and troponin T, with high-sensitivity cardiac troponin I (hs-cTn) being especially recommended due to its heart-specific nature and sensitivity. Acute myocardial injury is defined by the detection of elevated cardiac troponin values above the 99% upper reference limit (URL) and is accompanied by a rise or fall of these cardiac troponin values. It's crucial to distinguish between MI and other heart conditions leading to myocardial injury, such as anemia, ventricular tachyarrhythmia, heart failure, and so on. Without clinical evidence of acute ischemic myocardial injury, these conditions are termed "myocardial injury" rather than MI. The distinction is essential for accurate diagnosis and treatment (Domienik-Karłowicz et al., 2021). There are 2 types of MI, known as ST-segment–elevation MI (STEMI) and non–ST-segment–elevation MI (NSTEMI) (Soliman et al., 2015). STEMI represents a critical manifestation of coronary artery disease, characterized by a significant percentage of morbidity and mortality rate. This condition predominantly arises from a complete thrombotic occlusion, originating from an atherosclerotic plaque rupture in an epicardial coronary artery (Vernon et al., 2019). The only optimal methods to reduce the consequences of STEMI are early diagnosis and immediate reperfusion. The gold standard for reperfusion in STEMI patients is primary percutaneous coronary intervention (PCI). However, if PCI does not occur within 120 minutes after MI, specific fibrinolytic agents are injected to lyse the thrombus. Establishing 24/7 cardiac catheterization services and implementing standardized hospital protocols have effectively shortened the delay to reperfusion treatment. Together with advancements in antithrombotic therapies and preventive strategies, these measures have contributed to a decline in STEMI-related mortality. However, a significant proportion of STEMI patients still remain susceptible to recurrent cardiovascular events (Vogel et al., 2019; Scholz et al., 2018).

Another type of MI is NSTEMI that arises due to a mismatch between myocardial oxygen demand and consumption. This mismatch can be caused by various factors, including plaques, vasospasm, coronary embolism, or coronary arteritis. Non-coronary injuries such as cardiac contusion, myocarditis or the presence of cardiotoxic substances may also lead to NSTEMI. Finally, factors not directly linked to the coronary vessels or the heart muscle, like hypotension, hypertension, tachycardia, aortic stenosis, and pulmonary embolism can result in NSTEMI due to

the heart's inability to meet the heightened need for oxygen (Basit et al., 2023). Patients with NSTEMI often experience pressure-like substernal pain, which can be accompanied by symptoms like dyspnea, nausea, or fatigue. The diagnosis of NSTEMI relies on the patient's history, ECG results, and the increase of specific markers, like - cardiac troponin (Jiménez-Méndez et al., 2021). The primary treatment is focused on reducing cardiac damage and preventing fatal outcomes. An immediate treatment often includes administration of oxygen, aspirin, and nitrate medications. In addition if NSTEMI is confirmed or highly suspected, anticoagulation treatment is initiated. Those patients who are diagnosed with NSTEMI are usually admitted to specific cardiac care units for comprehensive care, that includes beta-blockers, ACE inhibitors, high-dose statins, and potential interventions like angiography (Somma et al., 2012). The overall morbidity and mortality are influenced by factors, such as the level of troponin biomarker and other health issues, including the diabetes, presence of peripheral vascular disease, presence of renal dysfunction, and dementia (Sanchis et al., 2011)

2.1.2 Biological Consequences of MI: Cellular death, Inflammation, and Scar Tissue Formation.

Infarction usually occurs as an extreme consequence of ischemia, which in turns, develops when the blood supply to the heart is blocked or partially restricted (White et al., 2008; Eltzschig et al., 2011). In the majority of cases ischemia is the result of atherosclerosis, a condition in which the inside of a vessel narrows due to the formation of plaques. However, there are other conditions that lead to infarction, including coronary artery spasm, coronary artery embolism, Takotsubo cardiomyopathy, coronary artery dissection, vasculitis, anomalous coronary artery, increased blood viscosity, oxygen supply and demand mismatch. We will now consider some of those conditions and their role in MI occurrence.

Atherosclerosis is a chronic inflammatory condition characterized by the accumulation of plaques and fibrous elements inside large arteries. The plaques are built from the agents found in the blood, such as fat, cholesterol and minerals which trigger inflammation, leading to irregular blood flow and culminating in atherosclerotic cardiovascular disease (ASCVD). (Pahwa et al., 2023) Risk factors, that lead to atherosclerosis include oxidation, obesity/insulin resistance, inflammation, low HDL-C, sedentary lifestyle, smoking, triglyceride and remnant lipoproteins, hypertension, platelet reactivity and low density lipoproteins (LDL) (Glaucylara et al., 2018).

Beyond MI, atherosclerosis leads to a broad range of complications, including aortic aneurysms, carotid and cerebrovascular disease (ischemic attack, small vessel disease), aortic valve disease and peripheral vascular disease (Makover et al., 2022).

A primary trigger for atherosclerosis is the accumulation of LDL within the subendothelial matrix. This buildup is accentuated when circulating LDL levels rise, especially in areas predisposed to lesion formation. The retention of LDL in the vessel wall is facilitated by interactions between LDL constituent, apolipoprotein B (apoB), and matrix proteoglycans. Over time, LDL undergoes oxidative modifications, leading to the formation of so-called “foam cells”, that are macrophages that have eaten oxidized LDL. These foam cells aggregate beneath the endothelium, forming early 'fatty streak' lesions. As these lesions evolve, they accumulate lipid-rich necrotic debris and smooth muscle cells (SMCs), giving rise to advanced lesions characterized by a fibrotic cap of SMCs and extracellular matrix that encloses a lipid-rich necrotic core. (Lusis, 2000; Jebari-Benslaiman et al., 2022).

In addition to LDL, other apoB-containing lipoproteins, such as lipoprotein(a) and remnants, also accumulate in the arterial wall. Lipoprotein(a) is especially interesting to note. While it structurally resembles LDL, it contains an additional polypeptide, that is apolipoprotein(a), which is linked to apoB. This structure imparts to lipoprotein(a) its particularly atherogenic properties, influencing fibrinolysis and SMC growth. As the disease progresses, inflammation enhances with the recruitment of monocytes and lymphocytes but not neutrophils to the wall area induced by the accumulation of oxidized LDL. Monocytes adhere to the endothelium, migrate into the intima, differentiate into macrophages, and uptake lipoproteins, further contributing to foam cell formation. Various proinflammatory factors and cytokines are expressed at this point. The cytokine macrophage colony-stimulating factor (M-CSF) plays a pivotal role in the process, stimulating macrophage proliferation and differentiation (Watson et al., 1997). Vulnerable plaques are characterized with thin fibrous cap and elevated inflammatory cell level.

Advanced atherosclerotic lesions are vulnerable to rupture, leading to thrombosis. The stability of these lesions is influenced by various factors, including calcification, neovascularization, and the presence of tissue factor, a key protein initiating the coagulation cascade, thereby setting the stage for potential vascular events like MIs or strokes (Lusis, 2000; Jebari-Benslaiman et al., 2022)

Additionally, individuals who have survived AMI are at risk for potential future events. The reasons for that are not yet clear. However, a recent study revealed that AMI can accelerate atherosclerosis and enhance inflammation in plaques distantly. Thus, experiments on Apoe−/− mice who were previously experienced with AMI showed that they developed larger and more advanced atherosclerotic lesions. This progression was linked to a notable rise in monocyte recruitment. The source of these extra monocytes was traced back to the release of hematopoietic stem cells as well as progenitor cells from the bone marrow niches following the MI through sympathetic signaling. These cells, driven by sympathetic nervous system signals, migrated to the spleen. Those cells then moved to the spleen, contributing to a sustained increase in monocyte production (Dutta et al., 2012).

Overall, atherosclerosis, a once predominantly Western concern, is now a global issue impacting various demographics, including younger populations, women, and numerous ethnicities. Its understanding has undergone significant changes, shifting the spotlight from traditional risk factors like LDL cholesterol, blood pressure, and smoking. Recent research in this area emphasizes the potential roles of triglyceride-rich lipoproteins in atherosclerosis development. Moreover, additional factors, such as sleep disturbances, lack of physical activity, microbiome imbalances, air pollution, and environmental stresses, have emerged as potential contributors. Inflammatory processes and leukocytes serve as a bridge between both conventional and emerging risk factors, affecting arterial wall cell behavior. Some other studies highlight the strategic role of bone marrow, revealing that somatic mutations in stem cells can lead to clonal hematopoiesis, a newfound and potent factor that elevates cardiovascular disease risk. The mechanisms underpinning thrombotic complications have also evolved in understanding, offering a new therapeutic view of this condition (Libby, 2021).

Again, the primary cause of MI is plaque rupture that causes intracoronary thrombus formation in the coronary artery. Yet, MI with nonobstructive coronary artery disease (MINOCA) represents a set of conditions with similar angiographic results. MINOCA is defined by the lack of significant (≥50%) coronary narrowing and no signs of broken atherosclerotic plaque. It's found in 5–8% of acute coronary syndrome cases (Monin et al., 2022). MINOCA has various causes and can be categorized based on the underlying pathological process into epicardial (such as unstable plaques at angiography, epicardial spasms, and coronary dissection) or microvascular origins. The microvascular category can be further split into intrinsic causes (such as coronary artery spasm,

Takotsubo syndrome, and coronary embolism) and extrinsic ones, like myocarditis (Niccoli & Camici, 2020).

Coronary artery spasm (CAS) involves intense narrowing of the coronary arteries, resulting in reduced blood flow to the heart muscle and eventually causing AMI (Seitz et al., 2022). It accounts for 3% to 95% of cases of MINOCA, varying by the registry. Tests that show positive results using intracoronary, adenosine, or ergonovine indicate a poorer outlook. Such positive tests correlate with increased mortality rates, more cardiac-related deaths during monitoring, a higher frequency of MI hospital readmissions, and poorer management of angina symptoms. Moreover, spasms in the main heart arteries have worse outcomes than those in smaller vessels (Vidal-Perez et al., 2019).

Coronary embolisms (CE) originating from the left heart can lead to MINOCA due to the effects on microcirculation. Genetic conditions that predispose individuals to clotting, like factor V Leiden or deficiencies in protein C/S, are commonly seen. In patients with MINOCA, screening for clotting disorders revealed that approximately 14% had such conditions (Niccoli & Camici, 2020). Other reasons causing CE include: thrombus formation in heart structures, such as the left atrial appendage or valves, paradoxical emboli, which transition from the venous to the systemic circulation through openings like a patent foramen ovale, commonly originating from deep vein thrombosis and finally, medical procedures, especially percutaneous coronary interventions and aortic valve replacements that can inadvertently introduce iatrogenic emboli into the coronary arteries (Monin et al., 2022).

Another condition that can lead to MINOCA is Takotsubo cardiomyopathy. Takotsubo cardiomyopathy, alternatively known as broken heart syndrome, stress cardiomyopathy, or apical ballooning syndrome, develops when an intense emotional or physical stressor results in dilation of the heart's left ventricle, precipitating acute heart failure. The principal treatment approach is supportive care. The administration of angiotensin-converting enzyme (ACE) inhibitors and angiotensin II receptor blockers (ARBs) may diminish the risk of subsequent episodes. The prognosis in general is favorable, with around 95% of affected individuals experiencing a complete recovery (Boyd & Solh, 2020).

In general, MI occurs due to a mismatch between the heart's oxygen supply and demand. When the heart muscle doesn't receive enough oxygen, it can lead to tissue damage. This imbalance can be a result of various factors, including a blocked artery or heightened cardiac demands that

aren't met by the corresponding blood supply. Prompt diagnosis and treatment are crucial to minimizing damage and improving patient outcomes. The prevention of MI often focuses on managing risk factors such as hypertension, diabetes, and high cholesterol.

2.1.3 Cellular Death

MI results in tissue death. Long-term ischemia activates the process called the ischemic cascade. Cardiomyocytes in the injured area, where the blood supply stopped and the left coronary artery is blocked, die (Stillman et al., 2018). Instead of contractile cardiac cells a collagen fibrotic tissue is formed. The combination of tissue death and fibrosis leads to impaired conduction pathways of the entire heart. This, in turns, may result in arrhythmias, inflammation and rupture of the heart wall, leading to death (Prabhu et al., 2016). Mechanisms underlying cellular death in MI are diverse, intricate, and largely interconnected. They include necrosis, apoptosis, and autophagy, as well as the factors influencing cellular death, such as duration of ischemia, oxygen and nutrient deprivation and reperfusion injury (Del Re et al., 2019 ; Sun et al., 2019)

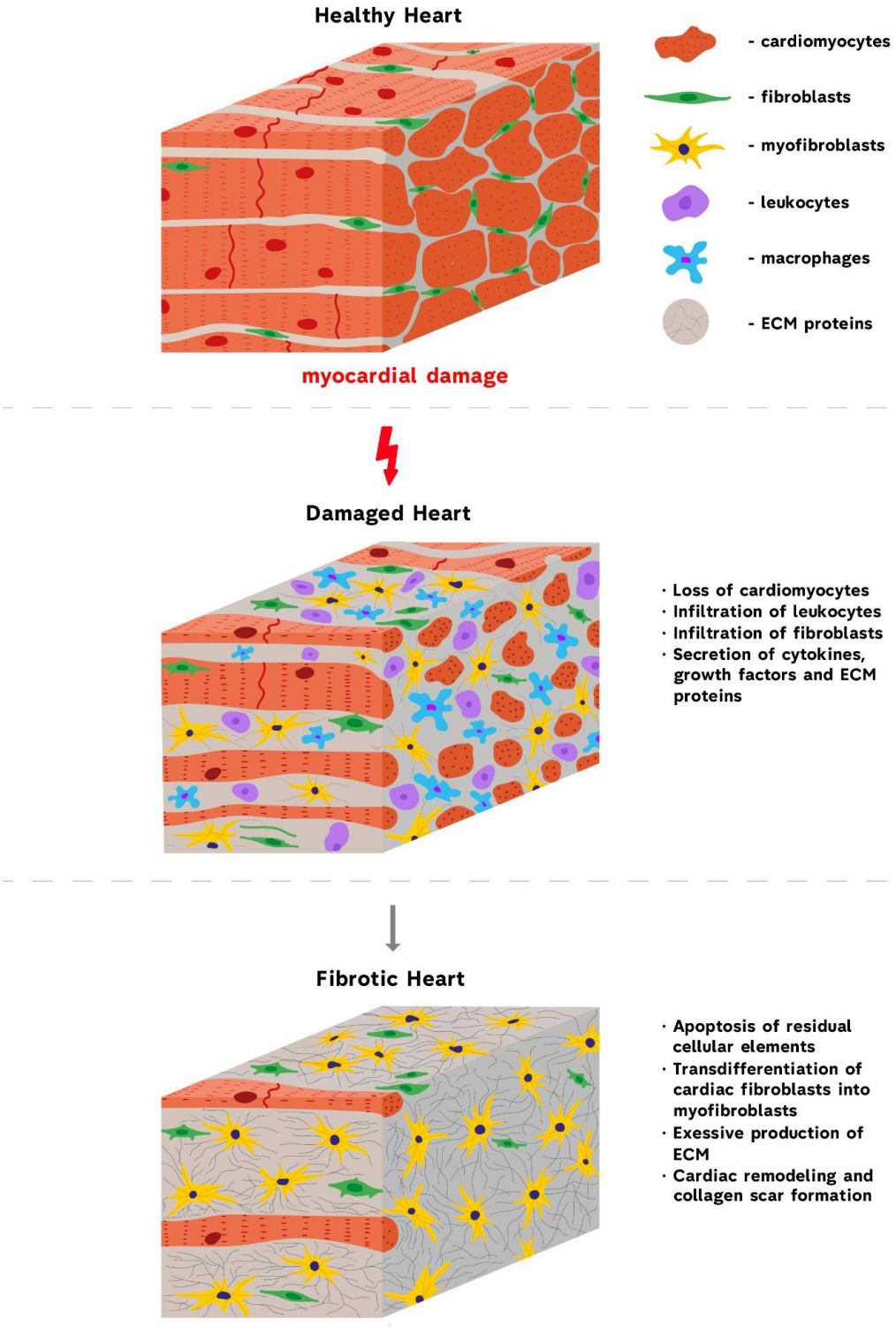

Figure 1. Tissue fibrosis development following MI (Raziyeva et al., 2022).

Necrosis is defined as a form of cell injury leading to the uncontrolled death of cells due to factors external to the cell, such as severe injury, infection or toxins. This leads to the release of the contents of cells into adjacent tissues and causing further harm (D'Arcy, 2019). In the context of MI, necrosis is a primary player. When coronary blood flow ceases or diminishes significantly, it leads to a deprivation of oxygen and essential nutrients to the myocardial cells. Unable to sustain their metabolic needs, these cells undergo irreversible injury and eventually die, leading to a necrotic way of cell death. The necrotic cells release their intracellular content, which can further exacerbate inflammation and damage (D'Arcy, 2019). Recent studies have revealed various pathways of regulated necrosis, commonly referred to as "programmed necrosis" or "necroptosis." Two primary pathways, the receptor-mediated and mitochondrial mechanisms, play significant roles in myocardial necrosis. Activation of receptor-interacting (RIP) kinases 1 and 3 has been observed in ischemic heart tissues, with these kinases being pivotal mediators of myocardial necroptosis. The compound Necrostatin-1, an inhibitor of the RIP1 kinase, has shown promise in curtailing myocardial cell demise and shrinking infarct dimensions in cardiac infarction models (Oerlemans et al., 2012). In the realm of myocardial I/R injury, a noteworthy discovery highlights the role of RIP3 in guiding necroptosis by targeting the Ca(2+)-calmodulin-dependent protein kinase II (Zhang et al., 2016). Another group identified the role of the Fas-associated death domain protein in regulating I/R and oxidative stress-triggered cardiomyocyte necrosis via its impact on the receptor-interacting serine/threonine-protein kinase (RIPK)/RIPK3 complex (Wang et al., 2015). Additionally, a central mechanism of necrosis revolves around the opening of the mitochondrial permeability transition pore (mPTP), which is modulated by cyclophilin-D (CypD). Yet, the overall comprehension of the primary processes underlying myocardial necroptosis, particularly the mPTP-CypD-associated death pathway, remains limited (Sun et al., 2019).

Apoptosis, often referred to as programmed cell death, is a process in which cells undergo self-destruction in a controlled and regulated manner (D'Arcy, 2019). Unlike necrosis, apoptosis is an organized form of death, ensuring that dying cells minimally affect neighboring cells. Apoptosis contributes significantly to myocardial cell loss following AMI and is involved in the subsequent changes in left ventricular structure and the onset of symptomatic heart failure. During the initial phases of ischemia, a controlled apoptosis can be protective, removing cells that have been irreversibly damaged without causing inflammation. It primarily causes myocytes death in peri-infarct areas. During MI's subacute phase, elevated levels of apoptosis are evident and are

closely linked to left ventricular (LV) remodeling. Importantly, patients who experienced heart failure shortly after AMI displayed higher apoptosis rates. Thus, apoptosis directly impacts infarct size, LV remodeling, and early heart failure onset following AMI(Teringova & Tousek, 2017).

Autophagy, in turn, is a cellular process wherein cells degrade their own components, especially during instances of stress, to recycle nutrients and ensure survival. Autophagy maintains heart health and performance under normal circumstances and is triggered during stress to reduce damage. It minimizes harm and sustains heart function during ischemia. Additionally, it lessens the chronic structural changes from long-term limited blood flow and helps the heart adjust to increased pressure by preventing the buildup of faulty proteins, mitochondrial issues, and oxidative damage. Disruptions in autophagy are linked to diabetes and age-related heart abnormalities. Such defects can lead to heart protein disorders and doxorubicin-induced cardiomyopathy. Yet, excessive autophagy can harm the heart during specific stressful events, like the return of blood supply after a blockage (Sciarretta et al., 2018).

Additionally, during MI, the extent of cellular death is influenced by several key factors. Ischemia, the reduced blood flow to heart tissues, can lead to reversible cell damage initially, but prolonged ischemia results in irreversible cell injury and death. Cardiomyocytes are heavily dependent on a consistent supply of oxygen and nutrients, and deprivation leads to metabolic distress, forcing cells to switch to less efficient energy pathways, resulting in toxicity and cellular death (Wu et al., 2018). Moreover, while reestablishing blood flow is crucial, the process can cause reperfusion injury, leading to oxidative stress and inflammation, worsening cellular damage. Thus, interventions should be focused not only on restoring blood flow but also on mitigating associated risks (Kalogeris et al., 2012).

2.1.4 Inflammation

Following MI, the heart muscle undergoes sequential healing processes, starting with inflammation then shifting to anti-inflammation, and finally leading to tissue repair, culminating in scar formation in the infarction zone (Fig.1). The heart's response to MI is mainly driven by two phases. First, invading leukocytes release proteases to degrade the extracellular matrix (ECM), an essential action for clearing dead cardiomyocytes. Subsequently, the creation of a new ECM, which forms the scar, is directed mainly by cardiac fibroblasts, the primary agents of ECM regeneration. Leukocytes play a central role in this transition, shifting from a pro-inflammatory stance to anti-

inflammatory and repair-oriented phenotypes. The balance between these phases results in the quality and size of scar, which then affects long-term post-MI consequences(Chalise et al., 2022).

Initiation of Inflammation

MI leads to immediate and robust immune response, a process that is essential for repair and scar formation but can also enhance tissue damage (Fig.1) This immune response is stimulated by the death of cardiac cells and the release of cellular debris and damage-associated molecular patterns (DAMPs) to the surrounding area. Upon the release of DAMPs, the earliest responders are usually neutrophils, followed by monocytes that differentiate into M1 macrophages in the tissue. These cells migrate to the site of injury, responding to chemotactic cues and signaling molecules. Activated platelets, in turn, cause immediate vascular blockage and enhance inflammation through interactions with neutrophils, monocytes, and lymphocytes (Paolisso et al., 2021). Thus, the recruitment and activity of these cells are crucial for clearing necrotic debris, setting the stage for subsequent tissue repair (Raziyeva et al., 2021). In addition, recent studies indicated that ratios like neutrophil-to-lymphocyte (NLR), platelet-to-lymphocyte (PLR), and neutrophil-to-platelet (NPR) can serve as systemic inflammation indicators and are linked to adverse outcomes in several cardiovascular conditions, including acute coronary syndromes (Paolisso et al., 2021 ; Yu et al., 2022).

Resolution of Inflammation

Inflammation, while essential for repair, needs to be timely resolved to prevent extended damage. Anti-inflammatory cytokines are vital for counterbalancing the pro-inflammatory state and initiating the reparative phase post-MI (Liu et al., 2020). Thus, during the repair phase, the anti-inflammatory cytokines IL-10 and TGF-β are activated to suppress pro-inflammatory molecules. TGF-β transforms cells into myofibroblasts, promotes production of external matrix proteins, and prevents matrix breakdown. It also aids in the migration of bone marrow MSCs to assist myocardial repair after MI by modulating the SDF-1/CXCR4 pathway (Zhang et al., 2016). Over time, sustained cytokine expression triggers changes in myocytes characteristics and activates matrix metalloproteinase to support cardiac remodeling (Nian et al., 2004). Specialized pro-resolving mediators, including lipoxins, resolvins, protectins, and maresins, play a significant role in curtailing inflammation. These SPMs not only promote the resolution of inflammation but also

enhance tissue repair and regeneration (Halade & Tourki, 2019). For instance, resolvin D1 has been shown to limit neutrophil infiltration and promote macrophage-mediated clearance of debris in MI models(Kain et al., 2015).

Inflammatory Mediators

Cytokines are a diverse group of small proteins, glycoproteins, or peptides that serve as molecular messengers and modulate cellular response during immune reactions. The role of cytokines in MI is crucial as they regulate inflammation, cell death, and tissue repair. Shortly after an MI an expression of pro-inflammatory cytokines, such as TNF-α, IL-1 and IL-6 is markedly increased. These cytokines not only amplify the inflammatory response but also play a role in myocardial cell apoptosis, matrix degradation, and might influence the heart's remodeling process. Also, pro-inflammatory cytokines activate endothelial cells, making them more receptive to leukocytes, thus promoting their recruitment and activation to the site of injury. In addition, IL-10 which is typically viewed as an anti-inflammatory cytokine is increased during the later stages of inflammation and aids in resolving inflammation, clearing tissue, and promoting healing (Liberale et al., 2021).

Chemokines are a specialized category of cytokines, and are crucial for immune cell trafficking. They navigate immune cells to the injury area. Damaged cardiomyocytes activate the complement system, generate reactive oxygen species, and stimulate cytokine production. These cytokines attract leukocytes to the injury site with the help from chemokines. Elevated levels of specific chemokines, such as CCL2, CCL3, and CCL5, play a pivotal role in recruiting monocytes, neutrophils, and lymphocytes to the site of myocardial damage. This directed migration is essential for both the clearance of dead cells and the initiation of repair mechanisms (Lu et al., 2022). In the I/R model, studies by Vajen et al. a group observed a reduction in MI area and a diminished count of neutrophils in the infarct zone through the blockage of the isomerization of CXCL4 with CCL5. The research also showed that introducing external CXCL4 to MI mice hindered macrophage phagocytosis and elevated post-MI mortality rates. Moreover, CXCL5, augmented by cardiomyocytes, enhances neutrophil recruitment, intensifying myocardial I/R injuries (Vajen et al., 2018). Further research reveals an elevated presence of CXCL8 due to Ang II in infarcted heart muscles, also leading to an increased infiltration of inflammatory cells (Sun et al., 2019). The application of FR183998 notably mitigated CXCL8 levels and MI occurrences, highlighting the

potential promote role of CXCL8 in myocardial ischemia (Ohara et al., 2002). CXCL10, likewise elevated in infarcted myocardium, has shown in animal studies to play a protective role in MI, by inhibiting fibroblast migration and promoting wound contraction, despite causing over-repair and scarring in its absence (Bujak et al., 2009).

The role of CXCL12 in MI is multifaceted and debated. While elevated levels of CXCL12 plasma are observed in MI patients, implying a protective role against IRI and a promoter of cardiomyocyte proliferation, opposing studies suggest it impairs cardiac functionality, causing increased cardiac fibrosis post-MI. These contrasting findings could result from varying experimental models. CXCL12 transgenic rats showed augmented inflammation and fibrosis post-MI induction. However, early administration of external CXCL12 has shown signs of enhanced cardiac functionality post-MI (Ghadge et al., 2011). Finally, elevated plasma levels of CXCL16 in MI mice demonstrated its protective role by enhancing macrophage phagocytosis. The disruption of the CXCL16-CXCR6 axis in CXCR6 KO mice indicated reduced infarct sizes and improved cardiac function under I/R induction (Zhao et al., 2013).

In addition to cytokines and chemokines, adhesion molecules, which are proteins expressed on the surface of cells, also play a role in MI inflammatory process. As the endothelium gets activated by various factors, the expression of adhesion molecules is upregulated. Molecules such as ICAM-1, VCAM-1 and selectins become critical players in the inflammatory response post-MI. They not only attach circulating leukocytes to the endothelium but also help during diapedesis, ensuring cell arrival at the inflamed myocardial tissue. This interaction between leukocytes and endothelial cells, facilitated by adhesion molecules, is a cornerstone of the acute inflammatory response seen after MI (Weil & Neelamegham, 2019).

2.1.5 Scar Tissue Formation

The process of fibrosis development after MI is similar to other tissues. It's characterized by an excessive production and reduced degradation of ECM proteins and an accumulation of myofibroblasts. This alters the heart's regular structure and functions, impacting mechano-electric interactions, which leads to the stiffness of left ventricle, delayed systole–diastole cycle, and arrhythmias (Raziyeva et al., 2022) (Fig.1).

Three types of cardiac fibrosis exist, which are replacement fibrosis, reactive fibrosis and infiltrative fibrosis (Webber et al., 2020; Karamitsos et al., 2020). Replacement fibrosis is

characterized by the replacement of dead cardiomyocytes with fibrotic tissue. Although healthy cardiomyocytes die during this process, ventricles' anatomical integrity is still preserved. Reactive fibrosis involves widespread collagen in the ECM. Unlike replacement fibrosis, cardiomyocytes do not die during a reactive type of fibrosis. Instead, it's triggered by ongoing issues like inflammation and hemodynamic stress, causing the mechanical stiffness of the myocardial tissue (Heymans et al., 2015). Thus, although it initially defends against increased wall tension, it eventually leads to issues like cardiac systolic and diastolic dysfunction, arrhythmias and metabolic impairment, marking a pathologic state of fibrosis (Tanaka et al., 2020). Infiltrative fibrosis is characterized by the abnormal accumulation of substances such as amyloid, iron, or glycosphingolipids. Cardiac amyloids are pathological extracellular proteins with a stable and fibrous structure. In the heart, significant amyloids include transthyretin (TTR) and immunoglobulin light chains (Kyriakou et al., 2018). Their presence in the heart can diminish both its muscle contraction and electrical activity (Hara et al., 2017).

During the proliferative phase, lasting several days to a month, immune cells such as macrophages, mast cells and lymphocytes are attracted (Raziyeva et al., 2021). These cells release mediators, prompting cardiac fibroblasts to transform into myofibroblasts, which are responsible for cell migration, ECM protein production, and bioactive molecule secretion (Ceauşu et al., 2021).

Under normal circumstances, a healthy heart comprises endothelial cells, smooth muscle cells, fibroblasts, and cardiomyocytes, varying in number based on factors like age and species (Yousefi et al., 2020). Post-injury, fibroblasts turn into myofibroblasts, which are cells with characteristics of both fibroblasts and smooth muscle cells. Myofibroblasts are typically absent in a healthy heart (Talman & Ruskoaho, 2016). They control ECM production, particularly collagen types I and III. Excessive ECM production by these cells results in cardiac remodeling (Ni et al., 2019). Myofibroblasts replace dying cardiomyocytes post-injury, and this leads to scar formation in the injured site. The transformation process is complex, and influenced by molecules including TGF-β, TNF-α, CTGF, RAAS, Gal-3 and IL-11 (Webber et al., 2020). Additionally, although myofibroblasts primarily arise from cardiac fibroblasts, other cells like pericytes can also transdifferentiate into them. However, the role of such cells in fibrosis development remains unclear (Talman & Ruskoaho, 2016).

Other cell types such as endothelial cells, pericytes, smooth muscle cells, and cardiomyocytes are also involved in the proliferative phase (Frangogiannis, 2020).

Activated fibroblasts support injury repair by enabling oxygen and nutrient flow and promoting vascular network development. The proliferative phase finished with an expression of anti-fibrotic mediators like IFN-γ, angiotensin AT2-receptor, and CXCL10 that help to stop fibrotic tissue formation (Aujla & Kassiri, 2021).

In the final maturation phase, residual fibroblasts and vascular cells in the injured region undergo apoptosis. Neighboring fibroblasts respond to altered infarct zones, producing additional ECM proteins (Dobaczewski et al., 2012). Myofibroblasts eventually transition into matrix fibrocytes, supporting mature scars by secreting specific proteins. In general, scar development is a complex process, involving various cells such as macrophages, endothelial cells, lymphocytes and trans-differentiated cardiac fibroblasts (Raziyeva et al., 2022).

Overall, heart tissue has a limited ability to recover by itself. Cardiomyocytes are cardiac muscle cells that regulate contractile functions of the heart. They are lost in infarcted tissue and cannot be regenerated once dead (Awada et al., 2016). Without properly working cardiac cells the heart may stop beating. In addition, MI also leads to gradual loss of healthy vessels, composed of endothelial cells (ECs) (Thirunavukkarasu, 2018) and smooth muscle cells (SMCs). Therefore, a strategy that would work for both cardiomyocytes and vascular cell replenishment is highly demanded.

2.2 Current Treatments and Their Limitations

An effective, on-time treatment of MI is pivotal. Rapid intervention not only helps to save the heart muscle and its function but also reduces the risk of life-threatening complications. The overall goal of any strategy remains to minimize myocardial damage, ensure patient survival, and improve the quality of life post-event (Reed et al., 2017). Figure 2 illustrates the current strategies applied to the treatment of infarction.

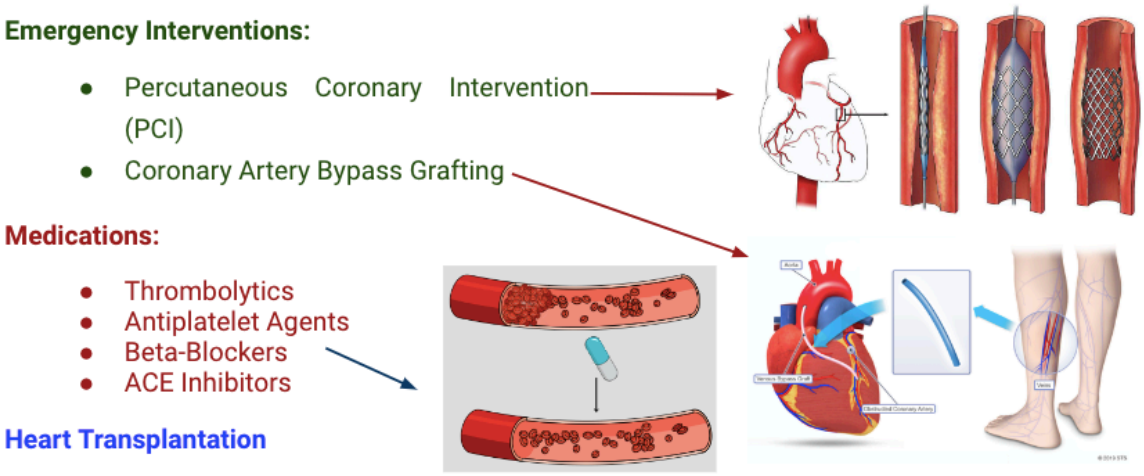

Figure 2. Current treatment of MI

2.2.1 Coronary Reperfusion Therapies

While rapid reperfusion therapy has demonstrated efficacy in reducing mortality, minimizing infarct dimensions, and enhancing left ventricular functions in STEMI, notable morbidity and mortality remain. Even with advancements in reperfusion therapy, there is a high chance that reestablishing blood circulation can induce detrimental outcomes. Such repercussions, known as reperfusion injury, contribute to fatal cellular demise and can represent nearly half of the final infarct dimension (Bainey & Armstrong, 2014).

Percutaneous Coronary Intervention (PCI)

Antithrombotic treatments aim to stabilize the plaque and facilitate natural fibrinolytic mechanisms to reestablish vessel patency. Percutaneous coronary intervention (PCI) is commonly used to enhance blood circulation and prevent further ischemic episodes. The European Society of Cardiology (ESC) guidelines call for prompt coronary artery reperfusion in patients diagnosed with STEMI. They emphasize that primary PCI, when accessible, is the recommended approach (Kristensen et al., 2014).

PCI is an invasive, non-operative technique aimed at alleviating the constriction or blockage within the coronary artery to enhance perfusion to the ischemic tissue. Typically, this is realized through various techniques. For example, balloon dilation of the constricted area or stent

placement to maintain arterial patency are the most prevalent methods among all (Ahmad et al., 2023).

Blood stream access is achieved via the femoral or radial artery routes. The catheter's position and surrounding tissues are visualized using real-time X-ray fluoroscopy. The catheter is progressed to the ascending aorta. Distinct catheters are used for engaging the right and left coronary arteries. Intravenous contrast is administered within the coronary artery to outline its structure. Imaging of the coronary arteries is captured from varied perspectives to evaluate the three-dimensional aspect of the constriction (Ahmad et al., 2023).

Ideally, PCI should be conducted within 24 hours post-NSTEMI. However, data indicates that in low-risk scenarios, this window could extend up to 48-72 hours without adverse outcomes. Yet, PCI beyond the initial 24-hour window has shown correlations with extended hospital stays, leading to heightened expenses and potentially compromising care quality. In contrast, for STEMI, the primary goal is swift reperfusion to minimize heart muscle damage, with antithrombotic treatments playing a supportive role. Furthermore, NSTEMI patients presenting significant risk factors necessitate prompt revascularization, underlining the critical nature of early risk evaluation.

Fibrinolytic Therapy

While PCI is the favored reperfusion method in contemporary STEMI management, fibrinolysis remains a central approach in areas with geographical limitations and restricted healthcare services, especially in developing countries (Wu et al., 2023). Fibrinolytic therapy, also frequently called thrombolytic therapy, plays a pivotal role in the management of MI. Overall, this therapeutic approach involves the administration of specific drugs designed to dissolve blood clots, which obstruct the coronary arteries and precipitate the MI. By promoting the breakdown of fibrin, a major component of clots, these agents work to restore blood flow to the injured myocardium. When administered promptly, fibrinolytic therapy can significantly reduce the extent of heart muscle damage and improve overall patient outcomes. The newest, most frequently used bolus fibrinolytics encompass tissue plasminogen activator (tPA) derivatives such as tenecteplase (TNK-tPA) and reteplase (rPA), both of which have initial plasma half-lives ranging from 15 to 30 minutes. These agents optimize prehospital fibrinolysis and minimize potential medication errors. Although their mortality reduction capability mirrors that of the 90-minute weight-adjusted accelerated t-PA regimen, TNK-tPA's enhanced fibrin specificity notably diminishes systemic

bleeding. On the other hand, while the combined use of intravenous glycoprotein IIb/IIIa (IV GP IIb/IIIa) inhibitors augments epicardial flow, myocardial perfusion, and curtails reinfarction, anticipated survival benefits remain elusive. In fact, concerns arose due to increased systemic bleeding and a noticeable uptick in intracranial hemorrhages among STEMI patients aged over 75, prompting a re-evaluation of combined reperfusion's appropriateness involving IV GP IIb/IIIa inhibitors and a diminished dose of fibrinolysis. Currently, combining a full dose of fibrinolysis with low molecular weight heparin or a direct antithrombin appears promising, attributed to reduced reinfarction and recurrent ischemic episodes (Armstrong et al., 2003).

The timing of the intervention and patient selection are crucial to its success and safety (Bendary et al., 2017). Thus, although fibrinolytic therapy was linked to a notable decline in mortality, it quickly became evident that it had multiple restrictions. Data from the TIMI-9 registry revealed that 10.3% of patients had factors that exclude the use of thrombolysis. These contraindications encompassed previous episodes of stroke or transient ischemic attack, recent cardiopulmonary resuscitation, trauma, surgery, recent hemorrhage, sustained hypertension, and serious medical conditions (Kunadian & Gibson, 2010).

Coronary Artery Bypass Grafting (CABG)

Coronary artery bypass grafting (CABG) ranks among the most frequently used procedures to treat MI. Its role in treating MI has been recognized for many years, and extensive research showed the comparative advantages of CABG over alternative PCI in different clinical situations (Shi & Smith, 2018).

CABG is an invasive surgical strategy that involves grafting blood vessels taken from another part of the patient's body, usually the leg or chest, to reroute blood flow around blocked or narrowed coronary arteries (Thielmann et al., 2021). The main objective of this procedure is to ensure that the heart muscle receives an adequate blood supply, thereby alleviating symptoms such as chest pain and potentially preventing heart attacks (Thilak et al., 2021). The success of CABG lies in its ability to offer long-term relief to patients with multi-vessel coronary artery disease, particularly when compared to less invasive methods like PCI.

However, similar to other surgical procedures, CABG has a number of challenges and limitations. It requires a more extended recovery period compared to PCI. Furthermore, there are risks associated with the surgery itself, including bleeding, infections, and complications from

anesthesia. Over time, the grafts used in the procedure can become narrowed or blocked, necessitating further intervention. Moreover, not every patient with coronary artery disease is a suitable candidate for CABG, as individual health factors and the extent of arterial blockage play crucial roles in determining the best course of treatment (Bachar et al., 2023). Despite these limitations, CABG remains a vital tool in the arsenal of treatments available for MI, offering hope and improved quality of life for many patients.

2.2.2 Medications for MI

Various clinical studies have shown that medications can reduce the risk of death and other complications after MI. Specifically, long-term use of oral antithrombotic agents (including antiplatelet agents and oral anticoagulants), beta blockers, ACE inhibitors, and statins have shown positive results in these studies (E van der Elst et al., 2007).

Antiplatelet agents are pivotal in the management of MI. Their primary mechanism of action is the reduction of platelet aggregation, a process that can lead to clot formation in the coronary arteries. By doing so, these agents play a significant role in preventing the formation of these clots, and thereby, the recurrence of cardiac events post-MI. The positive effects of daily aspirin therapy in the initial five weeks following a MI are well-documented. Aspirin works by blocking the enzyme cyclooxygenase I in platelets, which reduces platelet aggregation at doses much lower than those needed for anti-inflammatory purposes. Even though aspirin is quickly removed from the body (with a plasma half-life of 30 minutes), doses starting at 75 mg can cause a lasting inhibition of cyclooxygenase I. This results in sustained antiplatelet effects for several days (Maxwell & Waring, 2000).

The use of antiplatelet agents still has limitations. First, chronic aspirin intake results in gastrointestinal toxicity with an increased risk of bleeding and ulceration. Second, they have certain contraindications, making them unsuitable for some patients (Maxwell & Waring, 2000). Beta-blockers in MI reduce the heart rate and the workload on the heart by saving the myocardium from further injury and preventing the onset of arrhythmias.

In individuals with AMI, the sympathetic nervous system typically activates due to chest pain, anxiety, and reduced cardiac function. This activation stimulates cardiac beta-1 adrenergic receptors, which leads to the raise in both the heart rate and the heart muscle's contractility. This subsequently elevates cardiac output and blood pressure. Also, extended activation can intensify myocardial ischemia by raising the heart's oxygen requirements and can also trigger ventricular arrhythmias. In this context, beta-blockers act to decrease heart rate, myocardial contractility, and high blood pressure, thus lowering the heart's oxygen needs. Additionally, they increase an oxygen supply to myocardium via enhanced coronary diastolic perfusion. Ventricular arrhythmias, both fatal and non-fatal, are potential complications in post-AMI heart. Beta-blockers act as class II antiarrhythmic agents, decreasing the heart response in the scarred myocardium post-infarction, mitigating the risk of serious ventricular arrhythmias after AMI (Joo, 2023).

Nevertheless, beta-blockers are not recommended for patients with specific respiratory conditions, and their administration can lead to side effects that necessitate close monitoring. Also for patients who don't have reduced ejection fraction or heart failure, the advantages and ideal length of beta-blocker treatment remain uncertain (Kezerashvili et al., 2012).

ACE Inhibitors are another class of medications frequently prescribed post-MI. Their mechanism of action involves vasodilation and a subsequent reduction in blood pressure which is crucial in preventing myocardial remodeling. Precisely, within the renin-angiotensin-aldosterone system, ACE facilitates the transformation of angiotensin I into angiotensin II. By acting as competitive inhibitors of ACE, ACE inhibitors hinder this conversion. As a result, the vasoconstrictive actions of angiotensin II are suppressed, leading to vessel dilation and reduced aldosterone release, which collectively lower blood pressure (Chen et al., 2018). For all STEMI cases, ACE inhibitors should be introduced within the first 24 hours, particularly for those with anterior MI, heart failure, or an LV ejection fraction (EF) not exceeding 40% (Goyal et al., 2023). Nevertheless, patients taking those medications might experience side effects such as a persistent cough, hyperkalemia angioedema, hypotension, which requires potential dose adjustments or medication changes (Ghouse et al., 2021 ; Kostis et al., 1996 ; Khera et al., 2021).

Finally, statins play an indispensable role in the post-MI medication regimen. Statins inhibit hydroxymethylglutaryl-CoA reductase and are recognized for their pleiotropic effects, including anti-inflammatory, antithrombotic, and antioxidant properties. As a result, they play a pivotal role in MI prevention. Research indicates that pre-treatment with statins can significantly decrease the incidence of MI (Han et al., 2018). In addition, statins play a role in stabilizing vascular structures, also resulting in decreasing risk of recurrence of cardiac events (Brooks et al., 2015). While statins undeniably benefit patients with MI, they can also induce side effects. The most well-documented adverse effects from both observational studies and clinical trials are a heightened risk of myopathy and a rise in diabetes incidence. Other side effects include hemorrhagic stroke, possibility to affect memory and cognition, as well as contribution to the development of cataracts (Pinal-Fernandez et al., 2018).

2.2.3 Heart Transplantation

Heart transplantation stands as the ultimate therapeutic solution for patients with end-stage heart failure post-MI (Perez-Villa et al., 2021). During the procedure an injured heart of the patient is removed and is being replaced with a healthy donor heart. It's typically reserved for patients who have exhausted all other therapeutic options and continue to experience debilitating symptoms or have a deteriorating heart function (Shah et al., 2019). The decision to proceed with a heart transplant is complex and is based on a comprehensive assessment by a multidisciplinary team. To be allowed for the transplantation a patient should be tested positively on several factors. These include the patient's overall health, age, and the presence of other complicating conditions. Once a patient is deemed suitable, they are placed on a waiting list, with priority determined by the severity of their condition and the likelihood of finding a matching donor (NHS, 2023)

The procedure itself is intricate, demanding significant expertise from the surgical team. While heart transplantation can provide an improved quality of life and extended survival, there are inherent limitations and challenges (Mehra et al., 2016). One of the foremost challenges is the scarcity of donor hearts, leading to prolonged waiting times. After the surgery, recipients must adhere to lifelong immunosuppressive medications to prevent transplant rejection, which comes with its own set of potential side effects. There's also the risk of surgical complications, graft failure, and other post-operative concerns (Hsich, 2016). In summary, while heart transplantation post-MI offers a new lease on life for many, it is a complex procedure with its own set of challenges and limitations.

Overall, the current treatment of MI is based on several basic therapies used in clinical practice and directed to reestablish blood flow to the affected heart muscle and prevent additional cardiac damage. Those therapies include coronary reperfusion therapy (such as percutaneous coronary intervention, fibrinolytic therapy and coronary artery bypass grafting), medications and heart transplantation (Raziyeva et al., 2020). However, all those strategies have limitations. Coronary reperfusion therapy is only intended to stop further tissue damage, however it doesn't recover an already injured area. The restrictions of the heart transplantation includes limited availability of an appropriate donor heart, price and immunocompatibility (Raziyeva et al., 2020).

2.3 Regenerative Medicine for the Treatment of Heart Failure

Traditional treatment strategies, such as medications and surgical interventions showed notable limitations in efficacy and long-term tissue recovery. These restrictions highlight an urgent need for innovative therapeutic solutions. Regenerative medicine is a rapidly evolving interdisciplinary field that combines engineering with life sciences to promote the recovery of damaged tissues and organs as well as reconstruction and substitution of the lost components of various organs, with the objective of closely replicating the original structure (Arjmand et al., 2021). This relatively young field has developed potential strategies targeting areas including wound healing and CVD treatment. Some of the strategies are now FDA-approved and commercially available (Mao & Mooney, 2015). Regenerative approaches are focused on tissue restoration and cellular rejuvenation, and aim to reduce the tissue damage post-MI. As the limitations of conventional treatments become increasingly evident, regenerative medicine emerges as a promising alternative option in MI therapeutic strategies (Gazit et al., 2019).

In general, regenerative medicine investigates the phenomenon of self-healing, wherein the human body exploits its natural mechanisms, occasionally with the assistance of exogenous biological substances, to regenerate cells and restore the integrity of tissues and organs. This field also includes tissue engineering, which uses the integration of scaffolds, cells, and physiologically active chemicals to create functional tissues. The phrases "tissue engineering" and "regenerative medicine" are frequently used interchangeably within the area, as there is a common focus on exploring curable approaches rather than conventional treatments for complex and frequently chronic disorders (Tissue Engineering and Regenerative Medicine, n.d.).

Regenerative medicine includes such therapies as cell therapy, where cells, most frequently stem cells are used to repair or replenish an injured tissue, gene therapy, where the genetic material is introducing or altering within the patient's cells to treat or prevent the disease, immunomodulatory therapy, where an inflammation is reduced due to immune modulations as well as the use of biologics and small molecules (Law et al., 2013; Arjmand et al., 2021; Muñoz et al., 2012). In tissue engineering, scaffolds are commonly utilized components. Those are biocompatible 3D structures that provide an environment for cell growth and tissue formation as well as sustained release of molecules ((Berillo et al., 2021; Smagul et al., 2020) (Fig.3).

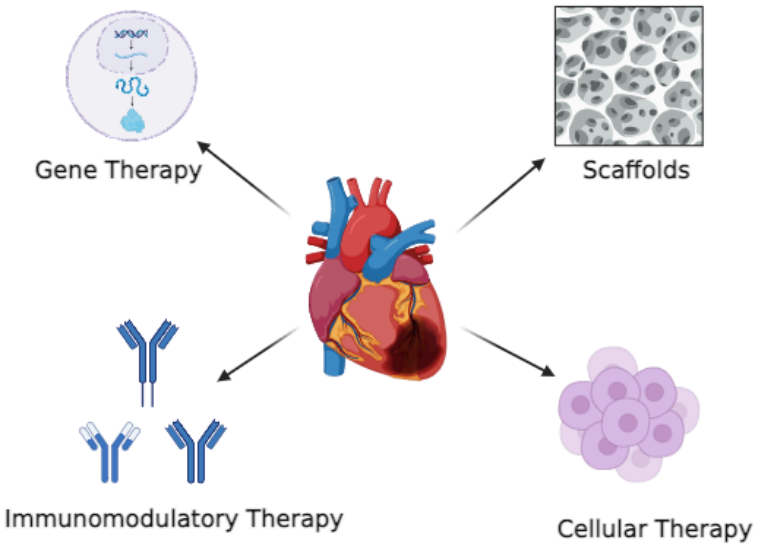

Figure 3. Regenerative medicine for MI treatment.

Overall, in order to achieve successful outcomes in regenerative medicine strategies, it is important that the materials used, mostly comprising combinations of scaffolds, growth factors,

and stem cells, have the capacity to effectively substitute the impaired tissue while also exhibiting the ability to emulate the functionality of the original tissue or facilitate its regeneration (Dzobo et al., 2018).

2.3.1 Stem Cell Therapy in Regenerative Medicine

Stem cells play a fundamental part in the formation of all tissues and organ systems inside the body, and they are involved in a wide range of functions related to disease progression, development, and tissue repair in the host organism. Stem cells can be classified into four categories based on their transdifferentiating potential, namely: unipotent, multipotent, pluripotent, and totipotent cells (Fortier, 2005). A zygote, which is the only totipotent stem cell found in the human organism, possesses the ability to generate an entire organism via transdifferentiation. Cells derived from the inner cell mass (ICM) of the embryo have pluripotent nature, meaning that they have the capacity to differentiate into cell types that represent the three germ layers, but are unable to differentiate into cells of the extraembryonic tissue (Mahla, 2016; Liu et al., 2019). Multipotent stem cells, such as hematopoietic stem cells (HSCs) have the ability to differentiate into various distinct cell types within a particular tissue. Unipotent cells have the capacity to develop exclusively into one specific cell type, such as cardiac-like cells found in myocardial tissue (Dulak et al., 2015). The potency and differentiation capacity of embryonic, extraembryonic, fetal, or adult stem cells are contingent upon the functional state of pluripotency factors such as OCT4, cMYC, KLF44, NANOG, SOX2, and other relevant proteins (Thomson et al., 2011). A separate type of stem cells are induced pluripotent stem (iPS) cells. Those are a category of pluripotent stem cells that originate from adult somatic cells. IPSCs undergo genetic reprogramming to reach a state similar to embryonic stem cells. This reprogramming is achieved by artificially inducing the expression of specific genes and factors that play a crucial role in preserving the characteristic features of embryonic stem cells (Ye et al., 2013).

In term of regenerative medicine stem cells can be classified into several categories, such as embryonic stem cells (ESCs), tissue-specific progenitor stem cells (TSPSCs), mesenchymal stem cells (MSCs), umbilical cord stem cells (UCSCs), bone marrow stem cells (BMSCs), and induced pluripotent stem cells (iPSCs) (Rajabzadeh et al., 2019). Cells can be transplanted either via autologous, allogeneic or syngeneic way. To avoid negative consequences of stem cell transplantation, such as host-versus-graft rejections, it is advisable to use tissue typing of human

leukocyte antigens (HLA) for tissue and organ transplantation, as well as the use of immunosuppressive agents (Petersdorf et al., 2007).

When considering the selection of suitable stem cells for their intended use of cardiovascular tissue regeneration and functional repair, several factors should be taken into account: The collection of sufficient stem cells, the effectiveness of ex vivo expansion, the most suitable method of administration, and the efficiency of in vitro differentiation and functional integration (Sun et al., 2014).

Moreover, there is a list of limitations that restrict the use of stem cell therapy in regenerative medicine to treat disorders including heart failures. Most important obstacles are listed further. First, there is tumorigenicity, which is the risk that injected stem cells might form teratomas or other types of tumors after transplantation. Stem cells share similar characteristics to cancer cells, including prolonged lifespan, resistance to programmed cell death, and the capacity for continuous proliferation over longer durations. Furthermore, stem cells and cancer cells share similar growth regulators and control mechanisms. Due to these factors, it's crucial to evaluate the potential oncogenic properties of these cells (Li et al., 2006).

The risk that transplanted cells would differentiate not into the desired cell type in-vivo is the next obstacle (Herberts et al., 2011). Further, immune rejection, when transplanted stem cells are recognized as foreign by the recipient's immune system, leading to graft rejection is also an issue to consider (Nussbaum et al., 2007). Other general qualms include the risk of low cell survival rate, meaning that once transplanted, there is a possibility for cells to die due to factors like lack of nutrients, inflammation, or immune response and bad integration with host tissue, meaning that transplanted cells may not integrate functionally and structurally with the patient's existing cells (Herberts et al., 2011). Apart from general limitations, there are also specific barriers of using stem cells in heart failure treatment. Those barriers include tissue targeting and timing of the therapy. In the first case, the direct cell injection into the myocardium often requires invasive procedure, while intravascular methods, such as intracoronary injections, are safer but pose challenges in accurately targeting the affected heart region. Timing of therapy, in turn, requires finding an optimal timing of stem cell injection post-MI (Tang et al., 2018).

Overall, stem cells therapy comprises one of the directions in regenerative medicine. It shows promising results in treating injured tissues including post-MI heart due to such features of stem cells as high multipotentiality, secretome and abilities to modulate and suppress immune

response (Smagul et al., 2020). Thus, stem cell therapy in MI promotes tissue regeneration by repairing and recovering the damaged heart tissue, reduces scar formation by limiting fibrosis and preserving heart muscle elasticity and function, improves heart function via enhancing cardiac function post-MI and reducing the risk of further heart failure (Fig.4). Moreover, stem cells possess the remarkable ability to undergo indefinite cell division and can differentiate into various cell types. Therefore, various stem cell types, each offering unique regenerative potentials, can be utilized in regenerative medicine for MI treatment. Consequently, they have emerged as a prominent source in the field of regenerative medicine, offering potential solutions for the repair of tissue and organ abnormalities resulting from genetic disorders, diseases, and the effects of aging (Mason & Dunnill, 2008).

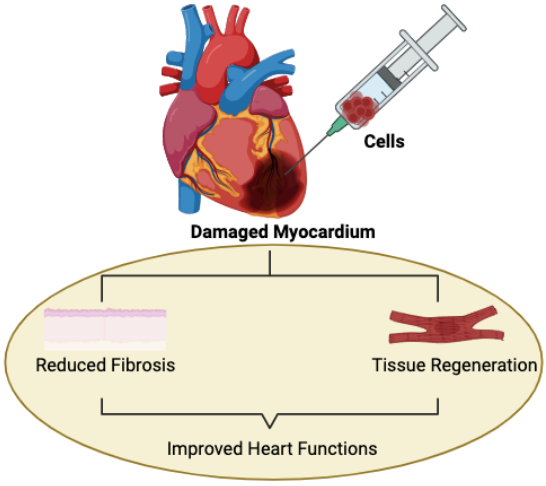

Figure 4. Cellular therapy in MI treatment.

2.3.2 Mesenchymal Stem Cells (MSCs) and Pre-differentiated Cells

Mesenchymal stem cells (MSCs) are bone marrow derived populations of non-hematopoietic cells with multipotent and self-renewal properties (Wei, 2020). They are characterized by the presence of specific cell surface markers, such as CD73, CD105, CD29, CD44, and CD90 and the absence of hematopoietic stem cells markers, including CD34 and CD45 (Madigan, 2018). MSCs are found in many tissues in the adult body including placenta, cord blood and adipose tissue; their isolation is relatively safe and with no ethical controversy. Therefore, MSCs are now considered as a potential target for stem cell therapy (Ying, 2014; Sid-Otmane, 2020). The beneficial impact of MSCs on myocardial tissue was shown in preclinical and clinical

studies (Squillaro, 2016). At such, there is now a growing number of recruiting and already completed clinical studies examining the effect of MSCs on acute myocardial infarcted heart, such as NCT04340609, NCT01394432, NCT00114452, NCT01392105 (*Safety and Efficacy of Intracoronary Adult Human Mesenchymal Stem Cells After Acute MI (SEED-MSC)*. (n.d.)). Results of those studies give a deeper understanding of the safety and efficacy issues associated with MSCs therapy.

There are direct and indirect mechanisms of cardiac tissue repair port-MI. The direct repair involves differentiation of MSCs into heart-specific cell types, whereas the indirect method involves angiogenesis, immunosuppression, inhibition of apoptosis and tissue fibrosis and activation of local immune and stem cells (Sid-Otmane, 2020). The indirect mechanism mainly involves paracrine factors. Nevertheless, pre-differentiated cells still exhibit characteristics similar to MSC including immune regulation, angiogenesis and functional repair.

One of the major impacts of MSCs on cardiac tissue repair is associated with autocrine, paracrine and endocrine factors, released by cells (Sid-Otmane, 2020) (Fig.5). Those factors are known to promote angiogenesis, prevent apoptosis, suppress an immune response and modulate fibrosis (Wei, 2020). For example, the culturing of MCP-1 injured adult rat cardiomyocytes in MSC-derived conditioned medium attenuated the damage caused by MCP-1, signifying the role of paracrine factors (Ohnishi, 2007). MSCs can regulate immune responses and avoid immune recognition (Fig.5). The precise mechanism is not clear yet, but it's assumed that the inflammatory microenvironment activates the processes. Thus, induced by the pro-inflammatory stimuli, such as IFN-gamma and TNF-α, MSCs can activate and recruit local immune cells, such as macrophages, neutrophils, dendritic cells, T cells, B cells, and natural killer (NK) cells as well as endogenous stem cells (Domenis, 2018). As such, MSCs can switch pro-inflammatory phenotypes of macrophages and dendritic cells toward anti-inflammatory via the suppression of immune activators, such as TNF-α, IL-6, IL-12, IL-1β, IL-23 and IL-12 and upregulation of IL-10 (Favaro, 2015; Selleri et al., 2016). They also modulate immune responses through regulation of T cell activity. In this case, MSCs may either directly activate Tr1 and Treg cells or suppress proinflammatory T cells subsets through EPHB2/ephrinB1 interaction, which was shown to inhibit the expression of TNF-α, IL-2 and IL-17 (Lianga et al., 2017; Nguyen et al., 2013).

Paracrine factors released from MSCs are also responsible for anti-fibrotic effects via the regulation of cardiac fibroblasts proliferation and collagen deposition . Thus, the proliferation of cardiac fibroblasts cultured in MSC-conditioned medium significantly decreased compared with CFB-conditioned medium. This is due to the upregulation of antiproliferation-related genes caused by MSC-conditioned medium. Moreover, the MSC-conditioned medium significantly downregulated the expression of type I and III collagen (Ohnishi et al., 2007).

MSCs promote neovascularization of damaged vessels through the secretion of various proangiogenic factors such as VEGF, bFGF, HGF, and angiopoietins (Matsushita, 2020). Moreover, VEGF, HGF and IGF released from MSCs reduce apoptosis and induce increased proliferation of cardiomyocytes ((Zhao et al., 2016; Burdick & Vunjak-Novakovic, 2009).

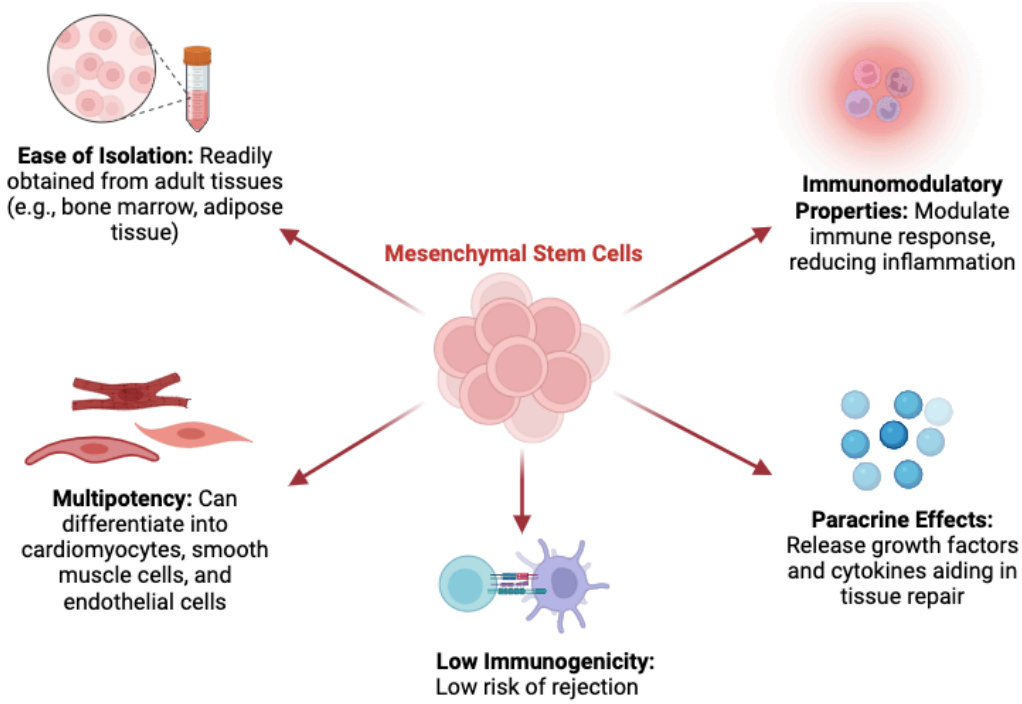

Figure 5. Advantages of utilizing MSCs in regenerative medicine.

MSCs can directly differentiate into subtypes of cells found in myocardium, as well as release paracrine factors leading to the reduced apoptosis, decreased fibrosis, neovascularization and suppression of immune response. Together with such advantages of MSCs as an ease of isolation from various tissues and immune tolerance, they become a highly prospective therapeutic option in regenerative medicine to eliminate negative consequences of MI.

However, when transplanted into the infarcted heart, stem cells are faced with a harsh environment, and this can result in a low engraftment and survival rates as well as weak proliferation of cells (Zhao et al., 2018). Other limitations include uncontrolled differentiation, when MSCs once injected into the heart environment may differentiate into the cell type not native to the tissue and limited direct cardiac repair, when MSCs do not directly transform into fully functional cardiomyocytes. This unpredictability in differentiation reduces the overall beneficial effect of MSC therapy in cardiac tissue repair (Fig.6).

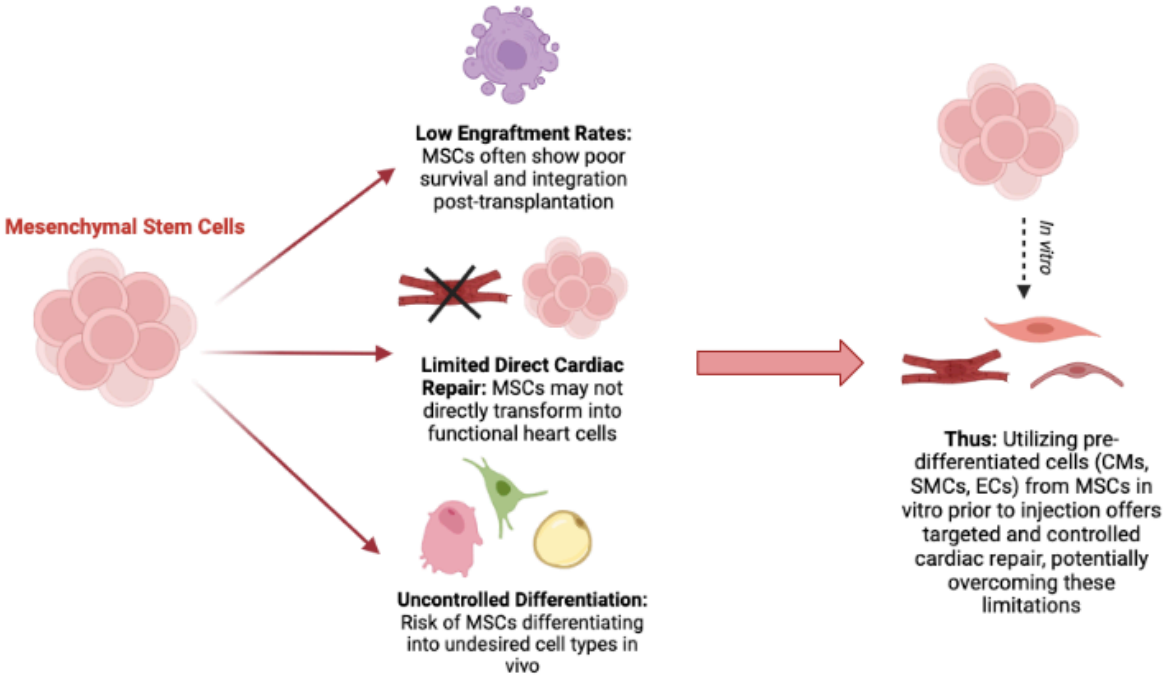

Figure 6. Limitations potential solutions of using MSCs in cardiac regeneration.

One way to eliminate such restrictions is to precondition MSCs *in vitro* prior transplantation into the heart. Several strategies to precondition cells are now applied, including heat shock, hypoxia, genetic modification, pre-treatment with chemical substances, and physical stimulation. An alternative approach involves the use of cells after the administration of cytokines and growth factors, which would create an optimal environment with decreased toxicity and harshness. In addition, various *in vivo* studies have proven engraftment and differentiation of stem cells into CM, ECs and SMCs after MI (Rigol et al., 2013). For example, intramyocardial transplantation of hBMSCs after MI resulted in enhanced engraftment and differentiation of cells into cardiomyocytes, endothelial and smooth muscle cells (Yoon, 2005). Finally, MSCs can be pre-

differentiated into heart cell types to further enhance their engraftment, stimulate angiogenesis and replenish the pool of lost or damaged cells (Kahn-Krell et al., 2022; Pittenger et al., 1999) (Fig.6).

2.4 MSC Differentiation

2.4.1 MSC Differentiation Toward Cardiomyocytes

Cardiomyocytes and their role in heart functions

The heart is the first organ that develops during embryonic growth. Throughout the process of fetal and postnatal development, cardiomyocytes undergo terminal differentiation, transforming into muscle cells. They interact with each other in a linear manner providing coordinated contractile activity. The contraction and relaxation process of cardiomyocytes is regulated by periodic changes in intracellular calcium levels, which are triggered by the depolarization of the sarcolemma and maintained through the release and reuptake of calcium by the sarcoplasmic reticulum. In both in vivo and in vitro models, cardiomyocytes when in stress show hypertrophic growth and apoptotic responses that eventually lead to heart failure (Woodcock & Matkovich, 2005).

The definition and description of cardiomyocytes can vary based on the specific field of study. From a histological point of view, the myocardium primarily consists of cardiomyocytes, which display centrally located nuclei, regular cross striations, and a dense capillary network in close proximity, reflecting their high requirement for oxygen (Maxwell, 1994). According to cell biology, a cardiomyocyte can be defined as a cardiac cell that exhibits contractile and excitable properties. It possesses a centrally located nucleus and expresses distinct sarcomeric protein isoforms, which serve as distinguishing features from other types of muscle cells. In addition, cardiomyocytes demonstrate rhythmic contraction without experiencing periods of rest (Cell Biology, 2017). From a cardiology view, the cardiomyocyte is the cellular component that controls the contraction of the heart. This process is assisted by a complex network of contractile proteins and ion transporters, which enable the cardiomyocyte to effectively carry out the contraction-relaxation cycle (Zipes, 2018). Overall, a cardiomyocyte can be characterized as a myocyte that performs several key functions: 1) they are located in myocardium, 2) they facilitate the contraction of the heart, 3) they develop from myoblasts, 4) possess centrally located nucleus, 5) they are smaller compared to skeletal myocytes and 6) finally, they have abundant sarcoplasm (Keepers et al., 2020).

In conclusion, cardiomyocytes are the key players in the myocardium. They possess unique structural, electrophysiological, and physiological properties as well as regulate coordinated contraction and relaxation cycles in the heart, enabling the effective circulation of blood.

Potential benefits of using MSC-derived cardiomyocytes in MI repair

Again, cardiomyocytes are the main players in myocardium, which are responsible for the construction of the heart and the maintenance of cardiac function. Their loss during infarction creates a significant gap that current therapeutic interventions still cannot fully fill. The difficulty in sourcing cardiomyocytes for cardiac repair stimulated research groups all over the world to search for alternative methods, such as using stem cell reprogramming into cardiomyocytes (Lin & Pu, 2014). MSCs have demonstrated their suitability as a promising choice for the generation of cardiomyocytes. Apart from protecting the myocardium by reducing inflammation levels and promoting the differentiation of local myocardial cells around infarct areas, MSCs are also comparatively more accessible than other stem cell types (Guo et al., 2020).

Human perivascular stem cells were shown to improve cardiac functions after the MI through multiple cardioprotective mechanisms. The treatment of the MI mice model resulted in the formation of new vessels, reversion of ventricular remodeling, shortening of the scar size and reduction of chronic inflammation (Chen et al., 2013). Another study demonstrated that combination of direct myocardial injection of cardiomyocytes from human induced pluripotent stem cells and cardiac patches implanted directly to left ventricular space contributed to synergetic effect, regeneration of post-MI tissue, enhanced angiogenesis and anti-fibrotic actions (Soon-Jung et al., 2019).

Cardiomyocytes, pre-differentiated from stem cells, are also utilized in clinical trials for the treatment of MI. Thus, a recent study (ClinicalTrials.gov ID - NCT05068674), registered in Stanford Hospital uses human embryonic stem cells derived cardiomyocytes to improve heart survival and functionalities in patients with chronic left ventricular dysfunction secondary to MI (Pilot Study of Human Embryonic Stem Cell-Derived Cardiomyocytes in PaTients With ChrOnic Ischemic Left VentRicular Dysfunction (HECTOR), n.d.). The study is currently in the first phase of clinical trials.

Differentiation of MSCs into cardiomyocyte-like cells

MSCs show significant promise as an alternative option for cell-based therapeutics, offering a more favorable approach compared to existing invasive methodologies. MSCs can undergo differentiation into several mesenchymal lineages, including cardiac cell types. Yet the goal of complete differentiation into fully functional cardiac cells has not been achieved so far (Szaraz et al., 2017).

Three phases determine stem cell differentiation into cardiomyocytes (Raziyeva et al., 2020). First, stem cells are differentiated into cardiac mesoderm under the exposure of Activin A, BMP 4, FGF2, VEGF, and Wnt/β-catenin (Yassa et al., 2018). Second, cardiac mesoderm is introduced to DKK1 and Activin/Nodal and becomes cardiac progenitors (Jiang & Lian, 2020). Finally, HGF, PGF, Neuregulin-1, Notch-1 and Wnt/β-catenin factors regulate cardiac progenitors differentiation and proliferation into fully activated cardiomyocytes (Farzaneh et al., 2019). Various signaling pathways are involved in the process of differentiation and proliferation. For example, the PI3K pathway is activated by FGF and promotes cardiac maturation, while the Akt pathway is regulated by PGF and is crucial for cell proliferation (Hodgkinson et al., 2016; Guo et al., 2018). Differentiated cardiomyocytes can be characterized by the specific markers, such as NKX2.5, Mef2c and GATA4 which appear first and cTnT, MYH6 and Cx43, that are found in mature cells (Szaraz et al., 2017). There are several ways to induce cardiac reprogramming, including genetic modification, electrical stimulation and direct introduction of modulating factors (Raziyeva et al., 2020). Chemicals such as 5-Azacytidine (5-aza) are also widely utilized as agents for inducing cardiac reprogramming (Guo et al., 2018). One study showed that treatment of MSCs with 5-Azacytidine for 3 weeks led to the formation of beating cardiomyocyte-like cells (Lee et al., 2009). Another study demonstrated that the differentiation potential of rat BMMSCs into cardiomyocyte-like cells was enhanced by a combined treatment of low doses of TGF-β1 and 5-AZA, evidenced by increased cell markers and reduced apoptosis compared to individual treatments. Also, the combined treatment stimulated an expression of troponin I, α-actin, and p-ErK1/2, suggesting the role of p-ErK1/2 in the differentiation process (Shi et al., 2016). In addition, incubation of MSCs in cardiac conditioned medium for hypoxic preconditioning resulted in the differentiation into myocardial-like cells (Xie et al., 2006). Finally, stimulation with ascorbic acid facilitated ES cells differentiation toward cardiac cells (Takahashi et al., 2003).

2.4.2 Smooth Muscle Cells (SMCs) Derived from MSCs

Role of SMCs in heart health and function

Smooth muscle cells (SMCs) are often found in the tunica media of blood vessels, where they are primarily involved in regulating vascular contraction and producing the extracellular matrix (ECM). SMCs also have a notable impact on the obedience and elastic rebound of the artery in response to the hemodynamic situation. Nevertheless, in the presence of damaged or stressful conditions, SMCs may undergo a transition in phenotype, shifting from a contractile state to a synthetic state and transforming into other cell types. This phenotypic switching can have either beneficial or negative implications for the progression of diseases. In addition, multiple studies have shown that alterations in the functionality of SMCs play a significant role in the development and progression of many cardiovascular disorders, including MI (Zhuge et al., 2020).

Thus, one of the recent studies investigated the transcriptome alterations in aortic vascular SMCs (VSMCs) in MI patients. Study group obtained results using laser capture microdissection (LCM) from patients diagnosed with and without MI. Gene expression analysis revealed the identification of a novel 21 genes classifier associated with SMCs. This classifier has demonstrated the ability to differentiate the response of SMCs to MI at the level of gene expression. Patients with acute MI exhibited upregulation of genes associated with VSMCs, such as ATP1A2, MYOCD, and SOD1 (Wongsurawat et al., 2018). Another study identified that the hypoxia signals played a significant role in the activation of SMCs in MI patients. Study group observed an upregulation of HIF-1A, UBE2, and CREB1 genes which are associated with the hypoxia signaling pathway (Russo et al., 2006). In addition, a study conducted by Guohong Ye and colleagues discovered that in hypoxia state VSMCs release bFGF into the surrounding environment, followed by the activation of the PI3K/AKT signaling pathway via the binding to the FGFR1 present in cardiomyocytes. This activation, in turn, attenuates the processes of apoptosis and autophagy in myocardial ischemia/reperfusion injury (Ye et al., 2018).

Potential advantages of utilizing MSC-derived SMCs in post-MI vascular repair

The differentiation of MSCs into SMCs has gained significant attention in the field of regenerative medicine, because MSCs are a more accessible cell source for differentiation into vascular cells compared to other stem cell types. Differentiation process is orchestrated by various factors, including microRNAs, making resultant SMCs suitable candidates for vascular tissue

grafts (Gu et al., 2018). Various studies that investigated smooth muscle differentiation from MSCs revealed the importance of MSC-derived SMCs in vascular health, due to their potential to contribute to vascular repair and atherosclerosis alleviation (Hegner et al., 2005).

One study investigated the effectiveness of a VSMC sheet in treating a rat MI model. The SMC-Tx group showed significant improvements in cardiac function, decreased left ventricular dilation and reduced fibrosis. In vitro experiments showed enhanced production of bFGF and less apoptotic cell death under hypoxia in the SMC-Tx group. Obtained results suggested that SMC sheet transplantation inhibited cardiac remodeling progression and improved cardiac function, possibly due to superior SMC survival (Harada et al., 2016). Another research focused on the restoration of viable muscle after MI via the cell transplantation. For this, a group injected various cell types, namely skeletal myoblasts, bone marrow stromal/stem cells and SMC and compared their impact on myocardial regeneration. Overall all cells showed hypoxic survival, VEGF expression and improved vasculogenesis after transplantation, proving an important role of SMC in heart regeneration (Kan et al., 2010). Additionally, Kawamura, M. et al, used rat bone marrow to isolate and reprogram MSCs into SMCs and covered them with endothelial progenitor cell (EPC) to create a bi-level cell sheets. The use of those SMC-EPC engineered sheets in the treatment of DMCM showed the preservation of cardiac function and prevention of unfavorable ventricular remodeling as evidenced by echocardiography and cardiac magnetic resonance imaging conducted 8 weeks after the induction of DMCM. Results of myocardial contrast echocardiography indicated that the treatment group exhibited intact myocardial perfusion and microvascular function in comparison to the control group. Finally, the histological analysis revealed a reduction in interstitial fibrosis and an increase in microvascular density in the group treated with SMC-EPC cell sheets (Kawamura et al., 2017).

Differentiation of MSCs into SMCs

MSCs are widely used in the field of vascular graft engineering, making them the most intensively studied among the different types of stem cells available for this application. MSCs are found in several types of tissue in adults or perinatal bodies, including bone marrow, adipose tissue and Wharton's jelly obtained from the umbilical cord. Due to their rapid proliferation rate, multipotency, and immunomodulatory features, MSCs now exhibit a strong potential as a viable candidate for vascular tissue engineering (Dan et al., 2015). In humans, hES-MCs (human

embryonic stem cell-derived mesenchymal cells) are the natural source of mesoderm-derived SMC progenitors (Boyd et al., 2009). hES-MCs can be naturally reprogrammed to differentiate into osteocytes, chondrocytes, and SMCs, where the differentiation into SMCs is stimulated by the TGF-β1 induction (Guo et al., 2013).

Overall, SMC differentiation is a complex process influenced by various factors, including growth factors, such as TGF-β and PDGF, signaling pathways, such as ECM-integrin signaling, retinoid signaling and Nox4-ROS signaling, microRNAs and epigenetic regulations (Shi & Chen, 2015). In vitro models provide valuable tools to understand the molecular mechanisms of SMC differentiation, which is crucial for developing strategies to prevent and attenuate heart failures. For example, serum response element (SRF), a transcription factor that regulates cardiac and skeletal development, plays a significant role in SMC differentiation (Sun et al., 2005). Myocardin and myocardin-related transcription factors A and B are also involved in SMC maturation (Pipes et al., 2006). MiR-503 and miR- 222-5p were identified to play the key role in SMC differentiation from MSC. Thus, miR-503 activates TGF-β1-mediated signaling pathways by directly targeting SMAD7. In addition miR-503 were shown to be associated with SMAD4, which is also a mediator of TGF-β signal transduction. In turn, miR-222-5p suppress an expression of ROCK2 and αSMA leading to the inhibition of SMC differentiation (Gu et al., 2018). Also, an activation of TGF-β1 stimulates the expression of specific smooth muscle genes in MSC. In detail, activated TGF-β1 induces an enhanced production of Notch ligand Jagged 1 (JAG1), leading to Notch activation and an expression of smooth muscle markers in MSC (Kurpinski et al., 2010).

Another key player in SMC differentiation is PDGF-B. Thus, a recent study showed that the cultivation of MSC for 4 days in media enriched with PDGF and TGFβ1 significantly increased the expression of SMC-specific markers and decreased MSC markers in comparison to the control media (Sivaraman et al., 2021). PDGF-B interacts with neuropilin-1 (NRP-1) in MSCs and by this regulates the differentiation and recruitment process in cells (Dhar et al., 2010).

2.4.3 Endothelial Cells (ECs) Derived from MSCs

Introduction to ECs and their significance in vascular systems

Blood vessels are composed of three layers. The innermost layer, known as the intima layer, consists of endothelial cells (EC). The middle layer, referred to as the media layer, is composed of SMCs. The outermost layer, called the adventitia, is composed of fibroblasts and extracellular

matrix (ECM) components. EC here are typically identified by the presence of VE-cadherin, CD31 (PECAM1), and vascular endothelial growth factor receptor 2 (VEGFR2). Additionally, they possess the ability to internalize acetylated low-density lipoproteins (ac-LDL), generate tubular structures in Matrigel, and secrete nitric oxide (Dan et al., 2015).

Five types of ECs are found in the heart, namely endocardial, coronary arterial, venous, capillary, and lymphatic, and each of them have their unique phenotype. For instance, coronary ECs are responsible for the development of a vascular network within the myocardium, whereas endocardial ECs contribute to the formation of a large epithelial sheet without exhibiting angiogenic sprouting into the heart. The coronary arteries, veins, capillaries, and lymphatic vessels do not exhibit fusion with the endocardium or have a direct contact with the heart chamber (Ishii et al., 2008).

MSC differentiation pathway to Endothelial cells

Autologous ECs in the human body can be isolated from adipose tissue. However, those isolated primary cells have restrictions in the form of limited proliferation potential when cultured in vitro (Zhang et al., 2021). In this scenario MSC emerges as the optimal candidate for EC differentiation. One important benefit of direct cell-based therapy is that endothelial cells, differentiated from MCSs, can directly participate in angiogenesis and subsequent blood floor restoration. Another approach involving vascular cell types is the use of bioengineered vessels for grafting, which typically consist of 3 components, namely cells, scaffold and mechanical signal (Naito et al., 2011).

The differentiation of stem cells into ECs and its subsequent injection into the myocardium contributes to repaired infarcted tissues as a result of the neo-angiogenesis and secreted paracrine factors (Funakoshi et al., 2016). The differentiation is regulated by factors that are similar to those responsible for cardiac differentiation, such as BMP-4, Activin A, VEGF and bFGF. This is because cardiac and endothelial cells share the similar signaling pathway in cardiogenic or hemogenic mesoderm (Jiang, 2020).

For example, one of the mechanisms by which VEGF induces differentiation in MSC is via stimulation of AT1R and AT2R expression and cellular localization (Ikhapoh et al., 2015). Also, the relationship between VEGF-165—VEGFR-2—Sox18 is critical for MSC differentiation into EC, as VEGF-165 stimulates Sox18 production, which in turn, enhances the expression of VEGFR-

2 in MSC. Furthermore, a knockdown of VEGFR-2 was shown to inhibit VEGF-165-mediated activation of Sox18 and subsequent EC differentiation (Ikhapoh et al., 2015). In addition, knockdown of Smad3 results in reduced VEGF production and hindered differentiation at both the early and late stages. Finally, a decreased amount of Smad1/5/8 phosphorylation has a beneficial impact on differentiation, and the effects of R-Smad are partially mediated by VEGF (Ai et al., 2015).

Thus, MSC were cultured in a medium enriched with VEGF, bFGF, IGF, EGF, ascorbic acid, and heparin. After 7 days of cultivation, the amount of CD31+ and CD34+ cells increased to 40%, with subsequent increase to 60% by day 14 (Wang et al., 2018). In vivo study in a canine chronic ischemia model showed that MSC, injected and differentiated into endothelial cells significantly enhanced vascularity and myocardial activity (Silva et al., 2005).

2.4.4 Challenges and Considerations in Using Cells Differentiated from MSCs

One of the limitations of using pre-differentiated cells in stem cell therapy is the heterogeneity in effectiveness and robustness of differentiation techniques.

For example, the heart is composed of a heterogeneous population of cells, including cardiomyocytes, cardiac fibroblasts, and endothelial cells. There are differentiation techniques available for the generation of cardiomyocytes and endothelial cells, however similar protocols are currently lacking for cardiac fibroblasts. Several investigations have achieved the generation of fibroblast-like cells that accurately replicate the appearance of cardiac fibroblasts. Nonetheless, the absence of distinct cell type markers exclusive to cardiac fibroblasts, other from the myofibroblast and mesenchymal genes that are shared throughout all fibroblast cell types, poses a challenge in assessing the effectiveness of differentiation regimens (Sharma et al., 2017). Moreover, variability in differentiation methods is observed even in cells with well-defined markers, such as cardiomyocytes and endothelial cells (Burridge et al., 2014). A contributing factor to this phenomenon is the continual improvement of protocols within the research field, which sometimes leads to a slower adoption of new protocols across various researchers. However, the ongoing enhancement of current protocols and the development of well-established protocols for cellular differentiation into new cell types will enhance the potential of stem cells in the field of regenerative medicine (Wnorowski et al., 2019).

Next limitation comes when stem cells differentiate into the specific cell type. The challenge lies in ensuring that these cells achieve a required adult phenotype that accurately reflects the characteristics of the damaged organ (Scott et al., 2013). A number of studies are currently involved in the development of various techniques focused on increasing the maturity of cardiomyocytes. These methods include electrical or mechanical stimulation, geometrical confinement, overexpression of maturation-related microRNAs, introduction of growth hormone, and prolonging the culture time (Kuppusamy et al., 2015). Recent studies showed that electrical stimulation of early stage iPSC-cardiomyocyte-derived tissue can lead to advanced maturation of 3D cardiac tissues (Ronaldson-Bouchard et al., 2018). Additionally, findings suggested that the implementation of moderate afterloads could significantly improve the development of hiPSC-CMs in engineered heart tissues. Conversely, high afterload conditions could mimic key characteristics of cardiac disease in humans that arise from increased mechanical strain (Leonard et al., 2018).

Another issue is the isolation of specific subtypes of cells. For example, cardiomyocytes have multiple subtypes, including atrial, ventricular, and nodal, and existing methods of differentiation commonly generate a combination of these three subtypes. Although there are protocols available to generate individual cell subtypes, it is more typical to find protocols that yield a heterogeneous population (Lee et al., 2017).

2.5 Introduction to Biomaterials: Definition, Properties and Applications

A biomaterial is either naturally derived or synthesized substance that is designed to interact with biological systems for therapeutics or diagnostic purposes (Biomaterials, n.d.). Currently biomaterials are extensively utilized in a broad array of applications in medicine, science, and bioengineering. In medicine, biomaterials are used to design medical implants, such as heart valves, stents, grafts, artificial joints, ligaments, tendons, hearing loss implants, dental implants, and nerve stimulation devices. In medicine, apart from implants, they are used for the healing of biological tissues via the use of sutures, clips, staples for wound closure, and dissolvable dressings. In addition, biomaterials applied for tissue regeneration purposes, where scaffolds are loaded with cells and various agents to engineer tissues, such as bone regenerating hydrogels or artificially grown human bladders. Furthermore, biomaterials, such as molecular probes and nanoparticles that are able to break through biological barriers, are employed for diagnostic purposes, such as for

example cancer imaging and therapy. Biosensors, which are designed to detect and transmit data regarding specific substances, are another application of biomaterials. Lastly, there are drug-delivery systems, also composed of biomaterials, that transport and administer various drugs or other biological agents to targeted disease sites. For example, such systems can deliver anti-inflammatory agents to specific cells, tissues and organs hence enhancing drug delivery efficiency and anti-inflammatory effectiveness, while avoiding toxicity issues (Tu et al., 2022). Through these diverse applications, biomaterials significantly contribute to advancements in the medical and bioengineering fields (Biomaterials, n.d.).

There are several features that are crucial for biomaterials, including biocompatibility, biodegradability, mechanical properties and bioactivity. Biocompatibility is the ability of biomaterials to perform their functions without inducing toxic effects while producing a suitable response in the host environment (Huzum et al., 2021). Such a feature not only depends on biomaterials themselves but extends to the interaction between biomaterials and the host system (Cacopardo, 2022). Various factors influence biocompatibility, including the physical, chemical, and biological properties of the material. For instance, the surface texture, chemistry, and mechanical properties of a material can significantly impact its interaction with the surrounding tissues and cells. Moreover, the environmental conditions at the site of administration, such as temperature, pH and mechanical stresses also affect biocompatibility. Overall, the assessment of biocompatibility before its approval for clinical use is crucial to ensure its reliability and safety in the host system. This means that it is essential to test that the biomaterial does not induce toxicity, inflammation, or other undesirable responses as well as to evaluate how the biomaterial behaves under various physiological conditions (Marin et al., 2020; Ghasemi-Mobarakeh et al., 2019).

Another important feature of biomaterials is biodegradability, which is the ability of a material to degrade into simple components under physiological conditions (Pires et al., 2022). Upon degradation, the biomaterial breaks down into non-toxic products that can either be absorbed or excreted by the body, ensuring safety and minimizing any adverse reactions. Biodegradation of material depends on various factors, including composition of material as well as morphology, structure, chemical and radiation treatments and molecular weight (Samir et al., 2022). Thus, each class of biomaterials has distinct degradation pathways influenced by environmental conditions inside the body (Hynes et al., 2023). Furthermore, the design of such biomaterials, in particular injectable ones, often means the use of natural or synthetic polymers. The biodegradation of such

materials is an essential attribute that influences their effectiveness in cardiac tissue engineering (Reis et al., 2014).

Biomaterials possess several characteristic features that make them similar to the microenvironment of natural extracellular matrices and therefore promote cell survival. Those features include molecular compatibility, porosity and mechanical strength (Burdick & Vunjak-Novakovic, 2009). Modern biomaterials in a form of 3D scaffolds are created in such a way to control functions and interactions of loaded cells via the bioactive components as well as physical and chemical signals presented in them. Thus, the biochemical and biophysical stem-cell–matrix interactions regulate the release of specific paracrine factors and the lineage-specific differentiation and proliferation of cells (Lutolf et al., 2009).

2.5.1 Types of Biomaterials

There are 2 major types of biomaterials based on their nature: natural, such as collagen, hyaluronic acid, gelatin, laminin and fiber and synthetic, including polymers, ceramics and metals (53,7). Among all, the most commonly used biomaterials formulations are polymeric micro- and nanospheres, nanoparticles (NPs), nanofibrous structures, coacervates, hydrogels, cryogels, and scaffolds (Smagul et al., 2020) (Fig.7).

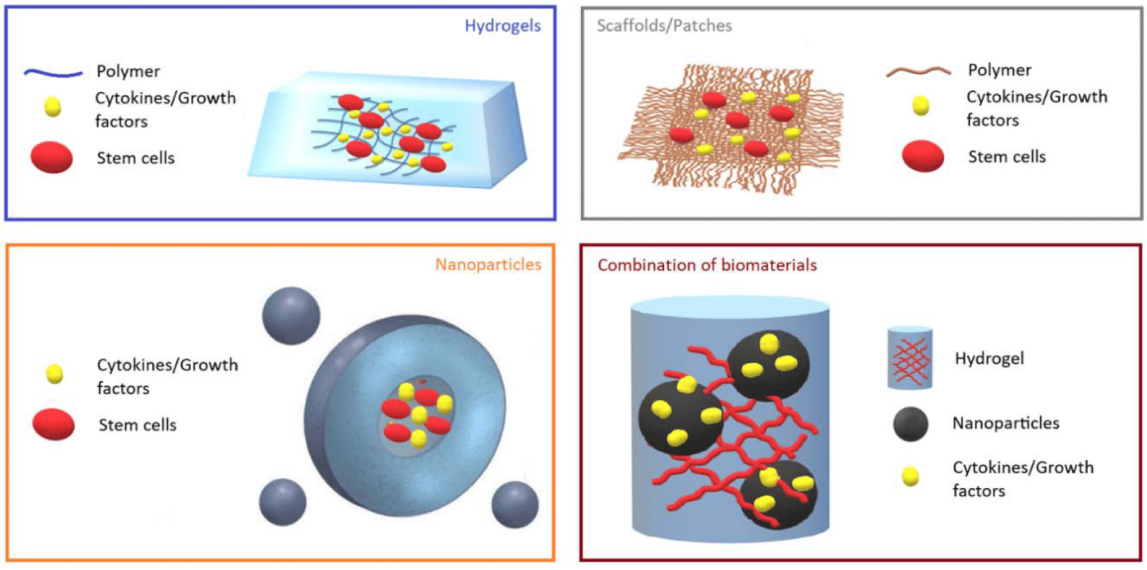

Figure 7. Types of biomaterials (Smagul et al., 2020).

Hydrogels that are composed of water and a cross-linked polymer are extensively used in cardiovascular studies (Li & Mooney, 2016). For example pre-clinical studies have investigated the use of hydrogels composed of cardiac extracellular matrix (ECM), alginate, hyaluronic acid (HA), natural biomaterials such as collagen, fibrin, and heparin, as well as synthetic polymers and microparticles, for the purpose of heart repair (Carlini et al., 2019). Hydrogel treatment has been found to produce multiple effects on post-MI heart, such as direct mechanical reinforcement, improved angiogenesis and myocardial tissue regeneration, decreased apoptosis and scar size as well as better recovery of heart function (Blackburn et al., 2015). Furthermore, some studies demonstrated that the use of hydrogels on their own had a positive impact on cells, such as macrophages, cardiomyocytes, fibroblasts, and endothelial cells in the post-MI environment (Lister et al., 2016).

Apart from naturally derived hydrogels, synthetic or hybrid ones are also utilized in the regenerative industry. Thus, the study conducted by Rufaihah and colleagues showed that the utilization of a synthetic glycosaminoglycan mimetic peptide nanofiber facilitated the process of angiogenesis and cardiomyocyte development in rats (Rufaihah et al., 2017). Another group developed a novel injectable hybrid hydrogel for cardiac tissue engineering from a temperature-responsive poly(N-isopropylacrylamide) and gelatin. The results showed that the hydrogel supported a high degree of survival for both cardiomyocytes and cardiac fibroblasts and promoted increased cytoskeletal organization in injured myocardium (Navaei et al., 2016). In addition to hydrogels, nanoscale carriers are also utilized for the heart tissue healing after MI. The desirable characteristics of nanoparticles (NPs) such as targeted administration, protein stability preservation, prolonged presence in the circulatory system and controlled release of loaded therapeutics contribute to their potential as carriers in cardiac therapy (Ho et al., 2016). Another type of biomaterials is cardiac patches that are directly administered into the myocardium. The efficacy of an acellular epicardial patch, derived from hydrogel, was demonstrated in its ability to reduce left ventricular remodeling and enhance cardiac function in rat models of acute and subacute MI (Lin et al., 2019).

The use of biomaterials in the field of regenerative medicine is currently undergoing rapid development as a novel strategy for the treatment of cardiac failures, including MI, where they are used as vehicles for a targeted and specific delivery of drugs and other agents to injured myocardium for anti-fibrotic, anti-inflammatory, pro-angiogenic and cardiac restoration purposes

(Domenech et al., 2016; Ashtari et al., 2019; Saghazadeh et al., 2018). They possess therapeutic effects when used alone as well as when combined with various biological agents, including factors, mediators and cells (Saludas et al., 2017). The regenerative effect exhibited by biomaterials, not loaded with any agents, on myocardial tissue can be explained by their ability to mimic the extracellular matrix (ECM) and provide direct mechanical support (Mihic et al., 2015). Additionally, biomaterials have the potential to enhance electrical conductance within a fibrotic scar region, a factor crucial for the normal operation of the heart (Wang et al., 2018).

Biomaterials for Drug Delivery and Release

The incorporation of biomaterials with biological agents such as cells, growth factors and cytokines significantly enhance the efficacy of the treatment compared to the administration of these agents alone. First, one of the primary advantages of using biomaterials is the delivery of agents to a specific zone of interest. Thus, biomaterials can direct the delivery of cells, growth factors, and cytokines to specific tissues or organs, which is a significant advantage over systemic delivery that distributes these agents throughout the body enhancing the risk of toxicity, allergy or decreased efficacy due to the reduced dose of therapeutics reaching the injured area (Gaharwar et al., 2020). Second, biomaterials provide a conducive environment for biological agents. For example, scaffolds enhance a cell's survival and engraftment in harsh post-MI environments by providing mechanical support and modulating host cell recruitment, which is crucial for tissue regeneration (Cho et al., 2018; Bertsch et al., 2022). Third, biomaterials provide a controlled and sustained release of attached growth factors and cytokines, which allows to avoid repeated injection of therapeutics. This also helps to control the dose of released therapeutics to reduce the chance of overdose (Dormont et al., 2018). Fourth, biomaterials can protect administered therapeutics from premature degradation, thereby preserving their bioactivity (Hussey et al., 2018). Overall, biomaterials possess the potential to serve as a successful carrier for the controlled and prolonged administration of growth factors and cytokines in order to reduce inflammation, enhance angiogenesis, diminish fibrosis, and facilitate the development of healthy heart tissue (Fig.8).

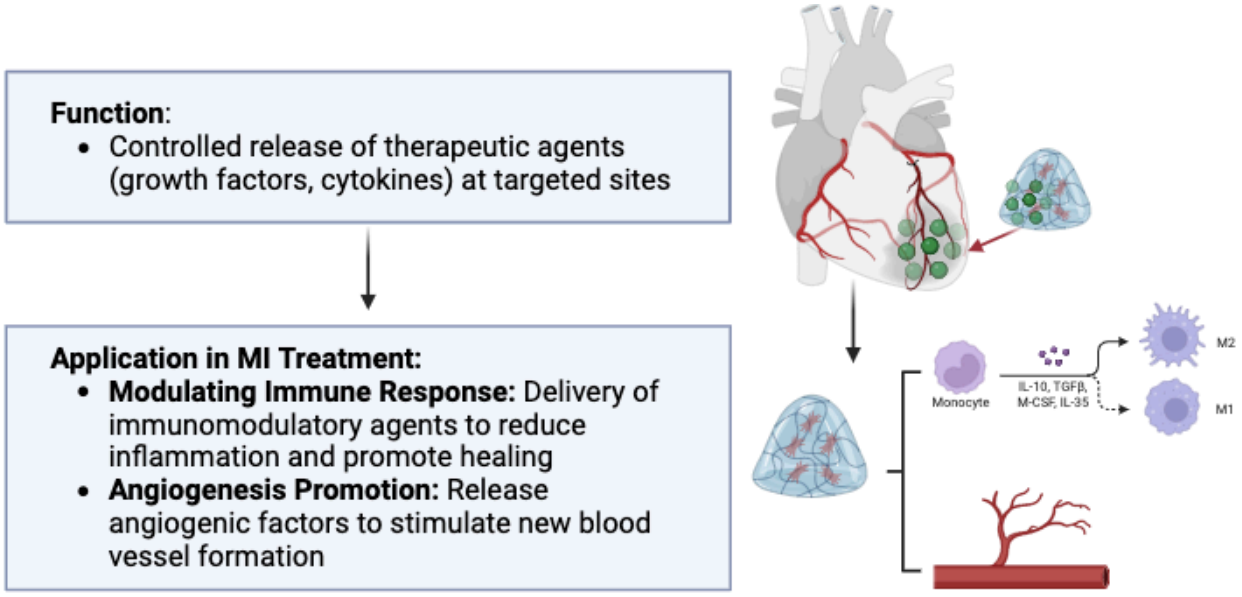

Figure 8. Biomaterials for the controlled release of therapeutics for cardiac regeneration.

In addition, the use of biomaterials provides a potential solution for challenges related to an application of cells for myocardial injury treatment. In particular, biomaterials can promote the survival and retention of cells, facilitate and support differentiation and proliferation processes, and ultimately enhance the overall therapeutic efficiency of therapy (Smagul et al., 2020).

2.5.2 Administration Routes of Biomaterials

Various anatomical routes can be used for the introduction of drugs into the human body. The selection of the administration route depends on various factors such as the specific condition being treated, the desired therapeutic outcome, and the availability of suitable pharmaceutical products. Therapeutic agents can be delivered either directly to the specific organ affected by a disease or systemically, with the intention of targeting the diseased organ (Jain, 2019). Drug delivery can be performed via oral, intravenous, transdermal, nasal, oromucosal, ocular and other routes (Berillo et al., 2021). Some scaffolds are also administered through surgical implantation (Fenton et al., 2018). Overall, therapeutic agents, including growth factors and cells can be either seeded with pre-formed scaffolds and introduced surgically to the damaged tissue or delivered via the injection.

Injectable scaffolds are gaining significant interest as delivery systems for cells and therapeutics due to their ability to uniformly distribute cells and biological agents within the

scaffold. Additionally, these biomaterials can be injected directly into cavities, including those with irregular shapes and sizes, in a minimally invasive manner (Hou et al., 2004).

Overall, the design of biomaterials includes several key aspects. Firstly, it involves the encapsulation of a sufficient amount of the drug within the biomaterial to achieve a prolonged release pattern, thereby facilitating efficient healing. Secondly, it requires maintaining the stability of the drug during transportation through the body and at the target site, while also preserving its biological activity for effective therapeutic outcomes. Thirdly, it requires a predictable release rate within the desired therapeutic period, which may last from days to years. Fourthly, the biomaterial and its degradation products must demonstrate biocompatibility and non-toxicity within the body. Lastly, the cost associated with the synthesis and/or fabrication of the biomaterial is also a crucial consideration (Adeosun et al., 2020).

2.6 Cryogels as Drug Release Systems

Cryogels are a subclass of hydrogels that are characterized as polymeric structures with a high degree of porosity. These structures are formed through the process of cryogelation, wherein mono- or polymers are subjected to freezing at subzero temperatures. Owing to their inherent interconnected macroporosity, simple synthesis process and compatibility with biological systems, there is a growing interest in exploring their potential in various biomedical fields, including 3D-bioprinting, drug delivery and wound healing (Memic et al., 2019; Jones et al., 2021).

Cryogel is a biodegradable substance that is a good candidate for cardiac tissue regeneration applications. It is biocompatible with the cells in myocardium as well as it possesses biological activity and supports cell differentiation and proliferation (Sultankulov et al., 2019). Also, cryogel presents in various forms, including powder, column, bead, sphere, membrane, and monolithic (Çimen et al., 2021). The powdered, injectable form of cryogel is a favorable candidate for tissue engineering as it allows minimally invasive surgery. In addition, cryogel alone has the ability to decrease left ventricular wall dilatation, promote angiogenesis, enhance endogenous tissue repair through cell recruitment, and preserve cardiac function (Vasu et al., 2021; Cui et al., 2016). Finally, cells grown in the cryogel systems show increased, long-term proliferation and differentiation (Fu et al., 2021).

The synthesis of cryogel includes a controlled freezing-thawing process using monomers/polymers and an initiator/activator pair. The polymerization, or crosslinking reaction,

occurs in a semi-solid phase that contains the monomer when the temperature is beneath the solvent's freezing point. Once the reaction ends, the product changes phase and assumes a molten state at room temperature. This process results in the formation of cryogels, which are distinguished by their loose and highly porous structure. In this synthesis water plays multiple roles as a solvent, a dispersing agent, and a porogen (Çimen et al., 2021). The cryogel's macroporous structure is facilitated by the presence of water, wherein a phase separation occurs, causing the frozen ice crystals to transiently convert into a completely linked cryogenic skeleton (Okay, 2014). The pore size of the cryogel is determined by various factors, including the initial concentration of monomers, physicochemical characteristics, and the degree of freezing. The pore wall thickness and density of the cryogel itself play a crucial role in determining its macroscopic mechanical properties (Çimen et al., 2021). Overall, the cryogels possess a highly porous interconnected structure that facilitates the diffusion of various substances, including macromolecules as well as colloid particles such as protein micelles and viruses. These characteristics make the cryogel a good candidate for the delivery of cell and other therapeutics.

Cryogel composition

The cryogel used in this study was designed in our laboratory by previous researchers. The cryogelation technique was used to fabricate macroporous scaffolds using a combination of chitosan (CHI), heparin (Hep), and polyvinyl alcohol (PVA), with the addition of a glutaraldehyde (GA) cross-linker. The inclusion of polyvinyl alcohol (PVA) in the reaction solution slowed the process of polyelectrolyte complex (PEC) synthesis between chitosan (CHI) and heparin (Hep) (Fig.9). This deceleration facilitated enhanced mixing and led to the production of a uniform matrix structure (Sultankulov et al., 2019).

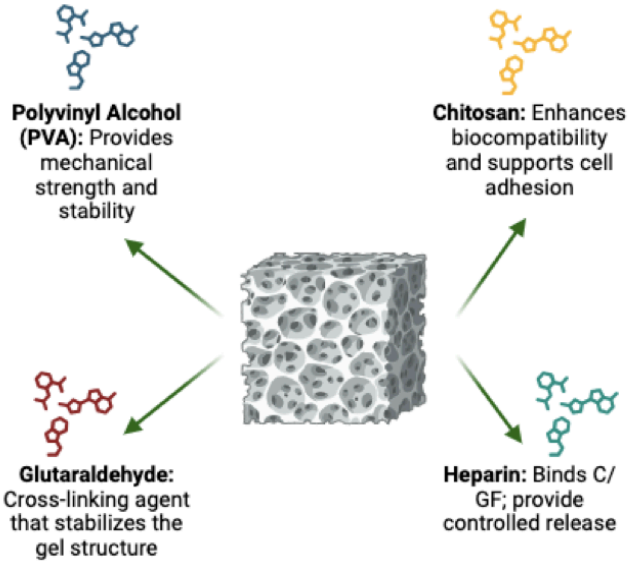

Figure 9. Cryogel composition.

In recent years, chitosan has emerged as a promising candidate for use in tissue engineering studies. Chitosan, a unique natural polysaccharide, derived from chitin, possesses remarkable characteristics such as biodegradability, biocompatibility, and antibacterial activity. It has the potential for chemical modification to enhance its functional capabilities, due to the presence of free amine groups within its backbone structure, which can be beneficial for the development of various biomaterials for the treatment of cardiac failures (Sultankulov et al., 2019).

Biomaterials based on chitosan have been shown to effectively promote in vivo regeneration and repair of a wide range of tissues and organs, such as bone, cartilage, dental, skin, nerve, cardiac, and others. Multiple preclinical models of various tissue injuries revealed de novo tissue development, differentiation of resident cells, and restoration of the extracellular matrix following therapy with chitosan-based biomaterials. Additionally, it was demonstrated that due to the ability to sustain release of therapeutic agents, chitosan can be used as a good carrier for drugs, genes, and bioactive substances (Kim et al., 2023). Overall, chitosan acts as a primary structural component in macroporous scaffolds due to its biocompatibility and ability to form complex biocomposites.

Heparin itself is the most popular anticoagulant drug, which belongs to the family of glycosaminoglycans (GAG) and is composed of sulphated polysaccharides found in connective-tissue-type mast cells (Oduah et al., 2016). It is kept within secretory granules together with histamine and a variety of mast cell proteases (Forsberg et al., 1999). In cryogel, heparin is used to

form polyelectrolyte complexes (PEC) with chitosan, which are essential for the development of the homogeneous matrix structure of the cryogel. Also, its highly sulfated nature allows for electrostatic drug binding and controlled release, which is vital for prolonged drug administration. This property is used in heparin-containing cryogel microcarriers to reduce toxic effects on tissue by controlling drug supply. Additionally, heparin may offer angiogenic benefits to the scaffold, promoting better vascularization and tissue integration (Kocak et al., 2022; Welzel et al., 2012).

PVA is a hydrophilic, biocompatible, non-toxic, and biodegradable synthetic polymer with excellent film-forming properties. Its hydroxyl groups presented in each repeating unit allow PVA to exhibit strong hydrophilic and hydrogen bonding character. This enables it to form cross-linked hydrogel, which is crucial for the cryogel's structure and performance (Wan et al., 2014; Păduraru et al., 2012). An addition of PVA to cryogel slows down the formation of the PEC between chitosan and heparin, thus allowing for more thorough mixing and a more uniform matrix structure.

Glutaraldehyde is a dialdehyde and a reduced form of the glutaric acid that is used in studies as a fixation agent for cells (Khapre et al., 2021). In scaffolds GA acts as a cross-linking agent for the formation of a stable structure. It facilitates the entrapment of biomolecules in polymeric matrices under mild conditions. An addition of GA to cryogel is important as it serves as a cross-linker during cryogelation, contributing to the formation of a stable and mechanically robust scaffold structure (Figueiredo et al., 2008).

In general, cryogel is a porous structure that was synthesized from CHI, Hep, PVA and GA. Chitosan serves as a primary structural component of cryogel and is essential for a homogeneous matrix structure. Heparin, in turn, is crucial for matrix homogeneity, and potentially promotes angiogenesis. PVA contributes to mechanical strength through its hydrogel-forming ability. Finally, GA acts as a cross-linking agent, solidifying the cryogel structure, and ensuring a stable, mechanically robust system suitable for the delivery of biological agents.

This organized combination of components, each with a specific role, results in a scaffold with suitable mechanical properties, a conducive environment for tissue integration and regeneration, and a controlled delivery system for potential biomedical applications (Omidian et al., 2023; Saylan & Denizli, 2019).

2.6.1 Chitosan-based Cryogel Microparticles (CCMPs) for the Release of Cytokines and Growth Factors

In recent decades the use of chitosan-based cryogels as a viable alternative to conventional treatments to restore damaged myocardial tissue has risen to prominence due to such properties of scaffolds as biocompatibility, biodegradability, and chemical adaptability (Evans et al., 2021).

Chitosan-based scaffolds have demonstrated a significant potential to enhance angiogenesis in the infarcted zone by stimulating the production of glycoprotein receptors of the VEGF family, which is crucial for the restoration of essential heart functions post-MI (Beleño Acosta et al., 2023). Furthermore, chitosan-based cryogels demonstrated an immunosuppressive effect driven by chitosan, which is able to suppress the inflammatory activity of macrophages leading to reduction of the inflammatory responses post-MI (Ayaz et al., 2021). Such characteristics combined with the controlled porosity that allows for nutrient exchange and stimulation of cell differentiation, highlights the promise of chitosan-based cryogels in cardiac tissue engineering applications.

Various studies report that cryogel allows a sequential delivery of growth factors and cytokines followed by cells. Such delivery of specific agents accelerated regeneration of post-MI hearts and improved functions. In addition, because cryogel offers a controlled and sustained release of cytokines and growth factors, such negative effects as overexposure of agents and repeat of injection are eliminated (Jimi et al., 2020).

Numerous studies have been conducted to investigate the significance of growth factors, cytokines, and various components of the extracellular matrix (ECM) in the treatment of MI (Thiagarajan et al., 2017). Thus, the anti-inflammatory and pro-healing effects of interleukin-10 (IL-10) and transforming growth factor-beta (TGF-β), together with the angiogenic and regenerative capabilities of vascular endothelial growth factor (VEGF) and fibroblast growth factor (FGF), have been extensively investigated (Fig.10).

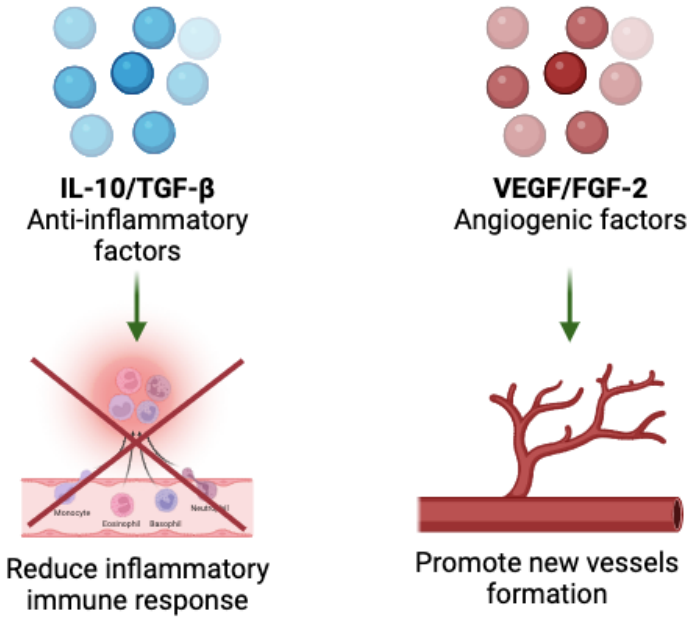

Figure 10. Cytokines and growth factors for cardiac tissue regeneration.

The use of a chitosan-based cryogel incorporated with IL-10/TGF-β and bFGF/VEGF potentially altered the inflammation and proliferation phases of wound healing, leading to an accelerated wound healing process and enhanced tissue regeneration, as was shown in previous studies conducted by our research group (Jimi et al., 2020). Anti-inflammatory cytokines IL-10 and TGF-β as well as pro-angiogenic growth factors, such as VEGF and FGF are actively utilized in the field of cardiovascular disease treatment (Smagul et al., 2020). TGF-β can stimulate macrophage activation via both Smad3-dependent and independent pathways. Smad3, in turn, participates in activation of phagocytosis, secretion of VEGF and TGF-β1, and protection against adverse cardiac tissue remodeling (Chen et al., 2019). The anti-inflammatory properties of IL-10 come from its role in the regulation of necrosis and neutrophil migration, since its lack was linked to increased necrosis and neutrophil recruitment resulting in increased infarct zone. Additionally, the deficiency of IL-10 leads to the upregulation of integrin-linked kinase, resulting in the impaired ability of endothelial progenitor cells to inhibit cellular apoptosis and diminish scar size (Yue et al., 2020). On the contrary, the administration of IL-10 can efficiently reduce inflammation, induce a shift in macrophage polarization towards the M2 phenotype, stimulate fibroblast activation, and subsequently improve left ventricular remodeling post-MI (Jung et al., 2017). VEGF is secreted by cardiac macrophages and participates in new vessel formation and myocardial tissue repair via the

regulation of endothelial cell proliferation, migration, and death (Ferraro et al., 2019). Also, VEGF promotes angiogenesis via the activation and regulation of various pathways, including PI3K, VRAP, Src tyrosine kinase, MAPK, and phospholipase C (Taimeh et al., 2013). In addition, VEGF and bFGF promote neovascularization of damaged heart tissue (Cahill et al., 2017). The mechanism by which bFGF functions involves its binding to the FGF receptor-heparin sulfate complex, leading to the subsequent activation of tyrosine kinase. The transmission of signals downstream occurs through the RAS-mitogen-activated protein kinase (MAPK) and phosphatidylinositide 3-kinase (PI3K) pathways (Itoh et al., 2016).

Nevertheless, the effective use of growth factors and cytokines in medical practices is restricted by their short lifespan, decreased stability, and susceptibility to enzymatic inactivation. For instance, the half-life of VEGF in plasma is around thirty four minutes (Oduk et al., 2018). Therefore, CCMPs possess considerable potential as effective instruments to protect, deliver, and facilitate the controlled release of growth factors and cytokines to the injured heart (Hachim et al., 2019).

To Conclude

MI, commonly known as a heart attack, is a life-threatening condition marked by the obstruction of blood flow to parts of the heart, leading to the destruction of heart muscle tissue. This condition, which is mainly a result of atherosclerosis and plaque formation in coronary arteries, remains a formidable challenge in modern medicine. Due to the persisting high incidence of MI and its profound impact on global health, there is now a high demand in alternative and more effective treatment. Traditional therapeutic methods do not effectively deal with the complex issues that follow MI, thus it is important to explore the new treatment options.

One of the treatment options emerging in the field of regenerative medicine is the use of pre-differentiated cells. This approach is focused on repairing or replenishing the damaged cardiac tissue. However, the effectiveness of such therapies is sometimes hindered by challenges such as the heterogeneity in cell differentiation and integration with the host tissue. Therefore, improving the effectiveness of these cell-based therapies has emerged as a crucial focus in research. One approach for that is to create a more favorable, conducive environment within the myocardium to soften the harsh conditions faced by cells post-injection, which would consequently facilitate a better integration and function of cells in MI-affected heart.

In the recent decades biomaterials demonstrated significant potential in boosting the therapeutic potential of regenerative medicine. They serve as scaffolds by providing a supportive matrix for the incorporation and sustained delivery of cytokines and growth factors. The unique properties of chitosan-based cryogels, including their biocompatibility and ability to mimic natural tissue environments, make them an ideal platform for tissue regeneration. Moreover, the ability of such cryogels to be loaded with cytokines and factors significantly enhances the therapeutic outcomes and promotes better integration and functionality of the transplanted cells within the cardiac tissue.

The innovative formulation of injectable CCMPs, specifically engineered for sequential delivery in MI treatment, marks a significant advancement in this area. CCMPs represent a cutting-edge approach, offering a controlled and phased release of cytokines and growth factors. This methodology addresses the complexities of MI treatment by ensuring a synchronized and targeted therapeutic intervention. The sequential delivery system optimizes the healing process, aligning the regenerative sequence with the natural healing stages of the heart. Such innovations not only hold the potential to revolutionize MI treatment but also exemplify the synergy between biomaterial science and cellular therapy, opening new horizons in cardiac regenerative medicine.

CHAPTER 1 : CRYOGEL MICROPARTICLES

METHODS

Cryogel Synthesis

To prepare a cryogel, a solution of precooled 5% PVA (1 g PVA + 20 ml dH_2O) and heparin (5 mg in 5 ml dH_2O at 1 mg/ml concentration) were mixed on a 600 rpm magnetic stirrer. A 2% Chitosan solution (0.4 g chitosan + 20 ml 1% acetic acid solution) was first prepared and placed on a hot plate at 50°C for 1-2 hrs at 500 rpm. It was then added to the PVA/heparin mixture followed by an addition of 400 µl of 25% glutaraldehyde (GA, Millipore USA, 354400, final concentration 0.5%), which was precooled and kept in the dark. The mixture was quickly stirred for approximately 5 seconds and poured into 20 ml beakers. For solidification, the cryogel was left in a refrigerated circulator (Julabo F34 HE, Seelbach, Germany) at -12°C for 12-18 hours. The next day, the cryogel was washed in a beaker with distilled water for 30 minutes at room temperature (RT) and neutralized on a shaker with 50 mM NaBH4 for 3 hours at RT. After neutralization, the cryogel was washed again with distilled water, frozen at -20°C for 1-2 hrs, and lyophilized overnight (Lyotrap Freeze Dryer, Core Facility).

Cryogel Microparticles Preparation and Sterilization

Cryogel was prepared in accordance with a previously established protocol. To receive a powder composition, the cryogel was first grinded using the micropore grater. Particles were collected in sterile 15 ml flasks. A two-tier sieve construction was assembled by placing a 50 µm sieve (Retsch, S/725857) on a petri dish, with a 100 µm sieve (Retsch, S/7261445) positioned on top. Cryogel powder was then poured onto the top 100 µm sieve, and the assembly was tightly covered with foil. Vortexing for 5 mins was conducted to allow cryogel of the appropriate size to uniformly pass through the top sieve. Powder was collected from the surface of the 50 mM sieve. Thus, cryogel microparticles in a range between 50-100 µm were obtained.

All subsequent steps were carried out under a cell culture hood. Cryogel powder was sterilized by leaving it in 70% ethanol for 10 minutes, followed by washing 3 times with sterile cold 1xPBS under the cell culture hood. Next cryogel powder was left for an additional UV light

sterilization for 40 minutes followed by washing 3 times with sterile cold 1xPBS to ensure removal of any contaminants.

SEM Microscopy

For SEM imaging, freeze-dried cryogel microparticles, obtained post lyophilization, were used without coating. Cryogel powder was gently stuck to adhesive tape to fix microparticles, and the tape was then adhered to the SEM stubs. Once secured, the SEM stubs with the adhered cryogel microparticles were loaded into the SEM chamber. The SEM imaging process was performed with variable accelerating voltage and magnifications as required to achieve detailed visualization.

Incorporation of Cytokines and Growth Factors into Cryogel Microparticles

Cryogel microparticles at the concentration of 10 μg/30 μl were loaded with either IL-10,TGF-β or FGF2,VEGF. First, a sterile 1 ml suspension of cryogel was prepared. For this, 0.333 mg of cryogel was measured and sterilized as described previously, then resuspended to a total volume of 1 ml in a 1.5 ml Eppendorf tube. All the following manipulations were performed under sterile conditions in a cell culture hood. The required amount of suspension was vortexed and pipetted into a new 1.5 ml Eppendorf tube, centrifuged to allow the cryogel to settle to the bottom, and the supernatant was removed. The cryogel was then loaded with the cocktails of cytokines and growth factors previously dissolved in sterile PBS and vortexed. Mouse recombinant IL-10,TGF-β, at the concentration of 1 μg/ml, and mouse recombinant VEGF, FGF-2 at the concentration of 10 μg/ml, were used in the study. To allow cryogel microparticles to successfully load cytokines and growth factors, the mixture was incubated on a shaker at 23°C for 4 hours at 700 rpm. After the incubation, the mixture was centrifuged again, and the supernatant was removed to eliminate non-bonded cytokines/growth factors. New cold 1xPBS was added under sterile conditions to prepare the mixture at a concentration of 10 μg/30 μl per mouse.

RESULTS

Cryogel microparticles preparation and characterization

Chitosan-based cryogel was synthesized and neutralized according to previously established protocol. Figure 11 demonstrates the process of cryogel microparticles preparation. The production of cryogel microparticles was achieved by grinding the cryogel mass into powder, which was then sized between 50-100 μm by using a dual-layer sieve setup. This specific size range was selected to ensure that the particles were small enough for injection while being large enough to maintain structural integrity. Cryogel was sterilized with both ethanol and UV light under aseptic conditions to ensure the elimination of any contaminants. This resulted in sterile uniform cryogel microparticles that were suitable for IL-10,TGF-β/VEGF,FGF-2 loading and injection into the heart.

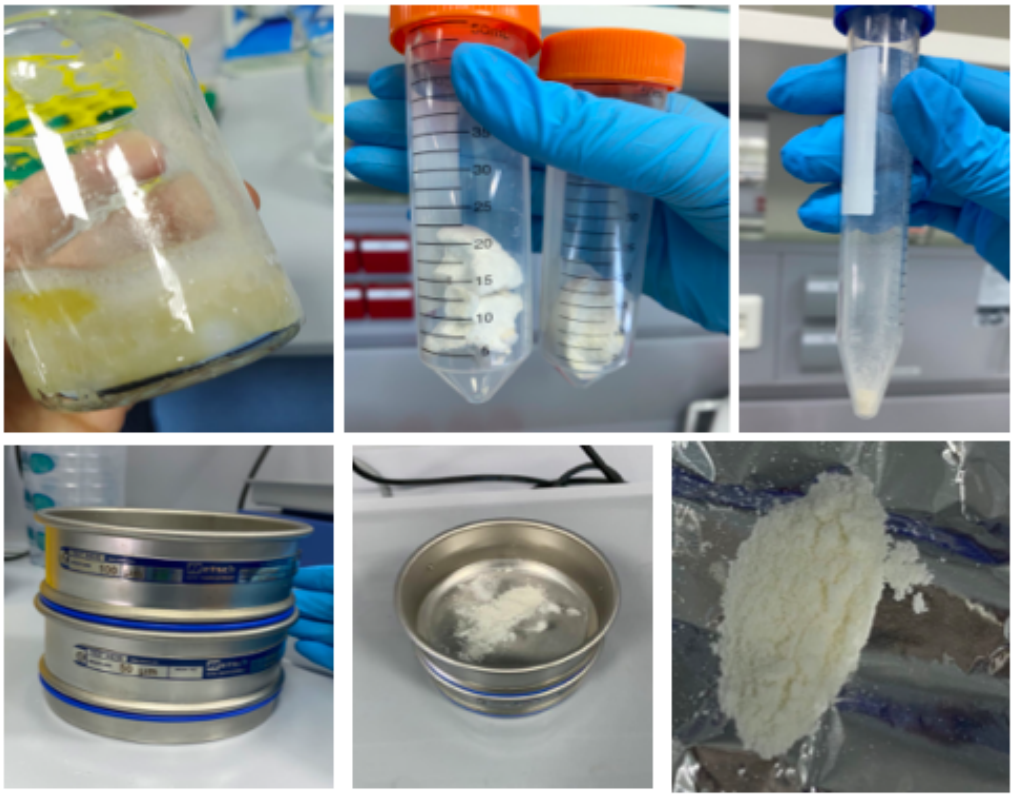

Figure 11. The process of cryogel microparticles preparation. A solid cryogel was first grinded to receive a powder condition, followed by passing through the sieves construction. Cryogel microparticles in a range of 50-100 μm were received.

SEM Microscopy

Further, SEM microscopy analysis under various magnifications was performed to explore the structural characteristics of obtained microparticles (Fig.12). SEM provided detailed images of the cryogel pore architecture, surface morphology and particle size distribution. Thus, cryogel microparticles possessed the rough surface texture, allowing them for more efficient attachment of C/GFs, homogeneous pore distribution and a rugged surface, which affirmed the scaffold's mechanical integrity and its capability for sustained biomolecule release. In addition, image analysis confirmed the consistent size range, which was pivotal to ensure a predictable and controlled release profile of cytokines. 100 μm magnification image showed that cryogel microparticles appeared to maintain distinct boundaries with minimal clumping, which is crucial for their uniform distribution upon injections. This characteristic is essential to ensure an even delivery of therapeutic agents to the myocardial tissue. Overall, SEM microscopy analysis validated the suitability of cryogel microparticles for myocardial injection, highlighting their size uniformity, surface morphology conducive for IL-10,TGF-β/VEGF,FGF-2 attachment, structural integrity, and favorable particle interaction. These features collectively underscored the potential of cryogel microparticles in the targeted delivery of cytokines and growth factors for myocardial tissue regeneration following infarction.

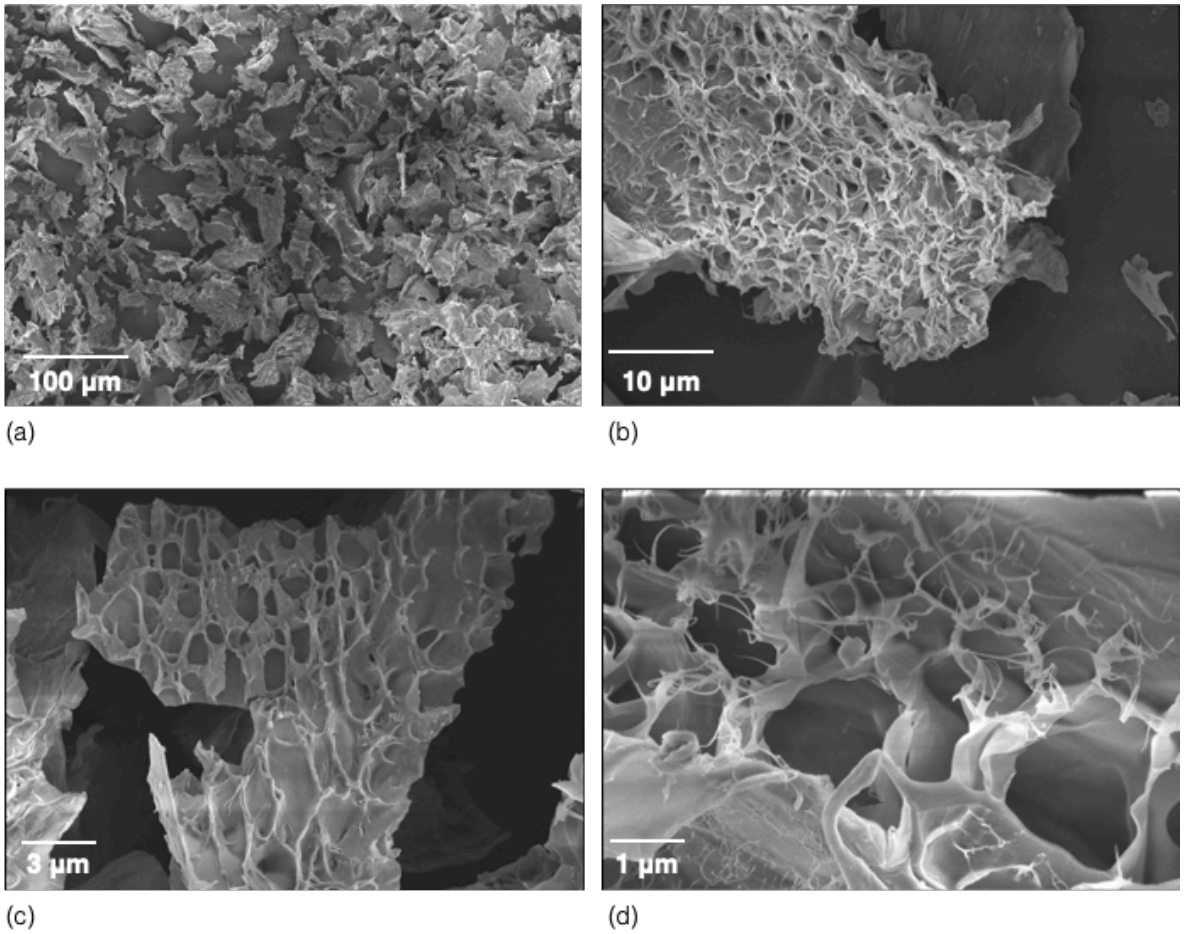

Figure 12. SEM imaging at 4 different magnifications, (a) 100 um, (b) 10 um, (c) 3 um, (d) 1 um, showing the structure of cryogel microparticles.

DISCUSSION

The cryogel was synthesized in our lab by a previous research group. Characteristics of cryogel were tested and analyzed. Thus, the primary objectives of the previous group were to create a cryogel scaffold that exhibits appropriate mechanical qualities for implantation, while also possessing the capacity to enhance tissue regeneration. Also, the scaffold needed to be compatible with tissue and capable of undergoing biodegradation. In addition, the previous study aimed to evaluate the potential of a single-step method for generating a scaffold that may be used for delivering growth factors, without the need for any extra chemical modifications. The findings of in vitro experiments indicated that cryogels derived from natural components, specifically Hep and CHI, exhibited favorable characteristics as carriers for promoting cell proliferation and differentiation. Newly synthesized cryogel allowed growth factors to be incorporated into cryogel matrices in a single-step process, without the need for chemical changes, while retaining their biological activity. Therefore, the selection of CHI, PVA, and Hep was made with the objective of producing cryogels that possess the capability to selectively and effectively adsorb growth factors without any supplementary modifications. The results of release kinetics and degradation experiments have demonstrated a high level of efficiency in the loading of BMP-2, with around 82.3% of the growth factor being successfully loaded. Furthermore, in vitro investigations have revealed that the release of the bound growth factors is reliant on the breakdown of the cryogel material (Sultankulov et al., 2019). Thus, in vitro study showed that the cryogel was biocompatible and biodegradable, allowing growth factors attachment and their sustained release in the biological system.

Further, the cryogel was tested *in vivo* on an internal splint wound healing model. The study investigated the sequential targeted delivery of growth factor/cytokine combinations with regulatory functions on inflammation and tissue regeneration. A cryogel was successfully integrated with four growth factors and cytokines, namely IL-10/TGF-β and VEGF/bFGF and demonstrated the ability to release these factors in a regulated and sustained manner, while preserving their biological functionalities (Jimi et al., 2020).

These cryogels were applied to the wound surface on day 0 and day 3, respectively, following the commencement of the wound. The cryogel group treated with C/GFs demonstrated

a statistically significant reduction in wound area starting from day 7. By day 10, the wound area in that group had reached about 10%, which was notably lower compared to the control groups where the wound area remained at around 60-65%. Moreover, previous in vivo studies on the cryogel showed that the administration of inflammation-modulating and wound healing components in a sequential manner resulted in the promotion of granulation tissue development, together with the facilitation of functional neovascularization, ultimately leading to the process of regenerated epithelialization (Jimi et al., 2020).

Overall, both in vitro and in vivo studies demonstrated that the cryogel possessed the ability to function as a controlled release mechanism, facilitating the sequential administration of several growth factors and cytokines. This feature enabled the cryogel to accelerate the process of tissue repair and regeneration.

The focus of the current research was aimed at studying heart injuries, in particular MI. The selection of MI as a model to test the efficacy of the cryogel was based on several reasons including both, the properties of the cryogel and the pathophysiological parallels between wound healing and myocardial repair post-infarction.

First, as it was described in literature review, the treatment of MI currently demands innovative therapeutic approaches due to the limited regenerative capacity of heart tissue. The tissue damage caused by MI leads to loss of cardiomyocytes and subsequent scar formation, which results in the mechanical and functional integrity of the heart. Thus, given that the cryogel previously demonstrated the ability to facilitate tissue repair and regeneration via the controlled release of C/GFs, these properties could be useful for heart tissue repair, which similarly requires support for cell proliferation, angiogenesis, and matrix remodeling to recover from injury.

Second, *in vivo* studies on skin wound healing models were successful and this fact also contributed to the selection of MI models. The processes of wound healing, such as inflammation modulation, granulation tissue development, and neovascularization, are similar to the healing process of infarcted myocardium. The idea behind was that the ability of cryogel to sequentially deliver various cytokines and growth factors in a controlled manner could also be beneficial for the healing of post-MI myocardium and could similarly result in the reduction of inflammation and the promotion of angiogenesis and tissue regeneration.

Furthermore, such features of the cryogel as biocompatibility and biodegradability that were demonstrated both in vitro and in vivo make it a suitable candidate for heart application. A

scaffold that could be gradually resorbed and removed from the body is ideal for cardiac tissue engineering, as it would minimize long-term foreign body reactions and allow for the natural restoration of cardiac tissue.

Finally, such a therapeutic strategy could be easily integrated into clinical practice due to the simple synthesis of cryogel and its single-step method for incorporating C/GFs, which simplifies the preparation and application processes.

Overall, the benefits of using cryogel in heart injury studies could be explained by its mechanical stability, biocompatibility, biodegradability, and controlled release abilities. Those features are crucial for successful cardiac tissue engineering. In addition, the previous studies provided strong reasons for cryogel application in the heart disorders, because of similar mechanisms of tissue repair and regeneration.

In previous studies cryogel was used in the form of thin round discs, as such form was the most convenient for the skin wound treatment. For the current research we chose a powdered form of the cryogel as it permits a minimally invasive approach via the administration through injection. The chosen particle size range (50-100 μm) was strategically optimized to minimize heart risks while being conductive for injection.

In previous studies the efficacy of C/GFs expression from cryogel was analyzed by a series of ELISA experiments as well as in vivo measurements. We measured the amount of cryogel used in previous research and calculated the equivalent amount of cryogel powder. Thus, in a previous study, cryogel samples (0.5 - 0.8 cm in diameter) were sliced into 3 mm thick disks. The mass of one disc was 10 ug, thus this mass of powder was used in our research. According to IACUC Policy for Dose Volumes in Laboratory Animals, the recommended dose of intramuscular injection in mice is 30 ul (Cate, 2022; Recommended Dose Volumes for Common LaboratoryAnimal,n.d.)

Species	PO gavage/in tragastric	IV* (bolus)	IV** (ml/kg/h)	IP@	SC@	IM***@	IN*** IT***	ID***
Mouse	**10** (20)	**5** (20)	**1** (4)	**10** (20)	**5** (10)	**0.03** (0.05)$	**0.03-0.05**[a]	**0.05** (0.1)
Rat	**10** (20)	**5** (20)	**1 or 2** (4)	**10** (20)	**5** (10)	**0.05** (0.1)$	**0.03-0.05**[a]	**0.05** (0.1)
Hamster	**10** (20)	**5** (10)	2-4	**10** (20)	**1-5** (10)	**0.05** (0.1)$	**0.03-0.05**	**0.05** (0.1)
Guinea pig	**10** (20)	**1** (5)	2-4	**10** (20)	**5** (10)	**0.05** (0.1)	**0.03-0.05** (0.2)	**0.05** (0.1)
Rabbit	**10** (20)	**1** (5)	**2-4**	Not recommended	**2.5** (10)	**0.05** (0.5)	**0.2** (0.5)	**0.05** (0.1)

Ideal maximum dose volumes are bolded, absolute maximum dose volumes are (smaller in parenthesis)

(Source: Cate, 2022).

Therefore, a concentration of 10 ug/ 30 ul was used per injection. Concentrations of IL-10,TGF-β/VEGF,FGF-2 were chosen according to previous results. Thus, sterile cryogel microparticles of known concentration were loaded with either IL-10,TGF-β or VEGF,FGF-2 and injected directly after therapeutic incorporation to avoid freeze thaw conditions. An effect of Cryo, Cryo/IL-10,TGF-β and Cryo/VEGF,FGF-2 injections are discussed later in the in vivo studies chapter.

CHAPTER 2: ISOLATION AND DIFFERENTIATION OF MSCS INTO ECS, SMCS, AND CMS

METHODS

Isolation of MSCs from Mouse Compact Bones

The use of animals was approved by the Institutional Animal Care and Use Committee of the autonomous organization of education “Nazarbayev University" (IACUC). All the manipulations were administered according to IACUC protocol.

A 2-3 week old male mouse (C57BL/6 strain) was euthanized via cervical dislocation. To minimize contamination risks, the animal was sterilized post-euthanasia by rinsing in 70% ethanol for 3 minutes. The mouse was then securely positioned on a 90 mm culture plate for dissection. The humeri, tibiae, and femurs were carefully dissected, ensuring complete removal of surrounding skin and muscle tissue. Once isolated, the bones were then rinsed in DMEM with 2% antibiotics. To prevent cross contamination with hematopoietic cells, the bone cavity was flushed 3 times using DMEM supplemented with 2% FBS + 1mM EDTA. The flushing was performed using an insulin syringe with a 30G needle. Subsequently, the bones were cleaned of any adhering muscles and tendons using sterile medical gauze, ensuring gentle and thorough wiping. After that, the cleaned bones were carefully cut into chips using sterile scissors. Those bone chips were then washed 3 times in DMEM supplemented with 2% FBS + 1mM EDTA. The washed bone chips were transferred into a 50 ml flask containing a Collagenase solution (DMEM, 10% FBS, 1% antibiotics, 2% collagenase type 2) and left in an incubator shaker (37 °C) for one hour at 160 rpm. Post-incubation, the bone chips were centrifuged and subsequently washed twice with DMEM medium supplemented with 20% FBS +1% antibiotics. The chips were then resuspended in a complete DMEM medium and transferred to a new T25 flask. They were then cultured at 37 °C in a 5% CO2 incubator. On day 3, the medium was replaced, and bone chips were left to let all the MSCs leave the bones. On day 7, the isolated cells were transferred to a new T25 flask to promote uniform and homogeneous growth of MCS. The media was replaced by DMEM supplemented with 10% FBS + 1% antibiotics. On day 14, cells were analyzed by IF analysis and used for further studies.

MSCs Differentiation to CMs, SMCs and ECs

For cell differentiation study, primary MSCs cultures at passage 2, cultivated for 15 days, were used. The cells were detached from the T25 flask using trypsin and subsequently counted using a haemocytometer. Cells were then seeded to 48-well plates at a concentration of 100.000 cells per well. The cells were incubated overnight (37 °C in a 5% CO2 incubator) in DMEM media supplemented with 10% FBS + 1% antibiotics to facilitate cell attachment.

Next day, the media were replaced with fresh inducing media, with 300 µL of media per well. According to the type of cells, 3 inducing media were prepared. For CM differentiation, DMEM was supplemented with 2.5 ng/mL TGF-β, 5 ng/mL Activin-A, 5 ng/mL BMP4, 50 ng/mL IGF, 10 ng/mL bFGF, 5% FBS, 1% antibiotics, and 1 µmol/L ascorbic acid. For EC differentiation, DMEM was enhanced with 5 ng/mL VEGF, 10 ng/mL bFGF, 20 ng/mL IGF, 5 ng/mL EGF, 5% FBS, 1% antibiotics, and 1 µmol/L ascorbic acid. For SMC induction, DMEM was fortified with 10 ng/mL PDGF-BB, 5 ng/mL TGF-β, 5% FBS, 1% antibiotics, and 1 µmol/L ascorbic acid. For control groups, DMEM supplemented with 5% FBS and 1% antibiotics was used to compare cell differentiation.

The inducing media for CMs, ECs, and SMCs, as well as the culture media for control groups, were refreshed every other day. After 12 days of induction (37°C in a 5% CO2 incubator) the phenotypes of the cells were analyzed using IF and polymerase chain reaction (PCR) analyses.

Cell Imaging

For immunofluorescent analysis, pre-differentiated cells were initially washed three times with cold 1xPBS, for 5 mins each time. The cells were then fixed in 4% paraformaldehyde for 15 minutes at RT. This was followed by three washes with cold 1xPBS each lasting for 5 mins. Subsequently, cells were permeabilized with PBS containing 0.3% Triton X-100 for 15 mins at RT, followed by another set of three washes with cold PBS.

After permeabilization, cells were treated with a blocking solution (5% bovine serum albumin (BSA) and 5% normal goat serum (NGS) in 1xPBS) for 1 hour at RT to prevent non-specific antibody binding. Cells were then incubated overnight at 4°C with primary antibodies at a concentration of 1:500 in antibody dissolving solution (1% BSA in PBS). The primary antibodies used included recombinant anti-CD31 mAb for ECs, anti-alpha SMA mAb for SMCs, anti-GATA mAb and anti-cardiac Troponin I pAb for CMs. Additionally, recombinant anti-CD105 mAb was

used for staining non-differentiated MSCs as a positive control, and differentiated cells as a negative control.

The following day, cells were washed three times with cold PBS for 5 mins each. Cells were then treated with either AlexaFluor 647 or AlexaFluor-488 goat anti-rabbit secondary antibody at a concentration of 1:1000, protected from light, for 60 minutes at RT. Afterward, cells were washed and counterstained with DAPI at a concentration of 1:2000. The analysis was performed using the EVOS cell imaging system.

PCR Analysis for Cell Specific Markers

PCR was performed to analyze the expression of specific gene markers in CMs, ECs and SMCs. On day 12 of differentiation, pre-differentiated cells were harvested and quantified using a haemocytometer. Total RNA extraction from the cells was performed using Trizol reagent and the PureLink RNA mini kit. The concentration and the purity of RNA were determined using the NanoDrop spectrophotometer system. For cDNA synthesis, 1 µL of total RNA from each sample was used with the Invitrogen SuperScript IV First-Strand Synthesis System. To ensure robustness, at least three RNA samples from different differentiation batches were processed for each cell type. The quantity and quality of synthesized cDNAs were assessed by NanoDrop.

The PCR reaction mixtures were prepared with a total volume of 25 µL, comprising 0.5 µL of 10 µM forward primer, 0.5 µL of 10 µM reverse primer, 12.5 µL of Taq 2X Master Mix (New England Biolabs, Inc.), and an adjusted volume of template cDNA to achieve a target concentration of 500 ng. Nuclease-free water was added to reach the final volume.

Gene markers targeted included Nkx2.5, Tbx5, and cardiac Troponin T (CTNT) for CMs; platelet endothelial cell adhesion molecule-1 (Pecam1) and CD34 for ECs; and alpha-smooth muscle actin (α-SMA or Acta2), Calponin3, and myosin heavy chain 11 (Myh11) for SMCs. The PCR amplification used a thermocycler with the following thermal profile: an initial denaturation at 95°C for 30 seconds, followed by 30 cycles of denaturation at 95°C for 30 seconds, annealing at temperatures optimized for each primer set (53°C for Tbx5, CTNT, Myh11; 55°C for Nkx2.5, Acta2, Calponin, Pecam1, CD34) for 30 seconds, and extension at 68°C for 1 minute, ending with a final extension at 68°C for 5 minutes.

Post-amplification, PCR products were mixed with DNA loading dye and subjected to agarose gel electrophoresis for size-based separation. A 1.5% agarose gel, stained with Ethidium

Bromide was prepared. The gel was run in a 1x TBE buffer at 100 V until the dye front had migrated appropriately. The gel was then visualized under UV light, and the DNA bands were compared against a 1000bp DNA ladder to determine the size of the amplified products. Bio-Rad Chemi-Doc MP system was used for results visualization.

Primers were self-designed and synthesized at the Nazarbayev University, Core Facility using the DNA-oligonucleotide synthesizer ASM-800. Primer sequences can be found in the Appendix section.

RESULTS

MSCs isolation and culture

Primary MSC cultures were efficiently isolated from mouse compact bones in accordance with the protocol outlined in Nature Protocols (Zhu et al., 2010) and maintained in culture for 14 days. The sequential steps of the isolation process are visually represented in Fig.13A, showing the details of bone extraction, cleaning, cutting and the setting of bone chips for cell culture.

During the initial week post-isolation (Day 1-7), the cells were cultivated in DMEM supplemented with 1 % antibiotics and 20% FBS optimizing conditions for robust cell growth and survival.

Morphological changes were closely monitored and are depicted in Fig.13(C). On Day 1, cells began to emerge from the bone chips, initially appearing rounded as they adapted to the in vitro environment. By Day 3 a subset of these cells had begun to display early signs of elongation, indicative of their mesenchymal stem cell nature and plasticity. By Day 3, throughout this period, care was taken to minimize disturbances to the culture to preserve the integrity of cell migration from the bone chips. As the culture progressed to Day 5, an increase in the number of migrated cells was observed, with the majority now completely separated from the bone fragments and exhibiting a more distinct spindle shape. This morphological change signals the MSCs' response to the culture conditions and their innate capacity to proliferate and differentiate. By Day 7, the cells were less crowded, by Day 14, the MSCs had undergone substantial morphological evolution; they were now densely populated with pronounced fibroblast-like features, including broader cytoplasmic extensions and increased cell-to-cell contact, indicating a high level of proliferation. The culture presented a variety of cell shapes, which is typical of MSCs approaching confluence, ranging from spindle-like to larger, flatter cells, and some retaining a smaller, more rounded form.

Immunofluorescence staining for CD105 was performed on the 15th day to confirm the MSC phenotype. The results, displayed in Fig.13(D), demonstrated robust CD105 expression on the cell membranes, co-localized with DAPI nuclear staining. This confirmed that the cells retained their MSC identity after two weeks of culture, validating the culture conditions and the potential of cells for further studies. The evident morphological transformations and consistent CD105

expression throughout the culture period substantiate the successful establishment of the MSC culture, priming it for further experimental use.

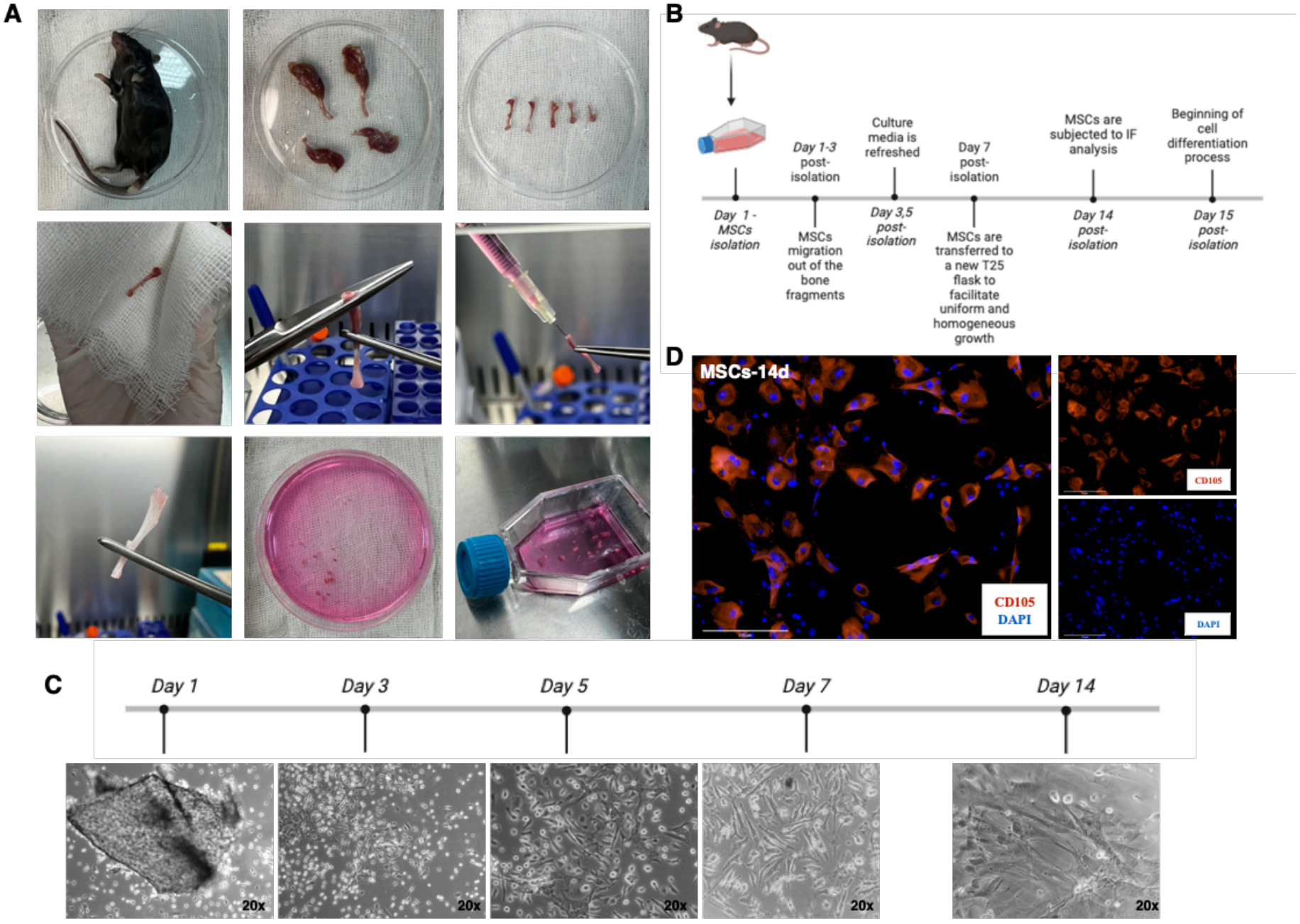
A
B
Day 1 - MSCs isolation
Day 1-3 post-isolation
MSCs migration out of the bone fragments
Culture media is refreshed
Day 3,5 post-isolation
Day 7 post-isolation
MSCs are transferred to a new T25 flask to facilitate uniform and homogeneous growth
MSCs are subjected to IF analysis
Day 14 post-isolation
Beginning of cell differentiation process
Day 15 post-isolation
D
MSCs-14d
CD105
DAPI
CD105
DAPI
C
Day 1
Day 3
Day 5
Day 7
Day 14
20x
20x
20x
20x
20x

Figure 13. Isolation, cultivation, and characterization of mouse MSCs. A) Detailed process of MSC isolation from a mouse: starting from the top left, a mouse is euthanized, followed by the extraction of long bones (humeri, tibiae, and femurs). The bones are cleaned and bone marrow is flushed. The final images shows the process of bone chips preparation and the seeding of chips into a culture dish. B) Schematic representation of the MSC cultivation protocol, illustrating the timeline and key milestones from initial bone chips seeding to cell culture. C) Morphological assessment at Days 1, 3, 5, 7, and 14 post-isolation under 20x magnification, depicting MSCs as they adopt a fibroblast-like morphology. D) IF analysis at Day 15: The left panel confirms MSC identity with CD105 (endoglin) expression on the cell membranes (red), with nuclei counterstained with DAPI (blue). Right panels exclusively show CD105 (endoglin) and nuclear DAPI staining. Scale bars are 100 µm.

MSC Differentiation Toward CM, EC, SMC

Cardiomyocyte Differentiation:

The direct differentiation of MSCs towards cardiomyocytes was assessed over a 12-day period. The cardiogenic differentiation of MSCs was induced by a cocktail of TGF-β (2.5 ng/mL) Activin-A (5 ng/mL), BMP-4 (5 ng/mL), IGF (50 ng/mL), bFGF (10ng/mL), and ascorbic acid (1 µmol/L) and led to significant morphological and molecular changes, characteristic of early cardiomyocytes (Fig.14).

The morphological assessment captured a time-lapse transformation of MSCs, where an elongation of cell bodies was evident from Day 1 to Day 12 post-induction. This elongation, particularly notable at Day 12, is a morphological cornerstone of cardiomyocyte maturation, reflecting the cytoarchitectural adaptations consistent with the development of cardiac-specific structures (Fig.14A).

The induced expression of GATA-4, a zinc-finger transcription factor imperative for early cardiac development, and Troponin I, was observed in MSCs-CM d12 group. The control MSC group was cultured in DMEM with 5% FBS and 1% antibiotics, similarly, for 12 days. Staining of the control group did not reveal GATA or Troponin expression (Fig.14B).

PCR assays were performed on Day 12 post-induction to analyze the successful cardiac induction on molecular level. Gene expression analysis confirmed the upregulation of cardiac markers Nkx2.5, Tbx5 and CTNT, that are regulators of cardiac gene expression and

morphogenesis. The 1.5% agarose gel electrophoresis showed clear bands for all tested genes, NxT2.5 (392 bp), Tbx5 (577bp) and CTNT (650 bp). Control group, also cultured similarly for 12 days, showed no expression of those genes on PCR, suggesting the molecular differentiation toward a cardiac phenotype (Fig.14C).

Smooth Muscle Cell Differentiation:

MSC differentiation into SMCs was thoroughly examined, showing significant changes in cell morphology and gene expression (Fig.5). The differentiation was similarly achieved through the application of a targeted differentiation regime. MSCs were subjected to the influence of TGF-β (5 ng/mL), PDGF-BB (10 ng/mL) and ascorbic acid (1 μmol/L) over a period of 12 days before performing analyses.

The MSCs, upon induction with TGF-β and PDGF-BB, underwent a transition from their inherent spindle shape to a more elongated and aligned morphology reminiscent of mature SMCs. This change was evident by Day 5 and became more pronounced by Day 7, reaching a peak at Day 12. The morphological changes are indicative of the cytoskeletal reorganization intrinsic to SMCs, which are known for their role in the contractile apparatus of the vascular system (Fig.5A).

IF staining for α-SMA, a definitive marker for SMCs, showed a marked increase in expression within the induced MSC population after 12 days of induction. Staining of induced cells showed the presence of α-SMA in stress fibers (Fig.5B) In contrast, the control MSCs, also cultured for 12 days at similar condition in DMEM with 5% FBS and 1% antibiotics showed no visible staining for α-SMA.

The expression of SMC-specific genes was assessed using PCR. A distinct upregulation of Acta, Calponin and Myh11 was observed in the MSCs-SMCs 12 d group and was absent in the control MSCs. Fig.5C shows the bands for Acta (722 bp), Calponin (682 bp) and Myh11 (661 bp). This gene expression profile is consistent with a mature SMC phenotype, corroborating the IF findings.

Endothelial Cell Differentiation

The endogenic differentiation of MSCs was induced by a cocktail of VEGF (5 ng/mL), bFGF (10 ng/mL), IGF (20 ng/mL), EGF (5 ng/mL) and ascorbic acid (1 μmol/L).

Morphological transition of MSCs to an endothelial phenotype over a 12-day period (Fig.6) was observed. Upon treatment, MSCs initially exhibited a characteristic spindle-shaped morphology. However, by Day 12, a visible shift towards a cobblestone pattern, typical of endothelial monolayers, was detected. This change suggests endothelial maturation and the establishment of cell-cell interactions, characteristic of in vivo endothelial networks.

IF staining provided an assessment of endothelial differentiation. MSCs-EC induced for 12 days showed a strong expression Pecam 1, as seen in Fig.6B. Control culture of MSCs cultured at similar conditions, however, without addition of GFs and ascorbic acid, showed minimal expression of Pecam 1. Molecular characterization through PCR analysis revealed the upregulation of EC-specific markers Pecam1 and Cd34 in MSCs post-induction (Fig.6C). 1.5% agarose gel electrophoresis detected bands for Pecam 1 (352 bp) and CD 34 (588 bp). Notably, expression of Pecam 1 and CD34 genes are absent in control MSC culture that was cultivated in similar conditions for 12 days at DMEM supplemented with 5% FBS and 1% antibiotics.

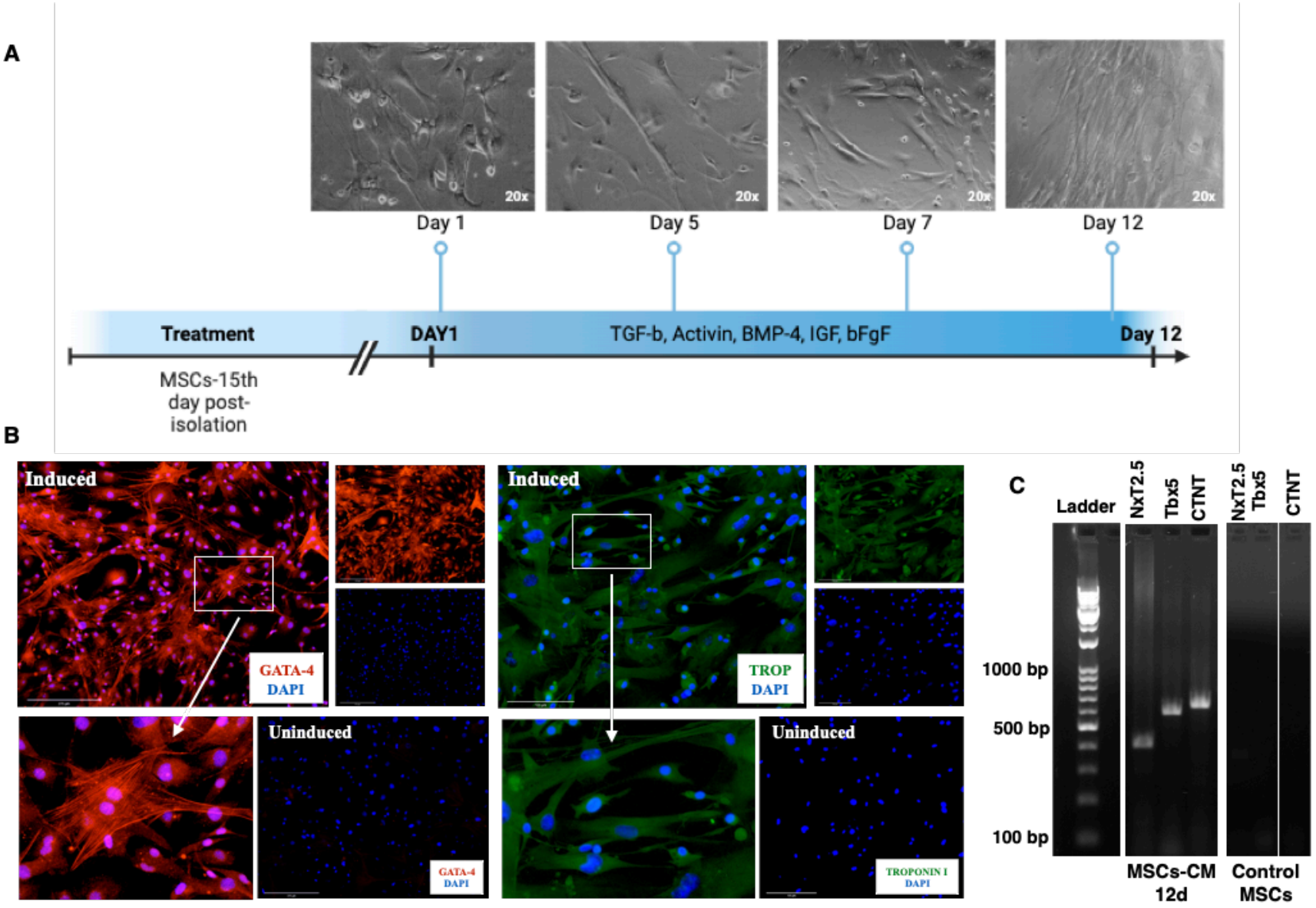
A
20x
20x
20x
20x
Day 1
Day 5
Day 7
Day 12
Treatment
DAY1
TGF-b, Activin, BMP-4, IGF, bFgF
Day 12
MSCs-15th day post-isolation
B
Induced
GATA-4
DAPI
Induced
TROP
DAPI
Uninduced
GATA-4
DAPI
Uninduced
TROPONIN I
DAPI
C
Ladder
NxT2.5
Tbx5
CTNT
NxT2.5
Tbx5
CTNT
1000 bp
500 bp
100 bp
MSCs-CM 12d
Control MSCs

Figure 14. Differentiation of MSCs into cardiomyocytes (A) Morphological changes in MSCs over a 12-day culture period post-induction with TGF-β, Activin, BMP-4, IGF, and bFGF. Images at 20x magnification. B) Immunofluorescence analysis of MSCs. Induced cells display strong nuclear GATA-4 expression (upper left panel, red), indicative of cardiomyocyte type commitment, with nuclei counterstained with DAPI (blue). Scale bar, 275 μm. Troponin I (TROP I) expression in induced cells (upper right panel, green) further validates cardiomyogenic differentiation, with DAPI counterstaining (blue). Scale bar, 125 μm. Uninduced MSCs show minimal GATA-4 (lower left panel) and TROP I (lower right panel) staining, demonstrating specificity of the differentiation protocol. Scale bars, 275 μm and 125 μm, respectively. Insets: Higher magnification of boxed areas to highlight specific marker expression. C) PCR analysis confirming the upregulation of cardiomyocyte-specific genes Nkx2.5, Tbx5, and CTNT in induced MSCs compared to undifferentiated control MSCs at day 12. A 1000 bp DNA ladder is included for size reference.

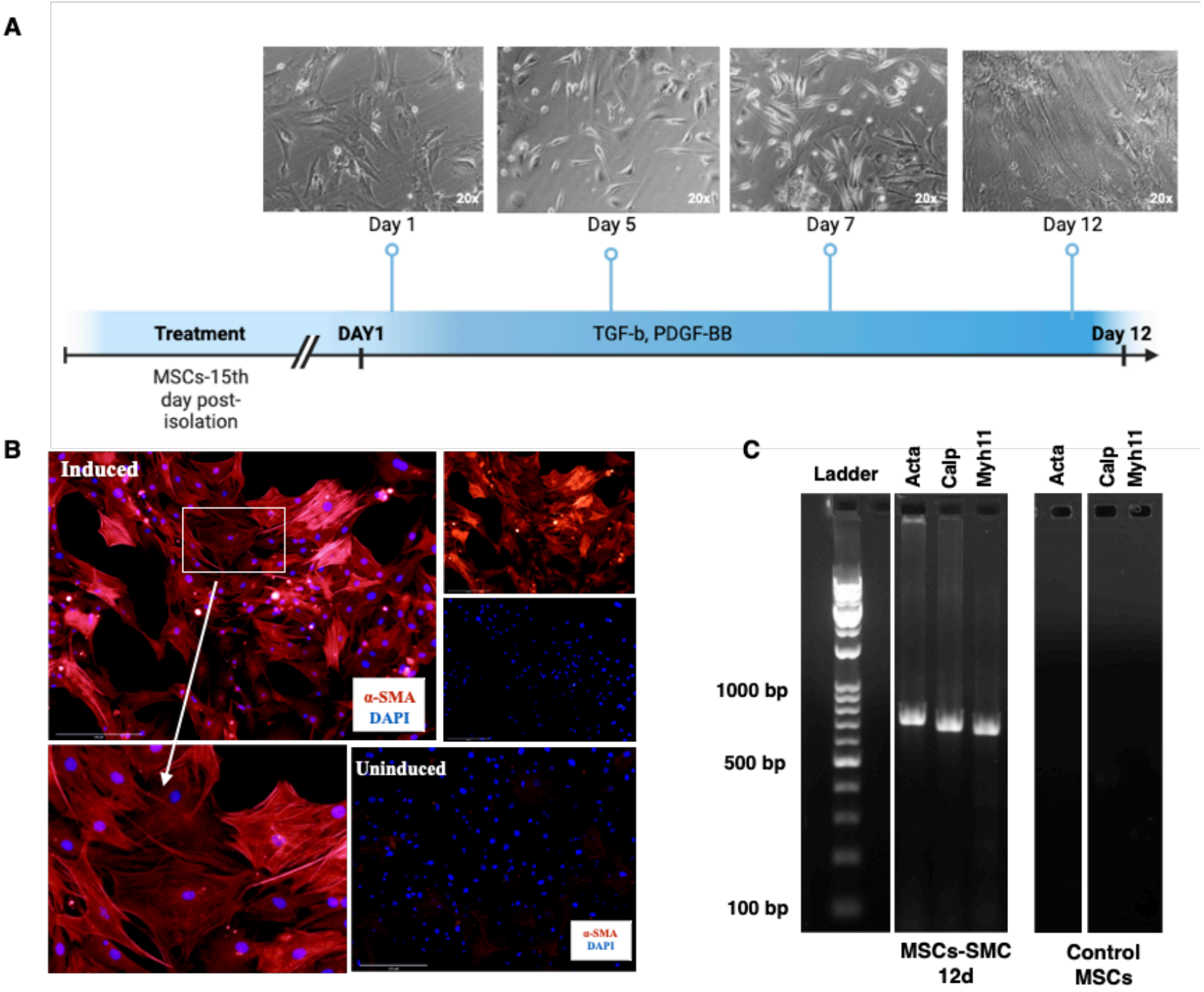
A
20x
20x
20x
20x
Day 1
Day 5
Day 7
Day 12
Treatment
DAY1
TGF-b, PDGF-BB
Day 12
MSCs-15th day post-isolation
B
Induced
α-SMA
DAPI
Uninduced
α-SMA
DAPI
C
Ladder
Acta
Calp
Myh11
Acta
Calp
Myh11
1000 bp
500 bp
100 bp
MSCs-SMC 12d
Control MSCs

Figure 15. Differentiation of MSCs into SMCs. A) Morphological changes in MSCs over a 12-day culture period with TGF-β and PDGF-BB treatment, captured at 20x magnification. B) Immunofluorescence analysis: Induced cells exhibit strong α-SMA expression (upper panel, red), a marker for SMC differentiation, with nuclear counterstaining by DAPI (blue). Scale bar, 200 μm. Lower panel shows uninduced MSCs with minimal α-SMA staining, confirming the specificity of the induction protocol. Insets: Higher magnification of boxed areas to highlight specific marker expression. C) PCR analysis demonstrating the expression of SMC-specific genes Acta2 (α-SMA) and Myh11 in induced MSCs-SMC at day 12, with no significant expression detected in control MSCs. A 1000 bp DNA ladder provides size reference.

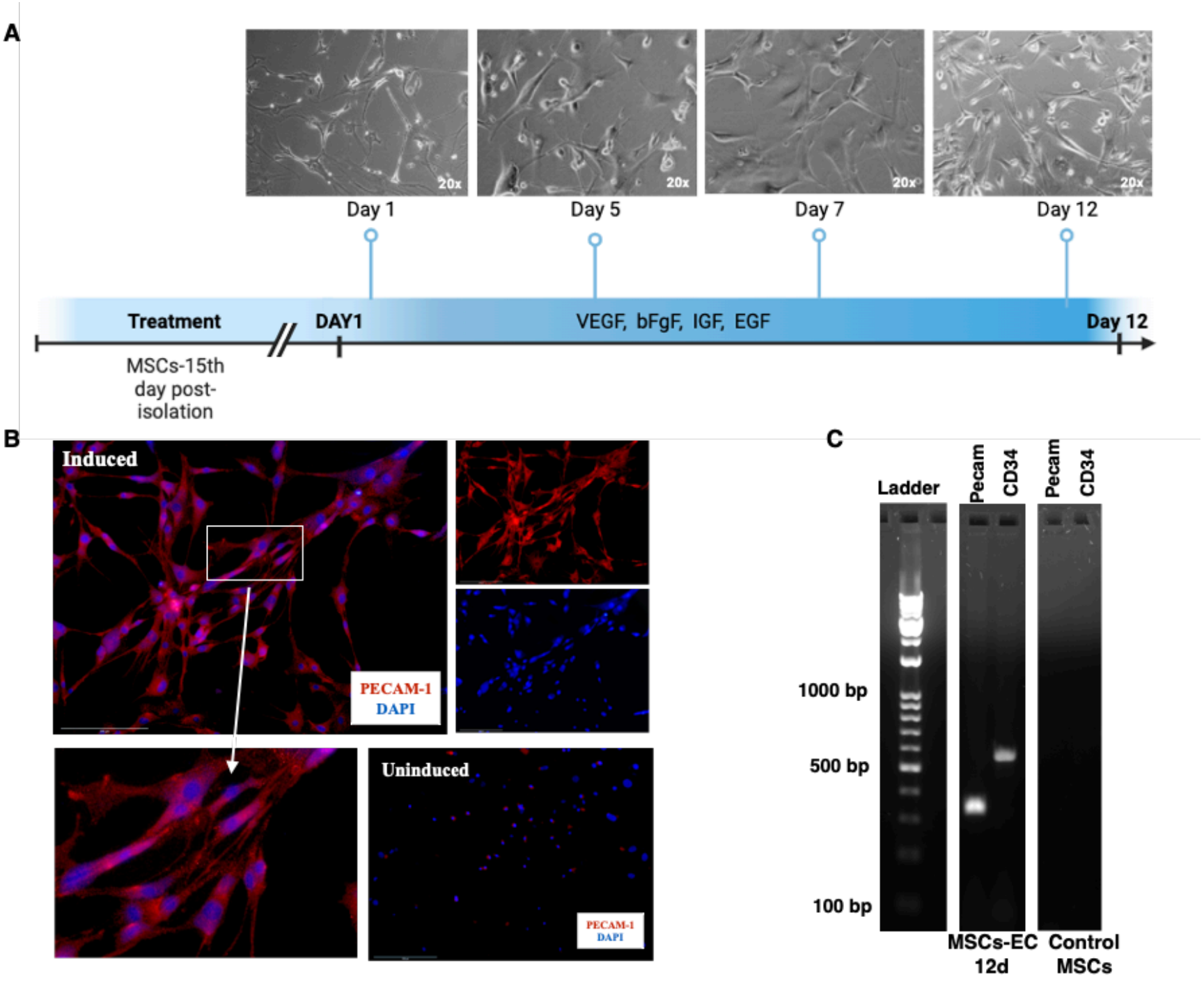
A
20x
20x
20x
20x
Day 1
Day 5
Day 7
Day 12
Treatment
DAY1
VEGF, bFgF, IGF, EGF
Day 12
MSCs-15th day post-isolation
B
Induced
PECAM-1
DAPI
Uninduced
PECAM-1
DAPI
C
Ladder
Pecam
CD34
Pecam
CD34
1000 bp
500 bp
100 bp
MSCs-EC 12d
Control MSCs

Figure 16. Differentiation of MSCs into ECs. A) MSCs exhibit morphological changes throughout a 12-day culture period following induction with VEGF, bFGF, IGF, and EGF, shown at 20x magnification. B) Immunofluorescence staining indicates that induced cells express PECAM-1 (upper panel, red), a marker indicative of EC differentiation, with nuclei counterstained with DAPI (blue). Scale bar, 200 μm. The absence of PECAM-1 expression in the lower panel confirms the specificity of staining in uninduced MSCs. Insets: Higher magnification of boxed areas to highlight specific marker expression. C) PCR results show the presence of Pecam1 and Cd34 mRNA in induced MSCs-EC at day 12, while these EC-specific markers are not detected in control MSCs. A DNA ladder is included to estimate the size of the PCR products.

DISCUSSION

The presence of heterogeneous outcomes among patients who receive treatment with autologous stem cells is known as a barrier to wider clinical acceptance of cell-based therapy in cardiovascular medicine. Some research shows that there are people who possess MSCs with an inherent ability to regenerate cardiac tissue. The reparative stem cells were identified by an increase in the expression of cardiac transcription factors. This indicates that a proactive cardiac specification could potentially improve the effectiveness of MSC therapy. (Clavel & Verfaillie, 2008; Dimmeler & Leri, 2008)

MSCs are the preferred source for use in regenerative medicine, including cardiac repair, due to their ease of access from various tissues in the adult body, relatively simple isolation, and general immune tolerance. Their positive effect on cardiac tissue was shown in preclinical and clinical studies. However, therapeutic efficacy is compromised due to phenotype heterogeneity among patients (Psaltis et al., 2008).

Assessment of adult stem cells having inherent reparative abilities revealed characteristics linked to their regeneration effectiveness, which correlate with the activation of both early and late cardiac transcription factors (Behfar et al., 2010). Cardiac transcription factors are also present in embryonic stem cells and play a crucial role in their response to specific cardiogenic stimuli. Pluripotent stem cells also have a unique ability to easily undergo a process of lineage specification, driven by coordinated and targeted signaling, leading to cardiac differentiation (Behfar et al., 2007; Faustino et al., 2008).

Adult stem cells, however, do not possess similar plasticity and are mainly guided by the environmental conditions *in vivo* (Orlic et al., 2001). The heart after MI loses its main player, cardiomyocytes, the cells responsible for normal heart functionality and construction. The loss of cardiomyocytes during the MI is irreversible. In addition, the post-MI environment demands new vessel formation, meaning the need for new EC and SMC. However, injection of adult stem cells, which are the easy source of stem cells compared to embryonic or pluripotent stem cells, has risks, such as the shift to the different differentiation fate of donor cells. Thus, pre-differentiation of those cells in vitro to trigger their cell fate specification is a favorable approach to minimize cell heterogeneity, enhance the efficacy of cell therapy and decrease the healing period.

In the current study, we used various cocktails of recombinant growth factors to pre-differentiate MSCs in vitro prior to their injection into mouse hearts with MI.

MSCs were isolated from mouse compact bones according to a published protocol (Zhu et al., 2010). Cells were cultured for 14 days in DMEM enriched with 20% FBS for better cell growth on days 1–7, with a subsequent decrease of FBS to 10%. The culture was cleaned from other cell types, such as hematopoietic stem cells, and reached 80% confluence before it was used in further manipulations. Fig.17 demonstrates the process that MSCs underwent to differentiate into required types.

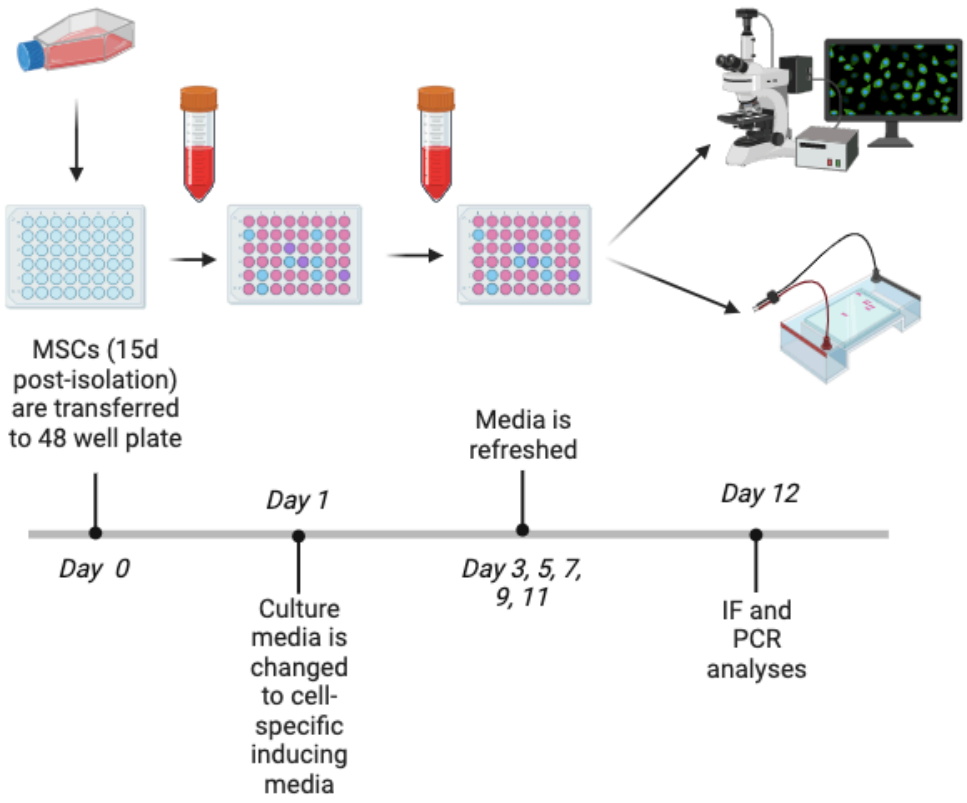

Figure 17. Diagram demonstrating the process of MSCs differentiation into specific cells.

The choice of growth factors, their combination, and concentration were done in accordance with previously published data (Behfar et al., 2010; Lin & Lilly, 2014; Brun et al., 2015; Wang et al., 2018). Thus, a cocktail for cardiac differentiation was chosen based on the study of the treatment of chronic MI in humans with MSCs guided to cardiac cell type (Behfar et al., 2010). Yet, the composition of growth factors was modified and optimized for our study. In addition, retinoic acid was substituted with ascorbic acid. An optimal growth factor combination TGF-β (2.5

ng/mL), Activin-A (5 ng/mL), BMP-4 (5 ng/mL), IGF (50 ng/mL), bFGF (10 ng/mL), and ascorbic acid (1 μmol/L) for cardiac cells was determined. Also, conditions, such as the period of media refreshment, temperature and the induction period were optimized. In previous experiments, where media were refreshed every 3 days, the differentiation process extended and cells started to differentiate in parallel into non-desired cell types, such as adipose cells, thereby disrupting the homogeneity of the culture. Similarly, inducing cells for more than 3 weeks resulted in the appearance of non-specific cells as well as apoptotic cells. Various concentrations of growth factors were analyzed during the study. It was revealed that the shiftment into more concentrated media (higher growth factors concentration) also resulted in apoptotic cell appearance. Less concentrated media did not give the required differentiation level. Therefore, for cardiac differentiation, primary MSCs-15d culture incubated for 12 days in 5% DMEM (with 1% antibiotics), enriched with TGF-β (2.5 ng/mL), Activin-A (5 ng/mL), BMP-4 (5 ng/mL), IGF (50 ng/mL), bFGF (10 ng/mL), where media is refreshed every other day was established as a good strategy for our research (Fig.18). The results were analyzed and confirmed by IF and PCR analyses.

To choose growth factor cocktails for SMC and EC, various studies were taken into account, and the most optimal growth factors and their concentrations were chosen and examined (Narita et al., 2008; Gong et al., 2009; Sivaraman et al., 2021; Hegner et al., 2016; Khaki et al., 2018; Yao et al., 2020). Thus, for SMC, the cocktail was composed of TGF-β (5 ng/mL), PDGF-BB (10 ng/mL), and ascorbic acid (1 μmol/L). For EC differentiation, cells were cultured with VEGF (5 ng/mL), bFGF (10 ng/mL), IGF (20 ng/mL), EGF (5 ng/mL), and ascorbic acid (1 μmol/L). Similarly, the conditions for EC and SMC were identical to CM, where cells were induced for 12 days with the fresh media introduced every other day (Fig.18).

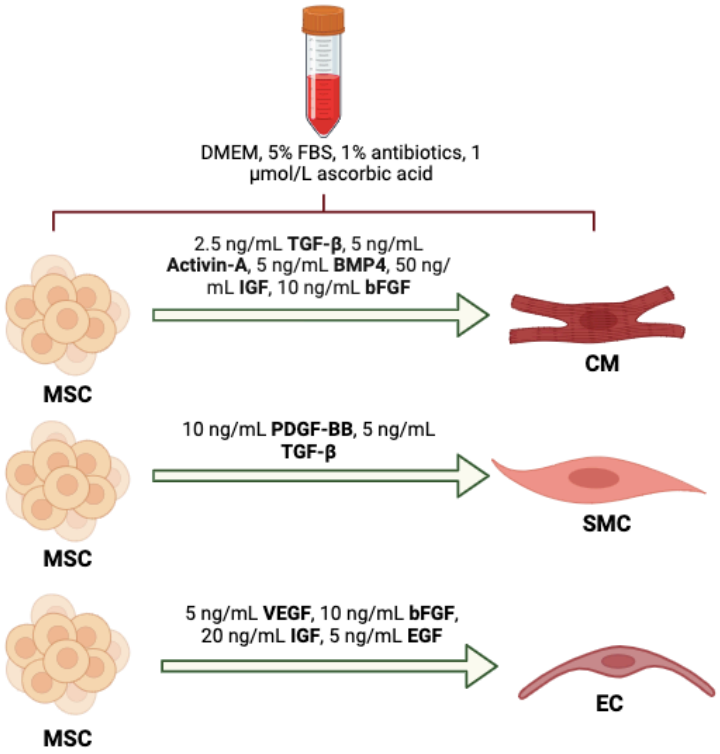

Figure 18. Inducing media for cell differentiation into CM, SMC and EC.

Overall, IF staining and PCR analysis for all 3 types of cells showed a good differentiation profile. IF staining results presented in this study proved the successful in vitro differentiation of MSCs into three types. The selective expression of GATA-4 and cardiac Troponin I in the induced MSCs, as illustrated in the IF staining, aligns with their expected localization in CMs, indicating not only lineage commitment but also a functional specialization. Similarly, the appearance of α-SMA in a pattern characteristic of SMCs corroborates the effective differentiation of MSCs into the SMC. Furthermore, the EC differentiation was indicated by CD31 staining, which is essential for forming the intercellular junctions that are a signature of endothelial networks.

The selected markers are cell-specific, meaning they are distinct identifiers for the corresponding cell types and serve as a reliable framework for confirming the differentiation process. The nuclear localization of transcription factors such as GATA-4 and the cytoplasmic distribution of structural proteins like cardiac Troponin I and α-SMA serve as additional confirmation of cellular identity and maturity. The contrast in staining between the MSC-treated and MSC-control groups clearly shows the difference between the populations that have undergone differentiation and those that have not.

To further analyze the differentiation capacity of MSC-treated groups PCR analysis on cell-specific genes was performed. The selection of specific genes was done due to the established roles these genes play in the development, function, and identification of each cell type.

Thus, for CM molecular analysis, the expression of three genes was studied. Nkx2.5 encodes a homeobox-containing transcription factor that is critical for early heart development. It is one of the earliest markers of cardiac lineage commitment and is involved in the development of the heart's conduction system and the regulation of other cardiac-specific genes (Akazawa & Komuro, 2005). Next, Tbx5 is another essential transcription factor that is involved in the regulation of heart development (Steimle & Moskowitz, 2017). CTNT, in turn, is part of the troponin complex of muscle fibers and is integral to muscle contraction. The cardiac isoform of Troponin T is specific to the heart muscle and is a reliable marker for the presence of functional cardiomyocytes (England et al., 2016).

In terms of Acta2, Calponin, and Myh11 expressions, Acta2 encodes an isoform of actin that is specific to smooth muscle cells. It is part of the contractile apparatus and is essential for SMC function. Its expression is a hallmark of mature SMCs (Moiseenko et al., 2017). Calponin is involved in the regulation of the contractile state of smooth muscle and is used as a marker of smooth muscle differentiation (Miano & Olson, 1996). Myh11 encodes smooth muscle myosin, which is a major contractile protein. It is specific to smooth muscle cells and is crucial for their motility and contractility (Myh11 Myosin, Heavy Polypeptide 11, Smooth Muscle [Mus Musculus (House Mouse)] - Gene - NCBI, n.d.)

Finally, for EC molecular typing, the Pecam1 and CD34 genes were chosen. PECAM1 is a cell adhesion molecule expressed on the surface of endothelial cells and plays a role in the formation of intercellular junctions. It is involved in endothelial cell-cell interactions and in the transmigration of leukocytes across the endothelium (Baldwin et al., 1994). CD34, in turn, is a well-known marker of hematopoietic stem cells but is also expressed on the surface of endothelial progenitor cells and mature endothelial cells, particularly those that line the blood vessels of the heart. It is implicated in the modulation of endothelial cell adhesion and is commonly used as a marker to identify endothelial cells (Hassanpour et al., 2023).

Overall, the expression of these genes, as seen in results, confirmed the identity of the differentiated cells and also demonstrated the functional state of the cells, which is crucial for their intended therapeutic roles in cardiac regeneration.

The morphological and molecular characteristics of the induced cells align with those expected of CM, EC and SMCs. These findings, supported by both phenotypic observations and molecular assays, affirm the potential of MSC-derived CM, EC, and SMC for use in repairing the damaged myocardium and vasculature in the heart following an MI event, marking a significant stride towards the realization of MSC-based therapies in clinical settings.

In conclusion, the successful transformation of MSCs into CMs, SMCs, and ECs as verified by both morphological and molecular markers, confirms their suitability for use in in vivo studies. The cells demonstrated in vitro differentiation markers and thus can be further injected into animal models of MI for research purposes. This allows their regenerative potential to be used for tissue repair and functional recovery. The comprehensive characterization ensures that the differentiated cells meet the essential requirements for translational research, providing a foundation for their use in preclinical models of cardiac injury.

CHAPTER 3: IN VIVO ANALYSIS OF REGENERATIVE TREATMENTS POST-MI

METHODS

Mice

Male C57BL/6 mice, aged 10-12 weeks were purchased from the Jackson Laboratory ((Strain #:000664, RRID:IMSR_JAX:000664, Common Name: B6J, B6/J)

The use of animals was approved by the Institutional Animal Care and Use Committee of the autonomous organization of education “Nazarbayev University" (IACUC). All the manipulations were administered according to IACUC protocol. Mice were housed in cages containing wood fiber bedding, 65 % relative humidity, and 12:12 light-dark cycle. To minimize the pain during the study, all the manipulations were conducted using anesthesia.

Left Anterior Descending (LAD) Model of MI

150 C57BL6 mice aged 10 to 12 weeks were used for in vivo experiments. The protocol for the study was reviewed and approved by the Nazarbayev University's Institutional Animal Care and Use Committee. MI was induced by the permanent ligation of the LAD coronary artery. Briefly, the animals were first anesthetized with 4 % isoflurane and 100 % oxygen for 2-3 min in the anesthesia induction chamber. Following that, endotracheal intubation was performed, and the animal was connected to the MINIVENT mouse ventilator set at tidal volume of 240 µl/stroke and ventilation rate of 140 strokes/minute with 2 % isoflurane and 100 % oxygen. Next, thoracotomy at the 3rd intercostal space between 3rd and 4th ribs was performed, and the heart was adequately exposed using self-made chest retractors. The pericardium was then removed, and the LAD was visualized with the ZEISS Stemi 508 stereo microscope. The vessel was ligated using 7-0 suture 2–3 mm below the auricle of the left atrium. The successful occlusion was confirmed by discoloration of the left ventricle below the ligature. After the ligation, the chest wall and skin were closed, the anesthesia was switched off, and the animal was monitored until the appearance of spontaneous breathing. The animal was then extubated and placed into a clean cage.

The detailed protocol for LAD surgery is available at the appendix section.

Cryo/GFs Injections

Cryo/GFs were prepared as previously described. For in vivo study, intramyocardial injections of Cryo/GFs were administered at two different time points. Cryo/IL-10/TGF-β1 (30 μL) was injected right after the LAD ligation and induction of MI into three points (10 μL each) of the infarction border zone. Second, Cryo/VEGF/bFGF (30 μL) injection was delivered through a 27-G needle using an ultrasound-guided closed-chest procedure on day 4 post-MI. The syringe was fixed in a micromanipulator (VisualSonics) prior to the injection and both the needle and RMV scanhead probe were aligned along the long-axis of LV. Under the control of ultrasound field-of-view, the needle tip was positioned in the desired location within the myocardium for the delivery of injections.

Pre-differentiated Cells Injections

MSCs were subjected to CM, EC, SMC inducing media for two weeks prior to injections. The differentiation status was accessed using IF and PCR analyses targeting specific biomarkers. On the day of injection, pre-differentiated cells were harvested, counted using a haemocytometer. Cell suspensions were then prepared, comprising 76% CM (456,000 cells), 10% EC (60,000 cells), and 14% SMC (84,000 cells), resulting in a final concentration of 600,000 cells per 30 μL injection. The cells were resuspended in sterile 1x PBS and aliquoted into sterile 1.5 mL Eppendorf tubes. Each cell suspension was apportioned according to the number of mice in the study and maintained on ice at +4°C until administration. Intramyocardial injection was administered at one LV site near the infarct border zone. 30 μL of cell suspension was delivered through a 27-G needle using an ultrasound-guided closed-chest procedure. The syringe was fixed in a micromanipulator (VisualSonics) prior to the injection and both the needle and RMV scanhead probe were aligned along the long-axis of LV. Under the control of ultrasound field-of-view, the needle tip was positioned in the desired location within the myocardium for the delivery of injections.

Transthoracic Echocardiography

Transthoracic echocardiography was performed on operated mice 2 times, on week 1 and week 4 post-MI, under the anesthesia with 2% isoflurane. Measurements of left ventricles were collected on a short axis view using M- and B- modes at the level of papillary muscles. Measurements were performed on VEVO 2100 Imaging System. Vevo LAB software was used to

analyze collected data (left ventricular ejection fraction (EF), fractional shortening (FS), systolic diameter (SD), diastolic diameter (DD)) after the final round of echocardiography.

Immunohistochemical Analysis (IHC)

IHC analysis was performed at 2 time points, at week 1 and week 4. For the analysis, mice were euthanized by cervical dislocation. The hearts were extracted, washed 3 times with cold PBS for 5 mins each and fixed in 4% paraformaldehyde solution for 24 hours at + 4°C. This was followed by leaving hearts in 15% and 30% sucrose solution for 12-24 hours. Next, hearts were transferred into individual pre-labeled tissue base molds and fully covered with cryo-embedding media (OCT). After that, hearts in base molds were placed into liquid nitrogen to ensure tissue is completely frozen. Frozen tissue was stored at -80°C until sectioning.

At the day of sectioning, frozen hearts were transferred into a cryotome cryostat (-20C) and cut into 5-µm-thick sections at the specific LV regions with expected infarction zone (CryoStar™ NX70 Cryostat). Sections were placed into pre-labeled positively charged glass slides and stored at -80°C until the staining procedure.

IHC started with washing sections with cold 1xPBS for 3 times 5 mins each. Sections were then blocked in blocking solution (5% BSA + 0.1% Triton X-100 in 1X PBS) for 1 hour at RT, followed by staining with 1'Ab (Troponin I, alpha-SMA, CD31, CD68, CD206 and CD3 to stain cardiomyocytes, smooth muscle cells, endothelial cells, M1 macrophages, M2 macrophages and T cells respectively) overnight at +4°C in a concentration of 1:500. Next day sections were washed 3 times with cold PBS and 2' Ab (goat anti-mouse Alexa 647) in a concentration of 1:1000 were added, followed by incubation for 1 hour at RT in the dark. Next, sections were washed 2 times with cold PBS, and counterstained with DAPI for 10 mins at the concentration of 1:2000. This was followed by a final wash with PBS. Mounting buffer was dropped carefully to slides, which were then covered with coverslips and the edges were fixed with transparent nail polish. Slides were stored in the dark at +4°C until analyzed. Analysis was performed using the EVOS FL Auto 2 Cell imaging system.

Histological Analysis

To assess scar size, tissue sections were stained using Masson's Trichrome stain (Carl Roth GmbH). Initially sections were rinsed under running tap water for 10-15 minutes. Subsequently,

the sections were stained with Goldner's Stain I (Ponceau-Fuchsin solution) for 10 minutes, followed by a brief rinse in a 1% acetic acid solution for 30 seconds. Then, Goldner's Stain II (Phosphotungstic acid-Orange G solution) was added for 30 minutes for connective tissue decolorization. After another rinse in the 1% acetic acid solution, the sections were counterstained with Goldner's Stain III (Light green SF yellowish solution) for 5 minutes. Finally, slides were washed in a 1% acetic acid solution for 5 minutes, and dehydrated by ascending alcohol series. Slides were then cleared in xylene, and mounted with a mounting medium.

Masson's Trichrome stained cytoplasm and muscle fibers in red and the scar tissue in green. The color differentiation allowed for a precise evaluation of scar size in the heart tissue.

Detection of pro- and anti-inflammatory cytokines expression via qPCR

Real-time PCR analysis was performed for each experimental group (Control, Cells, Cryo/GFs, Cryo/GFs/Cells), targeting specific genes as markers of interest: TGF-β, IL-10, IL-4, IL-6, IL-1β, and TNF-β. Total RNA was extracted from the samples using the Invitrogen PureLink RNA Mini Kit (cat-12183018A). The extracted RNA was then reverse-transcribed into complementary DNA (cDNA) using the Abcam cDNA Synthesis Kit (ab286905). The cDNA synthesis protocol was as follows: 1 µl of RNA sample was added to 1 µl of primers, 1 µl of dNTP Mix, and nuclease-free water up to 20 µl. This mixture was supplemented with 4 µl of 5X RT Buffer and 1 µl of Novo RTase (200 U/µl), the latter containing RNaseOFF Ribonuclease Inhibitor. The reaction mixture was gently mixed and briefly centrifuged before incubating for 15 minutes at 53°C. The reaction was then halted by heating at 85°C for 5 minutes. The resultant first-strand cDNA was stored at -20°C until use. The purity and concentration of obtained RNA and synthesized cDNA was accessed using the NanoDrop system.

Custom-designed and synthesized primers, produced at the National Center for Biotechnology, Astana, Kazakhstan, were utilized for the amplification of the targeted genes. The primers were labeled with Fam-cytokine-BHQ1. Alongside these genes, Actin served as a housekeeping gene for data normalization.

TaqMan Fast Advanced Master Mix (10 µl) was mixed with primer mix (1 µl forward primer (0.5 uM), 1 µl reverse primer (0.5 uM), 0.5 µl probe(0.2 uM)), cDNA (1 µl of diluted cDNA) and nuclease-free water up for the 20 µl reaction.

The PCR amplification was carried out using a Real-time PCR system (CFX96, Bio-Rad). The cycling conditions were set as follows: initial denaturation at 94°C for 3 minutes, followed by 50 cycles of denaturation at 94°C for 10 seconds, and annealing at 57°C. The TaqMan probe labeled Fam-cytokine-BHQ1 was incorporated to enable real-time detection of the amplified product. Rox-Actin-BHQ2 primer was incorporated into Actin for data normalization.

The analysis was performed in triplicate for each target gene to ensure the accuracy and reproducibility of results. These triplicates included both technical replicates, to control for variation in the PCR process, and biological replicates, to account for biological variability among samples. The mean value of the triplicate measurements was used for subsequent statistical analysis.

Data analysis was conducted using the double delta Ct method to determine relative gene expression levels. Statistical analysis of the data was performed using one-way ANOVA with Tukey's post-hoc test, employing GraphPad Prism software (version 10).

Primer sequences for this study can be found in appendix(B) section.

Statistical Analysis

All the groups were first checked for normality. One-way ANOVA test was then used to compare means of the treatment groups for echocardiography, IHC, Real-time PCR and fibrotic area measurements. Tukey's post-hoc test was done to compare groups. The data presented as means and standard deviations. Significance level was set as p values < 0.05. Statistical analysis and graph plotting were performed employing GraphPad Prism software (version 10).

RESULTS AND DISCUSSION

1. LEFT ANTERIOR DESCENDING (LAD) MODEL OF MI

In the present study, an *in vivo* model of MI using mice was developed to evaluate the therapeutic efficacy of various treatments on cardiac functions. The model was established following a protocol to ensure consistency and reliability across all experimental groups.

Prior to the induction of MI, mice were anesthetized using a ventilation system delivering 4% isoflurane and 100% oxygen to maintain sedation without compromising the animals' physiological stability. Anesthesia was initiated with an induction phase of 1-2 minutes, ensuring a depth sufficient for the duration of the surgical procedure.

Post-induction, the mice were intubated to secure an airway, facilitating mechanical ventilation. This critical step was performed quickly, within a 30-second window, to minimize stress and prevent hypoxia. Subsequently, the animals were connected to a ventilator system, ensuring they received a consistent tidal volume and optimal respiratory rate throughout the surgical procedure.

The surgical induction of MI was achieved by ligating the left anterior descending (LAD) artery. The procedure commenced with a left thoracotomy to expose the heart, followed by the identification and ligation of the LAD artery (Fig.19A). This critical step was accurately carried out under magnification to ensure precision and to minimize unintended tissue damage. Upon successful ligation, which was typically achieved within 20-30 minutes after the beginning of the surgery, the ischemic area was visibly pale, confirming the occlusion of the artery and the establishment of an MI model (Fig.19B).

Following the surgical procedure, the chest wall was sutured and the mice were closely monitored during the recovery phase to ensure their well-being and to identify any immediate post-operative complications (Fig.19C).

To confirm the successful establishment of a MI model, and to validate the use of the control group for comparison with subsequent treatments, 3 groups of mice were compared: control: LAD ligation without treatment (number of mice in group - 5), sham operated: open chest operation without LAD ligation (number of mice in group - 6) and healthy: no intervention, (number of mice in group - 6). Cardiac activity was assessed at week 1 post-intervention via the US. Analysis revealed significant impairment in the control group compared to both the healthy and sham

operated groups. Marked negative alterations were observed in EF (control: 23±6.4%, sham: 56±5.5%, healthy: 60±3.0%), FS (control: 10±3.1%, sham: 29±3.5%, healthy: 32±2.1%), SD (control: 4.3±0.37 mm, sham: 3.0±0.33 mm, healthy: 2.9±0.14 mm), and DD (control: 5.0±0.42 mm, sham: 4.2±0.39 mm, healthy: 4.3±0.14 mm) in the control group compared to the sham and healthy cohorts (Fig.19D).

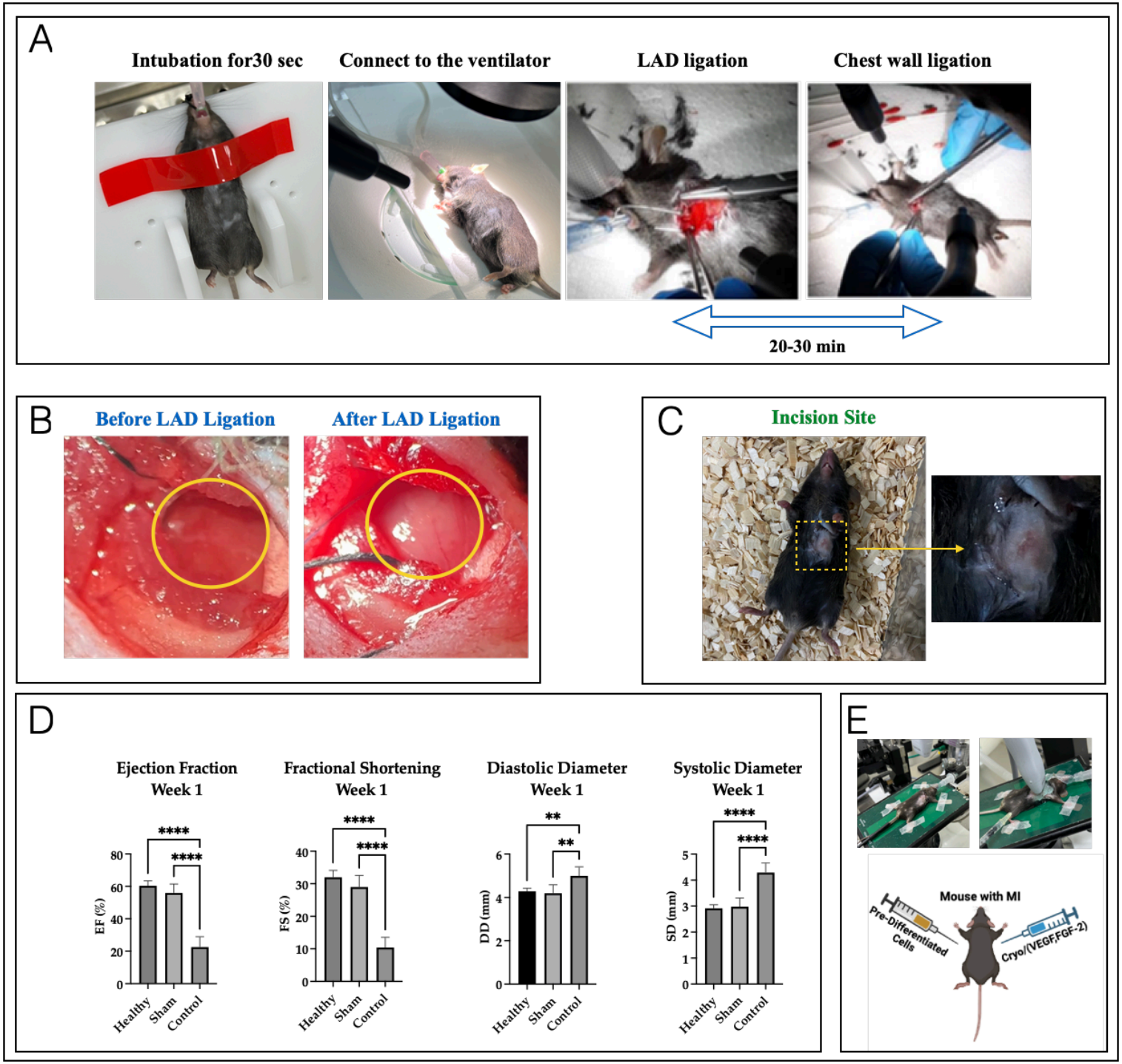
A
Intubation for30 sec
Connect to the ventilator
LAD ligation
Chest wall ligation
20-30 min
B
Before LAD Ligation
After LAD Ligation
C
Incision Site
D
Ejection Fraction Week 1
Fractional Shortening Week 1
Diastolic Diameter Week 1
Systolic Diameter Week 1
EF (%)
FS (%)
DD (mm)
SD (mm)
Healthy
Sham
Control
E
Mouse with MI
Pre-Differentiated Cells
Cryo/(VEGF,FGF-2)

Figure 19. Overview of the LAD ligation procedure and equipment used in the study A) LAD coronary artery ligation in C57BL6 mice, for inducing MI as part of an experimental murine MI model. B) Cardiac region before and after MI induction. Pale region indicates successful ligation. C) Mouse post-surgery, with an indication of the incision site. D) Evaluation of heart functions across three groups: healthy (no intervention, n=6), sham (open chest operation without LAD ligation, n=6), and control (LAD ligation without any treatment, n=5), conducted at week 1 through US analysis. Cardiac functionality in the control group was significantly reduced as indicated by alterations in EF, FS, SD, and DD, confirming the successful induction of MI in the control group. E) The ultrasonographic system used in the study. The system facilitates the non-invasive administration of the therapeutic agents (Cryo/VEGF,FGF-2, cells) into the murine subject, guided by ultrasonic imaging. Right images demonstrate the fixation of the mouse prior the injection of treatment as well as ultrasound analysis to detect the right injection site.

2. IDENTIFICATION OF OPTIMAL TIMING FOR CELLULAR INJECTION POST-MI

To define the ideal post-infarct window for pre-differentiated cell injection, a detailed analysis of the cardiac microenvironment at multiple time points following MI induction was conducted. Analysis included echocardiographic measurements at week 4 post-infarction on parameters including ejection fraction, fractional shortening, diastolic diameter, systolic diameter, and cardiac output (Fig.20). Manipulations were performed on mouse-MI models that did not receive any treatments (control MI model).

Day 6 was chosen as an optimal timing for cell injection due to consideration of several factors. First, data from ultrasound analysis revealed the improvement in both EF (Control-Day 6: 49.16±8.2 %, Control-Day 3: 30.8±14 %, Control-Day 1: 38.2±3.1), and FS (Control-Day 6: 26.74±7.1 %, Control-Day 3: 24.9±5.4 %, Control-Day 1: 5.6±4.3 %) in the Control-Day 6 group compared to other treatment groups. These parameters are critical indicators of systolic function, thus even minimal improvements can indicate the recovery potential of the heart. Systolic (Control-Day 6: 3.4±0.6mm, Control-Day 3: 3.6±0.4mm, Control-Day 1: 4.5±1.4mm) and Diastolic diameter (Control-Day 6: 4.5±0.4mm, Control-Day 3: 4.8±0.2mm, Control-Day 1: 5.3±1.3mm) measurements indicated a comparatively more favorable cardiac dimension stability within the Control-Day 6 group. The preservation of consistent cardiac dimensions post-MI is critical for the therapeutic interventions, as significant variances could potentially prevent the homing and functional integration of administered cellular therapies. Those results were taken into consideration when choosing the most appropriate timing.

While the data is not statistically significant, it can reflect a critical window where the myocardium is most receptive to cell therapy.

Second, in addition to echocardiography results, it was taken into consideration that overwhelming the heart with too many injections at once could reduce the efficacy of the treatment. As the injection of Cryo/(IL-10,TGF-β) was set on day of operation, and injection of Cryo/(VEGF/FgF2) was set on day 4, it was suggested that spacing out the injections might be beneficial. Although cytokines and cells can be injected together in some protocols ((Deuse et al., 2009; Nguyen et al., 2010; Spiroski et al., 2022) for the current study, it was decided to choose Day 6 as cell injection timing as it might be advantageous to provide the cytokines and factors first to

create a conducive environment and then perform cell injection. The hypothesis behind stated that Cryo/(IL-10,TGF-β) injection at day of operation would first decrease the degree of inflammation, followed by the injection of Cryo/(VEGF,FgF2), that might provide an environment for new blood vessels formation, thus ensuring better survival and integration of injected pre-differentiated cells.

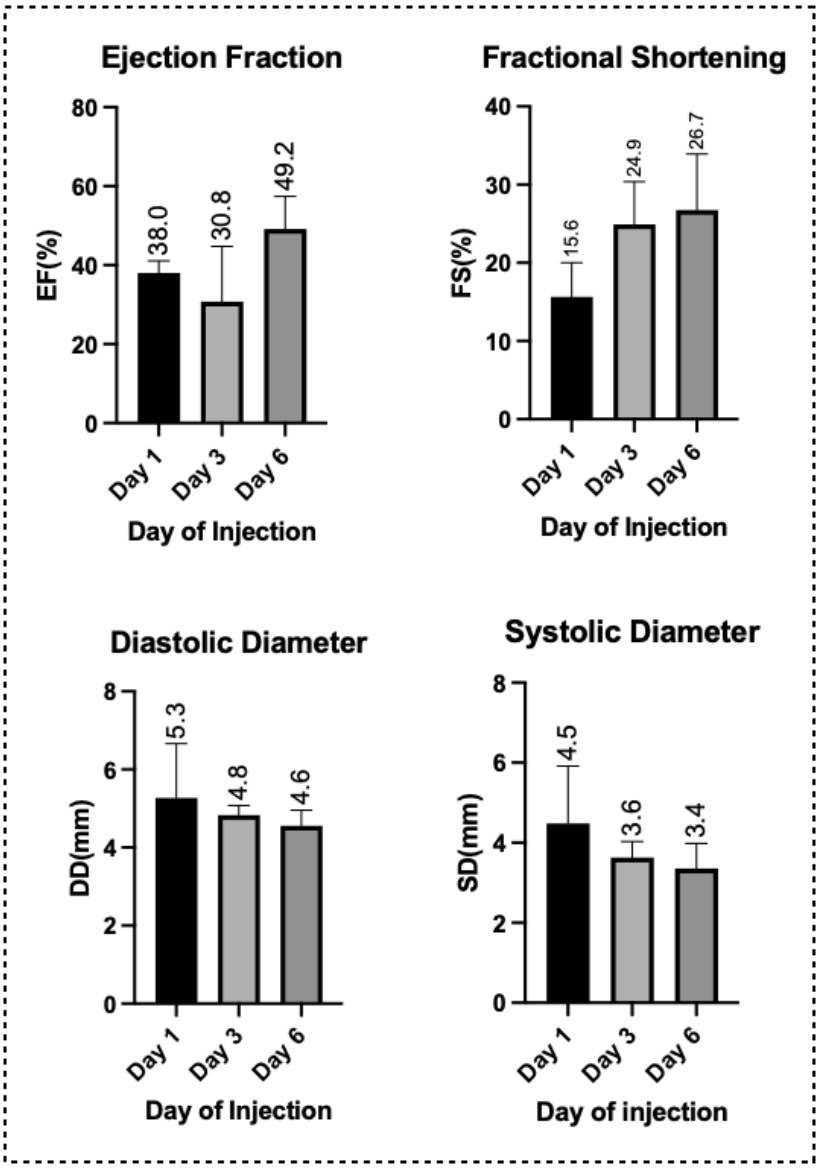

Figure 20. Evaluation of cellular integration and cardiac function at week 4 post-cell injection to determine the optimal timing for therapeutic intervention. The bar graphs present the ejection fraction, fractional shortening, diastolic diameter and systolic diameter, providing quantitative measures of cardiac performance at Days 1, 3, and 6 post-cell injection. Data are presented as mean ± SD, indicating the stabilization of cardiac function by day 6, suggesting this as the optimal time point for intervention.

3. SELECTION OF OPTIMAL TREATMENT GROUPS THOUGH COMPARATIVE ANALYSIS

To establish the most effective therapeutic strategy for myocardial repair post-infarction, we evaluated various treatment modalities across two experimental sets. These sets comprised different combinations of cryogel, growth factors, and cellular therapy. Fig.21 summarizes the combinations of treatment used in this study.

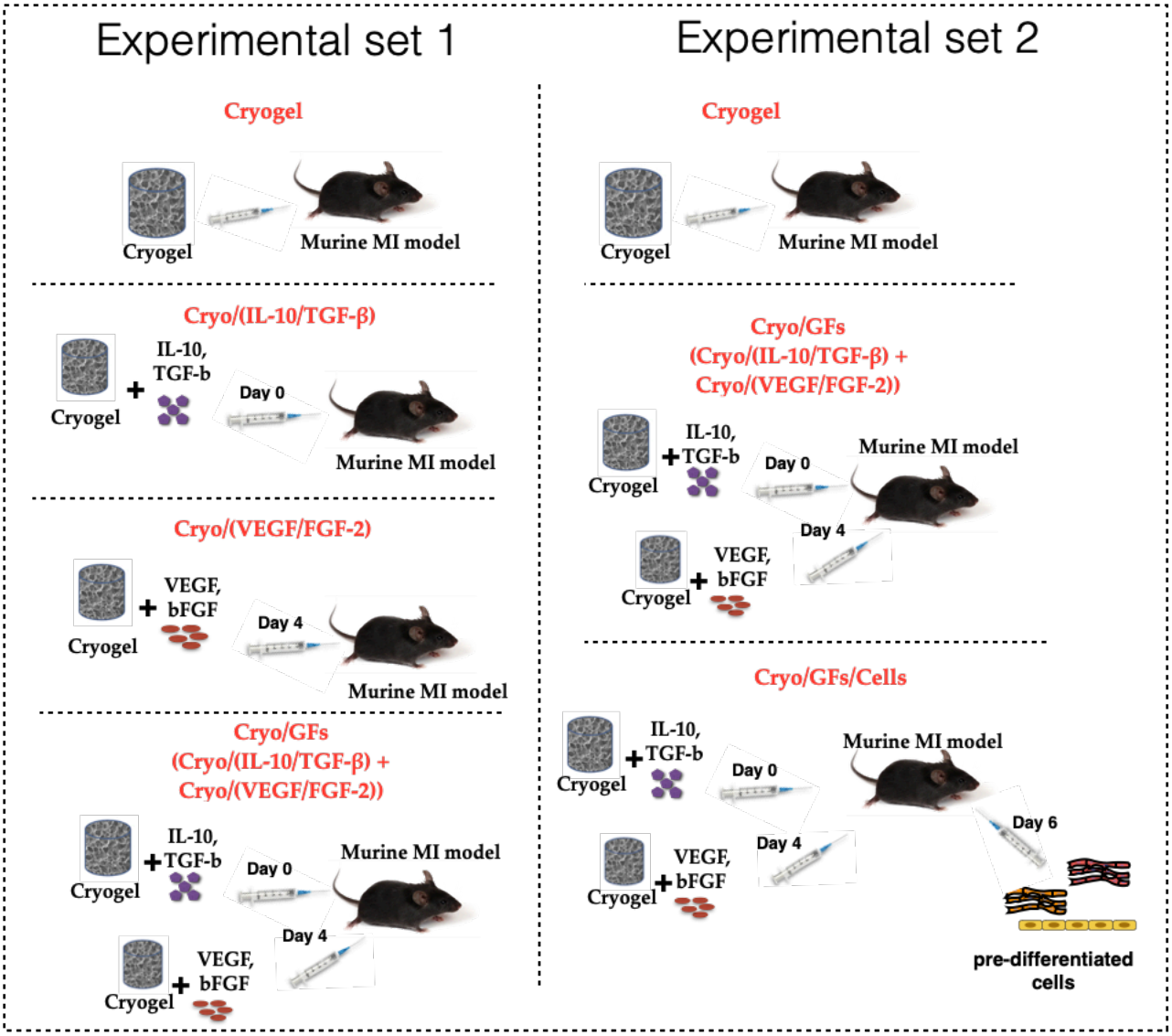

Figure 21. Treatment groups used in the study.

Mice were divided into following groups:

Experimental Set 1:

Group 1: MI-induced control - murine-MI model without any treatment (5 mice in group)

Group 2: Cryogel only - murine-MI model receiving an injection of cryogel immediately after the operation (5 mice in group).

Group 3: Cryo/(IL-10,TGF-β) - murine-MI model receiving an injection of cryogel loaded with IL-10/TGF-β immediately after the operation (6 mice in group).

Group 4: Cryo/(VEGF,FGF-2) - murine-MI model receiving an injection of cryogel loaded with VEGF/FGF-2 at day 4 post-surgery via needle-guided navigation (5 mice in group).

Group 5: Cryo/(IL-10,TGF-β) + Cryo/(VEGF,FGF-2) - murine-MI model receiving first injections of Cryo/(IL-10,TGF-β) directly after the surgery and second injections of Cryo/(VEGF,FGF-2) at day 4 post-surgery via needle-guided navigation.

Experimental Set 2:

Group 1: MI-induced control - murine-MI model without any treatment (9 mice in group).

Group 2: Cryogel only - murine-MI model receiving an injection of cryogel immediately after the operation (7 mice in group).

Group 3: Cryo/(IL-10,TGF-β) + Cryo/(VEGF,FGF-2) - murine-MI model receiving first injections of Cryo/(IL-10,TGF-β) directly after the surgery and second injections of Cryo/(VEGF,FGF-2) at day 4 post-surgery via needle-guided navigation (7 mice in group).

Group 4: Cryo/(IL-10,TGF-β) + Cryo/(VEGF,FGF-2) + Cells - murine-MI model receiving the full treatment, including Cryo/(IL-10,TGF-β) on the day of surgery, Cryo/(VEGF,FGF-2) on day 4, and a cocktail of pre-differentiated cells on day 6.

Guided injections of Cryo/(VEGF,FGF-2) and Cells were done by using the Vevo 3100 Ultra High Frequency ultrasound system. Injections were performed into the LV at the border of the MI zone in PSLAX view. The echocardiographic measurements were performed at week 4 post-surgery (Fig.22).

During the Set 1 experiment the Cryogel group did not exhibit significant improvements in myocardial recovery compared to the control group, as evidenced by ultrasound results (Fig.22A). A subsequent examination (experimental set 2) confirmed results from Set 1 and showed that the

group differed from the control only in Systolic Diameter (Fig.22B). Consequently, the Cryogel group was not included in further studies.

Subsequently, to determine whether the beneficial effects observed in the Cryo/GFs group (Cryo/(IL-10,TGF-β) + Cryo/(VEGF,FGF-2)) resulted from the synergistic action of both factor groups, we separated the group into Cryo/(IL-10,TGF-β) and Cryo/(VEGF,FGF-2). We then assessed their individual impacts on cardiac function. For this, ultrasound parameters including ejection fraction, fractional shortening, diastolic diameter and systolic diameter were analyzed (Fig 11(A)).

The Cryo/(IL-10/TGF-β) group demonstrated significant improvements in ejection fraction and fractional shortening compared to the control group. In contrast, the Cryo/(VEGF/FGF-2) group did not show significant enhancements in these parameters and exhibited a notable decline in regenerative capacity when compared to the combined Cryo/GFs group. This outcome supports the hypothesis that Cryo/(IL-10,TGF-β), administered on the day of the operation, could reduce inflammation and promote a pro-healing environment. Thus, when Cryo/(VEGF,FGF-2) is administered on Day 4, it may benefit a less hostile environment, enhancing its angiogenic effects. When isolated, without prior environmental preparation by IL-10,TGF-β, the VEGF,FGF-2 factors face a challenging environment, which could limit their effectiveness in promoting vessel formation. These results supported the theory of a synergistic effect between the two factor groups. Therefore, the Cryo/(IL-10,TGF-β) and Cryo/(VEGF,FGF-2) groups were also excluded from the further study.

The Cryo/GFs group showed significant cardiac function improvements, as evidenced by the results of set 1 and further confirmed by set 2 experiments. Similarly, the Cryo/GFs/Cells group demonstrated significant results on all parameters. Therefore, both Cryo/GFs and Cryo/GFs/Cells groups were selected for further investigation.

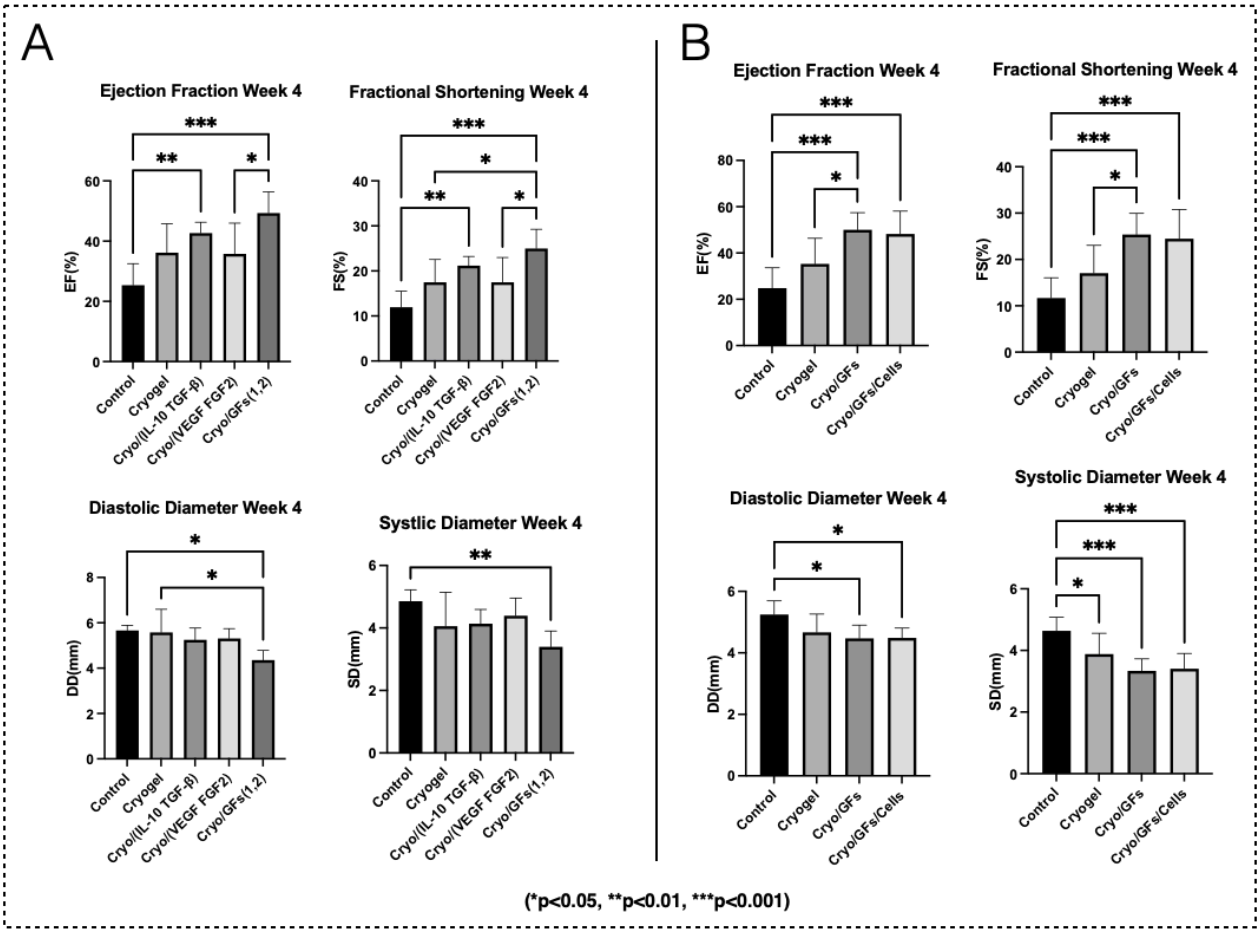

Figure 22. Comparative Analysis of Cardiac Function Following Different Treatment Regimens A) Ultrasound assessment of cardiac function at week 4 post-operation for an experimental set 1. The bar graphs represent the ejection fraction, fractional shortening, diastolic diameter and systolic diameter for the following groups: Control, Cryogel alone (Cryogel), Cryogel with IL-10/TGF-β, Cryogel with VEGF,FGF2, Cryogel with (IL-10,TGF-β)/(VEGF,FGF-2). Asterisks denote statistical significance compared to the control group (*p<0.05, **p<0.01, ***p<0.001). B) Ultrasound assessment of cardiac function at week 4 post-operation for an Experimental set 2. The bar graphs display the same cardiac function parameters as Set 1, for the following groups: Control, Cryogel alone, Cryo/GFs ((IL-10,TGF-β)/(VEGF,FGF2)) and Cryogel with GFs(IL-10,TGF-β)/(VEGF,FGF2) with pre-differentiated cells (Cryo/GFs/Cells). Asterisks indicate the level of statistical significance when compared to the control group (*p<0.05, **p<0.01, ***p<0.001). Data

represent mean ± SD, with statistical analyses conducted to determine the efficacy of each treatment regimen in restoring cardiac functions.

4. COMPREHENSIVE *IN VIVO* ANALYSIS OF CARDIAC REGENERATION ACROSS FOUR TREATMENT GROUPS

The final experimental series encompassed four groups: Control, Cells, Cryo/GFs and Cryo/GFs/Cells. A comprehensive *in vivo* examination was performed using a variety of research methods. Those included ultrasound measurements for accessing cardiac functions, IHC for the detection of specific cellular and molecular markers, histological examination to quantify fibrotic area and real-time PCR for evaluating the levels of pro-inflammatory and anti-inflammatory cytokines. Each analytical method was systematically applied to elucidate distinct aspects of cardiac regeneration and inflammatory response within the different treatment groups. The subsequent sections describe the results of these analyses in detail. In addition, an integrated discussion of individual findings are given for understanding of the overall experimental outcomes.

Ultrasound Measurement of All Groups

The ultrasound measurements were performed at the end of week 1 and week 4 for all groups. The key parameters analyzed included Ejection Fraction (the percentage of blood the left ventricle pumps out with each contraction), Fractional Shortening (the percentage of the diameter the ventricle reduces during contraction), Diastolic Diameter (internal dimension of the ventricle when it is filled with blood) and Systolic Diameter (internal dimension of the ventricle after it has pumped out blood) (Fig.23C). Measurements for other parameters, namely Cardiac Output, Stroke Volume, Diastolic Volume, and Systolic Volume were also performed and the data is provided in the appendix section. The post-hoc analysis, performed to analyze the efficacy of each group on MI treatment is also provided in the appendix section. Notably, at the end of week 1, none of these parameters showed significant differences among the groups (EF-control:46±14%, Cells:41±11%, (Cryo/GF):37±9.8%, (Cryo/GF/Cells):41±10%; FS-control:23±7.5%, Cells:18±5.4%, (Cryo/GF):20±6.1%, (Cryo/GF/Cells):20±5.3%; DD-control:4.5±0.65 mm, Cells:4.4±0.47 mm, (Cryo/GF):4.3±0.51 mm, (Cryo/GF/Cells):4.3±0.60 mm; SD-control:3.5±0.79 mm, Cells:3.6±0.38 mm, (Cryo/GF):3.4±0.51 mm, (Cryo/GF/Cells):3.4±0.57 mm).

This could indicate a similarity in the immediate post-treatment cardiac function across all experimental conditions. Although subsequent sections of the study (IHC, RT-PCR) identified statistically significant positive alterations by week 1, suggesting the activation of a pro-healing

mechanism at the molecular and cellular levels, it may not yet result in observable changes in overall cardiac function.

However, by week 4, significant changes were observed in treatment groups indicating and evaluating the impact of different strategies on cardiac recovery (EF-control:30±10%, Cells:41±7.7%, (Cryo/GF):51±7.0%, (Cryo/GF/Cells):54±7.4%; FS-control:14±5.1%, Cells:21±5.5%, (Cryo/GF):25±5.4%, (Cryo/GF/Cells):28±4.7%; DD-control:5.4±0.53 mm, Cells:4.8±0.35 mm, (Cryo/GF):4.8±0.55 mm, (Cryo/GF/Cells):4.4±0.22 mm; SD-control:4.7±0.72 mm, Cells:3.9±0.57 mm, (Cryo/GF):3.7±0.42 mm, (Cryo/GF/Cells):3.3±0.43 mm). Thus, most significant improvements in the EF, FS, SD and DD were observed in the Cryo/GFs/Cells group. The data are aligned with results observed at experimental set 2 (Fig.22B). These results suggest a potential synergistic effect of combining cell therapy with Cryo/GFs in promoting cardiac recovery post-MI, and highlight the efficacy of the treatments in improving cardiac function. Cryo/GFs group, again, as it was seen in previous Sets (Fig.22) showed significant improvement of all the parameters, with ejection fraction and fractional shortening being almost similarly effective as Cryo/GFs/Cells group, however less effective, yet still significantly better than control, in volumes (Fig.23C). The group with cells also demonstrated significant improvement of ejection fraction, systolic and diastolic volumes however, with no significance in fractional shortening.

The data obtained from ultrasound analysis proved the efficacy of various strategies on promoting cardiac recovery MI. In particular, ejection fraction and fractional shortening parameters, which are critical indicators of the heart's pumping efficiency were significantly improved in Cryo/GFs/Cells and Cryo/GFs groups, exhibiting the functional benefits of treatments. Other parameters, including systolic and diastolic diameters were also significantly reduced in all treatment groups (Cryo/GFs/Cells, Cryo/GFs, Cells), indicating less ventricular remodeling, a common MI consequence. Reduced ventricular dilation is associated with a lower risk of heart failure and better overall cardiac function.

The superior result in the Cryo/GFs/Cells group may be explained by combined benefits of a supportive scaffold, sustained release of reparative GFs, and the direct contributions of the therapeutic cells. Separately, the Cell group had less significant effect on cardiac function compared to Cryo/GFs/Cells and Cryo/GFs, possibly due to cell integration issues, meaning that without the supportive environment provided by the Cryo/GFs, their efficacy could be limited. The Cryo/GFs group, in turn, showed good overall improvement of heart tissue in all the parameters,

although slightly less than the combination therapy group. This suggests that, although growth factors are effective in enhancing cardiac repair, the addition of cells provides a critical component that further amplifies the recovery process.

M-mode echocardiography, which is used to measure and evaluate cardiac function, provided us with a one-dimensional view of the heart. The M-mode traces demonstrated the movement of the heart's walls and the change in ventricular dimensions during the cardiac cycle. The images highlighted more efficient heart movements in treated groups compared to the control (Fig.23D)

Overall, the ultrasound analysis demonstrated the effectiveness of combined Cryo/GF/cells therapy in improving key cardiac function parameters post-MI. The significant improvements observed in the treatment groups compared to the control, especially in parameters like ejection fraction and fractional shortening, offer promising insights into the potential of these therapies in cardiac regenerative medicine.

F-statistic and p-values as well results for post-hoc analysis are provided in the appendix section.

Histological and Immunohistochemical Analysis of Specific Marker Expression

Histology

Histological analysis using Masson's Trichrome staining kit was performed to examine and evaluate the fibrotic region in 3 treatment groups compared to control. For this, week 4 tissue sections with infarct zones from each group were stained and compared. The staining typically colors muscle fibers in red, and collagen in blue or green. It is particularly useful to identify fibrosis, that forms due to excess of fibrous connective tissue in injured heart during the reparative process. Fig.23A demonstrates heart tissue sections of the control group as well as of three treatment groups: Cells, Cryo/GFs, and Cryo/GFs/Cells.

Illustrations display the gradual decrease of fibrotic area from control to combined treatment groups, with Cell group showing lower fibrotic region compared to control, and Cryo/GFs showing similar dynamic towers Cell group. The Cryo/GFs/Cells section appears to have the least amount of blue staining among all the groups, suggesting that the combined therapy provided the most substantial reduction in fibrosis. Quantitative data of the percentage of fibrosis further supported the visual assumption (control: 60.8±3.7 %, cells: 43.3±7.1 %, Cryo/GFs: 36.7±7

%, Cryo/GFs/Cells: 31.6±9.5 %) (Fig.23B). The control group served as a baseline for comparison. All the treatment groups had a significantly lower fibrotic area in comers with control. Again, the Cryo/GFs/Cells group exhibited the lowest percentage of fibrosis.

The histological analysis suggests that all treatments were able to reduce the extent of fibrosis compared to the control. Combined therapy, however, demonstrated the greatest potential in mitigating fibrotic tissue development after MI. This could be indicative of improved cardiac repair and remodeling in response to the combined treatment strategy.

IHC

For IHC analysis heart sections with infarct zones were stained for 6 different markers to evaluate the regenerative capacity of the heart, receiving various treatment regimens.

The levels of Troponin, α-SMA, and CD31 expression were assessed in heart sections at week 4 post-surgery. By week 4, a significant change in troponin, α-SMA and CD31 levels would indicate the extent of myocardial repair and recovery. Quantitative data for each marker was measured using ImageJ software, and the area of each marker expression was analyzed and calculated. The statistical data was obtained by applying One-way ANOVA analysis, with a post-hoc test done to compare effectiveness of each group. The list of post-hoc results as well as p-value and F-value are given in the Appendix section.

The increased Troponin expression in Cell, Cryo/GFs and Cryo/GFs/Cells groups suggested a progressive improvement in myocardial condition (Fig.24). The control group (6.9±0.5 %) showed a certain level of Troponin staining, which may represent the baseline presence of cardiomyocytes involved in the natural response to injury. The cell group (14.1±1.4 %) exhibited a substantial increase in troponin area, which may suggest progressive tissue repair or regeneration over the period. An expression of Troponin in the Cryo/GFs group (13.6±1.2 %) was less than in the cell group. The cell group may have had a more direct and immediate effect on the tissue due to the introduction of pre-differentiated cells, where the major proportion of cells (76%) were of cardiac lineage (due to natural distribution of those cell types in heart) that contribute to troponin expression. In turn, GFs in the Cryo/GFs group could promote the migration and proliferation of native cells. However, this process might be slower or less efficient compared to the Cells group where pre-differentiated cells are already present. Cryo/GFs/Cells group (16.7±1.3 %) presented

the highest troponin area percentage, level suggesting that the synergistic effect of the scaffold, growth factors, and cell therapy led to the most significant regeneration of cardiac tissue.

Similar tendency was observed in the expression of α-SMA (Control: 5.5±0.5 %, Cells: 16.1±1.2 %, Cryo/GFs: 13.9±2.2 %, Cryo/GFs/Cells: 17.4±1.2 %) and CD31 (Control: 6.1±1.7 %, Cells: 14.2±1.6 %, Cryo/GFs: 13.7±1.1 %, Cryo/GFs/Cells: 18.1±0.8 %). The observed increase in α-SMA (Fig.25) and CD31 staining (Fig.26) in the group treated with pre-differentiated cells suggested enhanced vascular activity, which may indicate the integration of these cells into the tissue and contribution to new vessel formation. Cryo/GFs group also significantly contributed to the myocardium vascularization, compared to control, suggesting the critical role of second injection (Cryo/(VEGF/FgF-2)) in the process. Again, Cryo/GFs/Cells expression of both markers was the highest among all groups, supporting the hypothesis of synergistic effects of all the components of the treatment.

Other markers

Hearts from four experimental groups underwent tissue sectioning at the infarction zones for immunohistology analysis at week 1 and week 4 post-operation. Sections from both time points were stained for CD68 and CD206, while CD3 staining was performed on Week 4 sections. CD68 identifies M1 macrophages involved in the initial inflammatory response, while CD206 is indicative of the reparative M2 macrophage phenotype. Analyzing these markers at both week 1 and week 4 allows for the observation of the shift from an inflammatory to a healing macrophage profile, a crucial aspect of cardiac repair. CD3 is a T cell marker that is crucial for understanding the adaptive immune response during cardiac healing. By week 4, the presence and extent of T cell infiltration can be indicative of the ongoing immune processes and potential resolution of inflammation.

Control group (5.7±0.9 %) showed a strong expression of CD68 week 1. This expression level could reflect the typical acute inflammatory response post-MI without any intervention to modulate it. The Cells (3.1±0.7 %) and Cryo/GFs (2.9±0.2 %) groups, in turn, showed a lower percentage of CD68 expression compared to the control. Cell injection could modulate the inflammatory response via the paracrine response of cells. Meanwhile anti-inflammatory cytokines IL-10,TGF-β injected at the day of operation in Cryo/GFs groups could reduce the degree of inflammation. Thus, the combination of those factors with cells could enhance responses that led the Cryo/GFs/Cells group (1.4±0.4 %) to show less expression of M1 macrophages. Overall, results

for week 1 suggest that these treatments could be effective in suppressing the early inflammatory response, which is often associated with M1 macrophage activity. By week 4, the percentage area of CD68 expression in all groups has decreased (Control: 2.1±0.2 %, Cells: 1.7±0.2 %, Cryo/GFs: 1.7±0.3 %, Cryo/GFs/Cells: 1.1±0.3 %), as would be expected in the normal progression from an inflammatory to a reparative phase following tissue injury. Although all the treatment groups showed reduced CD68 expression, only the Cryo/GFs/Cells group had the statistically significant difference with the control. The reduction from week 1 to week 4 in all groups is consistent with the natural resolution of the acute inflammatory phase and the transition to the healing phase of cardiac repair. Overall, results suggest that treatments influence the early inflammatory environment post-operation, which could be beneficial for acceleration of cardiac repair (Fig.27).

The expression of CD206 at week 1 was significantly higher in all treatment groups compared to the control group (Control: 2.5±0.3 %, Cells: 5.6±0.5 %, Cryo/GFs: 6.1±0.4 %, Cryo/GFs/Cells: 7.8±0.9 %). This suggests an early induction of an anti-inflammatory reaction by the treatments. Meanwhile the combinatorial therapy (Cryo/GFs/Cells) showed the strongest expression of CD206, indicating the effective anti-inflammatory response driven by combination of cryogel with growth factors and cells early in the healing process. By week 4, there was a noticeable shift in the pattern of CD206 expression. The control group gave marked increase in CD206 expression. This could show the natural progression towards an anti-inflammatory state as part of the healing process. The Cryo/GFs group exhibited a significant decrease to a level that is comparable to the control, which could be explained by the anti-inflammatory cytokines expressed early in the healing process and could enhance the shift into anti-inflammatory state. The expression of CD206 was the lowest in Cryo/GFs/Cells group, indicating the fast healing process. These results highlight the dynamic nature of the immune response following MI and the potential modulatory effects of treatments on macrophage polarization and the inflammatory environment during cardiac repair (Fig.28).

Lastly, staining for CD3 revealed similar dynamic as staining for CD206 at week 4 (Control: 3.3±0.2 %, Cells: 1.6±0.3 %, Cryo/GFs: 1.7±0.3 %, Cryo/GFs/Cells: 0.7±0.3 %). The decrease in CD3 expression from the control through to the Cryo/GFs/Cells group suggests a gradation in the modulatory effects of the treatments on T cell infiltration at the site of injury (Fig.29).

Overall, data obtained from IHC analysis supported the hypothesis of the synergetic effect of combined treatment on cardiac restoration. Replenishment of injured heat with pre-differentiated cells could restore cardiac cells activity and enhance neovascularization, while administration of GFs with cryogel that support their sustained release may support accelerated pro-healing process in infarcted zone.

Real-time PCR on the expression of pro- and anti-inflammatory cytokines in treatment groups

The expression levels of six cytokine genes (TNF-α, IL-1β, IL-6, TGF-β, IL-10, and IL-4) were quantified via qPCR at week 1, week 2 and week 4 across four experimental groups: Control, Cells, Cryo/GFs, and Cryo/GFs/Cells (Fig.30).

Initially, the cycle threshold (CT) values were normalized against a housekeeping gene (Actin) to calculate the delta Ct (ΔCt) values for each sample. The ΔCt value for each target gene was determined by subtracting the CT value of the housekeeping gene from the CT value of the target gene, thus normalizing for variations in RNA input and reverse transcription efficiency. Subsequently, the delta delta Ct (ΔΔCt) values were obtained by subtracting the average ΔCt of the control group from each ΔCt value within the experimental groups. The relative quantification of gene expression was calculated using the 2^(-delta delta Ct) method, which provides the fold change in expression relative to the control group. Statistical analysis was conducted using one-way ANOVA to compare the relative expression levels of each cytokine gene among the four groups. Data analysis was performed using the GraphPad Prism tool. A p-value less than 0.05 was considered indicative of a statistically significant difference in gene expression between groups. The statistical data results of the one-way ANOVA are provided in the appendix section. The tables show the significance, p-value and F-value for each cytokine for all cytokines. The post-hoc analysis provided information regarding differences between groups, clarifying impacts of cell therapy, growth factors, and their combination on cytokine expression. The expression levels in the treatment groups were normalized to the control group for comparison.

Weeks 1, 2, and 4 time points for qPCR were chosen to provide a comprehensive view of the inflammatory and healing processes post-MI. Thus, week 1 shows the acute inflammatory response, which is crucial to assess the immediate effect of treatments on inflammation. Week 2 represents a transitional phase where inflammation decreases and reparative processes begin.

Finally, week 4 allows for the evaluation of longer-term treatment effects on anti-inflammatory activity and tissue repair, marking the progression from acute response to healing resolution.

Overall, pro-inflammatory cytokines (TNF-α, IL-1β, IL-6) showed a significant decrease in expression across the treatment groups when compared to the control over the observed period in most of the groups (Fig.30A). The Cryo/GFs/Cells group had the lowest level of pro-inflammatory gene expressions.

Anti-inflammatory cytokines (IL-10, IL-4), in turn, demonstrated an initial increase in gene expression in the treatment groups at week 1, which then considerably decreased by week 4 (Fig.30B). This initial increase in IL-10 and IL-4 level could be the result of the rapid activation of pro-healing processes triggered by treatments. Thus, anti-inflammatory factors secreted from cryogel scaffold, as well as paracrine factors secreted by cells could stimulate fast recovery of tissue. Over time, the tissue regeneration may have progressed more rapidly in those groups, leading to a subsequent reduction in the levels of these pro-healing cytokines. Anti-inflammatory factors secreted from the cryogel scaffold (IL-10,TGF-b), as well as paracrine factors released by the introduced cells, possibly contributed to the accelerated tissue recovery. Over time, as the tissue regeneration progressed, it may have led to a natural reduction in these pro-healing cytokines, which indicate a faster shift from an active healing phase to a more stabilized tissue state.

The expression of TGF-β varied and showed a small tendency to decrease in the treatment groups (Fig.30B). This observation may indicate its involvement in tissue repair and fibrosis. During the first week treatment groups, most notably Cryo/GFs, showed higher expression of TGF-B, possibly meaning the accelerated scaring processes. By week 4 we observed relatively high expression of TGF-β in the Cell group that could suggest extended fibrotic processes. Overall, the expression of TGF-β did not show specific trends like the other cytokines, most likely because of its complex involvement in the healing process.

TNF-α, IL-1β, IL-6, TGF-β, IL-10 and IL-4 cytokines were selected to evaluate the inflammatory and healing processes in the post-MI environment. Those cytokines were chosen for their known roles in inflammation and tissue regeneration. Thus, TNF-α and IL-1β are pro-inflammatory cytokines that are typically elevated in infarcted tissue and play a role in the acute inflammatory response. Another pro-inflammatory marker, IL-6 is involved in the transition from acute to chronic inflammation. IL-10 and IL-4 are anti-inflammatory cytokines responsible for resolving inflammation and facilitating tissue repair. TGF-β can have both pro- and anti-

inflammatory effects. It plays a crucial role in the fibrotic healing process and can contribute to scar tissue formation. Scar stabilizes the wounded area, but its excessive formation may lead to adverse cardiac remodeling.

The observed decrease in pro-inflammatory cytokines and increase in anti-inflammatory cytokines in the treated groups suggest the modulatory effect of treatment groups on the immune system. The combined treatment with Cryo/GFs/Cells appears to be particularly effective, potentially providing both a scaffold for the delivery of growth factors and cells that together work to enhance the reparative process by regulating anti-inflammatory cytokine levels.

Overall, the data suggests that the applied treatments can significantly modulate inflammatory and anti-inflammatory responses after infarction, which could potentially lead to enhanced cardiac healing. The trends in cytokine expression, as modulated by the treatments, reflect a shift from a pro-inflammatory state towards a more balanced or anti-inflammatory state, which may be beneficial for cardiac function recovery. The alterations in cytokine expression, influenced by the treatments, indicate a transition from an pro-inflammatory state to a more balanced anti-inflammatory profile, which could promote the recovery of heart function.

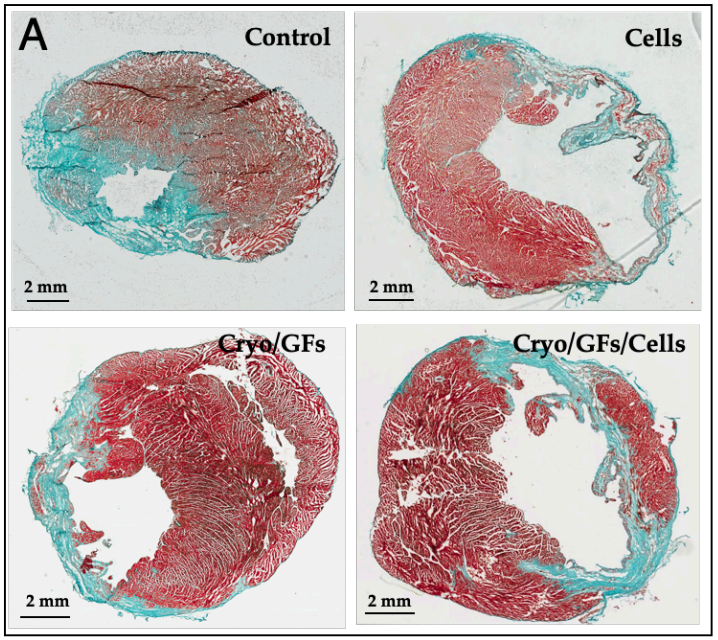
A
Control
Cells
Cryo/GFs
Cryo/GFs/Cells
2 mm
2 mm
2 mm
2 mm

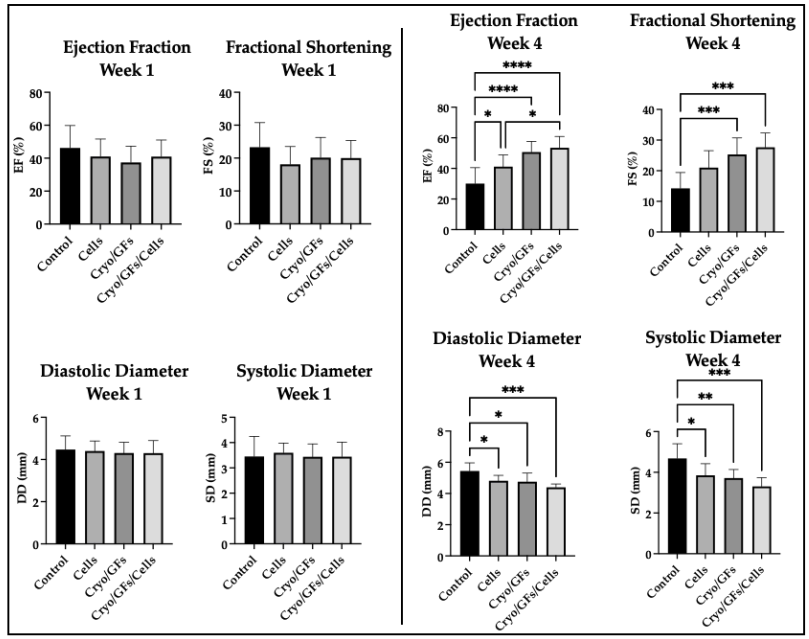
C
Ejection Fraction Week 1
Fractional Shortening Week 1
Ejection Fraction Week 4
Fractional Shortening Week 4
Diastolic Diameter Week 1
Systolic Diameter Week 1
Diastolic Diameter Week 4
Systolic Diameter Week 4
EF (%)
FS (%)
DD (mm)
SD (mm)
Control
Cells
Cryo/GFs
Cryo/GFs/Cells

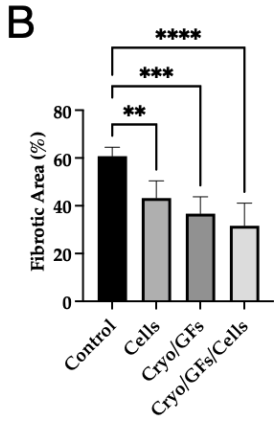
B
Fibrotic Area (%)
****
***
**
Control
Cells
Cryo/GFs
Cryo/GFs/Cells

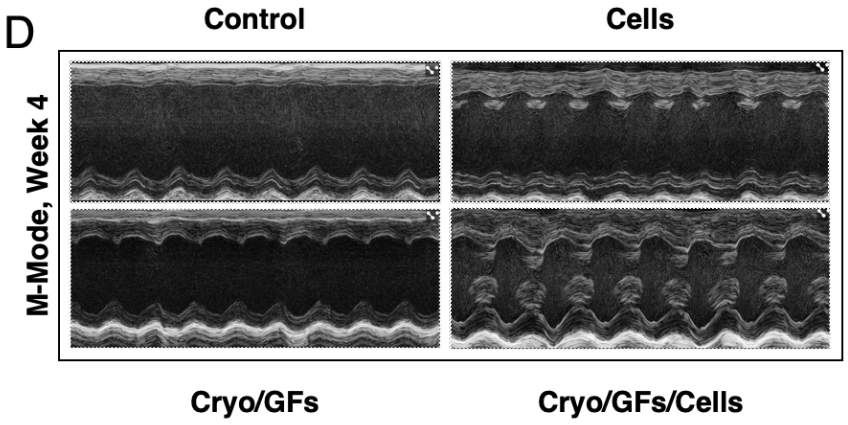
D
Control
Cells
M-Mode, Week 4
Cryo/GFs
Cryo/GFs/Cells

Figure 23. Comprehensive Evaluation of Cardiac Repair Interventions A) Masson's Trichrome staining of myocardial sections from control, cell-treated (Cells), cryogel with GFs (Cryo/GFs), and cryogel with C/GFs and cells (Cryo/GFs/Cells) groups. Staining highlights the collagen fibers in blue, indicating areas of fibrosis, and healthy myocardial tissue in red. Scale bars = 2 mm. B) Quantitative analysis of fibrosis percentage from histological sections, measured using ImageJ software. The bar graph represents the extent of fibrosis across different treatment groups, expressed as mean ± SD, with statistical significance annotated (***$p<0.001$, ****$p<0.0001$). C) Ultrasound analysis of cardiac function at week 1 and week 4 post-treatment, assessing ejection fraction, fractional shortening, diastolic diameter, and systolic diameter. Data are presented as mean ± SD. Statistical annotations represent comparisons between groups at each time point, indicating changes in cardiac function (*$p<0.05$, **$p<0.01$, ***$p<0.001$, ****$p<0.0001$). D) Representative M-Mode echocardiographic images from the ultrasound analysis at week 4, showing cardiac wall motion and chamber dimensions during the cardiac cycle for each group. Images provide a visual context for the quantitative ultrasound data, reflecting the functional status of the myocardium post-intervention.

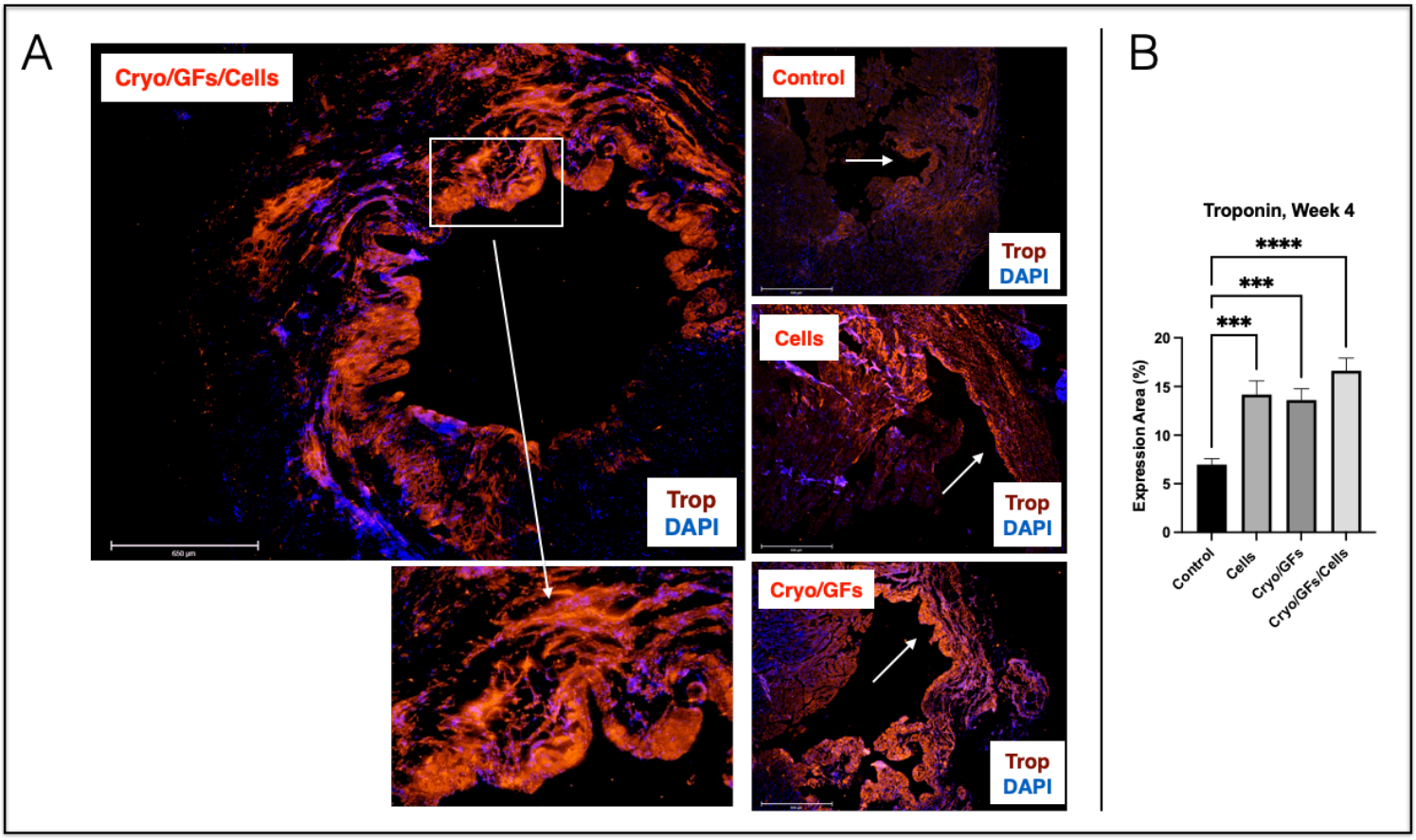

Figure 24. Troponin I IHC staining and Quantitative Analysis in Post-MI Tissue A) IHC staining of heart tissue sections at week 4 post-MI. Troponin I (Trop, red) marks cardiomyocytes, with nuclei counterstained with DAPI (blue). Images show sections from cryogel with GFs and cells (Cryo/GFs/Cells), control, cell-treated (Cells) and cryogel with GFs (Cryo/GFs) groups. Arrows indicate areas of Troponin I expression. Scale bars = 650 µm. B) Statistical analysis of Troponin I positive area percentage at week 4 post-infarction. Quantification was performed using ImageJ to calculate the percentage of the area that was Troponin I-positive in the tissue sections. Data represent mean ± SD, with statistical significance denoted as follows: ***$p<0.001$, ****$p<0.0001$

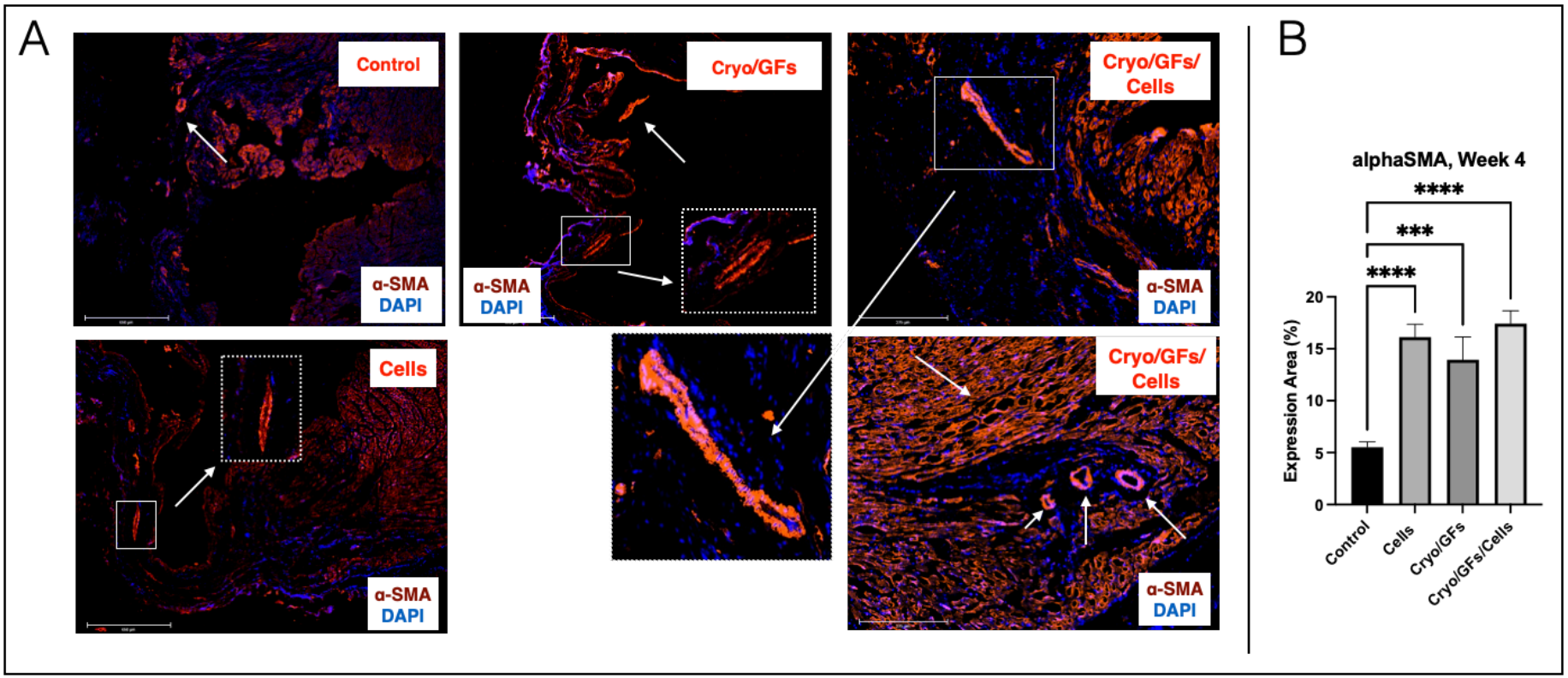

Figure 25. Analysis of α-SMA Expression in Myocardial Tissue Post-Intervention A) IHC staining for α-SMA (red) in heart tissue sections at week 4 post-infarction, with nuclei counterstained with DAPI (blue). The panels display staining of control, cell-treated (Cells), cryogel with GFs (Cryo/GFs), and cryogel with GFs and cells (Cryo/GFs/Cells) groups. White arrows point to regions with α-SMA expression, demonstrating new vessel formation. Insets show magnified areas (dotted boxes) highlighting the α-SMA positive structures. Scale bars - 650 µm. B) Quantitative analysis of α-SMA positive area percentage in myocardial tissue sections at week 4. The bar chart reflects the proportion of the area staining positive for α-SMA. Quantification was performed using ImageJ software. Data are expressed as mean ± SD, with ***$p<0.001$, ****$p<0.0001$ denoting significant differences compared to the control group.

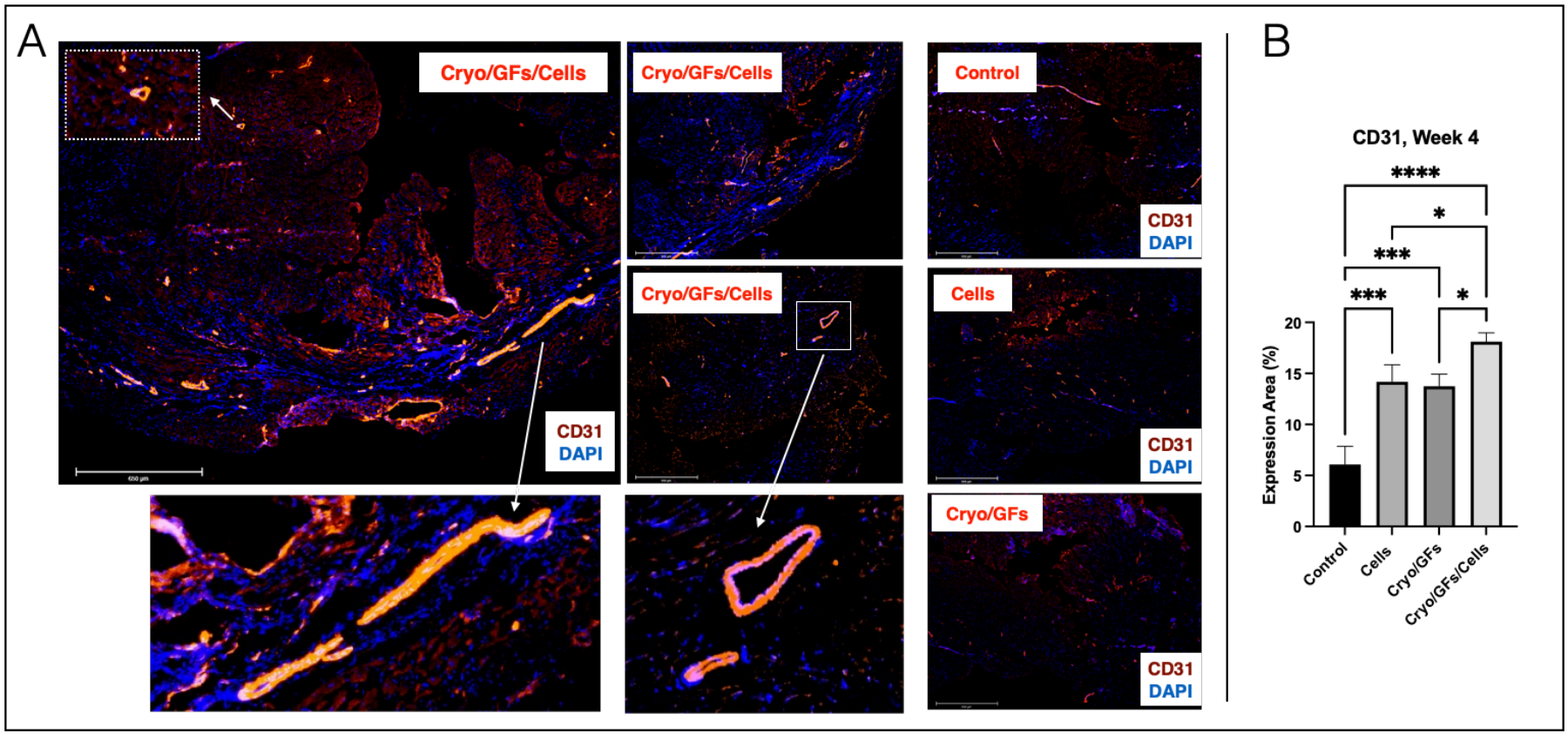

Figure 26. CD31 Expression and Quantification in Myocardial Tissue Post-Treatment A) IHC staining for CD31 (red), a marker for ECs, in heart tissue sections at week 4 post-treatment, with nuclei counterstained with DAPI (blue). Representative images from control, cell-treated (Cells), cryogel with GFs (Cryo/GFs), and the cryogel with GFs and cells (Cryo/GFs/Cells), groups are shown. Arrows indicate CD31-positive vascular structures. Insets (dotted boxes) are magnified to highlight the presence of CD31 expression, indicating angiogenesis.. Scale bars = 650 µm. B) Quantitative analysis of the percentage area positive for CD31, indicative of endothelialization and neovascularization in the tissue. Measurements were performed using ImageJ software, and data are presented as mean ± SD. Statistical significance is indicated by asterisks (*$p<0.05$, ***$p<0.001$, ****$p<0.0001$), demonstrating significant differences in CD31 expression between treatment groups compared to the control.

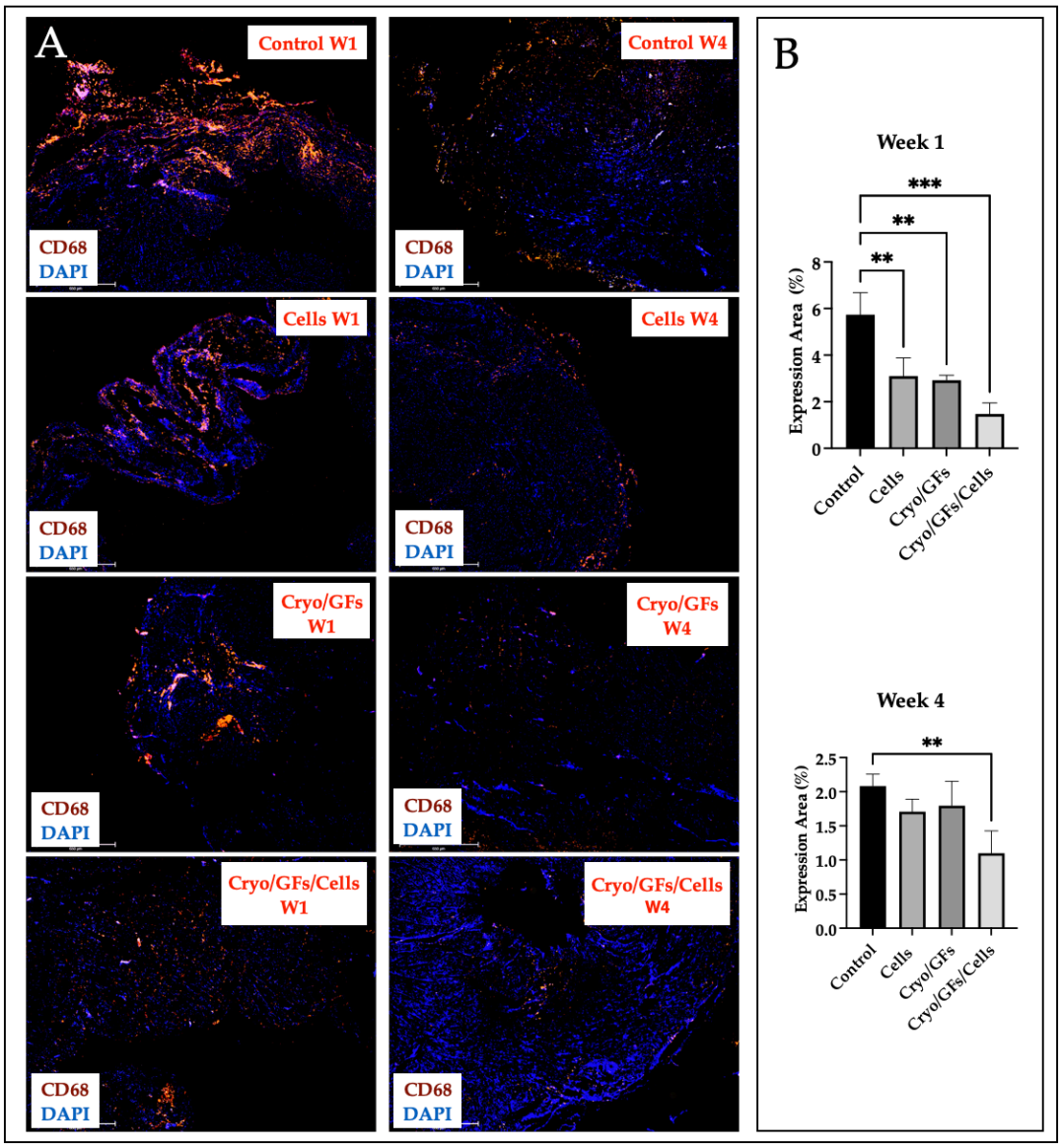

Figure 27. IHC Analysis of CD68+ Macrophages in Post-Treatment Myocardial Tissue A) IHC staining for CD68 (red), a marker of M1 pro-inflammatory macrophages, in myocardial tissue sections at week 1 (W1) and week 4 (W4) post-infarction. The sections from the control, cell-treated (Cells), cryogel with GFs (Cryo/GFs), and cryogel with GFs and cells (Cryo/GFs/Cells) groups are compared. Nuclei are counterstained with DAPI (blue). The presence of CD68+ macrophages indicates areas of inflammation. Scale bars = 650 µm. B) Quantitative analysis of the percentage area positive for CD68 at week 1 and week 4. The bar charts illustrate the proportion of the area exhibiting CD68 staining, reflecting the extent of macrophage infiltration and inflammation. Quantification was conducted using ImageJ software. Data are expressed as mean ± SD, with statistical significance indicated (**p<0.01, ***p<0.001), highlighting notable differences in inflammatory response between the groups at week 1, which appear to converge by week 4.

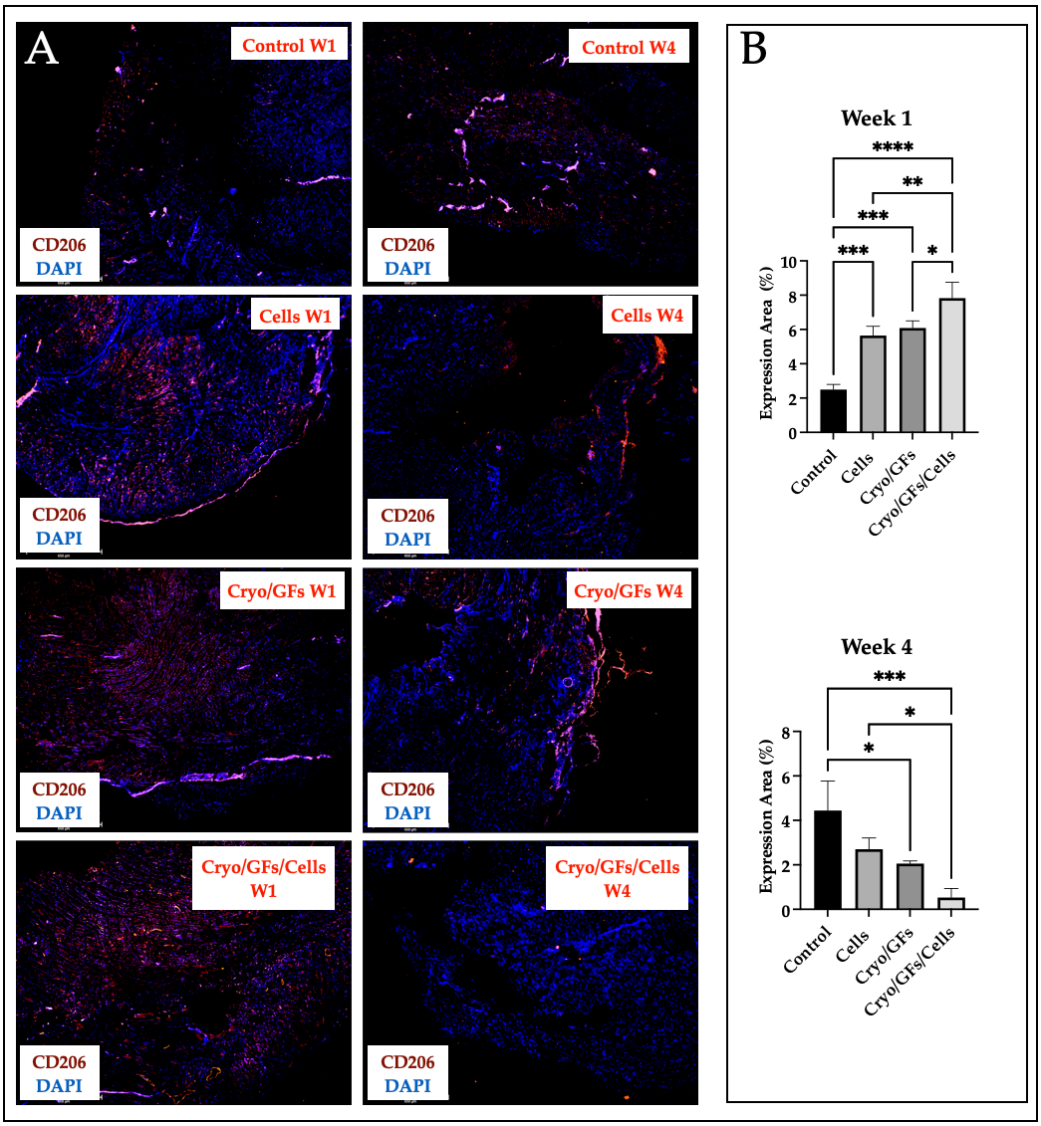

Figure 28. Characterization of M2 Macrophage Infiltration Post-Treatment Using CD206 Marker A) IHC detection of CD206 (red), indicative of M2 anti-inflammatory macrophages, in myocardial tissue at week 1 (W1) and week 4 (W4) after treatment. Sections from the control, cell-treated (Cells), cryogel with GFs (Cryo/GFs), and cryogel with GFs and cells (Cryo/GFs/Cells) groups are presented. Nuclei are counterstained with DAPI (blue). CD206 expression is used to identify areas of anti-inflammatory activity. Scale bars - 650 µm. B) Quantification of the percentage area positive for CD206 at week 1 and week 4. The bar charts show the extent of CD206+ area, representing the presence of anti-inflammatory macrophages within the tissue. Analysis was performed using ImageJ software, and the data are shown as mean ± SD. Statistically significant differences are marked, indicating the dynamic changes in the anti-inflammatory response between the groups from week 1 to week 4 (*p<0.05, **p<0.01, ***p<0.001, ****p<0.0001).

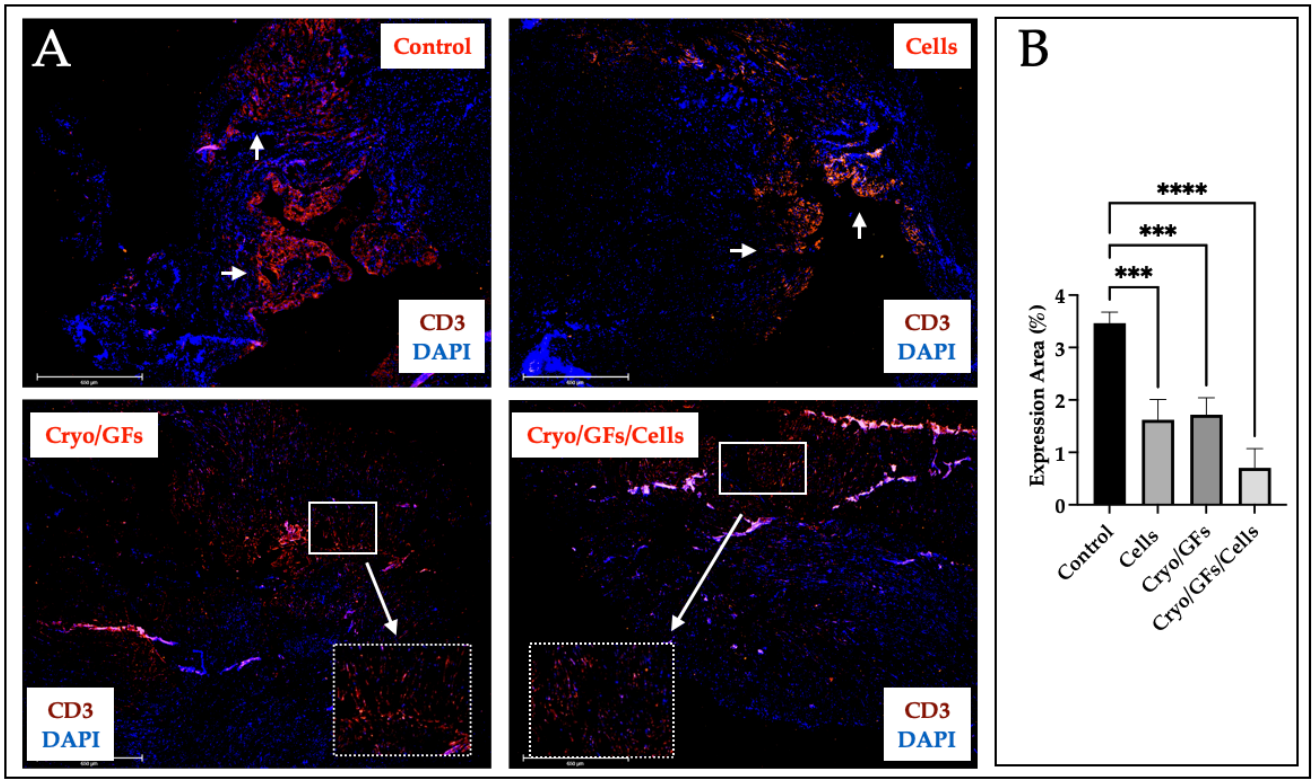

Figure 29. T-Cell Presence in Myocardial Tissue Analyzed with CD3 Marker A) IHC staining of myocardial sections for CD3 (red), a T-cell marker, at week 4 post-infarction. The images display tissue from control, cell-treated (Cells), cryogel with GFs(Cryo/GFs), and cryogel with GFs and cells (Cryo/GFs/Cells) groups. The presence of CD3+ T cells, indicated by arrows, reflects the immune response in the myocardium. Insets show enlarged areas of interest. Nuclei are counterstained with DAPI (blue). Scale bars = 650 µm. B) Quantitative assessment of the area positive for CD3 at week 4 post-infarction. The bar chart quantifies the percentage of CD3+ area, representing T-cell infiltration in each treatment group. Analysis was carried out using ImageJ software, with results expressed as mean ± SD. Significant differences in T-cell presence between groups are highlighted, with asterisks indicating the level of statistical significance (***p<0.001, ****p<0.0001

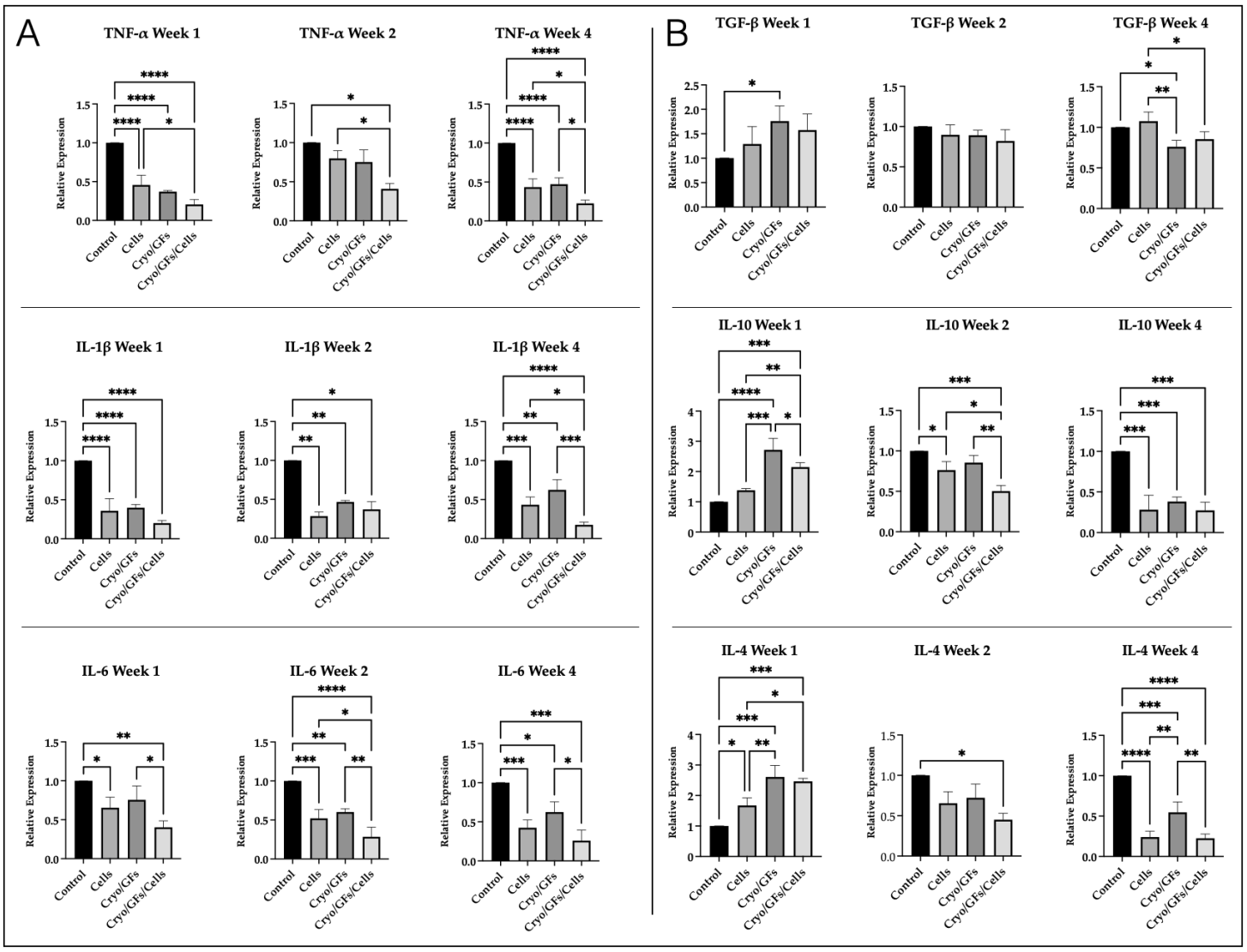

Figure 30. Real-time PCR Analysis of Cytokine Expression Post-Treatment A) Pro-inflammatory Cytokine Expression: Graphical representation of the expression levels of pro-inflammatory cytokines TNF-α, IL-1β, and IL-6 across four different treatment groups: Control, Cells, cryogel with GFs (Cryo/GFs), and cryogel with GFs and cells (Cryo/GFs/Cells) at weeks 1, 2, and 4 post-operation. Expression levels are normalized to a reference gene and shown relative to the control group. Data are presented as mean ± SD, with statistical annotations indicating significance compared to control (*$p<0.05$, **$p<0.01$, ***$p<0.001$, ****$p<0.0001$). B) Anti-inflammatory Cytokine Expression: Quantitative assessment of the expression levels of anti-inflammatory cytokines TGF-β, IL-10 and IL-6 at weeks 1, 2, and 4 post-operation. The role of TGF-β as an anti-inflammatory cytokine can be context-dependent, often exhibiting dual roles in inflammation and immune regulation. Like panel A, data are normalized and shown relative to the control group, with mean ± SD and statistical significance noted.

Key Insights From the *In Vivo* Cardiac Regeneration Study

An *in vivo* part of the study on cardiac regeneration included four groups: Control, Cells, Cryo/GFs, and Cryo/GFs/Cells. To analyze the effect of each treatment and to find the best working combination among groups, several methods were employed, such as ultrasound, IHC, histological analysis, and real-time PCR.

Ultrasound results for the week 1 post-surgery indicated no notable differences in cardiac function among the groups. Yet, by the fourth week, the Cryo/GFs/Cells group showed marked improvements in heart function, specifically in Ejection Fraction and Fractional Shortening, along with improvements in both Systolic and Diastolic Volumes. This suggests that the combination of cell therapy with Cryo/GFs could be particularly effective in aiding heart recovery.

Next, the histological analysis further supported those findings by demonstrating a significant reduction in fibrotic area in the Cryo/GFs/Cells group, indicating improved cardiac repair and remodeling. IHC results provided further evidence, showing the highest increase in troponin area in the Cryo/GFs/Cells group, a sign of substantial cardiac tissue regeneration. This group also demonstrated increased levels of α-SMA and CD31, indicating enhanced vascularization, which is critical for heart repair. In addition, IHC revealed a remarkable transition in macrophage types, from the inflammatory M1 to the healing M2 phenotype, in particular, in the Cryo/GFs/Cells group. Real-time PCR analysis highlighted that this group experienced a substantial regulation in inflammatory and anti-inflammatory cytokines, regulating the immune response favorably for heart repair.

In conclusion, *in vivo* study revealed the Cryo/GFs/Cells group as the most effective in terms of altering the post-MI environment towards regeneration and repair. This combination therapy improved overall heart function, prevented fibrosis and modulated the inflammatory response, which make it a potentially valuable method in the field of cardiac regenerative medicine.

MAIN OUTLINES AND CONCLUSION

MI is the most common cause of congestive heart failure which subsequently leads to death. The disease is the consequence of an acute coronary syndrome, where the normal blood flow in the coronary lumen is blocked due to the formation of plagues ((Yang et al., 2017). The current treatment is mainly based on drugs and surgery (Philip, 1996). However, such therapies cannot fully recover damaged myocardium: they are mainly focused on reducing the consequences of MI, such as the prevention of further clot formation, and reducing scarring of myocardium and cannot remodel fibrotic tissue and return the heart back to its normal, fully-functional state ((Shafei et al., 2017). Moreover, not only myocardium is damaged after MI. Blood vessels are also damaged, therefore, the new therapy focused on the repair of both muscles and vasculature is required (Park, 2019).

Stem cell transplantation is a promising strategy used in the field of regenerative medicine that can resolve many challenges which are currently unable to be solved by traditional treatments. However, when cells are injected directly to the heart, they are faced with a harsh post-MI environment such as ischemia, inflammation, and anoikis. Studies report that approximately 90% of stem cells die within the first 7 days after transplantation, which significantly reduces the efficacy of the therapy (Wu et al., 2019).

Another approach of regenerative medicine for cardiac tissue repair is the use of scaffolds loaded with anti-inflammatory cytokines and pro-angiogenic growth factors. This approach allows to prepare an optimal environment for the subsequent injection of cells by reducing the inflammation in the site of infarction and stimulating neovascularization. This preparatory step can help to eliminate such challenges of the cellular therapy as the low engraftment, bad proliferation and weak differentiation of cells in the injured area. Modern biomaterials, including the cryogel, are biodegradable, non-toxic and immune tolerant (Sultankulov et al., 2019). Combining pre-differentiated cells with C/GFs loaded into cryogel allows to enhance engraftment and survival rates of cells, stimulate their proliferations and increase the beneficial impact on heart regeneration post-MI (Sultankulov et al., 2019). The main aspects of the current study are summarized below (Fig.31).

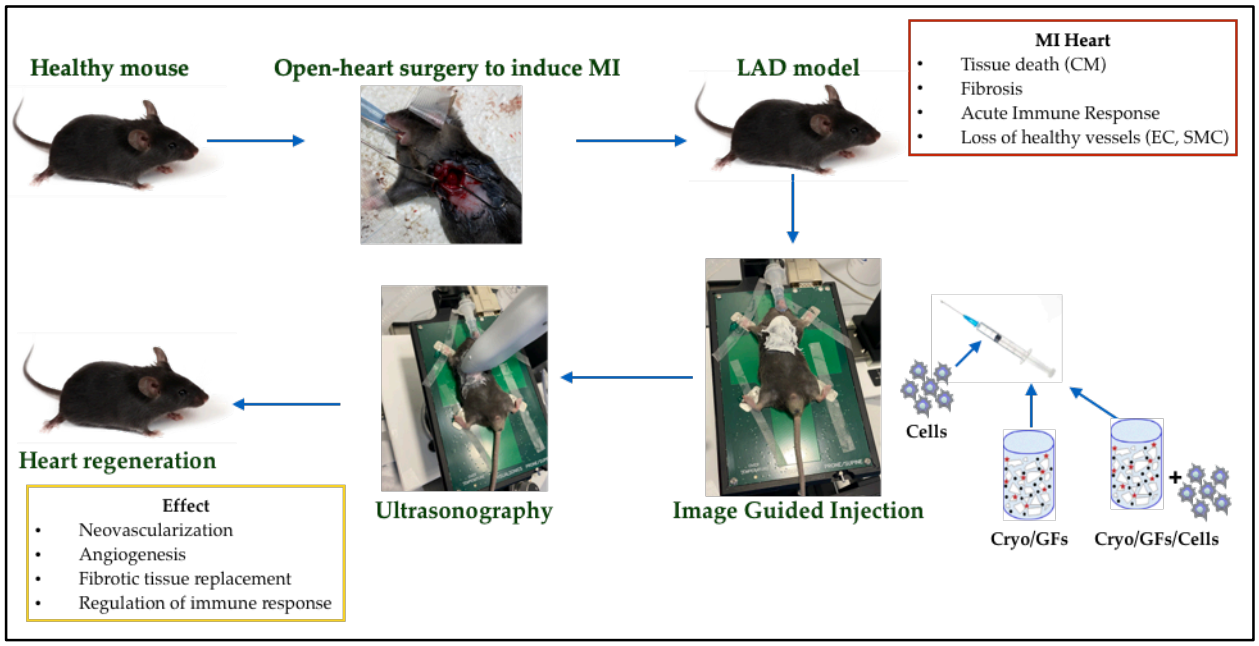

Figure 31. The workflow of the current research

The aim of the current study was to achieve the regeneration of the infarcted heart by subsequent administration of the Cryo/(IL-10,TGF-β), Cryo/(VEGF,FGF-2) and pre-differentiated cells. The first objective was the isolation of MSCs culture from mouse compact bones. MSCs were then exposed to culture mediums enriched with unique combinations of growth factors to receive CMs, ECs and SMCs, for their subsequent use in in vivo study.

The cryogel in a form of round discs was used in previous studies (Sultankulov et al., 2019). However, such form requires an open chest operation. The use of injection is a much less invasive approach. Therefore, for this study we prepared a powder with a particle size in a range between 50 to 100 um. Such particle size is small enough not to cause negative consequences to the heart and is convenient for the injection.

The challenge of MI recovery lies not just in restoring cardiac function but also in addressing the complex interplay of cellular responses post-injury. Our study's results shed light on the pivotal role of targeted therapeutic interventions at distinct post-MI phases. Our cryogel scaffold interconnects macroporous structure and ensures efficient and optimal delivery and release of therapeutic agents to the injured myocardium (Sultankulov et al., 2019; Kim et al., 2023). Powdered form of cryogel permits a minimally invasive injectable approach compared to disc form. The chosen particle size range (50-100μM) was strategically optimized to minimize heart risks while being conductive for injection. Injection of cryogel loaded with the combination of GFs,

followed by the injection of cells showed significant improvement in cardiac regeneration, compared to the control group.. Concentrations of injected GFs were chosen based on previous studies (Jimi et al., 2020) and were set to 1 ug/ml for Cryo/IL-10,TGF-β and 10 ug/ml for Cryo/VEGF,FGF-2. Cells were injected on day 6.

Our findings highlighted the importance of timing in the administration of treatments. The initial application of Cryo/(IL-10,TGF-β) on day of surgery worked as a preparatory phase, with IL-10 and TGF-β attenuating inflammation and setting the stage for tissue repair (Frangogiannis, 2014). The subsequent introduction of Cryo/(VEGF,FGF-2) on day 4 was strategic. VEGF and FGF-2 are potent stimulators of angiogenesis, crucial for re-establishing blood flow to the ischemic tissue, and for ensuring survival and integration of newly introduced cells (Simons et al., 2016). Furthermore, the results from the group receiving pre-differentiated cells after GFs injection highlighted the importance of cellular intervention. These cells likely acted synergistically with the growth factors, enhancing their therapeutic effects while also compensating for cell loss.

In the context of other murine studies, the current research demonstrated significant advancements in cardiac repair and regeneration, paralleling recent developments in cellular therapies. Recent advances in cellular therapies for cardiac regeneration have primarily focused on enhancing the maturity of stem cell-derived cardiomyocytes (PSC-CMs) (Tenreiro et al., 2021). For example, a study by Jiang et al. (2020), where human induced PSC-CMs were transplanted into a murine model of MI, showed an improvement in heart function with an EF of 54% on day 28 post-induction, which aligns with the results obtained in the current study for the Cryo/GF/Cells groups on day 28 (54±7.4%). Another regenerative study examining the role of MSCs as well as trophoblast SCs, differentiated into cardiomyocytes in vivo after transplantation, detected a decrease in fibrotic tissue from 58% to 39% and 38%, respectively (Li et al., 2017). Our study revealed that treatment with Cryo/GFs/Cells significantly reduced fibrotic tissue formation compared to the control group (31.6±9.5% vs 60.8±3.7%), emphasizing the efficacy of combining both strategies for myocardial regeneration. Furthermore, a biomaterial study focusing on the Ti2C-8-cryogel combined with CMs demonstrated that when transplanted into the infarcted heart of an MI rat model, the Ti2C-8-cryogel modulated the inflammatory response, evidenced by the expression of the M1 macrophage marker CD68 at week 4 (2.5% of positively stained area) (Ye et al., 2020). In comparison, our study revealed that by week 4, the percentage area of CD68

expression in all treatment groups decreased (Cells: 1.7±0.2%, Cryo/GFs: 1.7±0.3%, Cryo/GFs/Cells: 1.1±0.3%).

Overall, the current study, utilizing a novel chitosan-based cryogel loaded with anti-inflammatory and proangiogenic factors, supplemented with pre-differentiated cells, presents a unique approach. The sequential delivery of Cryo/GF/Cells for cardiac regeneration, to our knowledge, has not been previously explored. This methodology, especially in the context of MI, represents a significant advancement. The obtained results indicating improved heart function, prevented fibrotic tissue formation and modulation of the inflammatory response place the study as a potentially valuable method in cardiac regenerative medicine. In contrast to existing studies, the current approach is not focused on utilizing cellular therapy and scaffold-based therapy separately, but instead on combining the two strategies. This comprehensive approach could address some challenges noted in other studies, such as the cell survival and integration post-transplantation.

While this study provided promising insights into myocardial regeneration via the use of sequential Cryo/GF/Cells therapy, there were some limitations that may have impacted our findings.

In reflecting upon the methodologies employed in this study, it is acknowledged that a potential source of bias may have arisen from the singular involvement of the primary researcher in various critical stages. While stringent protocols and objective measures were implemented to ensure consistency and impartiality of the study, the potential for unconscious bias cannot be entirely dismissed. To address this issue, future studies should incorporate a blinded analysis, wherein independent examiners or pathologists who are not involved in the experimental procedures would perform certain analytical tasks. This modification would significantly reduce the risk of potential bias and enhance the reliability and replicability of the findings, further strengthening the reliability of our results in the field of experimental biomedical research.

The promising results of the current study obtained in the murine model emphasize the potential of this approach in cardiac tissue repair post-MI. However, before considering human trials it is important to advance from the current murine model to larger animal models such as porcines or canines, whose cardiac physiology and pathology more closely resemble those of humans. This transition is crucial, because although the main aspects shown in this study, such as immunomodulation, neovascularization, and cell replacement are likely applicable, there is still

need to assess the scalability of cryogel delivery, optimize cytokine `and growth factor dosages, and evaluate cell engraftment efficiency in a more human-like cardiac environment.

For the future clinical translation, the current strategy can be modified in order to reduce invasiveness and enhance applicability in humans. One such advancement could be the development of multilayered cryogel microparticles. Such a design would allow the outer layer to release anti-inflammatory factors immediately after and a middle layer to release pro-angiogenic factors a few days after delivery, as the cryogel naturally degrades, thereby eliminating the need of multiple injections. The delivery of such modified cryogel can be combined with percutaneous coronary intervention (PCI), a common treatment for MI. This potential approach can employ trans-catheter delivery methods to administer therapeutics concurrently with the restoration of blood flow via stent placement. Combination of these procedures may maximize therapeutic impact while minimizing additional invasive interventions. In addition, percutaneous epicardial delivery presents another promising approach, and offers a targeted delivery with reduced invasiveness, specifically for the delivery of pre-differentiated cells few days after the MI. Overall, an approach of combining bi-layered cryogel delivery with PCI and using percutaneous epicardial delivery for later cell therapy is innovative and could be feasible. However, each step needs to be carefully evaluated for safety, particularly in the post-MI period, when the heart is in a vulnerable state, and any intervention, even minimally invasive, needs to be evaluated for risks like inducing arrhythmias, damaging fragile tissue, or causing inflammation.

In conclusion, this study demonstrated significant myocardial repair in mouse cohorts treated with our chitosan-based cryogel combined with growth factors, with the following injection of cells (Cryo/GFs/Cells). This cryogel, proficiently loaded with anti-inflammatory and pro-angiogenic factors, appears to serve as a promising platform for the controlled release of therapeutics, essential in the post-MI healing process. The integration of pre-differentiated cells into this framework was shown to substantially enhance the regenerative effects, contributing to notable tissue repair and overall cardiac regeneration.

REFERENCES

1. Pamukçu, B. (Ed.). (2019). MI. IntechOpen. doi: 10.5772/intechopen.69907
2. Valgimigli, M., Bueno, H., Byrne, R. A., et al. (2021). 2017 ESC focused update on dual antiplatelet therapy in coronary artery disease developed in collaboration with EACTS: The Task Force for dual antiplatelet therapy in coronary artery disease of the European Society of Cardiology (ESC) and of the European Association for Cardio-Thoracic Surgery (EACTS). *Journal of the American College of Cardiology, 75*(17), 2133-2140. doi:10.1016/j.jacc.2020.11.010.
3. American College of Cardiology. (2020). CVD Burden and Deaths Rising Around the World.
4. Timmis, A., Vardas, P., Townsend, N., et al. (2022). European Society of Cardiology: cardiovascular disease statistics 2021. *Eur Heart J*, 43(8), 716-799. https://doi.org/10.1093/eurheartj/ehab892
5. Ohira, T., & Iso, H. (2013). Cardiovascular Disease Epidemiology in Asia: An Overview. _Circulation Journal_, 77(7), 1646-1652
6. Roth, G. A., Mensah, G. A., Johnson, C. O., Addolorato, G., Ammirati, E., Baddour, L. M., Barengo, N. C., Beaton, A. Z., Benjamin, E. J., Benziger, C. P., Bonny, A., Brauer, M., Brodmann, M., Cahill, T. J., Carapetis, J., Catapano, A. L., Chugh, S. S., Cooper, L. T., Coresh, J., . . . Fuster, V. (2020, December). Global Burden of Cardiovascular Diseases and Risk Factors, 1990–2019. Journal of the American College of Cardiology, 76(25), 2982–3021. https://doi.org/10.1016/j.jacc.2020.11.010
7. Bugiardini, R., & Cenko, E. (2020, JULY 11). Sex differences in MI deaths. *The Lancet Journal*, *396*(10244), 72-73. https://www.thelancet.com/journals/lancet/article/PIIS0140-6736(20)31049-7/fulltext
8. Salari, N., Morddarvanjoghi, F., Abdolmaleki, A., Rasoulpoor, S., Khaleghi, A. A., Hezarkhani, L. A., Shohaimi, S., & Mohammadi, M. (2023, April 22). The global prevalence of MI: a systematic review and meta-analysis. BMC Cardiovascular Disorders, 23(1). https://doi.org/10.1186/s12872-023-03231-w
9. Dugani, S. B., Hydoub, Y. M., Ayala, A. P., Reka, R., Nayfeh, T., Ding, J. F., McCafferty, S. N., Alzuabi, M., Farwati, M., Murad, M. H., Alsheikh-Ali, A. A., & Mora, S. (2021, August). Risk Factors for Premature MI: A Systematic Review and Meta-analysis of 77 Studies. Mayo Clinic Proceedings: Innovations, Quality & Outcomes, 5(4), 783–794. https://doi.org/10.1016/j.mayocpiqo.2021.03.009
10. Jortveit, J., Pripp, A. H., Langørgen, J., & Halvorsen, S. (2020, February 28). Incidence, risk factors and outcome of young patients with MI. Heart, 106(18), 1420–1426. https://doi.org/10.1136/heartjnl-2019-316067
11. Ojha N, Dhamoon AS. MI. (2023, August 8). MI Available from: https://www.ncbi.nlm.nih.gov/books/NBK537076/

12. Raziyeva, K., Kim, Y., Zharkinbekov, Z., Temirkhanova, K., & Saparov, A. (2022, September 2). Novel Therapies for the Treatment of Cardiac Fibrosis Following MI. Biomedicines, 10(9), 2178. https://doi.org/10.3390/biomedicines10092178
13. Goch, A., Misiewicz, P., Rysz, J., & Banach, M. (2009, April 20). The Clinical Manifestation of MI in Elderly Patients. Clinical Cardiology, 32(6). https://doi.org/10.1002/clc.20354
14. Shiraishi, J., Kohno, Y., Yamaguchi, S., Arihara, M., Hadase, M., Hyogo, M., Yagi, T., Shima, T., Sawada, T., Tatsumi, T., Azuma, A., Matsubara, H., & on behalf of the AMI-Kyoto Multi-Center Risk Study Group. (2005). Acute MI in Young Japanese Adults Clinical Manifestations and In-Hospital Outcome. Circulation Journal, 69(12), 1454–1458. https://doi.org/10.1253/circj.69.1454
15. Wong, C. P. (2012). Acute MI: Clinical features and outcomes in young adults in Singapore. World Journal of Cardiology, 4(6), 206. https://doi.org/10.4330/wjc.v4.i6.206
16. Shiraishi, J., Shiraishi, H., Hayashi, H., Sawada, T., Tatsumi, T., Azuma, A., & Matsubara, H. (2005). Interventional Treatment for Very Young Adults With Acute MI: Clinical Manifestations and Outcome. International Heart Journal, 46(1), 1–12. https://doi.org/10.1536/ihj.46.1
17. Rich, M. W. (2006, January). Epidemiology, Clinical Features, and Prognosis of Acute MI in the Elderly. The American Journal of Geriatric Cardiology, 15(1), 7–13. https://doi.org/10.1111/j.1076-7460.2006.05273.x
18. Domienik-Karłowicz, J., Kupczyńska, K., Michalski, B., Kapłon-Cieślicka, A., Darocha, S., Dobrowolski, P., Wybraniec, M., Wańha, W., & Jaguszewski, M. (2021, April 13). Fourth universal definition of MI. Selected messages from the European Society of Cardiology document and lessons learned from the new guidelines on ST-segment elevation MI and non-ST-segment elevation-acute coronary syndrome. Cardiology Journal, 28(2), 195–201. https://doi.org/10.5603/cj.a2021.0036
19. Soliman, E. Z., Lopez, F., O'Neal, W. T., Chen, L. Y., Bengtson, L., Zhang, Z. M., Loehr, L., Cushman, M., & Alonso, A. (2015, May 26). Atrial Fibrillation and Risk of ST-Segment–Elevation Versus Non–ST-Segment–Elevation MI. Circulation, 131(21), 1843–1850. https://doi.org/10.1161/circulationaha.114.014145
20. Vernon, S. T., Coffey, S., D'Souza, M., Chow, C. K., Kilian, J., Hyun, K., Shaw, J. A., Adams, M., Roberts-Thomson, P., Brieger, D., & Figtree, G. A. (2019, November 5). ST-Segment–Elevation MI (STEMI) Patients Without Standard Modifiable Cardiovascular Risk Factors—How Common Are They, and What Are Their Outcomes? Journal of the American Heart Association, 8(21). https://doi.org/10.1161/jaha.119.013296
21. Vogel, B., Claessen, B. E., Arnold, S. V., Chan, D., Cohen, D. J., Giannitsis, E., Gibson, C. M., Goto, S., Katus, H. A., Kerneis, M., Kimura, T., Kunadian, V., Pinto, D. S., Shiomi, H., Spertus, J. A., Steg, P. G., & Mehran, R. (2019, June 6). ST-segment elevation MI. Nature Reviews Disease Primers, 5(1). https://doi.org/10.1038/s41572-019-0090-3

22. Scholz, K. H., Maier, S. K. G., Maier, L. S., Lengenfelder, B., Jacobshagen, C., Jung, J., Fleischmann, C., Werner, G. S., Olbrich, H. G., Ott, R., Mudra, H., Seidl, K., Schulze, P. C., Weiss, C., Haimerl, J., Friede, T., & Meyer, T. (2018, February 14). Impact of treatment delay on mortality in ST-segment elevation MI (STEMI) patients presenting with and without haemodynamic instability: results from the German perspective, multicentre FITT-STEMI trial. European Heart Journal, 39(13), 1065–1074. https://doi.org/10.1093/eurheartj/ehy004
23. Basit, H., Malik, A., & Huecker, M. R. (2023). Non–ST-Segment Elevation MI. In *StatPearls*. StatPearls Publishing.
24. Jiménez-Méndez, C., Díez-Villanueva, P., & Alfonso, F. (2021). Non-ST segment elevation MI in the elderly. Reviews in Cardiovascular Medicine, 22(3), 779. https://doi.org/10.31083/j.rcm2203084
25. Somma, K. A., Bhatt, D. L., Fonarow, G. C., Cannon, C. P., Cox, M., Laskey, W., Peacock, W. F., Hernandez, A. F., Peterson, E. D., Schwamm, L., & Saxon, L. A. (2012, September). Guideline Adherence After ST-Segment Elevation Versus Non-ST Segment Elevation MI. Circulation: Cardiovascular Quality and Outcomes, 5(5), 654–661. https://doi.org/10.1161/circoutcomes.111.963959
26. Sanchis, J., Núñez, J., Bodí, V., Núñez, E., García-Alvarez, A., Bonanad, C., Regueiro, A., Bosch, X., Heras, M., Sala, J., Bielsa, O., & Llácer, A. (2011, April). Influence of Comorbid Conditions on One-Year Outcomes in Non–ST-Segment Elevation Acute Coronary Syndrome. Mayo Clinic Proceedings, 86(4), 291–296. https://doi.org/10.4065/mcp.2010.0702
27. Pahwa, R., & Jialal, I. (2023). Atherosclerosis. In *StatPearls*. StatPearls Publishing
28. Makover, M. E., Shapiro, M. D., & Toth, P. P. (2022, December). There is urgent need to treat atherosclerotic cardiovascular disease risk earlier, more intensively, and with greater precision: A review of current practice and recommendations for improved effectiveness. *American Journal of Preventive Cardiology*, *12*, 100371. https://doi.org/10.1016/j.ajpc.2022.100371
29. Lusis, A. J. (2000, September). Atherosclerosis. Nature, 407(6801), 233–241. https://doi.org/10.1038/35025203
30. Jebari-Benslaiman, S., Galicia-García, U., Larrea-Sebal, A., Olaetxea, J. R., Alloza, I., Vandenbroeck, K., Benito-Vicente, A., & Martín, C. (2022, March 20). Pathophysiology of Atherosclerosis. International Journal of Molecular Sciences, 23(6), 3346. https://doi.org/10.3390/ijms23063346
31. Watson, A. D., Leitinger, N., Navab, M., Faull, K. F., Hörkkö, S., Witztum, J. L., Palinski, W., Schwenke, D., Salomon, R. G., Sha, W., Subbanagounder, G., Fogelman, A. M., & Berliner, J. A. (1997, May). Structural Identification by Mass Spectrometry of Oxidized Phospholipids in Minimally Oxidized Low Density Lipoprotein That Induce Monocyte/Endothelial Interactions and Evidence for Their Presence in Vivo. Journal of Biological Chemistry, 272(21), 13597–13607. https://doi.org/10.1074/jbc.272.21.13597

32. Dutta, P., Courties, G., Wei, Y., Leuschner, F., Gorbatov, R., Robbins, C. S., Iwamoto, Y., Thompson, B., Carlson, A. L., Heidt, T., Majmudar, M. D., Lasitschka, F., Etzrodt, M., Waterman, P., Waring, M. T., Chicoine, A. T., van der Laan, A. M., Niessen, H. W. M., Piek, J. J., . . . Nahrendorf, M. (2012, June 27). MI accelerates atherosclerosis. Nature, 487(7407), 325–329. https://doi.org/10.1038/nature11260
33. Libby, P. (2021, April 21). The changing landscape of atherosclerosis. Nature, 592(7855), 524–533. https://doi.org/10.1038/s41586-021-03392-8
34. Monin, A., Didier, R., Leclercq, T., Chagué, F., Rochette, L., Danchin, N., Zeller, M., Fauchier, L., Cochet, A., & Cottin, Y. (2022, July). Coronary artery embolism and acute coronary syndrome: A critical appraisal of existing data. Trends in Cardiovascular Medicine. https://doi.org/10.1016/j.tcm.2022.07.004
35. Niccoli, G., & Camici, P. G. (2020, March 30). MI with non-obstructive coronary arteries: what is the prognosis? European Heart Journal Supplements, 22(Supplement_E), E40–E45. https://doi.org/10.1093/eurheartj/suaa057
36. Seitz, A., Martínez Pereyra, V., Sechtem, U., & Ong, P. (2022, July). Update on coronary artery spasm 2022 – A narrative review. International Journal of Cardiology, 359, 1–6. https://doi.org/10.1016/j.ijcard.2022.04.011
37. Vidal-Perez, R., Casas, C. A. J., Agra-Bermejo, R. M., Alvarez-Alvarez, B., Grapsa, J., Fontes-Carvalho, R., Veloso, P. R., Acuña, J. M. G., & Gonzalez-Juanatey, J. R. (2019, December 26). MI with non-obstructive coronary arteries: A comprehensive review and future research directions. World Journal of Cardiology, 11(12), 305–315. https://doi.org/10.4330/wjc.v11.i12.305
38. Niccoli, G., & Camici, P. G. (2020, March 30). MI with non-obstructive coronary arteries: what is the prognosis? *European Heart Journal Supplements*, *22*(Supplement_E), E40–E45. https://doi.org/10.1093/eurheartj/suaa057
39. Boyd, B., & Solh, T. (2020, March). Takotsubo cardiomyopathy. JAAPA, 33(3), 24–29. https://doi.org/10.1097/01.jaa.0000654368.35241.fc
40. Del Re, D. P., Amgalan, D., Linkermann, A., Liu, Q., & Kitsis, R. N. (2019, October 1). Fundamental Mechanisms of Regulated Cell Death and Implications for Heart Disease. Physiological Reviews, 99(4), 1765–1817. https://doi.org/10.1152/physrev.00022.2018
41. Sun, T., Ding, W., Xu, T., Ao, X., Yu, T., Li, M., Liu, Y., Zhang, X., Hou, L., & Wang, J. (2019, December 1). Parkin Regulates Programmed Necrosis and Myocardial Ischemia/Reperfusion Injury by Targeting Cyclophilin-D. Antioxidants & Redox Signaling, 31(16), 1177–1193. https://doi.org/10.1089/ars.2019.7734
42. D'Arcy, M. S. (2019, April 25). Cell death: a review of the major forms of apoptosis, necrosis and autophagy. Cell Biology International, 43(6), 582–592. https://doi.org/10.1002/cbin.11137
43. Oerlemans, M. I. F. J., Liu, J., Arslan, F., Ouden, K., Middelaar, B. J., Doevendans, P. A., & Sluijter, J. P. G. (2012, May 3). Inhibition of RIP1-dependent necrosis prevents adverse

cardiac remodeling after myocardial ischemia–reperfusion in vivo. Basic Research in Cardiology, 107(4). https://doi.org/10.1007/s00395-012-0270-8

44. Zhang, T., Zhang, Y., Cui, M., Jin, L., Wang, Y., Lv, F., Liu, Y., Zheng, W., Shang, H., Zhang, J., Zhang, M., Wu, H., Guo, J., Zhang, X., Hu, X., Cao, C. M., & Xiao, R. P. (2016, January 4). CaMKII is a RIP3 substrate mediating ischemia- and oxidative stress–induced myocardial necroptosis. Nature Medicine, 22(2), 175–182. https://doi.org/10.1038/nm.4017
45. Wang, J. X., Zhang, X. J., Li, Q., Wang, K., Wang, Y., Jiao, J. Q., Feng, C., Teng, S., Zhou, L. Y., Gong, Y., Zhou, Z. X., Liu, J., Wang, J. L., & Li, P. F. (2015, July 31). MicroRNA-103/107 Regulate Programmed Necrosis and Myocardial Ischemia/Reperfusion Injury Through Targeting FADD. Circulation Research, 117(4), 352–363. https://doi.org/10.1161/circresaha.117.305781
46. Teringova, E., & Tousek, P. (2017, May 1). Apoptosis in ischemic heart disease. Journal of Translational Medicine, 15(1). https://doi.org/10.1186/s12967-017-1191-y
47. Sciarretta, S., Maejima, Y., Zablocki, D., & Sadoshima, J. (2018, February 10). The Role of Autophagy in the Heart. Annual Review of Physiology, 80(1), 1–26. https://doi.org/10.1146/annurev-physiol-021317-121427
48. Wu, M. Y., Yiang, G. T., Liao, W. T., Tsai, A. Y., Cheng, Y. L., Cheng, P. W., Li, C. Y., & Li, C. J. (2018). Current Mechanistic Concepts in Ischemia and Reperfusion Injury. Cellular Physiology and Biochemistry, 46(4), 1650–1667. https://doi.org/10.1159/000489241
49. Kalogeris, T., Baines, C. P., Krenz, M., & Korthuis, R. J. (2012). Cell Biology of Ischemia/Reperfusion Injury. *International Review of Cell and Molecular Biology Volume 298*, 229–317. https://doi.org/10.1016/b978-0-12-394309-5.00006-7
50. Chalise, U., Becirovic-Agic, M., & Lindsey, M. L. (2022, October 23). The cardiac wound healing response to MI. WIREs Mechanisms of Disease, 15(1). https://doi.org/10.1002/wsbm.1584
51. Paolisso, P., Foà, A., Bergamaschi, L., Donati, F., Fabrizio, M., Chiti, C., Angeli, F., Toniolo, S., Stefanizzi, A., Armillotta, M., Rucci, P., Iannopollo, G., Casella, G., Marrozzini, C., Galiè, N., & Pizzi, C. (2021, February 2). Hyperglycemia, inflammatory response and infarct size in obstructive acute MI and MINOCA. Cardiovascular Diabetology, 20(1). https://doi.org/10.1186/s12933-021-01222-9
52. Raziyeva, K., Kim, Y., Zharkinbekov, Z., Kassymbek, K., Jimi, S., & Saparov, A. (2021, May 8). Immunology of Acute and Chronic Wound Healing. Biomolecules, 11(5), 700. https://doi.org/10.3390/biom11050700
53. Yu, J., Liu, Y., Peng, W., & Xu, Z. (2022, August 31). Serum VCAM-1 and ICAM-1 measurement assists for MACE risk estimation in ST-segment elevation MI patients. Journal of Clinical Laboratory Analysis, 36(10). https://doi.org/10.1002/jcla.24685
54. Liu, Y., Xu, J., Wu, M., Kang, L., & Xu, B. (2020, April 30). The effector cells and cellular mediators of the immune system involved in cardiac inflammation and fibrosis

after MI. Journal of Cellular Physiology, 235(12), 8996–9004. https://doi.org/10.1002/jcp.29732
55. Zhang, S. J., Song, X. Y., He, M., & Yu, S. B. (2016). Effect of TGF-β1/SDF-1/CXCR4 signal on BM-MSCs homing in rat heart of ischemia/perfusion injury. *European review for medical and pharmacological sciences*, *20*(5), 899–905
56. Nian, M., Lee, P., Khaper, N., & Liu, P. (2004, June 25). Inflammatory Cytokines and PostMI Remodeling. Circulation Research, 94(12), 1543–1553. https://doi.org/10.1161/01.res.0000130526.20854.fa
57. Halade, G. V., & Tourki, B. (2019). Specialized Pro-resolving Mediators Directs Cardiac Healing and Repair with Activation of Inflammation and Resolution Program in Heart Failure. Advances in Experimental Medicine and Biology, 45–64. https://doi.org/10.1007/978-3-030-21735-8_6
58. Kain, V., Ingle, K. A., Colas, R. A., Dalli, J., Prabhu, S. D., Serhan, C. N., Joshi, M., & Halade, G. V. (2015, July). Resolvin D1 activates the inflammation resolving response at splenic and ventricular site following MI leading to improved ventricular function. *Journal of Molecular and Cellular Cardiology*, *84*, 24–35. https://doi.org/10.1016/j.yjmcc.2015.04.003
59. Liberale, L., Ministrini, S., Carbone, F., Camici, G. G., & Montecucco, F. (2021, March 26). Cytokines as therapeutic targets for cardio- and cerebrovascular diseases. *Basic Research in Cardiology*, *116*(1). https://doi.org/10.1007/s00395-021-00863-x
60. Lu, X., Wang, Z., Ye, D., Feng, Y., Liu, M., Xu, Y., Wang, M., Zhang, J., Liu, J., Zhao, M., Xu, S., Ye, J., & Wan, J. (2022, May 20). The Role of CXC Chemokines in Cardiovascular Diseases. *Frontiers in Pharmacology*, *12*. https://doi.org/10.3389/fphar.2021.765768
61. Vajen, T., Koenen, R. R., Werner, I., Staudt, M., Projahn, D., Curaj, A., Sönmez, T. T., Simsekyilmaz, S., Schumacher, D., Möllmann, J., Hackeng, T. M., Hundelshausen, P. V., Weber, C., & Liehn, E. A. (2018, July 13). Blocking CCL5-CXCL4 heteromerization preserves heart function after MI by attenuating leukocyte recruitment and NETosis. Scientific Reports, 8(1). https://doi.org/10.1038/s41598-018-29026-0
62. Sun, Y., Wang, Y., Yang, H., Lu, Y., Zhu, G., Yang, L., Zhao, Y., Hu, B., & Ying, T. (2019, January). Interleukin 8 targeted contrast echocardiography is effective to evaluate myocardial ischemia-reperfusion injury in the rabbits. Biomedicine & Pharmacotherapy, 109, 1346–1350. https://doi.org/10.1016/j.biopha.2018.10.126
63. Ohara, F., Ohkubo, K., Maeda, K., Seki, J., & Goto, T. (2002, February). FR183998, a Na+/H+ exchange inhibitor, suppresses both IL-8 content and myocardial infarct size in a cardiac ischaemia-reperfusion model in rats. Journal of Pharmacy and Pharmacology, 54(2), 263–268. https://doi.org/10.1211/0022357021778295
64. Bujak, M., Dobaczewski, M., Gonzalez-Quesada, C., Xia, Y., Leucker, T., Zymek, P., Veeranna, V., Tager, A. M., Luster, A. D., & Frangogiannis, N. G. (2009, November 6). Induction of the CXC Chemokine Interferon-γ-Inducible Protein 10 Regulates the

Reparative Response Following MI. *Circulation Research*, *105*(10), 973–983. https://doi.org/10.1161/circresaha.109.199471

65. Ghadge, S. K., Mühlstedt, S., Özcelik, C., & Bader, M. (2011, January). SDF-1α as a therapeutic stem cell homing factor in MI. *Pharmacology & Therapeutics*, *129*(1), 97–108. https://doi.org/10.1016/j.pharmthera.2010.09.011
66. Zhao, G., Wang, S., Wang, Z., Sun, A., Yang, X., Qiu, Z., Wu, C., Zhang, W., Li, H., Zhang, Y., Zhao, J., Zou, Y., & Ge, J. (2013, September). CXCR6 deficiency ameliorated myocardial ischemia/reperfusion injury by inhibiting infiltration of monocytes and IFN-γ-dependent autophagy. *International Journal of Cardiology*, *168*(2), 853–862. https://doi.org/10.1016/j.ijcard.2012.10.022
67. Weil, B. R., & Neelamegham, S. (2019, February 27). Selectins and Immune Cells in Acute MI and Post-infarction Ventricular Remodeling: Pathophysiology and Novel Treatments. Frontiers in Immunology, 10. https://doi.org/10.3389/fimmu.2019.00300
68. Raziyeva, K., Kim, Y., Zharkinbekov, Z., Temirkhanova, K., & Saparov, A. (2022, September 2). Novel Therapies for the Treatment of Cardiac Fibrosis Following MI. Biomedicines, 10(9), 2178. https://doi.org/10.3390/biomedicines10092178
69. Webber, M., Jackson, S. P., Moon, J. C., & Captur, G. (2020, August 30). Myocardial Fibrosis in Heart Failure: Anti-Fibrotic Therapies and the Role of Cardiovascular Magnetic Resonance in Drug Trials. Cardiology and Therapy, 9(2), 363–376. https://doi.org/10.1007/s40119-020-00199-y
70. Karamitsos, T. D., Arvanitaki, A., Karvounis, H., Neubauer, S., & Ferreira, V. M. (2020, May). Myocardial Tissue Characterization and Fibrosis by Imaging. *JACC: Cardiovascular Imaging*, *13*(5), 1221–1234. https://doi.org/10.1016/j.jcmg.2019.06.030
71. Heymans, S., González, A., Pizard, A., Papageorgiou, A. P., López-Andrés, N., Jaisser, F., Thum, T., Zannad, F., & Díez, J. (2015, June 30). Searching for new mechanisms of myocardial fibrosis with diagnostic and/or therapeutic potential. European Journal of Heart Failure, 17(8), 764–771. https://doi.org/10.1002/ejhf.312
72. Tanaka, R., Umemura, M., Narikawa, M., Hikichi, M., Osaw, K., Fujita, T., Yokoyama, U., Ishigami, T., Tamura, K., & Ishikawa, Y. (2020, January 27). Reactive fibrosis precedes doxorubicin-induced heart failure through sterile inflammation. ESC Heart Failure, 7(2), 588–603. https://doi.org/10.1002/ehf2.12616
73. Kyriakou, P., Mouselimis, D., Tsarouchas, A., Rigopoulos, A., Bakogiannis, C., Noutsias, M., & Vassilikos, V. (2018, December). Diagnosis of cardiac amyloidosis: a systematic review on the role of imaging and biomarkers. BMC Cardiovascular Disorders, 18(1). https://doi.org/10.1186/s12872-018-0952-8
74. Hara, H., Takeda, N., & Komuro, I. (2017, July 17). Pathophysiology and therapeutic potential of cardiac fibrosis. Inflammation and Regeneration, 37(1). https://doi.org/10.1186/s41232-017-0046-5
75. Ceauşu, Z., Socea, B., Costache, M., Predescu, D., Şerban, D., Smarandache, C., Pacu, I., Alexandru, H., Daviţoiu, A. M., Jacotă-Alexe, F., Cîrstoveanu, C., Dimitriu, M., Pleş, L.,

& Ceauşu, M. (2021, January 25). Fibroblast involvement in cardiac remodeling and repair under ischemic conditions. *Experimental and Therapeutic Medicine*, *21*(3). https://doi.org/10.3892/etm.2021.9700

76. Yousefi, F., Shabaninejad, Z., Vakili, S., Derakhshan, M., Movahedpour, A., Dabiri, H., Ghasemi, Y., Mahjoubin-Tehran, M., Nikoozadeh, A., Savardashtaki, A., Mirzaei, H., & Hamblin, M. R. (2020, June 9). TGF-β and WNT signaling pathways in cardiac fibrosis: non-coding RNAs come into focus. *Cell Communication and Signaling*, *18*(1). https://doi.org/10.1186/s12964-020-00555-4
77. Talman, V., & Ruskoaho, H. (2016, June 21). Cardiac fibrosis in MI—from repair and remodeling to regeneration. *Cell and Tissue Research*, *365*(3), 563–581. https://doi.org/10.1007/s00441-016-2431-9
78. Ni, H., Li, W., Zhuge, Y., Xu, S., Wang, Y., Chen, Y., Shen, G., & Wang, F. (2019, October). Inhibition of circHIPK3 prevents angiotensin II-induced cardiac fibrosis by sponging miR-29b-3p. International Journal of Cardiology, 292, 188–196. https://doi.org/10.1016/j.ijcard.2019.04.006
79. Frangogiannis, N. G. (2020, November 2). Cardiac fibrosis. Cardiovascular Research, 117(6), 1450–1488. https://doi.org/10.1093/cvr/cvaa324
80. Aujla, P. K., & Kassiri, Z. (2021, February). Diverse origins and activation of fibroblasts in cardiac fibrosis. Cellular Signalling, 78, 109869. https://doi.org/10.1016/j.cellsig.2020.109869
81. Dobaczewski, M., de Haan, J. J., & Frangogiannis, N. G. (2012, September 7). The Extracellular Matrix Modulates Fibroblast Phenotype and Function in the Infarcted Myocardium. Journal of Cardiovascular Translational Research, 5(6), 837–847. https://doi.org/10.1007/s12265-012-9406-3
82. Reed, G. W., Rossi, J. E., & Cannon, C. P. (2017, January). Acute MI. The Lancet, 389(10065), 197–210. https://doi.org/10.1016/s0140-6736(16)30677-8
83. Bainey, K. R., & Armstrong, P. W. (2014, May). Clinical perspectives on reperfusion injury in acute MI. American Heart Journal, 167(5), 637–645. https://doi.org/10.1016/j.ahj.2014.01.015
84. Kristensen, S. D., Laut, K. G., Fajadet, J., Kaifoszova, Z., Kala, P., Di Mario, C., Wijns, W., Clemmensen, P., Agladze, V., Antoniades, L., Alhabib, K. F., De Boer, M. J., Claeys, M. J., Deleanu, D., Dudek, D., Erglis, A., Gilard, M., Goktekin, O., Guagliumi, G., . . . Sokolov, Y. (2014, January 12). Reperfusion therapy for ST elevation acute MI 2010/2011: current status in 37 ESC countries. European Heart Journal, 35(29), 1957–1970. https://doi.org/10.1093/eurheartj/eht529
85. Ahmad, M., Mehta, P., Reddivari, A. K. R., & Mungee, S. (2023). Percutaneous Coronary Intervention. In *StatPearls*. StatPearls Publishing.
86. Wu, C., Li, L., Wang, S., Zeng, J., Yang, J., Xu, H., Zhao, Y., Wang, Y., Li, W., Jin, C., Gao, X., Yang, Y., & Qiao, S. (2023, February 22). Fibrinolytic therapy use for ST-segment elevation MI and long-term outcomes in China: 2-year results from the China

Acute MI Registry. *BMC Cardiovascular Disorders*, *23*(1). https://doi.org/10.1186/s12872-023-03105-1
87. Armstrong, P. W., Collen, D., & Antman, E. (2003, May 27). Fibrinolysis for Acute MI. Circulation, 107(20), 2533–2537. https://doi.org/10.1161/01.cir.0000072930.64775.dc
88. Bendary, A., Tawfik, W., Mahrous, M., & Salem, M. (2017, December 30). Fibrinolytic therapy in patients with ST-segment elevation MI: Accelerated versus standard Streptokinase infusion regimen. Journal of Cardiovascular and Thoracic Research, 9(4), 209–214. https://doi.org/10.15171/jcvtr.2017.36
89. Kunadian, V., & Gibson, C. M. (2010, November 11). Thrombolytics and MI. Cardiovascular Therapeutics, 30(2). https://doi.org/10.1111/j.1755-5922.2010.00239.x
90. Shi, W. Y., & Smith, J. A. (2018). Role of Coronary Artery Bypass Surgery in Acute MI. Primary Angioplasty, 211–221. https://doi.org/10.1007/978-981-13-1114-7_16
91. Thielmann, M., Wendt, D., Slottosch, I., Welp, H., Schiller, W., Tsagakis, K., Schmack, B., Weymann, A., Martens, S., Neuhäuser, M., Wahlers, T., Choi, Y., Ruhparwar, A., & Liakopoulos, O. (2021, September 21). Coronary Artery Bypass Graft Surgery in Patients With Acute Coronary Syndromes After Primary Percutaneous Coronary Intervention: A Current Report From the North-Rhine Westphalia Surgical MI Registry. Journal of the American Heart Association, 10(18). https://doi.org/10.1161/jaha.121.021182
92. Thilak, A., Thacker, D., Shales, S., Das, D., Behera, S., Ghosh, A., & Narayan, P. (2021). Timing of coronary artery bypass grafting after acute MI: does it influence outcomes? Polish Journal of Cardio-Thoracic Surgery, 18(1), 27–32. https://doi.org/10.5114/kitp.2021.105184
93. Bachar, B. J., & Manna , B. (2023). Coronary Artery Bypass Graft. In *StatPearls*. StatPearls Publishing.
94. E van der Elst, M. E., Bouvy, M. L., de Blaey, C. J., & de Boer, A. (2007, October 1). Effect of drug combinations on admission for recurrent MI. Heart, 93(10), 1226–1230. https://doi.org/10.1136/hrt.2006.098053
95. Maxwell, S., & Waring, W. S. (2000, November). Therapeutics Drugs used in secondary prevention after MI: Case presentation. *British Journal of Clinical Pharmacology*, *50*(5), 405–417. https://doi.org/10.1046/j.1365-2125.2000.00287.x
96. Joo, S. J. (2023, August 31). Beta-blocker therapy in patients with acute MI: not all patients need it. Acute and Critical Care, 38(3), 251–260. https://doi.org/10.4266/acc.2023.00955
97. Kezerashvili, A., Marzo, K., & De Leon, J. (2012, June 1). Beta Blocker Use After Acute MI in the Patient with Normal Systolic Function: When is it "Ok" to Discontinue? Current Cardiology Reviews, 8(1), 77–84. https://doi.org/10.2174/157340312801215764
98. Chen, Y. J., Li, L. J., Tang, W. L., Song, J. Y., Qiu, R., Li, Q., Xue, H., & Wright, J. M. (2018, November 14). First-line drugs inhibiting the renin angiotensin system versus other first-line antihypertensive drug classes for hypertension. Cochrane Database of Systematic Reviews, 2018(11). https://doi.org/10.1002/14651858.cd008170.pub3

99. Goyal, A., Cusick, A. S., & Thielemier, B. (2023). ACE Inhibitors. In *StatPearls*. StatPearls Publishing.
100. Ghouse, J., Ahlberg, G., Andreasen, L., Banasik, K., Brunak, S., Schwinn, M., Larsen, I. H., Petersen, O., Sørensen, E., Ullum, H., Rasmussen, E. R., Eriksson, N., Hallberg, P., Wadelius, M., Bundgaard, H., & Olesen, M. S. (2021, August). Association of Variants Near the Bradykinin Receptor B2 Gene With Angioedema in Patients Taking ACE Inhibitors. Journal of the American College of Cardiology, 78(7), 696–709. https://doi.org/10.1016/j.jacc.2021.05.054
101. Kostis, J. B., Shelton, B., Gosselin, G., Goulet, C., Hood, W. B., Kohn, R. M., Kubo, S. H., Schron, E., Weiss, M. B., Willis, P. W., Young, J. B., & Probstfield, J. (1996, February). Adverse effects of enalapril in the Studies of Left Ventricular Dysfunction (SOLVD). American Heart Journal, 131(2), 350–355. https://doi.org/10.1016/s0002-8703(96)90365-8
102. Khera, R., Clark, C., Lu, Y., Guo, Y., Ren, S., Truax, B., Spatz, E. S., Murugiah, K., Lin, Z., Omer, S. B., Vojta, D., & Krumholz, H. M. (2021, July 6). Association of Angiotensin-Converting Enzyme Inhibitors and Angiotensin Receptor Blockers With the Risk of Hospitalization and Death in Hypertensive Patients With COVID-19. *Journal of the American Heart Association*, *10*(13). https://doi.org/10.1161/jaha.120.018086
103. Han, X., Zhang, Y., Yin, L., Zhang, L., Wang, Y., Zhang, H., & Li, B. (2018, March). Statin in the treatment of patients with MI. Medicine, 97(12), e0167. https://doi.org/10.1097/md.0000000000010167
104. Brooks, J. M., Cook, E., Chapman, C. G., Schroeder, M. C., A. Chrischilles, E., Schneider, K. M., Kulchaitanaroaj, P., & Robinson, J. (2015, April). Statin Use After Acute MI by Patient Complexity. Medical Care, 53(4), 324–331. https://doi.org/10.1097/mlr.0000000000000322
105. Pinal-Fernandez, I., Casal-Dominguez, M., & Mammen, A. L. (2018, May). Statins: pros and cons. Medicina Clínica, 150(10), 398–402. https://doi.org/10.1016/j.medcli.2017.11.030
106. Perez-Villa, B., Cubeddu, R. J., Brozzi, N., Sleiman, J. R., Navia, J., & Hernandez-Montfort, J. (2021, October 21). Transition to heart transplantation in post-MI ventricular septal rupture: a systematic review. Heart Failure Reviews, 28(1), 217–227. https://doi.org/10.1007/s10741-021-10161-2
107. Shah, K. S., Kittleson, M. M., & Kobashigawa, J. A. (2019, June 25). Updates on Heart Transplantation. Current Heart Failure Reports, 16(5), 150–156. https://doi.org/10.1007/s11897-019-00432-3
108. Website, N. (2023, April 21). *Heart transplant*. nhs.uk. https://www.nhs.uk/conditions/heart-transplant/
109. Mehra, M. R., Canter, C. E., Hannan, M. M., Semigran, M. J., Uber, P. A., Baran, D. A., Danziger-Isakov, L., Kirklin, J. K., Kirk, R., Kushwaha, S. S., Lund, L. H., Potena, L., Ross, H. J., Taylor, D. O., Verschuuren, E. A., & Zuckermann, A. (2016, January).

The 2016 International Society for Heart Lung Transplantation listing criteria for heart transplantation: A 10-year update. The Journal of Heart and Lung Transplantation, 35(1), 1–23. https://doi.org/10.1016/j.healun.2015.10.023

110. Hsich, E. M. (2016, April). Matching the Market for Heart Transplantation. Circulation: Heart Failure, 9(4). https://doi.org/10.1161/circheartfailure.115.002679

111. Arjmand, B., Abedi, M., Arabi, M., Alavi-Moghadam, S., Rezaei-Tavirani, M., Hadavandkhani, M., Tayanloo-Beik, A., Kordi, R., Roudsari, P. P., & Larijani, B. (2021, September 10). Regenerative Medicine for the Treatment of Ischemic Heart Disease; Status and Future Perspectives. Frontiers in Cell and Developmental Biology, 9. https://doi.org/10.3389/fcell.2021.704903

112. Mao, A. S., & Mooney, D. J. (2015, November 23). Regenerative medicine: Current therapies and future directions. *Proceedings of the National Academy of Sciences*, *112*(47), 14452–14459. https://doi.org/10.1073/pnas.1508520112

113. Gazit, Z., Pelled, G., Sheyn, D., Yakubovich, D. C., & Gazit, D. (2019). Mesenchymal Stem Cells. Principles of Regenerative Medicine, 205–218. https://doi.org/10.1016/b978-0-12-809880-6.00014-x

114. *Tissue Engineering and Regenerative Medicine*. (n.d.). National Institute of Biomedical Imaging and Bioengineering. https://www.nibib.nih.gov/science-education/science-topics/tissue-engineering-and-regenerative-medicine#pid-1156

115. Law, S., & Chaudhuri, S. (2013). Mesenchymal stem cell and regenerative medicine: regeneration versus immunomodulatory challenges. *American journal of stem cells*, *2*(1), 22–38

116. Arjmand, B., Abedi, M., Arabi, M., Alavi-Moghadam, S., Rezaei-Tavirani, M., Hadavandkhani, M., Tayanloo-Beik, A., Kordi, R., Roudsari, P. P., & Larijani, B. (2021, September 10). Regenerative Medicine for the Treatment of Ischemic Heart Disease; Status and Future Perspectives. Frontiers in Cell and Developmental Biology, 9. https://doi.org/10.3389/fcell.2021.704903

117. Muñoz Ruiz, M., & Regueiro, J. R. (2012). New Tools in Regenerative Medicine: Gene Therapy. Advances in Experimental Medicine and Biology, 254–275. https://doi.org/10.1007/978-1-4614-2098-9_17

118. Berillo, D., Yeskendir, A., Zharkinbekov, Z., Raziyeva, K., & Saparov, A. (2021, November 5). Peptide-Based Drug Delivery Systems. Medicina, 57(11), 1209. https://doi.org/10.3390/medicina57111209

119. Smagul, S., Kim, Y., Smagulova, A., Raziyeva, K., Nurkesh, A., & Saparov, A. (2020, August 19). Biomaterials Loaded with Growth Factors/Cytokines and Stem Cells for Cardiac Tissue Regeneration. International Journal of Molecular Sciences, 21(17), 5952. https://doi.org/10.3390/ijms21175952

120. Dzobo, K., Thomford, N. E., Senthebane, D. A., Shipanga, H., Rowe, A., Dandara, C., Pillay, M., & Motaung, K. S. C. M. (2018, July 30). Advances in

Regenerative Medicine and Tissue Engineering: Innovation and Transformation of Medicine. Stem Cells International, 2018, 1–24. https://doi.org/10.1155/2018/2495848

121. Fortier, L. A. (2005, September). Stem Cells: Classifications, Controversies, and Clinical Applications. Veterinary Surgery, 34(5), 415–423. https://doi.org/10.1111/j.1532-950x.2005.00063.x

122. Mahla, R. S. (2016). Stem Cells Applications in Regenerative Medicine and Disease Therapeutics. International Journal of Cell Biology, 2016, 1–24. https://doi.org/10.1155/2016/6940283

123. Liu, G., David, B. T., Trawczynski, M., & Fessler, R. G. (2019, November 23). Advances in Pluripotent Stem Cells: History, Mechanisms, Technologies, and Applications. *Stem Cell Reviews and Reports*, *16*(1), 3–32. https://doi.org/10.1007/s12015-019-09935-x

124. Dulak, J., Szade, K., Szade, A., Nowak, W., & Józkowicz, A. (2015). Adult stem cells: hopes and hypes of regenerative medicine. *Acta Biochimica Polonica*, *62*(3), 329–337. https://doi.org/10.18388/abp.2015_1023

125. Thomson, M., Liu, S., Zou, L. N., Smith, Z., Meissner, A., & Ramanathan, S. (2011, June). Pluripotency Factors in Embryonic Stem Cells Regulate Differentiation into Germ Layers. *Cell*, *145*(6), 875–889. https://doi.org/10.1016/j.cell.2011.05.017

126. Ye, L., Swingen, C., & Zhang, J. (2013, February 1). Induced Pluripotent Stem Cells and Their Potential for Basic and Clinical Sciences. *Current Cardiology Reviews*, *9*(1), 63–72. https://doi.org/10.2174/157340313805076278

127. Rajabzadeh, N., Fathi, E., & Farahzadi, R. (2019, July). Stem cell-based regenerative medicine. Stem Cell Investigation, 6, 19–19. https://doi.org/10.21037/sci.2019.06.04

128. Petersdorf, E. W., Malkki, M., Gooley, T. A., Martin, P. J., & Guo, Z. (2007, January 30). MHC Haplotype Matching for Unrelated Hematopoietic Cell Transplantation. *PLoS Medicine*, *4*(1), e8. https://doi.org/10.1371/journal.pmed.0040008

129. Li, H. C., Stoicov, C., Rogers, A. B., & Houghton, J. (2006). Stem cells and cancer: Evidence for bone marrow stem cells in epithelial cancers. *World Journal of Gastroenterology*, *12*(3), 363. https://doi.org/10.3748/wjg.v12.i3.363

130. Herberts, C. A., Kwa, M. S., & Hermsen, H. P. (2011, March 22). Risk factors in the development of stem cell therapy. *Journal of Translational Medicine*, *9*(1). https://doi.org/10.1186/1479-5876-9-29

131. Nussbaum, J., Minami, E., Laflamme, M. A., Virag, J. A. I., Ware, C. B., Masino, A., Muskheli, V., Pabon, L., Reinecke, H., & Murry, C. E. (2007, February 6). Transplantation of undifferentiated murine embryonic stem cells in the heart: teratoma formation and immune response. *The FASEB Journal*, *21*(7), 1345–1357. https://doi.org/10.1096/fj.06-6769com

132. Tang, J. N., Cores, J., Huang, K., Cui, X. L., Luo, L., Zhang, J. Y., Li, T. S., Qian, L., & Cheng, K. (2018, February 22). Concise Review: Is Cardiac Cell Therapy Dead?

Embarrassing Trial Outcomes and New Directions for the Future. Stem Cells Translational Medicine, 7(4), 354–359. https://doi.org/10.1002/sctm.17-0196

133. Mason, C., & Dunnill, P. (2008, January). A brief definition of regenerative medicine. *Regenerative Medicine*, *3*(1), 1–5. https://doi.org/10.2217/17460751.3.1.1

134. Kahn-Krell, A., Pretorius, D., Guragain, B., Lou, X., Wei, Y., Zhang, J., Qiao, A., Nakada, Y., Kamp, T. J., Ye, L., & Zhang, J. (2022, July 22). A three-dimensional culture system for generating cardiac spheroids composed of cardiomyocytes, endothelial cells, smooth-muscle cells, and cardiac fibroblasts derived from human induced-pluripotent stem cells. Frontiers in Bioengineering and Biotechnology, 10. https://doi.org/10.3389/fbioe.2022.908848

135. Woodcock, E. A., & Matkovich, S. J. (2005, September). Cardiomyocytes structure, function and associated pathologies. *The International Journal of Biochemistry & Cell Biology*, *37*(9), 1746–1751. https://doi.org/10.1016/j.biocel.2005.04.011

136. Maxwell, W. L. (1994, January). Wheater's functional histology–a text and colour atlas by H.G. Burkitt, B. Young, and J.W. Heath, 3rd edition, 416 pp. Edinburgh: Churchill livingston; 1993. (Distributed in the United States of America by Churchill Livingston, inc.). £27.50. Clinical Anatomy, 7(1), 52–53. https://doi.org/10.1002/ca.980070110

137. Microtubules and Centrosomes. (2017). *Cell Biology*, 593–612. https://doi.org/10.1016/b978-0-323-34126-4.00034-7

138. Zipes, D. (2018). Braunwald's Heart Disease: A Textbook of Cardiovascular Medicine, 11th Edition. *BMH Medical Journal - ISSN 2348–392X, 5*(2), 63. Retrieved from https://babymhospital.org/BMH_MJ/index.php/BMHMJ/article/view/163

139. Keepers, B., Liu, J., & Qian, L. (2020, March). What's in a cardiomyocyte – And how do we make one through reprogramming? *Biochimica Et Biophysica Acta (BBA) - Molecular Cell Research*, *1867*(3), 118464. https://doi.org/10.1016/j.bbamcr.2019.03.011

140. Lin, Z., & Pu, W. T. (2014, June 4). Strategies for Cardiac Regeneration and Repair. Science Translational Medicine, 6(239). https://doi.org/10.1126/scitranslmed.3006681

141. Guo, Y., Yu, Y., Hu, S., Chen, Y., & Shen, Z. (2020, May 11). The therapeutic potential of mesenchymal stem cells for cardiovascular diseases. *Cell Death & Disease*, *11*(5). https://doi.org/10.1038/s41419-020-2542-9

142. A Phase I, Pilot Study of Human Embryonic Stem Cell-Derived Cardiomyocytes in PaTients with ChrOnic Ischemic Left VentRicular Dysfunction (HECTOR) – CIRM. (n.d.). https://www.cirm.ca.gov/our-progress/awards/phase-i-pilot-study-human-embryonic-stem-cell-derived-cardiomyocytes-patients-chronic-ischemic-left-ventricular-dysfunction-hector/

143. Szaraz, P., Gratch, Y. S., Iqbal, F., & Librach, C. L. (2017, August 9). In Vitro Differentiation of Human Mesenchymal Stem Cells into Functional

Cardiomyocyte-like Cells. Journal of Visualized Experiments, 126. https://doi.org/10.3791/55757

144. Guo, X., Bai, Y., Zhang, L., Zhang, B., Zagidullin, N., Carvalho, K., Du, Z., & Cai, B. (2018, February 26). Cardiomyocyte differentiation of mesenchymal stem cells from bone marrow: new regulators and its implications. Stem Cell Research & Therapy, 9(1). https://doi.org/10.1186/s13287-018-0773-9

145. Shi, S., Wu, X., Wang, X., Hao, W., Miao, H., Zhen, L., & Nie, S. (2016). Differentiation of Bone Marrow Mesenchymal Stem Cells to Cardiomyocyte-Like Cells Is Regulated by the Combined Low Dose Treatment of Transforming Growth Factor-β1 and 5-Azacytidine. Stem Cells International, 2016, 1–11. https://doi.org/10.1155/2016/3816256

146. Zhuge, Y., Zhang, J., Qian, F., Wen, Z., Niu, C., Xu, K., Ji, H., Rong, X., Chu, M., & Jia, C. (2020). Role of smooth muscle cells in Cardiovascular Disease. *International Journal of Biological Sciences*, *16*(14), 2741–2751. https://doi.org/10.7150/ijbs.49871

147. Wongsurawat, T., Woo, C. C., Giannakakis, A., Lin, X. Y., Cheow, E. S. H., Lee, C. N., Richards, M., Sze, S. K., Nookaew, I., Kuznetsov, V. A., & Sorokin, V. (2018, April). Distinctive molecular signature and activated signaling pathways in aortic smooth muscle cells of patients with MI. *Atherosclerosis*, *271*, 237–244. https://doi.org/10.1016/j.atherosclerosis.2018.01.024

148. Russo A, Favero L, Saccà S, Caico SI, Cernetti C. (2006). Coronary artery aneurysms.*Cardiologia*. (7-8):409-417. DOI: 10.1714/1954.21240. PMID: 26228610.

149. Ye, G., Fu, Q., Jiang, L., & Li, Z. (2018, November). Vascular smooth muscle cells activate PI3K/Akt pathway to attenuate myocardial ischemia/reperfusion-induced apoptosis and autophagy by secreting bFGF. Biomedicine & Pharmacotherapy, 107, 1779–1785. https://doi.org/10.1016/j.biopha.2018.05.113

150. Gu, W., Hong, X., Le Bras, A., Nowak, W. N., Issa Bhaloo, S., Deng, J., Xie, Y., Hu, Y., Ruan, X. Z., & Xu, Q. (2018, May). Smooth muscle cells differentiated from mesenchymal stem cells are regulated by microRNAs and suitable for vascular tissue grafts. Journal of Biological Chemistry, 293(21), 8089–8102. https://doi.org/10.1074/jbc.ra118.001739

151. Hegner, B., Weber, M., Dragun, D., & Schulze-Lohoff, E. (2005, June). Differential regulation of smooth muscle markers in human bone marrow-derived mesenchymal stem cells. *Journal of Hypertension*, *23*(6), 1191–1202. https://doi.org/10.1097/01.hjh.0000170382.31085.5d

152. Harada, S., Nakamura, Y., Shiraya, S., Fujiwara, Y., Kishimoto, Y., Onohara, T., Otsuki, Y., Kishimoto, S., Yamamoto, Y., Hisatome, I., & Nishimura, M. (2016, August 5). Smooth muscle cell sheet transplantation preserve cardiac function and minimize cardiac remodeling in a rat MI model. *Journal of Cardiothoracic Surgery*, *11*(1). https://doi.org/10.1186/s13019-016-0508-x

153. Kan, C. D., Lee, H. L., & Yang, Y. J. (2010, September). Cell transplantation for myocardial injury: a preliminary comparative study. *Cytotherapy*, *12*(5), 692–700. https://doi.org/10.3109/14653241003786130

154. Kawamura, M., Paulsen, M. J., Goldstone, A. B., Shudo, Y., Wang, H., Steele, A. N., Stapleton, L. M., Edwards, B. B., Eskandari, A., Truong, V. N., Jaatinen, K. J., Ingason, A. B., Miyagawa, S., Sawa, Y., & Woo, Y. J. (2017, November 2). Tissue-engineered smooth muscle cell and endothelial progenitor cell bi-level cell sheets prevent progression of cardiac dysfunction, microvascular dysfunction, and interstitial fibrosis in a rodent model of type 1 diabetes-induced cardiomyopathy. *Cardiovascular Diabetology*, *16*(1). https://doi.org/10.1186/s12933-017-0625-4

155. Dan, P., Velot, M., Decot, V., & Menu, P. (2015, January 1). The role of mechanical stimuli in the vascular differentiation of mesenchymal stem cells. Journal of Cell Science. https://doi.org/10.1242/jcs.167783

156. Boyd, N. L., Robbins, K. R., Dhara, S. K., West, F. D., & Stice, S. L. (2009, August). Human Embryonic Stem Cell–Derived Mesoderm-like Epithelium Transitions to Mesenchymal Progenitor Cells. *Tissue Engineering Part A*, *15*(8), 1897–1907. https://doi.org/10.1089/ten.tea.2008.0351

157. Guo, X., Stice, S. L., Boyd, N. L., & Chen, S. Y. (2013, February 15). A novel in vitro model system for smooth muscle differentiation from human embryonic stem cell-derived mesenchymal cells. American Journal of Physiology-Cell Physiology, 304(4), C289–C298. https://doi.org/10.1152/ajpcell.00298.2012

158. Shi, N., & Chen, S. (2015, October 8). Smooth Muscle Cell Differentiation: Model Systems, Regulatory Mechanisms, and Vascular Diseases. Journal of Cellular Physiology, 231(4), 777–787. https://doi.org/10.1002/jcp.25208

159. Sun, Q., Chen, G., Streb, J. W., Long, X., Yang, Y., Stoeckert, C. J., & Miano, J. M. (2005, December 19). Defining the mammalian CArGome. *Genome Research*, *16*(2), 197–207. https://doi.org/10.1101/gr.4108706

160. Pipes, G. T., Creemers, E. E., & Olson, E. N. (2006, June 15). The myocardin family of transcriptional coactivators: versatile regulators of cell growth, migration, and myogenesis. *Genes & Development*, *20*(12), 1545–1556. https://doi.org/10.1101/gad.1428006

161. Kurpinski, K., Lam, H., Chu, J., Wang, A., Kim, A., Tsay, E., Agrawal, S., Schaffer, D. V., & Li, S. (2010, February 9). Transforming Growth Factor-β and Notch Signaling Mediate Stem Cell Differentiation into Smooth Muscle Cells. *Stem Cells*, *28*(4), 734–742. https://doi.org/10.1002/stem.319

162. Sivaraman, S., Hedrick, J., Ismail, S., Slavin, C., & Rao, R. R. (2021, September 25). Generation and Characterization of Human Mesenchymal Stem Cell-Derived Smooth Muscle Cells. *International Journal of Molecular Sciences*, *22*(19), 10335. https://doi.org/10.3390/ijms221910335

163. Dhar, K., Dhar, G., Majumder, M., Haque, I., Mehta, S., Van Veldhuizen, P. J., Banerjee, S. K., & Banerjee, S. (2010, August 5). Tumor cell-derived PDGF-B potentiates mouse mesenchymal stem cells-pericytes transition and recruitment through an interaction with NRP-1. *Molecular Cancer*, *9*(1). https://doi.org/10.1186/1476-4598-9-209
164. Dan, P., Velot, M., Decot, V., & Menu, P. (2015, January 1). The role of mechanical stimuli in the vascular differentiation of mesenchymal stem cells. *Journal of Cell Science*. https://doi.org/10.1242/jcs.167783
165. Ishii, Y., Langberg, J., Rosborough, K., & Mikawa, T. (2008, August 6). Endothelial cell lineages of the heart. *Cell and Tissue Research*, *335*(1), 67–73. https://doi.org/10.1007/s00441-008-0663-z
166. Zhang, Q., Bosch-Rué, L., Pérez, R. A., & Truskey, G. A. (2021, May 7). Biofabrication of tissue engineering vascular systems. *APL Bioengineering*, *5*(2). https://doi.org/10.1063/5.0039628
167. Naito, Y., Shinoka, T., Duncan, D., Hibino, N., Solomon, D., Cleary, M., Rathore, A., Fein, C., Church, S., & Breuer, C. (2011, April). Vascular tissue engineering: Towards the next generation vascular grafts. *Advanced Drug Delivery Reviews*, *63*(4–5), 312–323. https://doi.org/10.1016/j.addr.2011.03.001
168. Ikhapoh, I. A., Pelham, C. J., & Agrawal, D. K. (2015, January 6). Synergistic effect of angiotensin II on vascular endothelial growth factor-A-mediated differentiation of bone marrow-derived mesenchymal stem cells into endothelial cells. *Stem Cell Research & Therapy*, *6*(1). https://doi.org/10.1186/scrt538
169. Ikhapoh, I. A., Pelham, C. J., & Agrawal, D. K. (2015, March). Sry-type HMG box 18 contributes to the differentiation of bone marrow-derived mesenchymal stem cells to endothelial cells. *Differentiation*, *89*(3–4), 87–96. https://doi.org/10.1016/j.diff.2015.03.003
170. Ai, W. J., Li, J., Lin, S. M., Li, W., Liu, C. Z., & Lv, W. M. (2015, June). R-Smad Signaling-Mediated VEGF Expression Coordinately Regulates Endothelial Cell Differentiation of Rat Mesenchymal Stem Cells. *Stem Cells and Development*, *24*(11), 1320–1331. https://doi.org/10.1089/scd.2014.0253
171. Wang, C., Li, Y., Yang, M., Zou, Y., Liu, H., Liang, Z., Yin, Y., Niu, G., Yan, Z., & Zhang, B. (2018, February). Efficient Differentiation of Bone Marrow Mesenchymal Stem Cells into Endothelial Cells in Vitro. *European Journal of Vascular and Endovascular Surgery*, *55*(2), 257–265. https://doi.org/10.1016/j.ejvs.2017.10.012
172. Silva, G. V., Litovsky, S., Assad, J. A., Sousa, A. L., Martin, B. J., Vela, D., Coulter, S. C., Lin, J., Ober, J., Vaughn, W. K., Branco, R. V., Oliveira, E. M., He, R., Geng, Y. J., Willerson, J. T., & Perin, E. C. (2005, January 18). Mesenchymal Stem Cells Differentiate into an Endothelial Phenotype, Enhance Vascular Density, and Improve Heart Function in a Canine Chronic Ischemia Model. *Circulation*, *111*(2), 150–156. https://doi.org/10.1161/01.cir.0000151812.86142.45

173. Sharma, A., Burridge, P. W., McKeithan, W. L., Serrano, R., Shukla, P., Sayed, N., Churko, J. M., Kitani, T., Wu, H., Holmström, A., Matsa, E., Zhang, Y., Kumar, A., Fan, A. C., del Álamo, J. C., Wu, S. M., Moslehi, J. J., Mercola, M., & Wu, J. C. (2017, February 15). High-throughput screening of tyrosine kinase inhibitor cardiotoxicity with human induced pluripotent stem cells. *Science Translational Medicine*, *9*(377). https://doi.org/10.1126/scitranslmed.aaf2584

174. Burridge, P. W., Matsa, E., Shukla, P., Lin, Z. C., Churko, J. M., Ebert, A. D., Lan, F., Diecke, S., Huber, B., Mordwinkin, N. M., Plews, J. R., Abilez, O. J., Cui, B., Gold, J. D., & Wu, J. C. (2014, June 15). Chemically defined generation of human cardiomyocytes. *Nature Methods*, *11*(8), 855–860. https://doi.org/10.1038/nmeth.2999

175. Wnorowski, A., Yang, H., & Wu, J. C. (2019, February). Progress, obstacles, and limitations in the use of stem cells in organ-on-a-chip models. *Advanced Drug Delivery Reviews*, *140*, 3–11. https://doi.org/10.1016/j.addr.2018.06.001

176. Scott, C. W., Peters, M. F., & Dragan, Y. P. (2013, May). Human induced pluripotent stem cells and their use in drug discovery for toxicity testing. *Toxicology Letters*, *219*(1), 49–58. https://doi.org/10.1016/j.toxlet.2013.02.020

177. Kuppusamy, K. T., Jones, D. C., Sperber, H., Madan, A., Fischer, K. A., Rodriguez, M. L., Pabon, L., Zhu, W. Z., Tulloch, N. L., Yang, X., Sniadecki, N. J., Laflamme, M. A., Ruzzo, W. L., Murry, C. E., & Ruohola-Baker, H. (2015, May 11). Let-7 family of microRNA is required for maturation and adult-like metabolism in stem cell-derived cardiomyocytes. *Proceedings of the National Academy of Sciences*, *112*(21). https://doi.org/10.1073/pnas.1424042112

178. Ronaldson-Bouchard, K., Ma, S. P., Yeager, K., Chen, T., Song, L., Sirabella, D., Morikawa, K., Teles, D., Yazawa, M., & Vunjak-Novakovic, G. (2018, April). Advanced maturation of human cardiac tissue grown from pluripotent stem cells. *Nature*, *556*(7700), 239–243. https://doi.org/10.1038/s41586-018-0016-3

179. Leonard, A., Bertero, A., Powers, J. D., Beussman, K. M., Bhandari, S., Regnier, M., Murry, C. E., & Sniadecki, N. J. (2018, May). Afterload promotes maturation of human induced pluripotent stem cell derived cardiomyocytes in engineered heart tissues. *Journal of Molecular and Cellular Cardiology*, *118*, 147–158. https://doi.org/10.1016/j.yjmcc.2018.03.016

180. Lee, J. H., Protze, S. I., Laksman, Z., Backx, P. H., & Keller, G. M. (2017, August). Human Pluripotent Stem Cell-Derived Atrial and Ventricular Cardiomyocytes Develop from Distinct Mesoderm Populations. *Cell Stem Cell*, *21*(2), 179-194.e4. https://doi.org/10.1016/j.stem.2017.07.003

181. *Biomaterials*. (n.d.). National Institute of Biomedical Imaging and Bioengineering. https://www.nibib.nih.gov/science-education/science-topics/biomaterials#:~:text=Biomaterials%20may%20be%20natural%20or,sutures%20made%20from%20animal%20sinew

182. Tu, Z., Zhong, Y., Hu, H., Shao, D., Haag, R., Schirner, M., Lee, J., Sullenger, B., & Leong, K. W. (2022, February 28). Design of therapeutic biomaterials to control inflammation. *Nature Reviews Materials*, *7*(7), 557–574. https://doi.org/10.1038/s41578-022-00426-z
183. Huzum, B., Puha, B., Necoara, R., Gheorghevici, S., Puha, G., Filip, A., Sirbu, P., & Alexa, O. (2021, September 17). Biocompatibility assessment of biomaterials used in orthopedic devices: An overview (Review). *Experimental and Therapeutic Medicine*, *22*(5). https://doi.org/10.3892/etm.2021.10750
184. Cacopardo, L. (2022). Biomaterials and biocompatibility. *Human Orthopaedic Biomechanics*, 341–359. https://doi.org/10.1016/b978-0-12-824481-4.00038-x
185. Marin, E., Boschetto, F., & Pezzotti, G. (2020, March 31). Biomaterials and biocompatibility: An historical overview. *Journal of Biomedical Materials Research Part A*, *108*(8), 1617–1633. https://doi.org/10.1002/jbm.a.36930
186. Ghasemi-Mobarakeh, L., Kolahreez, D., Ramakrishna, S., & Williams, D. (2019, June). Key terminology in biomaterials and biocompatibility. *Current Opinion in Biomedical Engineering*, *10*, 45–50. https://doi.org/10.1016/j.cobme.2019.02.004
187. Pires, J. R. A., Souza, V. G. L., Fuciños, P., Pastrana, L., & Fernando, A. L. (2022, March 27). Methodologies to Assess the Biodegradability of Bio-Based Polymers—Current Knowledge and Existing Gaps. *Polymers*, *14*(7), 1359. https://doi.org/10.3390/polym14071359
188. Samir, A., Ashour, F. H., Hakim, A. A. A., & Bassyouni, M. (2022, August 19). Recent advances in biodegradable polymers for sustainable applications. *Npj Materials Degradation*, *6*(1). https://doi.org/10.1038/s41529-022-00277-7
189. Hynes, C. G., Morra, E., Walsh, P., & Buchanan, F. (2023). Degradation of biomaterials. *Tissue Engineering*, 213–259. https://doi.org/10.1016/b978-0-12-824459-3.00032-9
190. Reis, L., Chiu, L., Feric, N., Fu, L., & Radisic, M. (2014). Injectable biomaterials for cardiac regeneration and repair. *Cardiac Regeneration and Repair*, 49–81. https://doi.org/10.1533/9780857096715.1.49
191. Li, J., & Mooney, D. J. (2016, October 18). Designing hydrogels for controlled drug delivery. *Nature Reviews Materials*, *1*(12). https://doi.org/10.1038/natrevmats.2016.71
192. Carlini, A. S., Gaetani, R., Braden, R. L., Luo, C., Christman, K. L., & Gianneschi, N. C. (2019, April 15). Enzyme-responsive progelator cyclic peptides for minimally invasive delivery to the heart post-MI. *Nature Communications*, *10*(1). https://doi.org/10.1038/s41467-019-09587-y
193. Blackburn, N. J., Sofrenovic, T., Kuraitis, D., Ahmadi, A., McNeill, B., Deng, C., Rayner, K. J., Zhong, Z., Ruel, M., & Suuronen, E. J. (2015, January). Timing underpins the benefits associated with injectable collagen biomaterial therapy for the treatment of MI. *Biomaterials*, *39*, 182–192. https://doi.org/10.1016/j.biomaterials.2014.11.004

194. Lister, Z., Rayner, K. J., & Suuronen, E. J. (2016, July 18). How Biomaterials Can Influence Various Cell Types in the Repair and Regeneration of the Heart after MI. *Frontiers in Bioengineering and Biotechnology*, *4*. https://doi.org/10.3389/fbioe.2016.00062

195. Recommended Dose Volumes for Common Laboratory Animal. (n.d.). The International Consortium for Innovation and Quality in Pharmaceutical Development . https://iqconsortium.org/initiatives/leadership-groups/3rs-translational-and-predictive-sciences

196. Rufaihah, A. J., Yasa, I. C., Ramanujam, V. S., Arularasu, S. C., Kofidis, T., Guler, M. O., & Tekinay, A. B. (2017, August). Angiogenic peptide nanofibers repair cardiac tissue defect after MI. *Acta Biomaterialia*, *58*, 102–112. https://doi.org/10.1016/j.actbio.2017.06.009

197. Navaei, A., Truong, D., Heffernan, J., Cutts, J., Brafman, D., Sirianni, R. W., Vernon, B., & Nikkhah, M. (2016, March). PNIPAAm-based biohybrid injectable hydrogel for cardiac tissue engineering. Acta Biomaterialia, 32, 10–23. https://doi.org/10.1016/j.actbio.2015.12.019

198. Ho, Y. T., Poinard, B., & Kah, J. C. Y. (2016, March). Nanoparticle drug delivery systems and their use in cardiac tissue therapy. *Nanomedicine*, *11*(6), 693–714. https://doi.org/10.2217/nnm.16.6

199. Lin, X., Liu, Y., Bai, A., Cai, H., Bai, Y., Jiang, W., Yang, H., Wang, X., Yang, L., Sun, N., & Gao, H. (2019, April 15). A viscoelastic adhesive epicardial patch for treating MI. *Nature Biomedical Engineering*, *3*(8), 632–643. https://doi.org/10.1038/s41551-019-0380-9

200. Domenech, M., Polo-Corrales, L., Ramirez-Vick, J. E., & Freytes, D. O. (2016, December). Tissue Engineering Strategies for Myocardial Regeneration: Acellular Versus Cellular Scaffolds? *Tissue Engineering Part B: Reviews*, *22*(6), 438–458. https://doi.org/10.1089/ten.teb.2015.0523

201. Ashtari, K., Nazari, H., Ko, H., Tebon, P., Akhshik, M., Akbari, M., Alhosseini, S. N., Mozafari, M., Mehravi, B., Soleimani, M., Ardehali, R., Ebrahimi Warkiani, M., Ahadian, S., & Khademhosseini, A. (2019, April). Electrically conductive nanomaterials for cardiac tissue engineering. *Advanced Drug Delivery Reviews*, *144*, 162–179. https://doi.org/10.1016/j.addr.2019.06.001

202. Saghazadeh, S., Rinoldi, C., Schot, M., Kashaf, S. S., Sharifi, F., Jalilian, E., Nuutila, K., Giatsidis, G., Mostafalu, P., Derakhshandeh, H., Yue, K., Swieszkowski, W., Memic, A., Tamayol, A., & Khademhosseini, A. (2018, March). Drug delivery systems and materials for wound healing applications. *Advanced Drug Delivery Reviews*, *127*, 138–166. https://doi.org/10.1016/j.addr.2018.04.008

203. Saludas, L., Pascual-Gil, S., Prósper, F., Garbayo, E., & Blanco-Prieto, M. (2017, May). Hydrogel based approaches for cardiac tissue engineering. *International Journal of Pharmaceutics*, *523*(2), 454–475. https://doi.org/10.1016/j.ijpharm.2016.10.061

204. Mihic, A., Cui, Z., Wu, J., Vlacic, G., Miyagi, Y., Li, S. H., Lu, S., Sung, H. W., Weisel, R. D., & Li, R. K. (2015, August 25). A Conductive Polymer Hydrogel Supports Cell Electrical Signaling and Improves Cardiac Function After Implantation into Myocardial Infarct. *Circulation*, *132*(8), 772–784. https://doi.org/10.1161/circulationaha.114.014937
205. Wang, W., Tan, B., Chen, J., Bao, R., Zhang, X., Liang, S., Shang, Y., Liang, W., Cui, Y., Fan, G., Jia, H., & Liu, W. (2018, April). An injectable conductive hydrogel encapsulating plasmid DNA-eNOs and ADSCs for treating MI. *Biomaterials*, *160*, 69–81. https://doi.org/10.1016/j.biomaterials.2018.01.021
206. Gaharwar, A. K., Singh, I., & Khademhosseini, A. (2020, July 6). Engineered biomaterials for in situ tissue regeneration. *Nature Reviews Materials*, *5*(9), 686–705. https://doi.org/10.1038/s41578-020-0209-x
207. Cho, K. H., Uthaman, S., Park, I. K., & Cho, C. S. (2018, September 1). Injectable Biomaterials in Plastic and Reconstructive Surgery: A Review of the Current Status. *Tissue Engineering and Regenerative Medicine*, *15*(5), 559–574. https://doi.org/10.1007/s13770-018-0158-2
208. Bertsch, P., Diba, M., Mooney, D. J., & Leeuwenburgh, S. C. G. (2022, August 5). Self-Healing Injectable Hydrogels for Tissue Regeneration. *Chemical Reviews*, *123*(2), 834–873. https://doi.org/10.1021/acs.chemrev.2c00179
209. Dormont, F., Varna, M., & Couvreur, P. (2018, March). Nanoplumbers: biomaterials to fight cardiovascular diseases. *Materials Today*, *21*(2), 122–143. https://doi.org/10.1016/j.mattod.2017.07.008
210. Hussey, G. S., Dziki, J. L., & Badylak, S. F. (2018, May 29). Extracellular matrix-based materials for regenerative medicine. *Nature Reviews Materials*, *3*(7), 159–173. https://doi.org/10.1038/s41578-018-0023-x
211. Jain, K. K. (2019, August 22). An Overview of Drug Delivery Systems. *Drug Delivery Systems*, 1–54. https://doi.org/10.1007/978-1-4939-9798-5_1
212. Berillo, D., Zharkinbekov, Z., Kim, Y., Raziyeva, K., Temirkhanova, K., & Saparov, A. (2021, December 1). Stimuli-Responsive Polymers for Transdermal, Transmucosal and Ocular Drug Delivery. *Pharmaceutics*, *13*(12), 2050. https://doi.org/10.3390/pharmaceutics13122050
213. Fenton, O. S., Olafson, K. N., Pillai, P. S., Mitchell, M. J., & Langer, R. (2018, May 7). Advances in Biomaterials for Drug Delivery. *Advanced Materials*, *30*(29). https://doi.org/10.1002/adma.201705328
214. Hou, Q., De Bank, P. A., & Shakesheff, K. M. (2004). Injectable scaffolds for tissue regeneration. *Journal of Materials Chemistry*, *14*(13), 1915. https://doi.org/10.1039/b401791a
215. O. Adeosun, S., O. Ilomuanya, M., P. Gbenebor, O., O. Dada, M., & C. Odili, C. (2020, November 26). Biomaterials for Drug Delivery: Sources, Classification, Synthesis,

Processing, and Applications. *Advanced Functional Materials*. https://doi.org/10.5772/intechopen.93368

216. Memic, A., Colombani, T., Eggermont, L. J., Rezaeeyazdi, M., Steingold, J., Rogers, Z. J., Navare, K. J., Mohammed, H. S., & Bencherif, S. A. (2019, February 10). Latest Advances in Cryogel Technology for Biomedical Applications. *Advanced Therapeutics*, *2*(4). https://doi.org/10.1002/adtp.201800114
217. Jones, L. O., Williams, L., Boam, T., Kalmet, M., Oguike, C., & Hatton, F. L. (2021, October 14). Cryogels: recent applications in 3D-bioprinting, injectable cryogels, drug delivery, and wound healing. *Beilstein Journal of Organic Chemistry*, *17*, 2553–2569. https://doi.org/10.3762/bjoc.17.171
218. Çimen, D., Özbek, M. A., Bereli, N., Mattiasson, B., & Denizli, A. (2021, April 1). Injectable Cryogels in Biomedicine. *Gels*, *7*(2), 38. https://doi.org/10.3390/gels7020038
219. Vasu, S., Zhou, J., Chen, J., Johnston, P. V., & Kim, D. H. (2021). Biomaterials-based Approaches for Cardiac Regeneration. *Korean Circulation Journal*, *51*(12), 943. https://doi.org/10.4070/kcj.2021.0291
220. Cui, Z., Yang, B., & Li, R. K. (2016, March). Application of Biomaterials in Cardiac Repair and Regeneration. *Engineering*, *2*(1), 141–148. https://doi.org/10.1016/j.eng.2016.01.028
221. Okay, O. (Ed.). (2014). Polymeric Cryogels. *Advances in Polymer Science*. https://doi.org/10.1007/978-3-319-05846-7
222. Sultankulov, B., Berillo, D., Kauanova, S., Mikhalovsky, S., Mikhalovska, L., & Saparov, A. (2019, December 4). Composite Cryogel with Polyelectrolyte Complexes for Growth Factor Delivery. *Pharmaceutics*, *11*(12), 650. https://doi.org/10.3390/pharmaceutics11120650
223. Sultankulov, B., Berillo, D., Sultankulova, K., Tokay, T., & Saparov, A. (2019, September 10). Progress in the Development of Chitosan-Based Biomaterials for Tissue Engineering and Regenerative Medicine. *Biomolecules*, *9*(9), 470. https://doi.org/10.3390/biom9090470
224. Kim, Y., Zharkinbekov, Z., Raziyeva, K., Tabyldiyeva, L., Berikova, K., Zhumagul, D., Temirkhanova, K., & Saparov, A. (2023, March 1). Chitosan-Based Biomaterials for Tissue Regeneration. *Pharmaceutics*, *15*(3), 807. https://doi.org/10.3390/pharmaceutics15030807
225. Oduah, E., Linhardt, R., & Sharfstein, S. (2016, July 4). Heparin: Past, Present, and Future. *Pharmaceuticals*, *9*(3), 38. https://doi.org/10.3390/ph9030038
226. Forsberg, E., Pejler, G., Ringvall, M., Lunderius, C., Tomasini-Johansson, B., Kusche-Gullberg, M., Eriksson, I., Ledin, J., Hellman, L., & Kjellén, L. (1999, August). Abnormal mast cells in mice deficient in a heparin-synthesizing enzyme. *Nature*, *400*(6746), 773–776. https://doi.org/10.1038/23488

227. Kocak, F. Z., Yar, M., & Rehman, I. U. (2022, May 11). Hydroxyapatite-Integrated, Heparin- and Glycerol-Functionalized Chitosan-Based Injectable Hydrogels with Improved Mechanical and Proangiogenic Performance. *International Journal of Molecular Sciences*, *23*(10), 5370. https://doi.org/10.3390/ijms23105370
228. Welzel, P. B., Grimmer, M., Renneberg, C., Naujox, L., Zschoche, S., Freudenberg, U., & Werner, C. (2012, July 3). Macroporous StarPEG-Heparin Cryogels. *Biomacromolecules*, *13*(8), 2349–2358. https://doi.org/10.1021/bm300605s
229. Wan, W., Bannerman, A. D., Yang, L., & Mak, H. (2014). Poly(Vinyl Alcohol) Cryogels for Biomedical Applications. *Polymeric Cryogels*, 283–321. https://doi.org/10.1007/978-3-319-05846-7_8
230. Păduraru, O. M., Ciolacu, D., Darie, R. N., & Vasile, C. (2012, December). Synthesis and characterization of polyvinyl alcohol/cellulose cryogels and their testing as carriers for a bioactive component. *Materials Science and Engineering: C*, *32*(8), 2508–2515. https://doi.org/10.1016/j.msec.2012.07.033
231. Khapre, M. A., Pandey, S., & Jugade, R. M. (2021, November). Glutaraldehyde-cross-linked chitosan–alginate composite for organic dyes removal from aqueous solutions. *International Journal of Biological Macromolecules*, *190*, 862–875. https://doi.org/10.1016/j.ijbiomac.2021.09.026
232. Figueiredo, K. C. S., Alves, T. L. M., & Borges, C. P. (2008, December 11). Poly(vinyl alcohol) films crosslinked by glutaraldehyde under mild conditions. *Journal of Applied Polymer Science*, *111*(6), 3074–3080. https://doi.org/10.1002/app.29263
233. Omidian, H., Dey Chowdhury, S., & Babanejad, N. (2023, June 27). Cryogels: Advancing Biomaterials for Transformative Biomedical Applications. *Pharmaceutics*, *15*(7), 1836. https://doi.org/10.3390/pharmaceutics15071836
234. Saylan, & Denizli. (2019, April 17). Supermacroporous Composite Cryogels in Biomedical Applications. *Gels*, *5*(2), 20. https://doi.org/10.3390/gels5020020
235. Evans, C., Morimitsu, Y., Hisadome, T., Inomoto, F., Yoshida, M., & Takei, T. (2021, July). Optimized hydrophobically modified chitosan cryogels for strength and drug delivery systems. *Journal of Bioscience and Bioengineering*, *132*(1), 81–87. https://doi.org/10.1016/j.jbiosc.2021.03.008
236. Beleño Acosta, B., Advincula, R. C., & Grande-Tovar, C. D. (2023, February 17). Chitosan-Based Scaffolds for the Treatment of MI: A Systematic Review. *Molecules*, *28*(4), 1920. https://doi.org/10.3390/molecules28041920
237. Ayaz, F., Demir, D., & Bölgen, N. (2021, January 1). Differential anti-inflammatory properties of chitosan-based cryogel scaffolds depending on chitosan/gelatin ratio. *Artificial Cells, Nanomedicine, and Biotechnology*, *49*(1), 682–690. https://doi.org/10.1080/21691401.2021.2012184
238. Thiagarajan, H., Thiyagamoorthy, U., Shanmugham, I., Dharmalingam Nandagopal, G., & Kaliyaperumal, A. (2017, June 21). Angiogenic growth factors in MI:

a critical appraisal. *Heart Failure Reviews*, *22*(6), 665–683. https://doi.org/10.1007/s10741-017-9630-7

239. Jimi, S., Jaguparov, A., Nurkesh, A., Sultankulov, B., & Saparov, A. (2020, April 17). Sequential Delivery of Cryogel Released Growth Factors and Cytokines Accelerates Wound Healing and Improves Tissue Regeneration. *Frontiers in Bioengineering and Biotechnology*, *8*. https://doi.org/10.3389/fbioe.2020.00345

240. Chen, B., Huang, S., Su, Y., Wu, Y. J., Hanna, A., Brickshawana, A., Graff, J., & Frangogiannis, N. G. (2019, June 21). Macrophage Smad3 Protects the Infarcted Heart, Stimulating Phagocytosis and Regulating Inflammation. *Circulation Research*, *125*(1), 55–70. https://doi.org/10.1161/circresaha.119.315069

241. Yue, Y., Wang, C., Benedict, C., Huang, G., Truongcao, M., Roy, R., Cimini, M., Garikipati, V. N. S., Cheng, Z., Koch, W. J., & Kishore, R. (2020, January 31). Interleukin-10 Deficiency Alters Endothelial Progenitor Cell–Derived Exosome Reparative Effect on Myocardial Repair via Integrin-Linked Kinase Enrichment. *Circulation Research*, *126*(3), 315–329. https://doi.org/10.1161/circresaha.119.315829

242. Jung, M., Ma, Y., Iyer, R. P., DeLeon-Pennell, K. Y., Yabluchanskiy, A., Garrett, M. R., & Lindsey, M. L. (2017, April 24). IL-10 improves cardiac remodeling after MI by stimulating M2 macrophage polarization and fibroblast activation. *Basic Research in Cardiology*, *112*(3). https://doi.org/10.1007/s00395-017-0622-5

243. Ferraro, B., Leoni, G., Hinkel, R., Ormanns, S., Paulin, N., Ortega-Gomez, A., Viola, J. R., de Jong, R., Bongiovanni, D., Bozoglu, T., Maas, S. L., D'Amico, M., Kessler, T., Zeller, T., Hristov, M., Reutelingsperger, C., Sager, H. B., Döring, Y., Nahrendorf, M., . . . Soehnlein, O. (2019, June). Pro-Angiogenic Macrophage Phenotype to Promote Myocardial Repair. *Journal of the American College of Cardiology*, *73*(23), 2990–3002. https://doi.org/10.1016/j.jacc.2019.03.503

244. Taimeh, Z., Loughran, J., Birks, E. J., & Bolli, R. (2013, July 16). Vascular endothelial growth factor in heart failure. *Nature Reviews Cardiology*, *10*(9), 519–530. https://doi.org/10.1038/nrcardio.2013.94

245. Cahill, T. J., Choudhury, R. P., & Riley, P. R. (2017, July 21). Heart regeneration and repair after MI: translational opportunities for novel therapeutics. *Nature Reviews Drug Discovery*, *16*(10), 699–717. https://doi.org/10.1038/nrd.2017.106

246. Itoh, N., Ohta, H., Nakayama, Y., & Konishi, M. (2016, October 18). Roles of FGF Signals in Heart Development, Health, and Disease. *Frontiers in Cell and Developmental Biology*, *4*. https://doi.org/10.3389/fcell.2016.00110

247. Wang, Z., Wang, Z., Lu, W. W., Zhen, W., Yang, D., & Peng, S. (2017, October). Novel biomaterial strategies for controlled growth factor delivery for biomedical applications. *NPG Asia Materials*, *9*(10), e435–e435. https://doi.org/10.1038/am.2017.171

248. Oduk, Y., Zhu, W., Kannappan, R., Zhao, M., Borovjagin, A. V., Oparil, S., & Zhang, J. J. (2018, February 1). VEGF nanoparticles repair the heart after MI. *American*

Journal of Physiology-Heart and Circulatory Physiology, *314*(2), H278–H284. https://doi.org/10.1152/ajpheart.00471.2017

249. Hachim, D., Whittaker, T. E., Kim, H., & Stevens, M. M. (2019, November). Glycosaminoglycan-based biomaterials for growth factor and cytokine delivery: Making the right choices. *Journal of Controlled Release*, *313*, 131–147. https://doi.org/10.1016/j.jconrel.2019.10.018

250. Cate. (2022, February 28). IACUC Policy for Dose Volumes in Laboratory Animals. Bloomington Institutional Animal Care and Use Committee (BIACUC). Retrieved December 3, 2023, from https://research.iu.edu/doc/compliance/animal-care/bloomington/iub-biacuc-dose-volumes-in-laboratory-animals.pdf

251. Zhu, H., Guo, Z. K., Jiang, X. X., Li, H., Wang, X. Y., Yao, H. Y., Zhang, Y., & Mao, N. (2010, February 25). A protocol for isolation and culture of mesenchymal stem cells from mouse compact bone. *Nature Protocols*, *5*(3), 550–560. https://doi.org/10.1038/nprot.2009.238

252. Dimmeler, S., & Leri, A. (2008, June 6). Aging and Disease as Modifiers of Efficacy of Cell Therapy. *Circulation Research*, *102*(11), 1319–1330. https://doi.org/10.1161/circresaha.108.175943

253. Clavel, C., & Verfaillie, C. M. (2008, February). Bone-marrow-derived cells and heart repair. *Current Opinion in Organ Transplantation*, *13*(1), 36–43. https://doi.org/10.1097/mot.0b013e3282f428d1

254. Psaltis, P. J., Zannettino, A. C., Worthley, S. G., & Gronthos, S. (2008, July 3). Concise Review: Mesenchymal Stromal Cells: Potential for Cardiovascular Repair. *Stem Cells*, *26*(9), 2201–2210. https://doi.org/10.1634/stemcells.2008-0428

255. Behfar, A., Yamada, S., Crespo-Diaz, R., Nesbitt, J. J., Rowe, L. A., Perez-Terzic, C., Gaussin, V., Homsy, C., Bartunek, J., & Terzic, A. (2010, August). Guided Cardiopoiesis Enhances Therapeutic Benefit of Bone Marrow Human Mesenchymal Stem Cells in Chronic MI. *Journal of the American College of Cardiology*, *56*(9), 721–734. https://doi.org/10.1016/j.jacc.2010.03.066

256. Behfar, A., Perez-Terzic, C., Faustino, R. S., Arrell, D. K., Hodgson, D. M., Yamada, S., Puceat, M., Niederländer, N., Alekseev, A. E., Zingman, L. V., & Terzic, A. (2007, February 5). Cardiopoietic programming of embryonic stem cells for tumor-free heart repair. *The Journal of Experimental Medicine*, *204*(2), 405–420. https://doi.org/10.1084/jem.20061916

257. Faustino, R. S., Behfar, A., Perez-Terzic, C., & Terzic, A. (2008). Genomic chart guiding embryonic stem cell cardiopoiesis. *Genome Biology*, *9*(1), R6. https://doi.org/10.1186/gb-2008-9-1-r6

258. Orlic, D., Kajstura, J., Chimenti, S., Jakoniuk, I., Anderson, S. M., Li, B., Pickel, J., McKay, R., Nadal-Ginard, B., Bodine, D. M., Leri, A., & Anversa, P. (2001, April 5). Bone marrow cells regenerate infarcted myocardium. *Nature*, *410*(6829), 701–705. https://doi.org/10.1038/35070587

259. Behfar, A., Yamada, S., Crespo-Diaz, R., Nesbitt, J. J., Rowe, L. A., Perez-Terzic, C., Gaussin, V., Homsy, C., Bartunek, J., & Terzic, A. (2010, August). Guided Cardiopoiesis Enhances Therapeutic Benefit of Bone Marrow Human Mesenchymal Stem Cells in Chronic MI. *Journal of the American College of Cardiology*, *56*(9), 721–734. https://doi.org/10.1016/j.jacc.2010.03.066

260. Narita, Y., Yamawaki, A., Kagami, H., Ueda, M., & Ueda, Y. (2008, July 8). Effects of transforming growth factor-beta 1 and ascorbic acid on differentiation of human bone-marrow-derived mesenchymal stem cells into smooth muscle cell lineage. *Cell and Tissue Research*, *333*(3), 449–459. https://doi.org/10.1007/s00441-008-0654-0

261. Gong, Z., Calkins, G., Cheng, E. C., Krause, D., & Niklason, L. E. (2009, February). Influence of Culture Medium on Smooth Muscle Cell Differentiation from Human Bone Marrow–Derived Mesenchymal Stem Cells. *Tissue Engineering Part A*, *15*(2), 319–330. https://doi.org/10.1089/ten.tea.2008.0161

262. Sivaraman, S., Hedrick, J., Ismail, S., Slavin, C., & Rao, R. R. (2021, September 25). Generation and Characterization of Human Mesenchymal Stem Cell-Derived Smooth Muscle Cells. *International Journal of Molecular Sciences*, *22*(19), 10335. https://doi.org/10.3390/ijms221910335

263. Hegner, B., Schaub, T., Catar, R., Kusch, A., Wagner, P., Essin, K., Lange, C., Riemekasten, G., & Dragun, D. (2016, April 7). Intrinsic Deregulation of Vascular Smooth Muscle and Myofibroblast Differentiation in Mesenchymal Stromal Cells from Patients with Systemic Sclerosis. *PLOS ONE*, *11*(4), e0153101. https://doi.org/10.1371/journal.pone.0153101

264. Khaki, M., Salmanian, A. H., Abtahi, H., Ganji, A., & Mosayebi, G. (2018). Mesenchymal Stem Cells Differentiate to Endothelial Cells Using Recombinant Vascular Endothelial Growth Factor -A. *Reports of biochemistry & molecular biology*, *6*(2), 144–150.

265. Yao, Z., Liu, H., Yang, M., Bai, Y., Zhang, B., Wang, C., Yan, Z., Niu, G., Zou, Y., & Li, Y. (2020, June 8). Bone marrow mesenchymal stem cell-derived endothelial cells increase capillary density and accelerate angiogenesis in mouse hindlimb ischemia model. *Stem Cell Research & Therapy*, *11*(1). https://doi.org/10.1186/s13287-020-01710-x

266. Akazawa, H., & Komuro, I. (2005, August). Cardiac transcription factor Csx/Nkx2-5: Its role in cardiac development and diseases. *Pharmacology & Therapeutics*, *107*(2), 252–268. https://doi.org/10.1016/j.pharmthera.2005.03.005

267. Steimle, J., & Moskowitz, I. (2017). TBX5. *Current Topics in Developmental Biology*, 195–221. https://doi.org/10.1016/bs.ctdb.2016.08.008

268. England, J., Pang, K. L., Parnall, M., Haig, M. I., & Loughna, S. (2016, May 19). Cardiac troponin T is necessary for normal development in the embryonic chick heart. *Journal of Anatomy*, *229*(3), 436–449. https://doi.org/10.1111/joa.12486

269. Moiseenko, A., Kheirollahi, V., Chao, C. M., Ahmadvand, N., Quantius, J., Wilhelm, J., Herold, S., Ahlbrecht, K., Morty, R. E., Rizvanov, A. A., Minoo, P., El Agha, E., & Bellusci, S. (2017, April 3). Origin and characterization of alpha smooth muscle actin-positive cells during murine lung development. *Stem Cells*, *35*(6), 1566–1578. https://doi.org/10.1002/stem.2615

270. Miano, J. M., & Olson, E. N. (1996, March). Expression of the Smooth Muscle Cell Calponin Gene Marks the Early Cardiac and Smooth Muscle Cell Lineages during Mouse Embryogenesis. *Journal of Biological Chemistry*, *271*(12), 7095–7103. https://doi.org/10.1074/jbc.271.12.7095

271. *Myh11 myosin, heavy polypeptide 11, smooth muscle [Mus musculus (house mouse)] - Gene - NCBI*. (n.d.). https://www.ncbi.nlm.nih.gov/gene/17880

272. Baldwin, H. S., Shen, H. M., Yan, H. C., DeLisser, H. M., Chung, A., Mickanin, C., Trask, T., Kirschbaum, N. E., Newman, P. J., Albelda, S. M., & Buck, C. A. (1994, September 1). Platelet endothelial cell adhesion molecule-1 (PECAM-1 / CD31): alternatively spliced, functionally distinct isoforms expressed during mammalian cardiovascular development. *Development*, *120*(9), 2539–2553. https://doi.org/10.1242/dev.120.9.2539

273. Hassanpour, M., Salybekov, A. A., Kobayashi, S., & Asahara, T. (2023, April 17). CD34 positive cells as endothelial progenitor cells in biology and medicine. *Frontiers in Cell and Developmental Biology*, *11*. https://doi.org/10.3389/fcell.2023.1128134

274. Deuse, T., Peter, C., Fedak, P. W., Doyle, T., Reichenspurner, H., Zimmermann, W. H., Eschenhagen, T., Stein, W., Wu, J. C., Robbins, R. C., & Schrepfer, S. (2009, September 15). Hepatocyte Growth Factor or Vascular Endothelial Growth Factor Gene Transfer Maximizes Mesenchymal Stem Cell–Based Myocardial Salvage After Acute MI. *Circulation*, *120*(11_suppl_1). https://doi.org/10.1161/circulationaha.108.843680

275. Nguyen, B. K., Maltais, S., Perrault, L. P., Tanguay, J. F., Tardif, J. C., Stevens, L. M., Borie, M., Harel, F., Mansour, S., & Noiseux, N. (2010, February 26). Improved Function and Myocardial Repair of Infarcted Heart by Intracoronary Injection of Mesenchymal Stem Cell-Derived Growth Factors. *Journal of Cardiovascular Translational Research*, *3*(5), 547–558. https://doi.org/10.1007/s12265-010-9171-0

276. Spiroski, A. M., McCracken, I. R., Thomson, A., Magalhaes-Pinto, M., Lalwani, M. K., Newton, K. J., Miller, E., Bénézech, C., Hadoke, P., Brittan, M., Mountford, J. C., Beqqali, A., Gray, G. A., & Baker, A. H. (2022, October 10). Human embryonic stem cell-derived endothelial cell product injection attenuates cardiac remodeling in MI. *Frontiers in Cardiovascular Medicine*, *9*. https://doi.org/10.3389/fcvm.2022.953211

277. Kim, Y., Zharkinbekov, Z., Raziyeva, K., Tabyldiyeva, L., Berikova, K., Zhumagul, D., Temirkhanova, K., & Saparov, A. (2023, March 1). Chitosan-Based Biomaterials for Tissue Regeneration. *Pharmaceutics*, *15*(3), 807. https://doi.org/10.3390/pharmaceutics15030807

278. Frangogiannis, N. G. (2014, March 25). The inflammatory response in myocardial injury, repair, and remodeling. *Nature Reviews Cardiology*, *11*(5), 255–265. https://doi.org/10.1038/nrcardio.2014.28

279. Simons, M., Gordon, E., & Claesson-Welsh, L. (2016, July 27). Mechanisms and regulation of endothelial VEGF receptor signalling. *Nature Reviews Molecular Cell Biology*, *17*(10), 611–625. https://doi.org/10.1038/nrm.2016.87

280. Martin-Rendon, E., Brunskill, S. J., Hyde, C. J., Stanworth, S. J., Mathur, A., & Watt, S. M. (2008). Autologous bone marrow stem cells to treat acute MI: a systematic review. *European Heart Journal,* 29(15), 1807–1818, doi:10.1093/eurheartj/ehn220

281. Roth, G.A.; Abate, D.; Abate, K.H.; Abay, S.M.; Abbafati, C.; Abbasi, N.; Abbastabar, H.; Abd-Allah, F.; Abdela, J.; Abdelalim, A. (2018). Global, regional, and national age-sex-specific mortality for 282 causes of death in 195 countries and territories, 1980–2017: a systematic analysis for the Global Burden of Disease Study 2017. *The Lancet, 392*, 1736-1788.

282. Cambria, E.; Pasqualini, F.S.; Wolint, P.; Günter, J.; Steiger, J.; Bopp, A.; Hoerstrup, S.P.; Emmert, M.Y. (2018). Translational cardiac stem cell therapy: advancing from first-generation to next-generation cell types. *NPJ Regenerative medicine*, *2*, 17, doi:10.1038/s41536-017-0024-1.

283. White, H. D., & Chew, D. P. (2008). *Acute MI. The Lancet, 372(9638), 570–584.*doi:10.1016/s0140-6736(08)61237-4

284. Eltzschig, H. K., & Eckle, T. (2011). Ischemia and reperfusion—from mechanism to translation. Nature Medicine, 17(11), 1391–1401. doi:10.1038/nm.2507

285. Glaucylara Reis Geovanini, Peter Libby., (2018). Atherosclerosis and inflammation: overview and updates. *Clin Sci (Lond)*, 132 (12): 1243–1252.

286. Stillman, A. E., Oudkerk, M., Bluemke, D. A., de Boer, M. J., Bremerich, J., Garcia, E. V., Wintersperger, B. J. (2018). Imaging the myocardial ischemic cascade.*The International Journal of Cardiovascular Imaging, 34(8), 1249–1263.*doi:10.1007/s10554-018-1330-4

287. Prabhu, S. D., & Frangogiannis, N. G. (2016). The Biological Basis for Cardiac Repair After MI.*Circulation Research, 119(1), 91–112.*doi:10.1161/circresaha.116.303577

288. Awada, H.K.; Hwang, M.P.; Wang, Y. (2016). Towards comprehensive cardiac repair and regeneration after MI: Aspects to consider and proteins to deliver. *Biomaterials*, *82*, 94-112.

289. Thirunavukkarasu, M. (2018). Disruption of VEGF Mediated Flk-1 Signaling Leads to a Gradual Loss of Vessel Health and Cardiac Function During MI: Potential Therapy With Pellino-1. *Journal of the American Heart Association, 7(18).*https://doi.org/10.1161/JAHA.117.007601

290. Raziyeva K, Smagulova A, Kim Y, Smagul S, Nurkesh A, Saparov A. (2020). Preconditioned and Genetically Modified Stem Cells for MI Treatment. *Int J Mol Sci.*, 21(19):E7301. doi: 10.3390/ijms21197301. PMID: 33023264.

291. Wei, J. (2020). Immune modulation by mesenchymal stem cells. *Cell proliferation*, *53*(1), 12712. https://onlinelibrary.wiley.com/doi/full/10.1111/cpr.12712
292. Madigan, M. (2018, April 6). Therapeutic Use of Stem Cells for MI. *Bioengineering*, *5*(2), 28. https://www.mdpi.com/2306-5354/5/2/28/htm
293. Ying, W. (2014, November). Plasticity of mesenchymal stem cells in immunomodulation: pathological and therapeutic implications. *Nat. Immunol*, *15*(11), 1009-16. https://pubmed.ncbi.nlm.nih.gov/25329189/
294. Sid-Otmane, C. (2020). Mesenchymal stem cell mediates cardiac repair through autocrine, paracrine and endocrine axes. *Journal of Translational Medicine volume*, *18*(336). https://link.springer.com/article/10.1186/s12967-020-02504-8
295. Squillaro, T. (2016, may 1). Clinical Trials with Mesenchymal Stem Cells: An Update. *Cell Transplantation*, *25*(5), 829-848. https://journals.sagepub.com/doi/full/10.3727/096368915X689622
296. *Safety and Efficacy of Intracoronary Adult Human Mesenchymal Stem Cells After Acute MI (SEED-MSC)*. (n.d.). ClinicalTrials.gov. https://clinicaltrials.gov/ct2/show/NCT01392105?term=Mesenchymal+stem+cells&cond=acute+myocardial+infarction&draw=2&rank=1
297. Ohnishi, S. (2007, January). Transplantation of mesenchymal stem cells attenuates myocardial injury and dysfunction in a rat model of acute myocarditis. *Journal of Molecular and Cellular Cardiology*, *42*(1), 88-97. https://www.sciencedirect.com/science/article/abs/pii/S002228280600959X
298. Domenis, R. (2018, September 6). Pro inflammatory stimuli enhance the immunosuppressive functions of adipose mesenchymal stem cells-derived exosomes. *Scientific Reports*, *8*, 13325. https://www.nature.com/articles/s41598-018-31707-9
299. Favaro, E. (2015, November 23). Human mesenchymal stem cells and derived extracellular vesicles induce regulatory dendritic cells in type 1 diabetic patients. *Diabetologia*, *59*, 325–333. https://link.springer.com/content/pdf/10.1007/s00125-015-3808-0.pdf
300. Selleri, S. (2016, May 24). Human mesenchymal stromal cell-secreted lactate induces M2-macrophage differentiation by metabolic reprogramming. *Oncotarget.*, *7*(21), 30193–30210. https://www.ncbi.nlm.nih.gov/pmc/articles/PMC5058674/
301. Lianga, C. (2017, Jun 05). Interferon-γ mediates the immunosuppression of bone marrow mesenchymal stem cells on T-lymphocytes in vitro. *Hematology*, *23*(1), 44-49. https://www.tandfonline.com/doi/full/10.1080/10245332.2017.1333245
302. Nguyen, T. M., Arthur, A., Hayball, J. D., & Gronthos, S. (2013, October 15). EphB and Ephrin-B Interactions Mediate Human Mesenchymal Stem Cell Suppression of Activated T-Cells. *Stem Cells and Development*, *22*(20), 2751–2764. https://doi.org/10.1089/scd.2012.0676
303. Ohnishi, S., Sumiyoshi, H., Kitamura, S., & Nagaya, N. (2007, July 23). Mesenchymal stem cells attenuate cardiac fibroblast proliferation and collagen synthesis

through paracrine actions. *FEBS Letters*, *581*(21), 3961–3966. https://doi.org/10.1016/j.febslet.2007.07.028

304. Matsushita, K. (2020, April). Heart Failure and Adipose Mesenchymal Stem Cells. *Trends in Molecular Medicine*, *26*(4), 369–379. https://doi.org/10.1016/j.molmed.2020.01.003

305. Zhao, L., Liu, X., Zhang, Y., Liang, X., Ding, Y., Xu, Y., Fang, Z., & Zhang, F. (2016, May). Enhanced cell survival and paracrine effects of mesenchymal stem cells overexpressing hepatocyte growth factor promote cardioprotection in MI. *Experimental Cell Research*, *344*(1), 30–39. https://doi.org/10.1016/j.yexcr.2016.03.024

306. Burdick, J. A., & Vunjak-Novakovic, G. (2009, February). Engineered Microenvironments for Controlled Stem Cell Differentiation. *Tissue Engineering Part A*, *15*(2), 205–219. https://doi.org/10.1089/ten.tea.2008.0131

307. Zhao, L., Hu, C., Zhang, P., Jiang, H., & Chen, J. (2018). Novel preconditioning strategies for enhancing the migratory ability of mesenchymal stem cells in acute kidney injury. *Stem Cell Research & Therapy, 9(1)*.doi:10.1186/s13287-018-0973-3

308. Rigol, M., Solanes, N., Roura, S., Roqué, M., Novensà, L., Dantas, A. P., Martorell, J., Sitges, M., Ramírez, J., Bayés-Genís, A., & Heras, M. (2013, December 18). Allogeneic adipose stem cell therapy in acute MI. *European Journal of Clinical Investigation*, *44*(1), 83–92. https://doi.org/10.1111/eci.12195

309. Yoon, Y. (2005, February 1). Clonally expanded novel multipotent stem cells from human bone marrow regenerate myocardium after MI. *The Journal of clinical Investigation*, *115*(2), 326–338. https://www.jci.org/articles/view/22326

310. Pittenger, M. F., Mackay, A. M., Beck, S. C., Jaiswal, R. K., Douglas, R., Mosca, J. D., Moorman, M. A., Simonetti, D. W., Craig, S., & Marshak, D. R. (1999, April 2). Multilineage Potential of Adult Human Mesenchymal Stem Cells. *Science*, *284*(5411), 143–147. https://doi.org/10.1126/science.284.5411.143

311. Chen, C. W., Okada, M., Proto, J. D., Gao, X., Sekiya, N., Beckman, S. A., Corselli, M., Crisan, M., Saparov, A., Tobita, K., Péault, B., & Huard, J. (2013). Human pericytes for ischemic heart repair. *Stem cells (Dayton, Ohio)*, *31*(2), 305–316. https://doi.org/10.1002/stem.1285

312. Soon-Jung Park, Ri Youn Kim, Bong-Woo Park, Sunghun Lee, Seong Woo Choi, Jae-Hyun Park, Jong. (2019). Dual stem cell therapy synergistically improves cardiac function and vascular regeneration following MI. *Nature Communications*, doi.org/10.1038/s41467-019-11091-2

313. Yassa, M. E., Mansour, I. A., Sewelam, N. I., Hamza, H., & Gaafar, T. (2018, March). The impact of growth factors on human induced pluripotent stem cells differentiation into cardiomyocytes. Life Sciences, 196, 38–47. https://doi.org/10.1016/j.lfs.2018.01.009

314. Farzaneh, M., Rahimi, F., Alishahi, M., & Khoshnam, S. E. (2019, January 14). Paracrine Mechanisms Involved in Mesenchymal Stem Cell Differentiation into

Cardiomyocytes. Current Stem Cell Research & Therapy, 14(1), 9–13. https://doi.org/10.2174/1574888x13666180821160421

315. Jiang, Y., & Lian, X. L. (2020, March). Heart regeneration with human pluripotent stem cells: Prospects and challenges. Bioactive Materials, 5(1), 74–81. https://doi.org/10.1016/j.bioactmat.2020.01.003

316. Hodgkinson, C. P., Bareja, A., Gomez, J. A., & Dzau, V. J. (2016, January 8). Emerging Concepts in Paracrine Mechanisms in Regenerative Cardiovascular Medicine and Biology. Circulation Research, 118(1), 95–107. https://doi.org/10.1161/circresaha.115.305373

317. Lee, W. C. C., Sepulveda, J. L., Rubin, J. P., & Marra, K. G. (2009, April). Cardiomyogenic differentiation potential of human adipose precursor cells. International Journal of Cardiology, 133(3), 399–401. https://doi.org/10.1016/j.ijcard.2007.11.068

318. Xie, X. (2006, September). Differentiation of bone marrow mesenchymal stem cells induced by myo- cardial medium under hypoxic conditions. *Acta Pharmacologica Sinica*, *27*(9), 1153–1158. https://www.nature.com/articles/aps2006156.pdf?origin=ppub

319. Takahashi, T., Lord, B., Schulze, P. C., Fryer, R. M., Sarang, S. S., Gullans, S. R., & Lee, R. T. (2003, April 15). Ascorbic Acid Enhances Differentiation of Embryonic Stem Cells Into Cardiac Myocytes. Circulation, 107(14), 1912–1916. https://doi.org/10.1161/01.cir.0000064899.53876.a3

320. Funakoshi, S., Miki, K., Takaki, T., Okubo, C., Hatani, T., Chonabayashi, K., Nishikawa, M., Takei, I., Oishi, A., Narita, M., Hoshijima, M., Kimura, T., Yamanaka, S., & Yoshida, Y. (2016, January 8). Enhanced engraftment, proliferation and therapeutic potential in heart using optimized human iPSC-derived cardiomyocytes. Scientific Reports, 6(1). https://doi.org/10.1038/srep19111

321. Burdick, J. A., & Vunjak-Novakovic, G. (2009, February). Engineered Microenvironments for Controlled Stem Cell Differentiation. Tissue Engineering Part A, 15(2), 205–219. https://doi.org/10.1089/ten.tea.2008.0131

322. Lutolf, M. P., Gilbert, P. M., & Blau, H. M. (2009, November). Designing materials to direct stem-cell fate. Nature, 462(7272), 433–441. https://doi.org/10.1038/nature08602

323. Fu, C. Y., Chuang, W. T., & Hsu, S. H. (2021, February 18). A Biodegradable Chitosan-Polyurethane Cryogel with Switchable Shape Memory. ACS Applied Materials & Interfaces, 13(8), 9702–9713. https://doi.org/10.1021/acsami.0c21940

324. Lin, C. H., & Lilly, B. (2014, November). Endothelial Cells Direct Mesenchymal Stem Cells Toward a Smooth Muscle Cell Fate. Stem Cells and Development, 23(21), 2581–2590. https://doi.org/10.1089/scd.2014.0163

325. Brun, J. (2015, December 16). Smooth Muscle-Like Cells Generated from Human Mesenchymal Stromal Cells Display Marker Gene Expression and Electrophysiological Competence Comparable to Bladder Smooth Muscle Cells. *Plos One*, *10*(12), e0145153. doi:10.1371/journal.pone.0145153

326. Wang, C., Li, Y., Yang, M., Zou, Y., Liu, H., Liang, Z., Yin, Y., Niu, G., Yan, Z., & Zhang, B. (2018, February). Efficient Differentiation of Bone Marrow Mesenchymal Stem Cells into Endothelial Cells in Vitro. European Journal of Vascular and Endovascular Surgery, 55(2), 257–265. https://doi.org/10.1016/j.ejvs.2017.10.012

327. Yang, G., Xiao, Z., Ren, X., Long, H., Ma, K., Qian, H., & Guo, Y. (2017, February 3). Obtaining spontaneously beating cardiomyocyte-like cells from adipose-derived stromal vascular fractions cultured on enzyme-crosslinked gelatin hydrogels. Scientific Reports, 7(1). https://doi.org/10.1038/srep41781

328. Philip, A. (1996, April 1). Acute MI: early treatment. *Australian prescriber*, *19*(2), 52-54. 10.18773/austprescr.1996.054

329. Shafei, A. E., Ali, M. A., Ghanem, H. G., Shehata, A. I., Abdelgawad, A. A., Handal, H. R., Talaat, K. A., Ashaal, A. E., & El-Shal, A. S. (2017, December). Mesenchymal stem cell therapy: A promising cell-based therapy for treatment of MI. The Journal of Gene Medicine, 19(12). https://doi.org/10.1002/jgm.2995

330. Park, S.-J. (2019, July 16). Dual stem cell therapy synergistically improves cardiac function and vascular regeneration following MI. *Nature*, *10*(3123). https://www.nature.com/articles/s41467-019-11091-2

331. Wu, W. Q., Peng, S., Song, Z. Y., & Lin, S. (2019, March 14). Collagen biomaterial for the treatment of MI: an update on cardiac tissue engineering and myocardial regeneration. Drug Delivery and Translational Research. https://doi.org/10.1007/s13346-019-00627-0

332. Prabhu, S. D., & Frangogiannis, N. G. (2016, June 24). The Biological Basis for Cardiac Repair After MI. Circulation Research, 119(1), 91–112. https://doi.org/10.1161/circresaha.116.303577

333. Jiang, X., Yang, Z., & Dong, M. (2020, July 17). Cardiac repair in a murine model of MI with human induced pluripotent stem cell-derived cardiomyocytes. *Stem Cell Research & Therapy*, *11*(1). https://doi.org/10.1186/s13287-020-01811-7

334. Tenreiro, M. F., Louro, A. F., Alves, P. M., & Serra, M. (2021, June 1). *Next generation of heart regenerative therapies: progress and promise of cardiac tissue engineering*. Npj Regenerative Medicine. https://doi.org/10.1038/s41536-021-00140-4

335. Li, G., Chen, J., Zhang, X., He, G., Wang, T., Wu, H., Li, R., Chen, Y., Gu, R., Xie, J., & Xu, B. (2017, March 15). *Cardiac repair in a mouse model of acute MI with trophoblast stem cells*. Scientific Reports. https://doi.org/10.1038/srep44376

336. Ye, G., Wen, Z., Wen, F., Song, X., Wang, L., Li, C., He, Y., Prakash, S., & Qiu, X. (2020). Mussel-inspired conductive Ti2C-cryogel promotes functional maturation of cardiomyocytes and enhances repair of MI. *Theranostics*, *10*(5), 2047–2066. https://doi.org/10.7150/thno.38876

APPENDIX

Contents

APPENDIX A

List of Reagents

Purpose	Name of Reagent	Supplier	Additional Information
Cryogel preparation	Chitosan	Sigma-Aldrich	LOT: 448877-50G
	Heparin solution salt from porcine intestinal mucosa	Sigma-Aldrich	H6279-100KU
	Poly(vinyl alcohol)	Sigma-Aldrich	341584-25G
	Glutaraldehyde Solution	Millipore	LOT:354400
	Sodium borohydride	Sigma-Aldrich	452882-500G
	Acetic acid solution	Merck	CAS Number: 64-19-7
MSCs isolation	Collagenase type 2		
	0.22 um syringe filters	Sigma-Aldrich	SLMPL25SS
	Alpha MEM Eagle	Pan-biotech	Lot: P04-21500
	Fetal Bovine Serum, qualified, heat inactivated	Thermofisher	Cat.N: 16140071
	DMEM, low glucose, pyruvate	Gibco	Lot: 2646161
	Penicillin-Streptomycin	Thermofisher	Cat.N: 15140163
	Trypsin Solution B (0.25% in DPBS)	Biological Industries	Lot: 2028521
	Recombinant Anti-CD105 antibody (Rabbit monoclonal)	Abcam	ab221675
Cell Differentiation	L-Ascorbic acid solution (1.0 mg/mL in acetonitrile)	Sigma-Aldrich	Lot: 50-81-7
	Recombinant mouse IGF1 protein	Abcam	ab198569
	Recombinant mouse EGF protein	Abcam	ab206643
	Recombinant mouse PDGF-BB protein	Abcam	ab78593

	Recombinant mouse IL-10 protein	Abcam	ab222176
	Recombinant Mouse TGF beta 1 protein	Abcam	ab208466
	Recombinant mouse VEGF protein	Abcam	ab62134
	Recombinant mouse FGF2 protein	Abcam	ab229521
	Recombinant human TNF-α protein	Abcam	ab259410
	Recombinant mouse Activin A protein	Abcam	ab151687
	Recombinant mouse BMP-4 protein	Abcam	ab245810
	Goat anti rabbit IgG, Alexa fluor 488	Abcam	ab150077
	Mounting Medium With DAPI - Aqueous, Fluoroshield	Abcam	ab104139
	Anti-GATA4 antibody	Abcam	ab227512
	Normal Goat Serum	Abcam	ab7481
	Goat Anti-Rabbit IgG, Alexa Fluor 647	Abcam	ab150083
	DAPI Staining solution	Abcam	ab228549
	Recombinant anti-SMA (Rabbit pAb)	Abcam	ab5694
	Recombinant anti-CD-31 (Rabbit mAb)	Abcam	ab222783
	Recombinant anti-CD-Cardiac Troponin I (Rabbit)	Abcam	ab155047
PCR and rt-PCR	Triton X-100	Sigma-Aldrich	Lot: STBH8537
	Bovine Serum Albumin	Capricorn	Lot: CP21-4299
	Formaldehyde Solution	Sigma-Aldrich	Lot: MKCQ6645

	TRIzol Reagent	ambion (Life technologies)	15596018 (15596-018)
	PureLink RNA Mini Kit	Invitrogen	Lot: 2490883
	SuperScript IV First-Strand Synthesis System	Invitrogen	Ref: 18091050
	Taq 2X Master mIX	New England BioLabs	Lot: M0270L
	Ethidium Bromide Solution	Bio-Rad	Cat: 1610433
	Agarose for DNA SDS	Sigma-Aldrich	Lot: K50246836827
	DNA Gel Loading Dye (6X)	ThermoFisher	R0611
	TaqMan Fast Advanced Master Mix	ThermoFisher	4444557
	cDNA kit	Abcam	ab286905
In vivo surgery	Mice C57bl/6 male	Jackson Laboratory	000-664
	Mice C57bl/6 female	Jackson Laboratory	000-664
	Recombinant mouse IL-10 protein	Abcam	ab281800
	Mouse TGF-beta 1 Recombinant Protein	R&D Systems	7666 MB 005 CF
	FGF-Basic Recombinant Mouse Protein	Abcam	ab229521
	Wax Coated Braided Silk 75 cm	Coviden	VS-890
	50 µL Microliter Syringe Model 705 RN	Hamilton	Ref: 80530
Stainings	Trichrome Stain (Masson) Kit	ROTH	Cat: 3470.1
	OCT embedding medium	Tissue-Plus	23-730-571
	DPX Mountant for histology	Sigma-Aldrich	06522-100 ML
	Cardiac troponin I primary antibody	Invitrogen	Ref: PA5-85358
	Alpha-Smooth Muscle Actin pAb	Invitrogen	Ref: PA5-85070

	CD206 Monoclonal Antibody (MR5D3)	Invitrogen	Ref: MA5-16868
	Recombinant Anti-CD3 epsilon antibody	Abcam	ab237721
	Recombinant Anti-CD163 antibody	Abcam	ab182422
	Recombinant Anti-CD68 antibody	Abcam	ab283654

APPENDIX B

List of primers for cell differentiation

Cardiomyocytes:

Nkx2.5

Forward primer 5’ -CACCACTCTCTGCTACCCAC-3’

Reverse primer - 5’-AGCGCGCACAGCTCTTTT-3’

Product length - 392

NM_008700.2 Mus musculus NK2 homeobox 5 (Nkx2-5), mRNA

Tbx5

Forward primer 5’-ACCCGTTTGGACACATTATCCT-3’

Reverse primer 5’-TAGCCCGAGCGATAGAAGGT T-3’

Product length - 577

NM_011537.3 Mus musculus T-box 5 (Tbx5), mRNA

CTNT

Forward primer 5’-TGCCAAAATAGCAGCCAACAC-3’

Reverse primer 5’-CCCGACGCTTTTCGATCCTG-3’

Product length - 650

Mus musculus troponin T2, cardiac (Tnnt2), transcript variant X7, mRNA

Smooth muscle cells:

a-SMA (Acta2)

Forward primer 5’-TAACCCTTCAGCGTTCAGCC-3’

Reverse primer 5’-CTCACGCTCGGCAGTAGTC-3’

Product length - 722

NM_007392.3 Mus musculus actin alpha 2, smooth muscle, aorta (Acta2), mRNA

Calponin3

Forward primer 5’-TCTAGCAGGTCTGGCGAAAA-3’

Reverse primer 5’-GCTAGCTTGGGTCTCACTGG-3’

Product length - 682

Template NM_028044.2

Myh11

Forward primer 5’-CCCCGGAGTAGATCTGGGAC-3’

Reverse primer 5’-GATGCTGCTGTCTTTCTTGCC-3’

Product length - 661

NM_013607.3 Mus musculus myosin, heavy polypeptide 11, smooth muscle (Myh11), transcript variant 1, mRNA

Endothelial cells:

Pecam1

Forward primer 5’-CACGCTGGTGCTCTATGCAA-3’

Reverse primer 5’-CTTGGGCTTGGATACGCCAT-3’

Product length - 352

Between pos. 106605728 and 106590711 on NC_000077.7

Cd34

Forward primer 5’-TCCGAGTGCCATTAAGGGAGAA-3’

Reverse primer 5’-GGGTTGTGAGGTACTGTGAGG-3’

Product length - 588

NM_001111059.2 Mus musculus CD34 antigen (Cd34), transcript variant 1, mRNA

APPENDIX C

Detailed protocol for Murine MI-Model preparation

Intubation and Ventilation

1. A mouse was placed into an anesthesia induction chamber with 4 % isoflurane and 100 % oxygen with oxygen flow rate of 0.4 L/min for 2 min.
2. The mouse was suspended on the intubation stand by the upper incisors using a rubber wire from the intubation kit and fixed on the stand with a 10-cm plastic tape.
3. Using curved forceps, the animal's tongue was moved slightly upwards and to the side to get access to the larynx.
4. Fiber optic intubation laryngoscope was inserted into the animal's mouth and gently pressed against the palate until the vocal cords became visible.
5. 18 G plastic trocar cannula was used as the intubation tube. The intubation tube was inserted into the animal's mouth using the intubation guide from the mouse intubation kit and passed through the vocal cords.
6. As soon as the cannula passed through the vocal cords the intubation guide was quickly retracted whereas the intubation tube was advanced further.
7. The mouse was quickly transferred to a heating pad, and the intubation tube was connected to the MINIVENT mouse ventilator with the following settings: tidal volume – 240 µl/stroke and ventilation rate – 140 strokes/minute.
8. Isoflurane concentration was changed to 2 % and the intubation tube was fixed to the pad using 10-cm plastic tape.

Preparation for the Surgery

1. Animal was placed into the left recumbent position with the right front leg moved upwards and to the right to expose the thorax.
2. The animal's front and back legs were fixed to the pad with a 10-cm piece of plastic tape. Animal's lower right thorax was cleared from the fur by applying a small amount of hair removal crème.
3. The exposed skin was disinfected with 70 % ethanol.

Thoracotomy

1. A small, about 1-cm oblique incision in the direction from the tip of the sternum to the origin of the right front leg was made using scissors.
2. The underlying connective tissue and pectoralis muscle were carefully cut to expose the rib cage.
3. The small opening in the intercostal muscles in the 2nd intercostal space was made using cushion delicate forceps.
4. The rib cage was opened by placing a small curved needle holder in the incision (see 3) and opening it.

5. The ribs were further retracted using chest retractors to expose the heart.

Ischemia

1. Pericardium was gently removed using two cushion dissecting forceps.
2. LAD was located under the microscope. Specifically, LAD appears as a bright red pulsating vessel originating from the left border of the auricle of the left atrium and runs towards the apex of the heart.
3. A tight ligature was made about 2-mm below the left atrium auricle with 7-0 silk suture. The success of the ischemia was confirmed by blanching or white discoloration of the area under the ligation.

Chest closure and Extubation

1. Rib cage was closed using 5-0 surgical sutures.
2. Connective tissue and skin were stitched using continuous sutures with 5-0 surgical suture.
3. The anesthesia settings were changed to 0 % isoflurane.
4. The animal's lungs were reinflated by pinching the outflow tube and holding it for 3 seconds.
5. The animal was carefully observed on the heating pad until the normal breathing pattern was resumed and the animal became awake.
6. The animal was extubated by removing the intubation tube from its mouth.

APPENDIX D

List of primers for qPCR

TNF-alpha

Forward - GCTCTTCTGTCTACTGAA

Reverse - GCCATAGAACTGATGAGA

Fam probe -AGGCCATTTGGGAACTTCTCATG

IL - 1b

Forward - CCTCAATGGACAGAATATC

Reverse - ACAGGTATTTTGTCGTTG

Fam probe - ACCAACAAGTGATATTCTCCATGAGC

IL- 6

Forward - CTACCAAACTGGATATAATCA

Reverse - CAGGTAGCTATGGTACTC

Fam probe -TGCCTATTGAAAATTTCCTCTGGTCTT

TGF - b

Forward - ATCGCCCTTTCATTTCAG

Reverse - CCTGGCAATTGTTCTTTG

Fam probe - AAACCTGATCCAGACCCTGATGTT

IL - 10

Forward - CAGGTGAAGACTTTCTTTC

Reverse - AACCCAAGTAACCCTTAA

Fam probe -ACAACATACTGCTAACCGACTCCTT

IL - 4

Forward - GGAGATGGATGTGCCAAA

Reverse - CTTGGAAGCCCTACAGAC

Fam probe -CAGGAACGAAGAACACCACAGAG

Actin (HK gene)

Forward - CCAACCGTGAAAGATGAC

Reverse - CTGGATGGCTACGTACATG

Fam probe - CAGATCATGTTTGAGACCTTCAACACC

APPENDIX E

Ultrasound Results for Set 1

One-way ANOVA results for Set 1

Parameter	Significance (p<0.05)	P-value	F-value
Ejection Fraction	Significant	0.0003	7.710
Fractional Shortening	Significant	0.0003	7.756
Diastolic Diameter	Significant	0.0111	4.083
Systolic Diameter	Significant	0.0196	3.708

Post-hoc Analysis for Set 1

Parameter	Comparison	Summary	P-value (Post-hoc)
Ejection Fraction	Control vs. Cryogel	ns	0.1941
	Control vs. Cryo/(IL-10 TGF-β)	**	0.0075
	Control vs. Cryo/(VEGF FGF2)	ns	0.1957
	Control vs. Cryo/GFs(1,2)	***	0.0002
	Cryogel vs. Cryo/(IL-10 TGF-β)	ns	0.5707
	Cryogel vs. Cryo/(VEGF FGF2)	ns	>0.9999
	Cryogel vs. Cryo/GFs(1,2)	*	0.0401
	Cryo/(IL-10 TGF-β) vs. Cryo/(VEGF FGF2)	ns	0.5678
	Cryo/(IL-10 TGF-β) vs. Cryo/GFs(1,2)	ns	0.5501

	Cryo/(VEGF FGF2) vs. Cryo/GFs(1,2)	*	0.0397
Fractional Shortening	Control vs. Cryogel	ns	0.1941
	Control vs. Cryo/(IL-10 TGF-β)	**	0.0075
	Control vs. Cryo/(VEGF FGF2)	ns	0.1957
	Control vs. Cryo/GFs(1,2)	***	0.0002
	Cryogel vs. Cryo/(IL-10 TGF-β)	ns	0.5707
	Cryogel vs. Cryo/(VEGF FGF2)	ns	>0.9999
	Cryogel vs. Cryo/GFs(1,2)	*	0.0401
	Cryo/(IL-10 TGF-β) vs. Cryo/(VEGF FGF2)	ns	0.5678
	Cryo/(IL-10 TGF-β) vs. Cryo/GFs(1,2)	ns	0.5501
	Cryo/(VEGF FGF2) vs. Cryo/GFs(1,2)	*	0.0397
Diastolic Diameter	Control vs. Cryogel	ns	0.9995
	Control vs. Cryo/(IL-10 TGF-β)	ns	0.8214
	Control vs. Cryo/(VEGF FGF2)	ns	0.8889
	Control vs. Cryo/GFs(1,2)	*	0.0262
	Cryogel vs. Cryo/(IL-10 TGF-β)	ns	0.8925
	Cryogel vs. Cryo/(VEGF FGF2)	ns	0.9447
	Cryogel vs. Cryo/GFs(1,2)	*	0.0276
	Cryo/(IL-10 TGF-β) vs. Cryo/(VEGF	ns	0.9998

	FGF2)		
	Cryo/(IL-10 TGF-β) vs. Cryo/GFs(1,2)	ns	0.1283
	Cryo/(VEGF FGF2) vs. Cryo/GFs(1,2)	ns	0.094
Systolic Diameter	Control vs. Cryogel	ns	0.2321
	Control vs. Cryo/(IL-10 TGF-β)	ns	0.3263
	Control vs. Cryo/(VEGF FGF2)	ns	0.7173
	Control vs. Cryo/GFs(1,2)	**	0.005
	Cryogel vs. Cryo/(IL-10 TGF-β)	ns	0.9995
	Cryogel vs. Cryo/(VEGF FGF2)	ns	0.8986
	Cryogel vs. Cryo/GFs(1,2)	ns	0.4091
	Cryo/(IL-10 TGF-β) vs. Cryo/(VEGF FGF2)	ns	0.9602
	Cryo/(IL-10 TGF-β) vs. Cryo/GFs(1,2)	ns	0.2998
	Cryo/(VEGF FGF2) vs. Cryo/GFs(1,2)	ns	0.0887

APPENDIX F

Ultrasound Results for Set 2

One-way ANOVA results for Set 2

Parameter	Significance (p<0.05)	P-value	F-value
Ejection Fraction	Significant	<0.0001	12.03
Fractional Shortening	Significant	<0.0001	11.07
Diastolic Diameter	Significant	0.0084	4.867
Systolic Diameter	Significant	0.0001	10.55

Post-hoc Analysis for Set 2

Parameter	Comparison	Summary	P-value (Post-hoc)
Ejection Fraction	Control vs. Cryogel	ns	0.1621
	Control vs. Cryo/GFs	***	0.0001
	Control vs. Cryo/GFs/Cells	***	0.0003
	Cryogel vs. Cryo/GFs	*	0.0323
	Cryogel vs. Cryo/GFs/Cells	ns	0.0689
	Cryo/GFs vs. Cryo/GFs/Cells	ns	0.9849
Fractional Shortening	Control vs. Cryogel	ns	0.2349
	Control vs. Cryo/GFs	***	0.0002
	Control vs. Cryo/GFs/Cells	***	0.0005
	Cryogel vs. Cryo/GFs	*	0.0345

	Cryogel vs. Cryo/GFs/Cells	ns	0.0688
	Cryo/GFs vs. Cryo/GFs/Cells	ns	0.9883
Diastolic Diameter	Control vs. Cryogel	ns	0.0935
	Control vs. Cryo/GFs	*	0.0151
	Control vs. Cryo/GFs/Cells	*	0.0176
	Cryogel vs. Cryo/GFs	ns	0.8511
	Cryogel vs. Cryo/GFs/Cells	ns	0.8792
	Cryo/GFs vs. Cryo/GFs/Cells	ns	>0.9999
Systolic Diameter	Control vs. Cryogel	*	0.0397
	Control vs. Cryo/GFs	***	0.0002
	Control vs. Cryo/GFs/Cells	***	0.0005
	Cryogel vs. Cryo/GFs	ns	0.2089
	Cryogel vs. Cryo/GFs/Cells	ns	0.314
	Cryo/GFs vs. Cryo/GFs/Cells	ns	0.9941

APPENDIX G

Ultrasound Results for Set 3

One-way ANOVA results for Set 3

Parameter	Significance (p<0.05)	P-value	F-value
Cardiac Output Week 1	Not Significant	0.8220	0.3044
Cardiac Output Week 4	Significant	<0.0001	10.72
Diastolic Diameter Week 1	Not Significant	0.9059	0.1848
Diastolic Diameter Week 4	Significant	0.0008	7.420
Ejection Fraction Week 1	Not Significant	0.4576	0.8899
Ejection Fraction Week 4	Significant	<0.0001	13.15
Systolic Diameter Week 1	Not Significant	0.9226	0.1597
Systolic Diameter Week 4	Significant	0.0003	8.542
Fractional Shortening Week 1	Not Significant	0.3949	1.026
Fractional Shortening Week 4	Significant	0.0001	9.845
Stroke Volume Week 1	Not Significant	0.6904	0.4922
Stroke Volume Week 4	Significant	0.0014	6.682
Diastolic Volume Week 1	Not Significant	0.8994	0.1944
Diastolic Volume Week 4	Not Significant	0.4953	0.8164
Systolic Volume Week 1	Not Significant	0.9658	0.08858
Systolic Volume Week 4	Significant	0.0491	2.951

Post-hoc analysis for Set 3, only statistically significant data included

Parameter	Comparison	Summary	P-value (Post-hoc)
Cardiac Output Week 4	Control vs. Cells	**	0.0035
	Control vs. Cryo/GFs	***	0.0004
	Control vs. Cryo/GFs/Cells	***	0.0001
	Cells vs. Cryo/GFs	ns	0.8168
	Cells vs. Cryo/GFs/Cells	ns	0.4397
	Cryo/GFs vs. Cryo/GFs/Cells	ns	0.8968
Diastolic Diameter Week 4	Control vs. Cells	*	0.0317
	Control vs. Cryo/GFs	*	0.0169
	Control vs. Cryo/GFs/Cells	***	0.0004
	Cells vs. Cryo/GFs	ns	0.9928
	Cells vs. Cryo/GFs/Cells	ns	0.2557
	Cryo/GFs vs. Cryo/GFs/Cells	ns	0.3773
Ejection Fraction Week 4	Control vs. Cells	*	0.0448
	Control vs. Cryo/GFs	****	<0.0001
	Control vs. Cryo/GFs/Cells	****	<0.0001
	Cells vs. Cryo/GFs	ns	0.0869
	Cells vs. Cryo/GFs/Cells	*	0.0271
	Cryo/GFs vs. Cryo/GFs/Cells	ns	0.9013

Systolic Diameter Week 4	Control vs. Cells	*	0.0202
	Control vs. Cryo/GFs	**	0.0056
	Control vs. Cryo/GFs/Cells	***	0.0002
	Cells vs. Cryo/GFs	ns	0.9500
	Cells vs. Cryo/GFs/Cells	ns	0.2201
	Cryo/GFs vs. Cryo/GFs/Cells	ns	0.4640
Fractional Shortening Week 4	Control vs. Cells	ns	0.0582
	Control vs. Cryo/GFs	***	0.0009
	Control vs. Cryo/GFs/Cells	***	0.0002
	Cells vs. Cryo/GFs	ns	0.3230
	Cells vs. Cryo/GFs/Cells	ns	0.0786
	Cryo/GFs vs. Cryo/GFs/Cells	ns	0.8109
Stroke Volume Week 4	Control vs. Cells	*	0.0117
	Control vs. Cryo/GFs	**	0.0026
	Control vs. Cryo/GFs/Cells	**	0.0056
	Cells vs. Cryo/GFs	ns	0.9276
	Cells vs. Cryo/GFs/Cells	ns	0.9562
	Cryo/GFs vs. Cryo/GFs/Cells	ns	>0.9999
	Control vs. Cells	ns	0.7404

Systolic Volume Week 4	Control vs. Cryo/GFs	ns	0.1529
	Control vs. Cryo/GFs/Cells	*	0.0491
	Cells vs. Cryo/GFs	ns	0.6333
	Cells vs. Cryo/GFs/Cells	ns	0.2826
	Cryo/GFs vs. Cryo/GFs/Cells	ns	0.8944

APPENDIX H

Statistical Data for Cytokine Gene Expression

Statistical Analysis of Cytokine Gene Expression by One-way ANOVA Week 1

Cytokine	Significance ($p<0.05$)	P-value	F-value
TNF-alpha	Significant	<0.0001	70.75
IL-1β	Significant	<0.0001	54.75
IL-6	Significant	0.0020	12.88
TGF-β	Not Significant	0.0524	3.983
IL-10	Significant	<0.0001	42.14
IL-4	Significant	<0.0001	31.18

Statistical Analysis of Cytokine Gene Expression by One-way ANOVA Week 2

Cytokine	Significance ($p<0.05$)	P-value	F-value
TNF-alpha	Significant	0.0067	18.68
IL-1β	Significant	0.0012	94.40
IL-6	Significant	<0.0001	35.91
TGF-β	Not Significant	0.2461	1.688
IL-10	Significant	0.0003	21.96
IL-4	Significant	0.0132	11.17

Statistical Analysis of Cytokine Gene Expression by One-way ANOVA Week 4

Cytokine	Significance ($p<0.05$)	P-value	F-value
TNF-alpha	Significant	<0.0001	66.40
IL-1β	Significant	<0.0001	50.51
IL-6	Significant	0.0002	26.82
TGF-β	Significant	0.0063	8.894
IL-10	Significant	<0.0001	31.94
IL-4	Significant	<0.0001	64.45

Post-Hoc statistics for qPCR (cytokine expression)

Post-Hoc Analysis Results, Week 1

Cytokine	Comparison	Summary	P-value (Post-hoc)
TNF-alpha	Control vs. Cells	****	<0.0001
	Control vs. Cryo/GFs	****	<0.0001
	Control vs. Cryo/GFs/Cells	****	<0.0001
	Cells vs. Cryo/GFs	ns	0.4835
	Cells vs. Cryo/GFs/Cells	*	0.0105
	Cryo/GFs vs. Cryo/GFs/Cells	ns	0.0813
IL-1β	Control vs. Cells	****	<0.0001
	Control vs. Cryo/GFs	****	<0.0001
	Control vs. Cryo/GFs/Cells	****	<0.0001

	Cells vs. Cryo/GFs	ns	0.9276
	Cells vs. Cryo/GFs/Cells	ns	0.1672
	Cryo/GFs vs. Cryo/GFs/Cells	ns	0.0716
IL-6	Control vs. Cells	*	0.0309
	Control vs. Cryo/GFs	ns	0.1330
	Control vs. Cryo/GFs/Cells	**	0.0013
	Cells vs. Cryo/GFs	ns	0.7333
	Cells vs. Cryo/GFs/Cells	ns	0.1198
	Cryo/GFs vs. Cryo/GFs/Cells	*	0.0279
TGF-β	Control vs. Cells	ns	0.6270
	Control vs. Cryo/GFs	*	0.0487
	Control vs. Cryo/GFs/Cells	ns	0.1454
	Cells vs. Cryo/GFs	ns	0.2671
	Cells vs. Cryo/GFs/Cells	ns	0.6358
	Cryo/GFs vs. Cryo/GFs/Cells	ns	0.8627
IL-10	Control vs. Cells	ns	0.1822
	Control vs. Cryo/GFs	****	<0.0001
	Control vs. Cryo/GFs/Cells	***	0.0006
	Cells vs. Cryo/GFs	***	0.0002

	Cells vs. Cryo/GFs/Cells	**	0.0080
	Cryo/GFs vs. Cryo/GFs/Cells	*	0.0373
IL-4	Control vs. Cells	*	0.0302
	Control vs. Cryo/GFs	***	0.0001
	Control vs. Cryo/GFs/Cells	***	0.0003
	Cells vs. Cryo/GFs	**	0.0050
	Cells vs. Cryo/GFs/Cells	*	0.0132
	Cryo/GFs vs. Cryo/GFs/Cells	ns	0.8687

Post-Hoc Analysis Results, Week 2

Cytokine	Comparison	Summary	P-value (Post-hoc)
TNF-alpha	Control vs. Cells	ns	0.2047
	Control vs. Cryo/GFs	ns	0.3051
	Control vs. Cryo/GFs/Cells	*	0.0134
	Cells vs. Cryo/GFs	ns	0.9959
	Cells vs. Cryo/GFs/Cells	*	0.0214
	Cryo/GFs vs. Cryo/GFs/Cells	ns	0.1410
IL-1β	Control vs. Cells	**	0.0057
	Control vs. Cryo/GFs	**	0.0013
	Control vs. Cryo/GFs/Cells	*	0.0248

	Cells vs. Cryo/GFs	ns	0.0925
	Cells vs. Cryo/GFs/Cells	ns	0.7123
	Cryo/GFs vs. Cryo/GFs/Cells	ns	0.6065
IL-6	Control vs. Cells	***	0.0006
	Control vs. Cryo/GFs	**	0.0021
	Control vs. Cryo/GFs/Cells	****	<0.0001
	Cells vs. Cryo/GFs	ns	0.6556
	Cells vs. Cryo/GFs/Cells	*	0.0407
	Cryo/GFs vs. Cryo/GFs/Cells	**	0.0083
TGF-β	Control vs. Cells	ns	0.5958
	Control vs. Cryo/GFs	ns	0.5663
	Control vs. Cryo/GFs/Cells	ns	0.1941
	Cells vs. Cryo/GFs	ns	>0.9999
	Cells vs. Cryo/GFs/Cells	ns	0.7816
	Cryo/GFs vs. Cryo/GFs/Cells	ns	0.8085
IL-10	Control vs. Cells	*	0.0228
	Control vs. Cryo/GFs	ns	0.1713
	Control vs. Cryo/GFs/Cells	***	0.0002
	Cells vs. Cryo/GFs	ns	0.5089

	Cells vs. Cryo/GFs/Cells	*	0.0143
	Cryo/GFs vs. Cryo/GFs/Cells	**	0.0024
IL-4	Control vs. Cells	ns	0.1520
	Control vs. Cryo/GFs	ns	0.2945
	Control vs. Cryo/GFs/Cells	*	0.0208
	Cells vs. Cryo/GFs	ns	0.9915
	Cells vs. Cryo/GFs/Cells	ns	0.3764
	Cryo/GFs vs. Cryo/GFs/Cells	ns	0.2904

Post-Hoc Analysis Results, Week 4

Cytokine	Comparison	Summary	P-value (Post-hoc)
TNF-alpha	Control vs. Cells	****	<0.0001
	Control vs. Cryo/GFs	****	<0.0001
	Control vs. Cryo/GFs/Cells	****	<0.0001
	Cells vs. Cryo/GFs	ns	0.9120
	Cells vs. Cryo/GFs/Cells	*	0.0271
	Cryo/GFs vs. Cryo/GFs/Cells	*	0.0113
IL-1β	Control vs. Cells	***	0.0002
	Control vs. Cryo/GFs	**	0.0027
	Control vs. Cryo/GFs/Cells	****	<0.0001

	Cells vs. Cryo/GFs	ns	0.0922
	Cells vs. Cryo/GFs/Cells	*	0.0243
	Cryo/GFs vs. Cryo/GFs/Cells	***	0.0009
IL-6	Control vs. Cells	ns	0.6474
	Control vs. Cryo/GFs	ns	0.8484
	Control vs. Cryo/GFs/Cells	*	0.0330
	Cells vs. Cryo/GFs	ns	>0.9999
	Cells vs. Cryo/GFs/Cells	ns	0.4505
	Cryo/GFs vs. Cryo/GFs/Cells	ns	0.6668
TGF-β	Control vs. Cells	ns	0.6885
	Control vs. Cryo/GFs	*	0.0303
	Control vs. Cryo/GFs/Cells	ns	0.2094
	Cells vs. Cryo/GFs	**	0.0069
	Cells vs. Cryo/GFs/Cells	*	0.0438
	Cryo/GFs vs. Cryo/GFs/Cells	ns	0.5411
IL-10	Control vs. Cells	***	0.0002
	Control vs. Cryo/GFs	***	0.0005
	Control vs. Cryo/GFs/Cells	***	0.0001
	Cells vs. Cryo/GFs	ns	0.6702

	Cells vs. Cryo/GFs/Cells	ns	0.9997
	Cryo/GFs vs. Cryo/GFs/Cells	ns	0.6194
IL-4	Control vs. Cells	****	<0.0001
	Control vs. Cryo/GFs	***	0.0005
	Control vs. Cryo/GFs/Cells	****	<0.0001
	Cells vs. Cryo/GFs	**	0.0060
	Cells vs. Cryo/GFs/Cells	ns	0.9951
	Cryo/GFs vs. Cryo/GFs/Cells	**	0.0045

APPENDIX I

One-Way ANOVA Results for Histology

Parameter	Significance (p<0.05)	P-value	F-value
Percentage of Fibrosis (%)	Significant	<0.0001	15.79

Post-hoc Analysis for Histology

Parameter	Comparison	Summary	P-value (Post-hoc)
Percentage of Fibrosis (%)	**Control vs. Cells**	**	0.0067
	Control vs. Cryo/GFs	***	0.0004
	Control vs. Cryo/GFs/Cells	***	<0.0001
	Cells vs. Cryo/GFs	ns	0.4895
	Cells vs. Cryo/GFs/Cells	ns	0.0856
	Cryo/GFs vs. Cryo/GFs/Cells	ns	0.6791